Performance Evaluation of Mechanically Connected and Adhesive Bonded Steel-Concrete Composite Connections

Pankaj Kumar
(2013RCE9041)

Department of Civil Engineering
Malaviya National Institute of Technology Jaipur
May 2018

Performance Evaluation of Mechanically Connected and Adhesive Bonded Steel-Concrete Composite Connections

Submitted
in fulfillment of the requirements of the degree of Doctor of Philosophy

by
Pankaj Kumar
(2013RCE9041)

to the

Department of Civil Engineering
Malaviya National Institute of Technology Jaipur
May 2018

Candidate's Declaration

I hereby declare that the research work presented in this thesis entitles "*Performance Evaluation of Mechanically Connected and Adhesive Bonded Steel-Concrete Composite Connections*" submitted for the award of the degree of Doctor of Philosophy in the Department of Civil Engineering, Malaviya National Institute of Technology Jaipur, Jaipur is an authenticated record of my own research work carried out under the supervision of Dr. Sandeep Chaudhary, Associate Professor, Department of Civil Engineering, MNIT Jaipur (presently on lien to Indian Institute of Technology Indore as Associate Professor, Discipline of Civil Engineering) and Dr. Amar Patnaik, Assistant Professor, Department of Mechanical Engineering, MNIT Jaipur. Other researchers' works have been duly cited and listed in reference section.

The matter presented in this thesis has not previously been submitted in part or full to any other University or Institution for award of any degree in India or abroad.

May 2018

(Pankaj Kumar)
2013RCE9041

Certificate

It is certified that the work contained in this thesis entitled "*Performance Evaluation of Mechanically Connected and Adhesive Bonded Steel-Concrete Composite Connections*", by Mr. Pankaj Kumar (2013RCE9041), has been carried out under our supervision and that his work has not been submitted elsewhere for a degree.

(Amar Patnaik)
Assistant Professor
Department of Mechanical Engineering
Malaviya National Institute of Technology Jaipur

(Sandeep Chaudhary)
On lien from
Associate Professor
Department of Civil Engineering
Malaviya National Institute of Technology Jaipur

Presently
Associate Professor
Discipline of Civil Engineering
Indian Institute of Technology Indore

May 2018

Acknowledgements

Research is a collective effort; it is not and cannot be pursued and accomplished in isolation. Among the countless people who have helped me during my Ph.D. research journey, my supervisors, Dr. Amar Patnaik, and Dr. Sandeep Chaudhary, deserve the first mention. I am and will always be indebted to the two of them for their unfailing support and direction.

The entire Civil Engineering Department of MNIT-Jaipur has been kind enough to make my research process quite convenient and smooth, providing me with the best laboratory facilities and research database. The eminent members of the department have supplied me with the right guidance and friendly advice at numerous points during the last few years.

In my experimental/laboratory work, Mr. Deepak Sharma and Mr. Padam Chand (Industrial Corporation), Mr. Dinesh Kedia (R M Constructions), Mr. Inderchand Sharma (JEW), Mr. Meghraj Solanki (GSC-JSW), Mr. Prakash (Sharda Engineering), Mr. Vivek Sharma (JDA Jaipur) have offered immense support, for which no matter how much I thank them, it shall never be enough. Jal Singh, my laboratory assistant, deserves my special thanks, for his constant help and hard work over the years.

A lot my friends and work associates have tremendously helped my research, some technically, others emotionally and some both ways. Mr. Ankit Bhardwaj, Dr. Arnav Anuj Kasar, Dr. Bhavna Tripathi, Dr. M. P. Ramnawas, Dr. S. A. A. Naqvi, Dr. Trilok Gupta my seniors, deserves all my gratefulness and blessings for having been a great support to me, both personally and professionally. Other friends from MNIT: Ambika, Minhaj, Nawal, Neeraj, Nishant, Pankaj, Pooja, Rupesh, Salman, Vishisht, and some of my college friends from B. Tech years: Abhijeet, Anilji, Kedia, Deependra, Jaideep, Mansha, Mridual, Mukesh, Natwar, Prabhash, Prateek, Dr. Ramesh, Vinit, Vikram have supported and loved me unconditionally, in times when I found it difficult to move ahead with my work. I extend my heartfelt thanks and regards to the whole bunch and hope that I never let anyone down.

Abstract

Steel-concrete composites have emerged as one of the most effective composite material for construction of modern civil engineering structures. Owing to their numerous advantages over conventional civil engineering materials, steel-concrete composites offer lighter and more cost effective construction along with the high degree of flexibility and ease of construction. The most critical component of such members, that governs their overall performance, is the connection between the steel and concrete. Apart from the mechanical and physical properties of the connected elements, the behaviour of the composite members depends upon the strength and ductility of the connecting medium. The adeptness of a particular connection methodology for composite connection depends on the load-deformation characteristics, the energy absorption capacity of the different connection methodologies and the type of anticipated loading conditions.

In the present study, a set of experimental and analytical analyses have been carried out to gain insight on the various parameters affecting the strength, stiffness, deformability and relative slip of composite members. Two types of connection methodologies, namely, mechanical headed studs as flexible shear connection and structural adhesive as rigid shear connection have been analysed. The physical, mechanical, chemical and microstructural properties of each material have been obtained experimentally to understand their behaviour. The suitability of adhesive material, to act as a connecting medium between the composite interfaces has been demonstrated by conducting dynamic mechanical analysis.

The preliminary behaviour of each of the connection methodology has been analysed through push-out tests on standard steel-concrete composite specimens. The specimens have been subjected to incremental monotonic and impact loading to investigate the effect of loading conditions on the behaviour. Significant insight on the monotonic behaviour of composite connections has been obtained through the investigation of applied load vs engendered slip curves of the specimens. The comparative performance has been obtained, through critical analysis of the experimentally obtained load-slip curves, in terms of ultimate strength, effective stiffness and deformability of each of the considered connection methodology. The suitability of a particular connection methodology has been underscored on the basis of observed behaviour in terms of the strength and stiffness. Also, the optimum design requirements for each of the studied connection strategy have been critically evaluated. The results of the drop weight impact

tests have been analysed to determine the adeptness of a connection strategy on the basis of energy absorption capacity of connections, under extreme loading conditions.

Further, the effects of variation in two critical parameters, namely, concrete strength and amount and detailing of reinforcement, on the behaviour of headed stud connections have been critically analysed. A comprehensive set of push-out test specimens has been experimentally investigated for this purpose. The composite specimens with five different concrete strengths having different amount and detailing of reinforcement have been critically analysed. The variations in connection strength, ultimate engendered slip and failure pattern for each specimen have been observed and discussed in detail. The pre and post-yield shear stiffnesses of composite specimen have been estimated through bilinear idealization of the obtained load-slip curves using energy balancing approach.

The behaviour of adhesive bonded composite specimens has also been investigated in detail, and the effects of variation in the thickness of adhesive layer on the composite behaviour has been underlined. The optimum thickness of the adhesive layer, to ensure effective transfer of forces between the elements of the composite member, has been obtained through a critical analysis of the strength and failure patterns of the composite specimens. The finite element (FE) simulations of the load-slip behaviour of the composite specimens has been carried out, and the simulation results are found to depict close correspondence with the experimental results.

The performance of full-scale composite beams, connected using both the connection methodologies, has also been experimentally evaluated. The effects of two distinct arrangements of mechanical headed stud connectors, in inline and staggered pattern, have also been investigated and the observations have been reported. The simply supported beam specimens have been subjected to a two point monotonic flexural loading, and the observed failure pattern, along with the obtained load-slip and load-deflection curves have been obtained. Finally, a comparative statement on the performance of full-scale beam specimens, in terms of the degree of interaction and degree of connection along with the load deformation behaviours of the both connection methodologies has been reported.

Keywords: Steel-Concrete Composite; Mechanical Headed Stud; Structural Adhesive; Strength; Relative Slip; Deflection; Initial Shear Stiffness; Post-Yield Stiffness

Contents

Chapter: 8 Summary and Conclusions

List of Figures

List of Tables

List of Notations

a	Opening distance of the adherend
A_o	Empirical constant
A_c	Bearing area of concrete
A_r	Cross-section area of reinforcement
$A_{r\%}$	Cross-section area of reinforcement in percent
A_{bc}	Bonded area at steel-concrete connected interface
A_{ds}	Effective cross- section of demountable stud (80% of gross area
A_{spc}	Shear area of perfobond shear connector
A_{tr}	Total cross-section area of transverse reinforcement
A_{sh}	Cross-section area of headed stud connector
$A_{eff.}$	Effective influence area for mechanical headed stud
b_{ad}	Width of the adherend
B_o	Empirical constant
C_1	Characteristic compressive strength of concrete cube at 28 days (*32.50* MPa)
C_2	Characteristic compressive strength of concrete cube at 28 days (*38.55* MPa)
C_3	Characteristic compressive strength of concrete cube at 28 days (*46.50* MPa)
C_4	Characteristic compressive strength of concrete cube at 28 days (*57.71* MPa)
C_5	Characteristic compressive strength of concrete cube at 28 days (*73.46* MPa)
C3D8R	Three dimensional eight noded linear brick element with reduced integration
d_r	Diameter of reinforcement bar
d_s	Diameter of headed stud connector
d_{pc}	Diameter of rib holes
d_{ia}	Effective diameter of the influence area diameter of rib holes
D_o	Empirical constant
e_a	Energy under the actual load-slip curve
e_b	Energy under the bilinear curve
e_{a-b}	Area between the actual and bilinear curve
E_a	Young's modulus of elasticity of adhesive
E_c	Young's modulus of elasticity of concrete
E_s	Young's modulus of elasticity of steel

$E^{'}$	Storage modulus
$E_{dw,\mathrm{f}}$	Drop weight impact energy for final failure
$E_{dw,i}$	Drop weight impact energy for crack initiation
$f_c^{'}$	Compressive strength of concrete cylinder at 28 days
f_y	Yield strength of shear connector
f_u	Ultimate tensile strength of headed stud shear connector
f_{bo}	Ultimate biaxial compressive stress
f_{ck}	Compressive strength of concrete cube of size *150* mm at *28* days
f_{co}	Ultimate uniaxial compressive stress
f_{ct}	Flexural strength of concrete beam of size *100* × *100* × *500* mm at *28* days
f_t	Tensile stress in concrete
f_{to}	Maximum tensile stress in concrete
f_{yr}	Yield strength of reinforcement bars
Δf_c	Change in compressive strength of concrete
g	Earth gravitational acceleration (*9.81* m/s^2)
G_a	Shear modulus of adhesive
G_f	Fracture energy
$G_{IC(bulk)}$	Mode-I fracture energy of bulk adhesive specimen
$G_{IIC(bulk)}$	Mode-II fracture energy of bulk adhesive specimen
h_c	Height of the channel shear connector
h_d	Depth ratio of the rib of metal deck in profiled sheet
h_{ad}	Height of the adherend
h_{dw}	Releasing height of impacter
h_{pc}	Height of perfobond rib connector
h_s	Height of headed stud connector
k_i	Initial shear stiffness
k_{py}	Post-yield stiffness
K_c	Flow stress ratio
l_c	Length of channel shear connector measured in transverse direction of flange of beam
L	Length of the longitudinal span
L_b	Length of the bonded area
m	Mass of impacter
N	Number of cycles required upto the failure
N_i	Number of cycle corresponding to the i^{th} block of constant loading in a loading sequence

N_1	Number of blows required to crack initiation
N_2	Number of blows required for failure level
n_p	Number of holes in perfobond rib
P	Applied load at any point
P_u	Maximum applied load
P_1	Unique load point in bilinear idealization
$P_{concrete}$	Strength of concrete elements
P_{design}	Value of applied load at design limit
$P_{\max.}$	Peak load obtained for headed stud connector in cyclic loading
$P_{serviceability}$	Value of applied load at serviceability limit
P_{shear}	Shear strength of connection
$\left(P_{shear}\right)_{required}$	Minimum of ultimate strength of concrete and steel elements
$p(s)$	Applied load as function of slip
$p'(s)$	Load in bilinear idealisation as function of slip
P_{steel}	Strength of steel element
$P_{u,N}$	Reduced static load of headed stud connector after N number of cycles
$P_{u,o}$	Load capacity of headed stud connector
ΔP	Range of cyclic loading
Q	Shear strength of connector at any load level
Q_u	Maximum resistance/ultimate strength of a connector
ΔQ_u	Change in resistance/strength of a connector
r_y	First order plastic zone size under plane stress conditions
s	Relative slip (induced at steel-concrete interface)
s_u	Ultimate slip
s_y	Relative slip at the load level of s_y
s_1	Relative slip at the load level of P_1
s_{design}	Relative slip in connection at design limit
$s_{serviceability}$	Relative slip in connection at serviceability limit
$S_{\max.}$	Maximum Shear stress
$S_{\min.}$	Minimum shear stress
S_r	Range of shear stress $\left(S_{\max.}-S_{\min.}\right)$
t_a	Thickness of adhesive layer
t_{ad}	Thickness of the adherend
t_{fc}	Flange thickness of the channel shear connector

t_{pc}	Thickness of perfobond rib connector
t_{wc}	Web thickness of the channel shear connector
T_g	Glass Transition Temperature
u_c	Change in length of concrete element
u_s	Change in length of steel element
w_d	Width of the rib of metal deck in profiled sheet
w_{fc}	Flange width of the channel shear connector
$\tan\delta$	Damping factor
ε_1	Longitudinal strain *0.00005*
ε_2	Longitudinal strain at load level of *40%* of the ultimate load
ε_c	Strain in concrete in compression
$\varepsilon_c^{'}$	Strain in concrete at stress level of $\sigma_c^{'}$
ε_t	Strain in concrete in tension
$\varepsilon_t^{'}$	Strain in concrete at stress level of $\sigma_{tt}^{'}$
ε_{lc}	Longitudinal strain in concrete element at connected interface
ε_{ls}	Longitudinal strain in steel section at connected interface
ε_{cc}	Strain in concrete
ε_{to}	Maximum strain in concrete in tension
η	Degree of shear connection
γ_m	Material parameter (concrete)
γ_v	Partial safety factor for headed stud connector for connection design
τ_v	Shear stress
τ_{avg}	Average shear stress
σ_m	Hydrostatic stress in adhesive
σ_1, σ_2 and σ_3	Normal stresses in three orthogonal directions
σ_{ae}	Effective stress induced in the adhesive
σ_{ao}	Yield stress of the adhesive
σ_{as}	Shear stress in adhesive
σ_{cc}	Compressive stress in concrete
$\sigma_{cc}^{'}$	Compressive stress in concrete at any load level
σ_{ct}	Tensile stress in concrete
$\sigma_{ct}^{'}$	Tensile stress in concrete at any load level
σ_{ya}	Uniaxial yield strength of the adhesive
σ_{c1}	Stress corresponding to longitudinal strain *0.00005*

σ_{c2}	Stress corresponding to load level of *40%* of the ultimate load
$\sigma_{y\,ad}$	Uniaxial yield strength of the adherend
$\delta_{composite}$	Deflection in composite beam
$\delta_{non-composite}$	Deflection in non-composite beam
$\delta_{\max}$	Maximum deflection in composite beam
β	Angle of internal friction
ψ	Dilation angle
μ	Sensitivity of yielding of adhesive material
λ	Ratio of yield stress (uniaxial compression to uniaxial tension)

Chapter: 1

Introduction

1.1 Overview

The adeptness of composite member depends on the integrity and effectiveness of the connection. The combining ability of the connection at the connecting interface, is an essential and critical factor for homogeneity of a composite member. The degree of the connection determines its strength and also the efficiency of the transfer of forces at the composite interface, from one element to another. However, the effectiveness of the composite connection in terms of deformability and engendered relative slip, at the composite interface, determines the degree of interaction. The connection performance also depends on the connection material employed, connecting materials, and the function of a composite member in the structure.

1.2 Composite Member

1.2.1 General

An engineering combination of two and more elements, of different materials, acting as a single unit, is known as a composite member. Such members utilise the positive attributes of structural properties, and improve the shortcoming of each element (Hollaway 2003). These composite members are superior to the conventional members owing to their high strength, low weight, enhanced toughness, improved impact resistance, part consolidation, higher design flexibility, better sound damping, high insulating properties, higher durability, and enhanced corrosion resistance (Karbhari and Zhao 2000; Mette et al. 2016; Mottram and Zheng 1996). These properties render them suitable for various fields of engineering applications, for instance, aerospace, automotive, construction, marine and wind (Hollaway 2003; Mays and Hutchinson 2005; Täljsten 2006).

The use of conventional composites for construction of structures dates back to 1500 B.C., when early Egyptian and Mesopotamian settlers used a mixture of

mud and straw to create strong and durable dwellings. Straw has been widely used to provide reinforcement to ancient composites, including pottery and boats.

Composite members with steel and concrete elements are used for construction of structures since late 19th century. The first use of steel-concrete composite members is marked in the year 1884, when concrete encased beams were used in a bridge at *Iowa* state, and a building at *Pittsburgh*. Laboratory tests on steel-concrete composite columns were first performed at *Columbia University* in 1908, while a composite beam was first tested at the *Dominion Bridge Works* in *Canada*, in 1922. Metal decks were employed, for the first time, in early 1950s. In 1951, a partial interaction theory was proposed by a team of researchers from the *University of Illinois*. Welded studs were first tested at the *University of Illinois* in 1954; a design formula based on the strength of studs was proposed in the year 1956. Through deck stud welding was first used in the *Federal Court House* building at *Brooklyn*, in 1960 (Johnson 2008; Nethercot 2003; Ollgaard et al. 1971).

1.2.2 Steel-Concrete Composite

Steel-concrete composite members in construction of buildings and bridges are gaining rapid recognition owing to their superiority over non-composite and reinforced cement concrete (RCC) members. Some of their advantages include, a higher strength to weight ratio, greater flexural strength and stiffness, speedier and more flexible construction, ease of retrofitting and repair, higher durability and better aesthetics (Bouazaoui et al. 2007; Ellobody 2014; Gara et al. 2010; Souici et al. 2013; Yu-Hang et al. 2014). An effective and efficient utilisation of concrete in compression zone and steel in a tension zone in a composite member makes it economic, viable and more popular as compared to a conventional or non-composite member (Deric and Bradford 1995; Subedi and Coyle 2002).

1.3 Connection between Steel and Concrete

1.3.1 General

The connection at the interface of steel and concrete elements is the key factor in achieving the desired performance. The connection formed at the interface of steel and concrete elements must be able to effectively resist and transfer the

stresses/forces between the steel and concrete elements, with adequate rigidity (Colajanni et al. 2014; He et al. 2013; Lam and El-Lobody 2005). The performance of interfacial connection depends on the type of loading over composite member. The type of composite member (composite slab, composite beam, composite column) and its position in a structural system determines the predominant load type (flexural, shear, tensile, cyclic, impact, fire etc.) (Clouston et al. 2005; Gattesco et al. 1997; Shanmugam and Lakshmi 2001; Taranath 2016).

The feasibility of a composite section lies in the effective transfer of forces between the steel and concrete elements. A conventional steel-concrete composite beam, when subjected to transverse gravity loads, tends to deflect in the direction of load because of which relative slip at the interface of the steel and concrete is observed. The connection at the interface unites steel and concrete, thereby reducing the interfacial slip and deflection, as shown in *Fig. 1-1*.

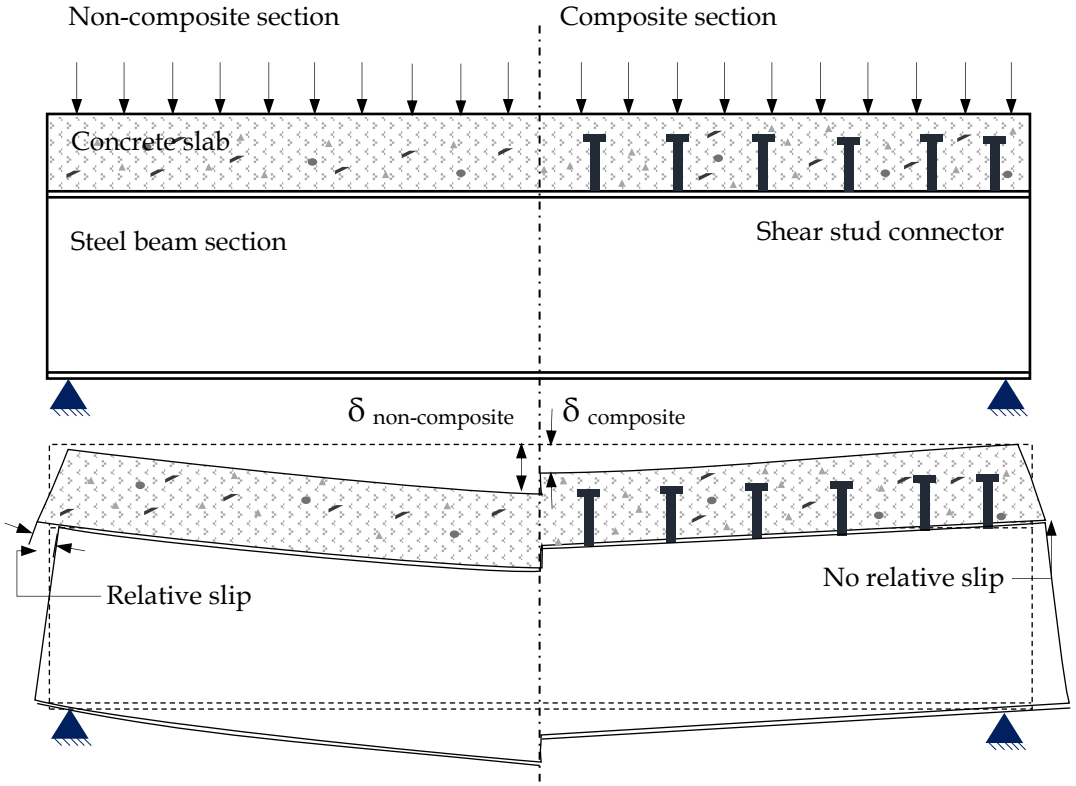

Fig. 1-1: Comparative behaviour of non-composite and composite section in terms of relative slip and deflection

1.3.2 Classification of Connections

The composite action between steel and concrete is controlled by the behaviour of connection, connection material used, and the function of composite member. Interfacial connections are characterised by the degree of shear connection and the degree of interaction.

1.3.2.1 Based on Member Function

The role of the composite member categorically depends on the desired function of that member in a particular structural system. On the basis of its function, a structural member can be classified as column, beam or floor.

Concrete encased steel sections and concrete filled steel tubes are the most common forms of steel-concrete composite columns. The advantages of these columns are better corrosion protection, enhanced fire resistance, increased strength and stiffness, reduced slenderness and increased buckling resistance (El-Tawil and Deierlein 1999; Han et al. 2014; Wang et al. 2004).

Composite beams, with cast in-situ or pre-cast concrete slabs laid over steel sections, are preferred for the construction of bridges. They facilitate a comparatively easier and faster construction, along with providing an increased efficiency in design, and improved riding comfort due to joint elimination (Brozzetti 2000; Nakamura et al. 2002).

Steel-concrete composite floor system, consisting of steel sheets below concrete slabs, are becoming popular choice for the construction of buildings. Apart from various structural advantages, such systems eliminate the need of shuttering, propping and false-work during the casting phase (Chen 2003; Lloyd and Wright 1990; Sadek et al. 2008; Wright et al. 1987).

Fig. 1-2 shows a cross-sectional view of some typical steel-concrete composite elements. *Fig. 1-2(a)* shows a concrete filled steel column section and partial concrete encased column section, while *Fig. 1-2(b)* depicts a typical solid RCC slab steel beam connected with mechanical shear studs. *Fig. 1-2(c)* shows a steel-concrete composite floor system having trapezoidal profile ribs parallel to

steel beam and *Fig. 1-2(d)* shows a steel-concrete composite connection having steel column connected with steel-concrete composite floor system.

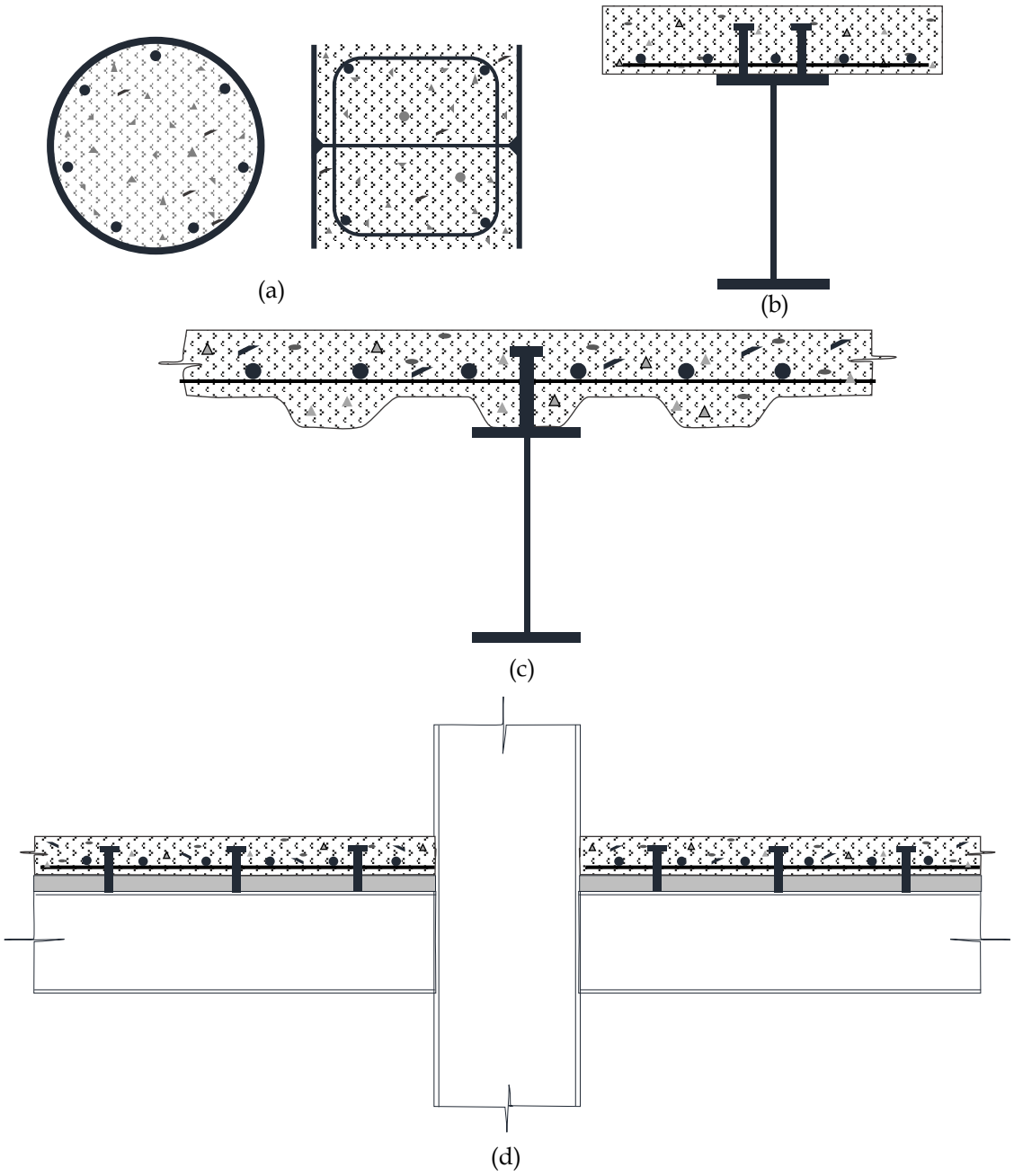

Fig. 1-2: Different steel-concrete composite system; (a) concrete filled and concrete encased column section, (b) steel-concrete composite beam, (c) steel-concrete composite floor system and (d) composite column-beam connection

1.3.2.2 Based on the Degree of Connection

The strength of connection at the interface with respect to the connected steel and concrete elements, defines the degree of connection in steel-concrete composite members. The degree of connection signifies the equilibrium of forces between the

components of a composite section. It depends upon the strength of the connection and also on the strength of steel and concrete elements. The degree of connection is defined as the ratio of strength of connection to the strength of individual (either steel or concrete) element. It is denoted by η and is expressed as

$$\eta = \frac{P_{shear}}{(P_{shear})_{required}} \qquad (1-1)$$

where, P_{shear} is the shear strength of connection and $(P_{shear})_{required}$ is the minimum of ultimate strengths of concrete and steel elements. Based on the degree of shear connection, connections are classified as either partial or full degree of connection.

Consider that the strength of steel element is (P_{steel}) and the strength of concrete section is $(P_{concrete})$, while shear strength of connection is (P_{shear}). A full degree of shear connection is attained when the connection between steel and concrete is such that the steel section is entirely in tension, while concrete section is under partial compression, i.e. $P_{concrete} > P_{steel}$, and the strength of connection is higher than that of steel $(P_{shear} \geq P_{steel})$. The neutral axis of such a section lies within the concrete element. Similarly, a full shear connection is also attained when the whole concrete section is in compression, while the steel section is under partial compression and tension, i.e. $P_{steel} > P_{concrete}$ and the strength of connection is higher than that of concrete $(P_{shear} \geq P_{concrete})$. The neutral axis of such composite sections lies within the steel element.

On the other hand, partial shear connections are attained when the ultimate strength of connection is lower than the ultimate strengths of both concrete and steel sections $(P_{concrete} > P_{shear}; P_{steel} > P_{shear})$. In such cases, both the steel and concrete sections are under partial tension and compression. Unlike full shear connections, partial connections have two neutral axes in the same section, one in concrete and the other in steel element. *Fig. 1-3* shows a schematic view of the three conditions of stress and strain distribution; two having full shear connection (*(a)* and *(b)*), and one *(c)*, having partial shear connection for the steel-concrete composite beam connected using headed studs.

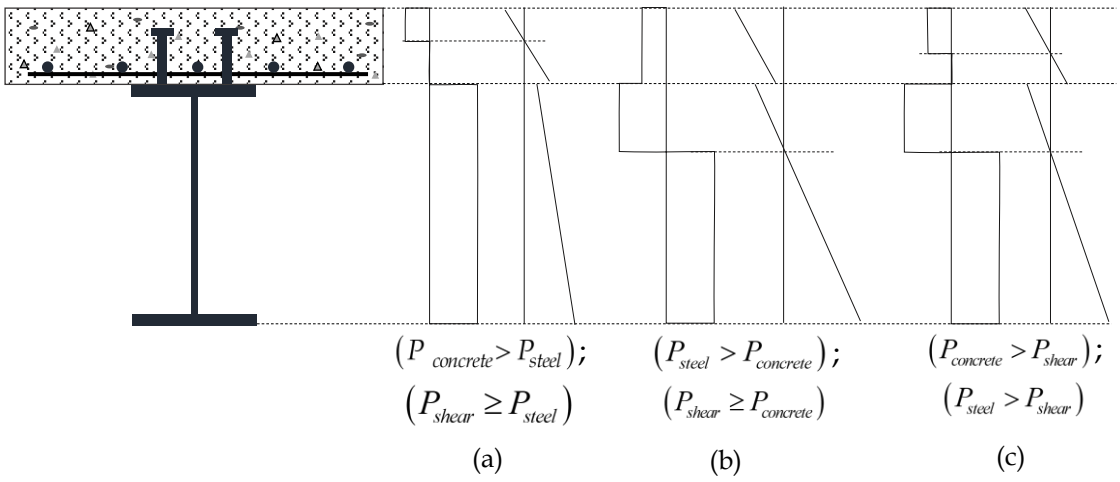

Fig. 1-3: Stress and strain distribution in a steel-concrete composite cross-section having; (a) and (b) with full shear connection and (c) with partial shear connection condition

1.3.2.3 Based on the Degree of Interaction

The degree of interaction is defined by the relative slip at the interface of steel and concrete elements of a composite member. The degree of interaction depends on the mode and extent of the deformation of connection, and the stiffness of connecting material. On the basis of the engendered slip at an interface, the degree of interaction can be classified as no interaction, partial interaction and full interaction. The interaction phenomena at steel-concrete composite section interface have been shown in *Fig. 1-4*.

When transverse gravity load is applied to conventional steel-concrete composite member, it undergoes flexural deformation. This leads to a contraction/elongation of concrete and steel elements due to compression/tension. This results in relative sliding of the concrete and steel at the interface, and is commonly termed as relative slip denoted by *s*, and expressed as,

$$s = (L + u_c) - (L + u_s) \qquad (1-2)$$

where, *L* is total length of the longitudinal span, while u_c and u_s represent the total change in length of the concrete and steel elements, respectively. The value of u_c and u_s may be obtained using equation (*1-3*) and (*1-4*),

$$u_c = \int_0^L \varepsilon_{lc} dx \qquad (1-3)$$

$$u_s = \int_0^L \varepsilon_{ls} dx \qquad (1-4)$$

where, ε_{lc} is the longitudinal strain in concrete element at connected interface and ε_{ls} is the longitudinal strain in steel section at the connected interface. Thus, the relative slip is

$$s = u_c - u_s = \int_0^L \varepsilon_{lc} dx - \int_0^L \varepsilon_{ls} dx \qquad (1-5)$$

The sudden change in strain at the connected interface of concrete and steel elements is known as slip strain. It can be derived by differentiating equation (*1-5*) as shown below.

$$\frac{ds}{dx} = \varepsilon_{lc} - \varepsilon_{ls} \qquad (1-6)$$

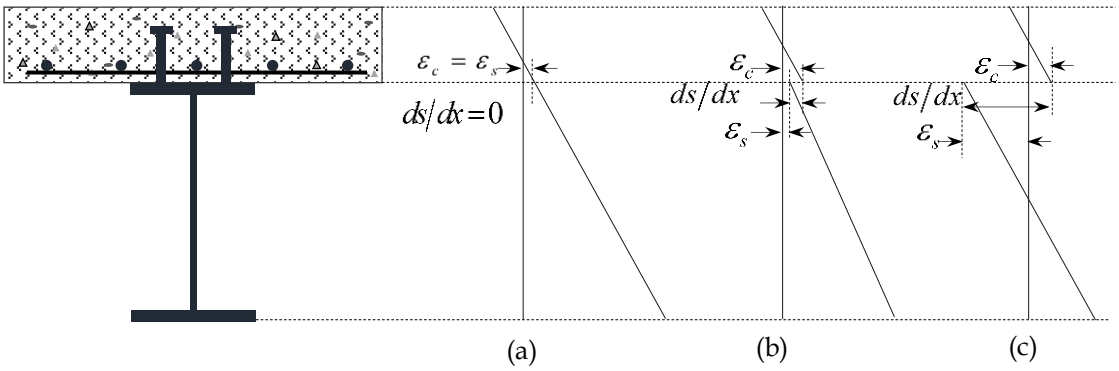

Fig. 1-4: Strain variation in a steel-concrete composite cross-section; (a) full interaction condition, (b) partial interaction condition and (c) no interaction condition

When there is no connection between the two elements of a composite member, no interaction between the two occurs (shown in *Fig. 1-4(c)*). This phenomenon is characterised by free slipping of two elements over each other, whilst maintaining the same curvature. Such connections are not recommended because the composite action is not achieved owing to no transfer of stresses/forces between the elements. The interfacial slip and slip strain (ds/dx) are maximum in this case.

On the other hand, when the interfaces are connected in a way that the interfacial slip (s) and slip strain (ds/dx) are zero, a full interaction at the interface is achieved, and the concrete and steel elements act as a single composite unit (shown in *Fig. 1-4(a)*).

All the other intermediate levels of interaction between no and full interaction, are called partial interaction conditions. The partial interaction condition have been shown in *Fig. 1-4(b)*.

1.3.2.4 Based on Connection Material

On the basis of connecting material, steel-concrete composite connections can broadly be classified under two heads, namely, mechanically connected and adhesive bonded (Bouazaoui et al. 2007; Larbi et al. 2007; Mays and Hutchinson 2005; Oehlers 1989; Selden et al. 2015; Souici et al. 2013). Mechanical connectors can be further classified into many types, a few of which are headed shear stud, demountable shear stud, angle, channel, T-shaped, perfobond and T-perfobond (Nie et al. 2014; Shariati et al. 2012; Shariati et al. 2016). Contrarily, adhesive bonded connections are formed by polymeric chains of various compounds such as epoxy resin, polyurethane and acrylic groups. Typical mechanically connected (*Fig. 1-5(a)*) and adhesive bonded (*Fig. 1-5(b)*) steel-concrete composite cross-sections have been shown.

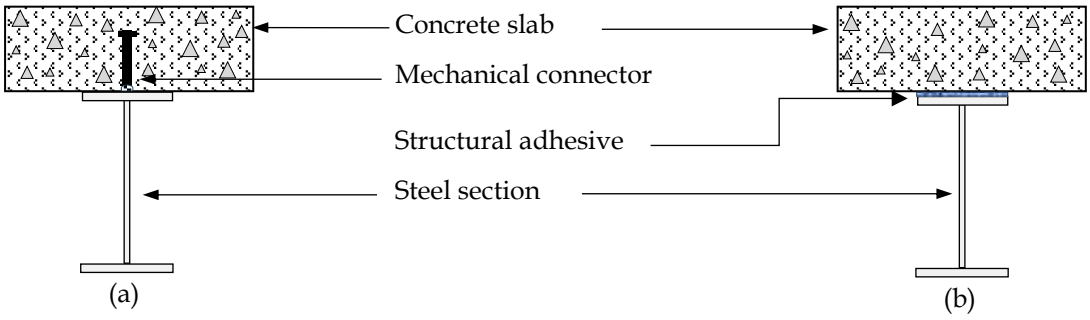

Fig. 1-5: Steel-concrete composite cross-section; (a) mechanical stud connected composite member and (b) adhesive bonded composite member

1.3.3 Characterization of Connections

Since the inception of steel-concrete composite member, the connection between steel and concrete has been critically analysed. As the performance of composite

member primarily depends on the behaviour of these connections, a need for characterisation of connections has been addressed by various researchers (Lukaszewska et al. 2008; O'Neill 2009; Oehlers and Bradford 1999). Initially, the connections between connecting surfaces were achieved through mechanical headed stud connectors, the design of which was first presented in American Institute of Steel Construction (AISC) specifications in the year 1961 (Ollgaard et al. 1971; Slutter and Driscoll Jr 1963). Improvements and design modifications have been presented in the design of such connections by various researcher and design codes. The connections between concrete and steel elements have been achieved through channel, angle, double angles, perfobond, T-perfobond, etc. These connections are supposed to be relatively more rigid than the connections with mechanical headed shear studs (Manfredi et al. 1999).

With the application of structural adhesives for composite connections between structural elements, a new era of such composite members has been initiated. These connections were deemed superior to the conventional mechanical shear studs, and thus, gained rapid recognition. Owing to their significantly larger connected area, the adhesive bonded connection offer greater shear strength with uniform stress transfer, but had exhibited limited ductility (rigid connection). This has led to a whole new domain of research, on the suitability of connections types, on the basis of application of the members and their functions.

A composite connection is generally characterised on the basis of its load-slip behaviour, provided that the connected elements do not yield. The initial slope of load-slip curve of any composite member provides a significant insight into the stiffness of connection. A typical schematic representation of load-slip behaviour of connections has been shown in *Fig. 1-6*. The adhesive bonded composite connections exhibit the highest degree of rigidity with brittleness, owing to a uniform stress distribution among the connected elements. However, the connections with channels, angles and T-perfobonds show lower stiffness than adhesive bonded, and higher stiffness than mechanical headed shear stud.

Connections with studs are the most flexible type of composite connections, and offer the highest ductility.

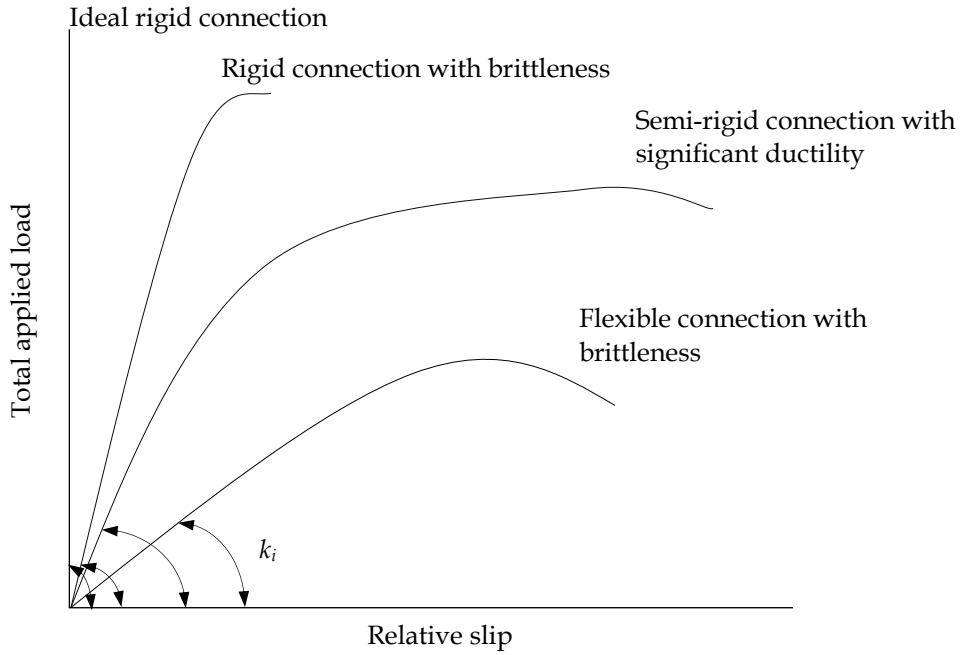

Fig. 1-6: Applied load-relative slip curve of steel-concrete composite connections having unlike behaviour

1.4 Organisation of the Thesis

This thesis document consists of *eight* relatively independent chapters. The *first chapter* presents a brief introduction to composite members and their behaviour. *Chapter two* presents a comprehensive study of pertinent literature, with a critical analysis of the state of the art. The *chapter* also points out the gaps in the area of steel-concrete composite connections and concludes with an elaborated scope of the work.

Chapter three outlines the mechanical and physical properties of materials used in the experimental investigation along with a detailed description of the experimental methodology and test setup. It also presents a numerical modelling procedure for the validation of experimental study carried out.

In *chapter four*, the behaviour of mechanically connected and adhesive bonded steel-concrete composite connections has been extensively discussed under monotonic and impact loading.

The behaviour of headed stud shear connectors has been discussed in detail in *chapter five*. The variation in the behaviour of headed stud connections, due to

variation in strength of concrete, change in distribution of confining reinforcement and change in density of reinforcement has been critically evaluated. The load-slip behaviour has also been taken into consideration in the light of the pre-and post-yield stiffness of connections.

In *chapter six*, the behaviour of adhesive bonded connections with variation in thickness of adhesive layer has been discussed, in detail. The load-slip behaviour of connections has been validated through the finite element analysis software *ABAQUS*.

Chapter seven presents a comparison between the performance of headed studs connected and adhesive bonded composite connections. The effect of staggering of headed studs has been studied through flexural testing of full scale composite beams with in-line and staggering effect.

Chapter eight presents the conclusions drawn from the present study. This chapter concludes with a brief summary of the present work and the scope for future research.

Chapter: 2

Literature Review

2.1 Overview

The performance of steel-concrete composite members is greatly influenced by the connection between the steel and concrete elements. Such connections are primarily characterised by their load-slip behaviours (*Fig. 2-1*). The initial/linear part of the load-slip curve represents the initial/elastic stiffness of the connections, while, the non-linear part depicts the post-yield behaviour of connections. On the basis of the slope of initial (linear) part of the curve, a connection can be classified as flexible, semi-rigid or rigid connection. Similarly, on the basis of post-yield behaviour, a connection can be categorized as ductile or brittle. The connection classification thus determines the suitability of a type of connection, depending upon the expected performance and function of member.

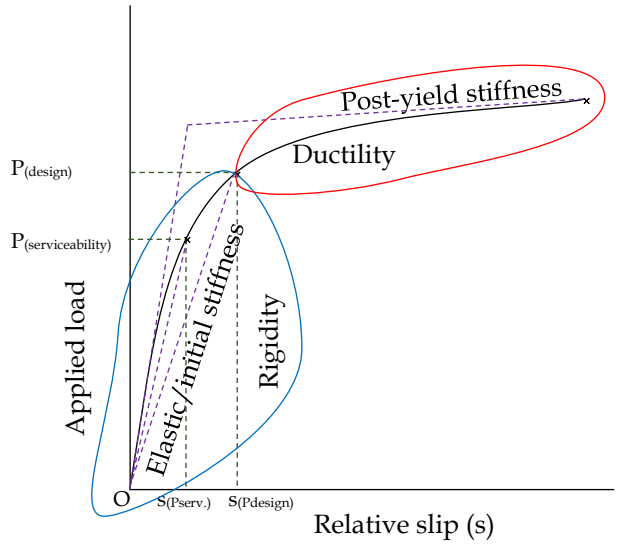

Fig. 2-1: Typical load-slip behaviour of composite connection

The ability of a steel-concrete composite member to meet the expected functionality objectives requires a justified estimation of the desired characteristics of the connection between elements. The characterisation of connection depends on a wide range of factors, including material used to form the connection, geometry of the connection, physical and mechanical properties of the connection material, connecting method (welding, bolting, adhesion etc.), type of loading on

the composite member, geometry of the composite member and location of member.

2.2 Development in Steel-Concrete Composite Member

The demand for affordable, low cost structures (Höök and Stehn 2008; Hui 2001; Teo et al. 2007), and economic repair and rehabilitation of deteriorating structures (Crasto et al. 2001; Tavakkolizadeh and Saadatmanesh 2003) along with strengthening and retrofitting of structure owing to enhanced functionality (Galambos 2000), exposed the frontier of composite construction. Efficiency of steel-concrete composite members is a function of the effectiveness of the interfacial connection, in terms of applied load, stiffness of member, mechanism of force transfer, durability of connection, etc. (Karayannis et al. 1998; Miller et al. 2001). The advancements in existing methods of interfacial connections and development of the new composite connections is an active field of research.

During the years of inception of composite construction, the transfer of shear force between the two connected elements of a composite member was achieved through mechanical shear connector (Badoux 1965; Roediger 1951; Viest 1951). Such early mechanical connectors were classified either as flexible (rolled channel connector, channel without top flange, Bent Z-plate, straight plate) or rigid connections (channel section, angle section and Tee-section), on the basis of their load-slip behaviour (Siess et al. 1952; Viest et al. 1952). Nevertheless, it was observed by the researchers that, apart from load-slip behaviour, the selection of a particular connection strategy (type) depends on several other factors such as uplift resistance, confinement, etc. It was observed that the behaviour of rigid mechanical connectors is determined by the effective bearing area of the connectors, while, for flexible mechanical connectors, the geometry of connectors is the key parameter (Siess and Viest 1952; Viest et al. 1952).

With the establishment of channel shear connectors as an effective connection strategy between the two elements of a composite member, a new domain of research and development began (Siess et al. 1952). It was observed that, irrespective of the mechanical properties of channel connectors, the flexibility of such connections was significant. Although, a certain amount of flexibility is

desirable for composite connections, the high flexibility induces large slip, and thereby decreases the degree of interaction. This led to numerous studies to; *a)* further investigate the behaviour and characteristics of channel connectors, and *b)* development of alternate connection strategies.

The observed high flexibility of hot rolled channel connectors, albeit offering high bearing area, characterised such connections as flexible, and not rigid (Viest et al. 1952). This led to almost simultaneous development of stud connectors, which were observed to be a superior alternative to channel shear connectors (Viest 1956). The first systematic elastic design procedure for shear connector was prescribed in the year 1957 by American Association of Highway officials (AASHO) (Culver and Coston 1961; Slutter and Driscoll Jr 1963). The preliminary studies on the behaviour of round stud connectors underscored their various advantages, such as, economy, simplicity in design, ease of installation, etc. (Culver and Coston 1961; Thurlimann 1958; Thurlimann 1959). Stud connectors, owing to their superior performance, gained rapid recognition in steel-concrete composite construction. With their increased popularity, the need to better understand the behaviour of such connections was addressed through push-out tests and full scale beam tests (Badoux 1965; Stallmeyer et al. 1965; Viest 1960).

With the evolution of plastic design concept, and owing to over conservative elastic design procedure, the need to develop a plastic design approach for mechanical connection was felt. The initial plastic design application underlined the high shape factor (1.46 - 1.67) of composite member, as compared to I-section steel beam (1.15) (Barnard and Johnson 1965; Chapman and Balakrishnan 1964; Driscoll Jr and Slutter 1961). Chapman and Balakrishnan (1964) and Yam and Chapman (1968) suggested that the design of composite connections shall be performed by considering only 80% of the connection strength obtained through experiments. It was also reported that the composite members having sufficient number of uniformly distributed studs offer adequate interaction (King et al. 1965; Slutter and Driscoll Jr 1963). Further, the alignment of composite specimens significantly affects the observed behaviour of connection under standard push-out tests (Slutter and Driscoll Jr 1963).

The various possible failure mechanisms in composite beams, i.e. flexural failure in concrete, shear failure in stud/beam and tensile failure in steel, were critically analysed by Toprac (1965), and the role of adequacy of stud shear connectors was discussed. Experimental investigations on composite beams suggested that the distributions of shear studs play a crucial role in determining their performance. It was observed that the transfer of shear stress through studs in a composite beam is not uniform throughout the span. The studs at the ends of the beam were observed to be subjected to much higher shear stresses, than the studs around the mid span and below the loaded area. It was therefore recommended that the spacing of the studs shall be varied throughout the span. It was also observed that the fatigue strength of stud connector is critical in determining the capacity of connection. On the basis of this observation, a modified design procedure based on static and fatigue strength of connector was proposed by (Slutter and Fisher 1965).

The ability to accurately estimate the strength of stud connectors along with enhanced design procedures further encouraged full scale experimental studies on single span and multi-span composite beams (Daniels and Fisher 1967; Daniels and Fisher 1968; Slutter and Fisher 1965). Initial studies on continuous composite beams were carried out under static loading and it was observed that the failure is primarily located around the mid support (Daniels and Fisher 1967). However, when subjected to moving loads, the continuous composite beams exhibited lesser ductility (Daniels and Fisher 1967). It was also observed that with the uniformly distributed studs across the beam length, inelastic shear deformation occurs in the shorter span. In another study, it was recommended that, under fatigue loading the number of stud shear connectors in a beam shall be decided on the basis of amount of longitudinal reinforcement provided in hogging region (Daniels and Fisher 1968). Nonetheless, the total strength of connectors in the hogging region shall not be less than that of the connector in sagging region (Fisher et al. 1972).

With the development of plastic design approach, the ultimate flexural capacity of a composite beam could be fairly estimated, thereby facilitating the horizontal shear force, which was supposed to be resisted through shear stud

connectors (Daniels and Fisher 1968). The contribution of transverse reinforcement on the behaviour of steel-concrete composite beams was first studied by El-Ghazzi (1972) and the contribution was found to be significant. The effect of geometrical properties of steel beams also plays a critical role in determining the strength of composite beams. It was reported that the thickness of top flange of steel section is more critical as compared to that of the bottom flange (Daniels and Fisher 1967; Daniels and Fisher 1968; El-Ghazzi 1972).

The behaviour of composite beams having pre-stressed concrete slab, under static loading was analysed by Sarnes Jr (1975). It was observed that the provision of pre-stressed concrete slab in hogging region reduced the cracking. Similar behaviour was observed in composite sections having regular concrete slabs with additional longitudinal reinforcement (Hamada and Longworth 1973). The presence of adequate longitudinal reinforcement in hogging region significantly affects the failure mode of composite section, and also reduces local buckling in steel flange.

The interaction, relative slip and uplift, at the interface of steel and concrete are governed by the shear strength of connectors. The partial interaction theory, for simply supported beam subjected to point load, was proposed by Newmark et al. (1951), with various assumptions. The experimental investigations conducted by Stras (1964) suggested that the interaction between steel beam and pre-stressed concrete slab is a critical parameter, and influences the deflection profile.

Taylor and Matlock (1968) developed a finite element method to estimate the degree of interaction at the connected interface. The authors concluded that the stiffness, strength and deflection of composite beam depends on the degree of interaction. It was also concluded that the degree of shear connection is governed by the amount, location, stiffness and strength of the connection. The unequal strains at the interface of steel and concrete leads to partial interaction between the two elements, thereby causing unequal deflections (Adekola 1968). The effect of shear lag phenomenon on degree of interaction was studied by Adekola (1974). It was observed that effective width is directly proportional to the degree of interaction, while, the deflection of composite beam varies inversely with the

degree of interaction. However, these relationships are valid only up to a certain limit.

The development of interaction theory, along with establishment of proper design guidelines (ACI 318 1977; AISC-ANSI 360 1978; BS 5400-5 1978; Pang 1979) for steel-concrete composite members, underlined the dependence of behaviour of such members on numerous factors, such as, design methodology, desired ductility, force transfer mechanism, materials used and function of the member. This encouraged various analytical as well as experimental studies (Daniels et al. 1993; Dorton et al. 1977; Mays and Vardy 1982; Van Gemert 1980), to gain insight upon the performance of composite members.

2.3 Shear Connectors

The various commonly available shear connectors for steel-concrete composite connections, along with their development and design, are discussed in this section. Shear connectors find their use not only as efficient connecting links between the elements, but also as an effective strengthening agent at the composite interface. The connectors such as, channel, headed stud, L-shape, T-shape, demountable, perfobond, T-perfobond, cristbond, Y-shape, J-shape, and structural adhesive are discussed in detail.

2.3.1 Channel Shear Connector

Channel shear connectors are the earliest flexible type shear connectors for steel-concrete composite (Siess et al. 1952; Viest 1951; Viest et al. 1952). The ease of availability and flexibility in design has made them a preferred choice over other contemporary connectors (spiral, angle etc.). Initial experimental studies, on different form of channel shear connectors suggested that the strength of connections primarily depends on the geometry of channel sections used and the strength of concrete slab (Siess et al. 1952; Viest et al. 1952). The flange thickness of channel connectors determines the location and mode of failure, while, the web thickness affects the ultimate strength of composite connection, although marginally. Literature also suggest that the connection strength varies linearly with the flange width of channel connectors (Hosain and Pashan 2006; Maleki and

Bagheri 2008b; Viest et al. 1952), while, the orientation and height of channel connector has marginal or no contribution on strength of connection (Slutter and Fisher 1966). The typical geometry of channel shear connector welded over steel I-section has been shown in *Fig. 2-2*.

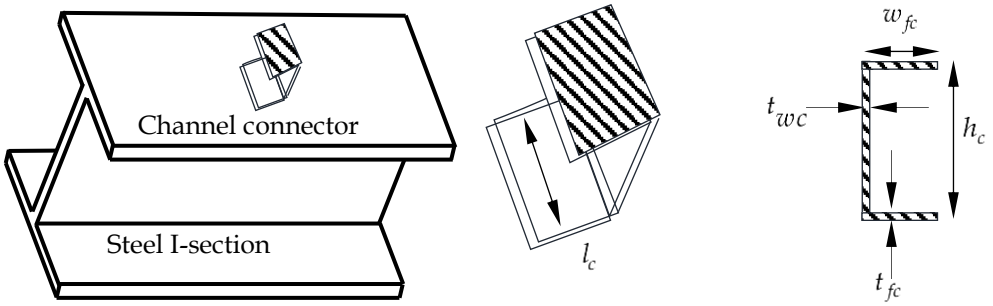

Fig. 2-2: Chanel shear connector welded over steel-section and typical geometric details

Further experimental studies on composite as well as non-composite steel-concrete continuous beams were conducted by Siess and Viest (1952). The effect of absence of connectors in the negative moment (hogging) region of the composite beams was also studied. It was observed that the elimination of connectors in negative moment region has no effect on the stresses induced in concrete slab. However, the beams having no shear connectors in the hogging region were found to have almost half the degree of interaction when compared to those having shear connectors in hogging region. Slutter and Fisher (1966) examined the fatigue behaviour of channel shear connectors in push out test specimens and observed that the failure initiates at the transverse fillet weld in the channel connectors. This is primarily attributed to the concentration of stresses at the bottom flange of the connectors, which is responsible for transfer of stresses, while, the remaining part of the connectors ensures fixity. It was also suggested that the thickness of weld of the bottom flange of connectors shall not be more than the flange thickness to prevent the failure of web of the connectors.

An empirical relation to predict the ultimate strength of channel shear connector Q_u (kip) was proposed by Slutter and Fisher (1966), as

$$Q_u = 550\left(t_{fc} + 0.5t_{wc}\right) l_c \sqrt{f_c'} \qquad (2-1)$$

where, t_{fc} is the flange thickness of channel (inches), t_{wc} is the web thickness (inches), l_c is the length of channel connector in the transverse direction of the flange of I-beam (inches) and $f_c^{'}$ is the compressive strength of concrete cylinder at 28 days in pound.

The current AISC-ANSI 360 (2010) provisions recommends a modified form relation to determine the ultimate strength Q_u (kN) of hot-rolled channel anchors embedded in solid slab of normal strength concrete, as

$$Q_u = 0.3\left(t_{fc} + 0.5t_{wc}\right) l_c \sqrt{f_c^{'} E_c} \qquad (2-2)$$

where, E_c is the modulus of elasticity of concrete in MPa.

A comprehensive study on the application of channel shear connectors on profiled concrete slabs in steel-concrete composites was carried out by Hosain and Pashan (2006) and Pashan and Hosain (2009). The primary observation, on the basis of experimental evaluation of composite specimens, having solid concrete slab as well as concrete slab with metal profile sheets, was that the connection strength in case of composite specimen with solid slab was higher. The difference in strength was of the order of about 33% for 150 mm high connectors and of 12% for 50 mm high channel connector. Another observation was that the prevalent design estimation, using equation (2-2), was very conservative. A modified empirical relation for estimation of ultimate strength of channel connector Q_u (kN) for solid concrete slab was thus proposed by Pashan and Hosain (2009), which is,

$$Q_u = \left(336\left(t_{wc}\right)^2 + 5.24 l_c h_c\right)\sqrt{f_c^{'}} \qquad (2-3)$$

where, h_c is the height of channel connector in mm. Also, the ultimate strength of embedded channel connector in ribbed metal deck composite slab Q_u (kN) is given as,

$$Q_u = \left(1.7 l_c h_c \frac{w_d}{h_d} + 275.4\left(t_w\right)^2\right)\sqrt{f_c^{'}} \qquad (2-4)$$

where, $\left(w_d / h_d\right)$ is the width to depth ratio of the rib in metal prefilled sheet (unit less).

An experimental study to determine the reverse cyclic behaviour of composite specimen connected using single channel connector was conducted by Maleki and Bagheri (2008a). It was observed that under reversed cyclic loading, the strength of connection undergoes a reduction of 10 to 23%, at a lower load intensity than the ultimate monotonic load. The specimens were observed to undergo failure in less than two cycles of 90% of the ultimate monotonic load capacity. However, no variation in the mode of failure was observed with change on loading type (monotonic and reverse cyclic). A parametric finite element study on the behaviour of connections with single channel shear connector was conducted by Maleki and Bagheri (2008b). The results of the study suggested that the strength as well as the stiffness of the connection reduces by approximately 16% when the orientation of channel connector is such that the flange toe is first to encounter the load. The observed behaviour was attributed to the concentration of stresses at the toe tip of channel flange, which led to the cracking of concrete in the vicinity of the toe. This observation was however contradictory to the established belief that the channel orientation has no effect on the ultimate strength of the connection (Slutter and Fisher 1966).

The effect of confinement of concrete on ultimate strength and ductility of composite connections with channel shear connectors was studied by Maleki and Mahoutian (2009). It was reported that in case of unconfined concrete the strength of connection is primarily governed by the grade of concrete only, leading to brittle failure of connection. However, the confinement of concrete, using stirrups enhances the strength and ductility of connections significantly.

Another set of experimental studies to examine the effect of orientation of specimens and height of channel connectors, on connections with single connector as well as a group of connectors were carried out by Baran and Topkaya (2012). The results suggest that the strength of connection in horizontal orientation is significantly higher than that in vertical orientation. It was also observed that the strength of connection changes with change in the height of connector, while, the stiffness remains unaffected. The ultimate strength of the connection with a single channel connector was also observed to be lesser than that of connections with a

group of connectors. The flexural behaviour of composite beam with channel shear connectors was studied by Baran and Topkaya (2014). The influence of degree of interaction on the strength and stiffness of connections was also observed. The authors concluded that when compared to beams with full degree of interaction, the beams with lower degrees of interaction (having two channel connectors in the whole span) has only 88% of the moment capacity and 71% of the maximum stiffness; while, the corresponding steel beam exhibited only 63% of moment capacity and 39% stiffness.

The plethora of research studies, to understand the behaviour of channel shear connectors suggest that these connectors, though effective and efficient, exhibit high deformability, lead to large slip at the connected interface. Also, the design and behaviour of channel shear connectors depends on a wide range of factors including the mechanical and geometrical properties of the channel connector along with the physical and mechanical properties of the connecting elements. These limitations, along with the availability of various forms of channel connectors, such as T-connector (Nie et al. 2014; Rodrigues and Laím 2014), L - shape connector (Soty and Shima 2011; Soty and Shima 2013) and C-shape connector (Alenezi et al. 2015), caused a lack of unequivocal design prescriptions for channel connectors. This gave way to development of alternate mechanical connectors, which had symmetrical geometry and uniform distribution of material, such as headed stud shear connectors.

2.3.2 Headed Stud Shear Connector

The investigations to understand the behaviour of headed stud shear connectors were initiated during the mid 1950s. Initial investigations by Viest (1956) highlighted the superiority of headed stud connectors for steel-concrete composite members. The behaviour of composite members, connected using headed stud connectors, depends up to various factors, including, nature of forces to be resisted, grade of materials of the two elements, geometry and spacing of headed stud connectors, and amount and detailing of the reinforcement in concrete (Chinn 1961; Driscoll Jr and Slutter 1961; Oehlers and Coughlan 1986; Oguejiofor and

Hosain 1994; Oguejiofor and Hosain 1997). The strength of headed stud connector is a function of

$$Q_u = f\left(E_c, E_s, f_c^{'}, f_u, A_{sh}, A_c, A_r\right) \qquad (2\text{-}5)$$

where, Q_u is maximum strength of connector, E_c is elastic modulus of concrete, E_s is elastic modulus of steel, $f_c^{'}$ compressive strength of concrete, f_u ultimate tensile strength of shear connector, A_{sh} is cross section area of stud shear connector, A_c is the bearing area of concrete and A_r is the cross section area of reinforcement (Lam and El-Lobody 2005; Oehlers and Bradford 1999).

The first reported empirical relationship to predict the strength of L bend stud shear connectors having shank diameter of *0.5* inch and height *2.25* inches, was proposed by Thurlimann (1959). The proposed stud connector strength Q_u under working load is given as,

$$Q_u = 120\sqrt{f_c^{'}} \qquad (2-6)$$

where, Q_u is the connector strength in kip and $f_c^{'}$ is the compressive strength of concrete cylinder at *28* days (Psi) and the allowable force in connector under working load is half of the connector strength, estimated using equation (*2-6*).

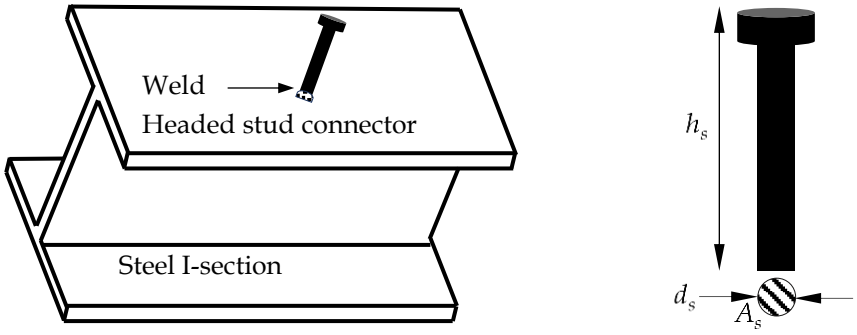

Fig. 2-3: Headed stud shear connector welded over steel-section and typical geometric details

The strength of steel-concrete composite connections, obtained using headed stud (*Fig. 2-3*) connectors under static as well as fatigue loading conditions, was investigated by Slutter and Driscoll Jr (1961). The authors also studied the effect of variation in geometrical properties of headed stud connectors on the performance on composite members, and proposed an empirical relationship to

estimate the strength of connections. Under static loads, the load carrying capacity of unit headed stud connector is given by

$$Q_u = \mathrm{A}_o \left(d_s\right)^2 \sqrt{f_c^{'}} \qquad (2-7)$$

where A_o is 330 and 932 suggested by AASHO (1957) and Slutter and Driscoll Jr (1961) respectively and d_s is the diameter of headed stud connector (inches). While, under fatigue loading, the load carrying capacity of connector is,

$$Q_u = \mathrm{B}_o\, h_s d_s \sqrt{f_c^{'}} \qquad (2-8)$$

Where, B_o is 80 and 222 suggested by AASHO (1957) and Slutter and Driscoll Jr (1961) respectively and h_s is the height of stud connector (inches). However, these relationships are applicable only for concrete strength greater than 20 MPa.

A mathematical relation between the number of cycles and the range of shear stress, to predict the fatigue behaviour of headed stud connectors, was established by Slutter and Fisher (1966) and expressed as

$$\log\left(N\right) = A_o + B_o\, S_r \qquad (2-9)$$

where, N is the number of cycle to failure, A_o and B_o are empirical constants, and have values of 8.072 and 0.1753 respectively. S_r is the range of shear stress calculated as, $\left(S_{\max.} - S_{\min.}\right)$ in ksi.

Later, another experimental investigation on behaviour of headed stud connectors with normal as well as lightweight concrete under push out test was conducted by Ollgaard et al. (1971). The results of push out tests suggested that the ultimate strength of connectors is a function of modulus of elasticity of concrete along with concrete compressive strength and cross-section area of stud connector. The connector load capacity (kips) is expressed as,

$$Q_u = 1.106\, \mathrm{A}_s \left(f_c^{'}\right)^{0.3} \left(E_c\right)^{0.44} \qquad (2-10)$$

where, A_s is the cross-section area of headed stud connector in (inches)^2 , $f_c^{'}$ and E_c are the compressive strength of concrete cylinder and Young's modulus of concrete, respectively. A load-slip relation for continuous loading is obtained as,

$$Q = Q_u \left(1 - e^{-18s}\right)^{2/5} \qquad (2-11)$$

where, Q is the shear strength of connector at any load level (kips), s is the slip engendered at the interface in inches. For multistep loading condition, the shear strength is given by,

$$Q = Q_u\left(\frac{80s}{1+80s}\right) \qquad (2-12)$$

Taplin and Grundy (1997) studied the growth of slip in composite specimen subjected to push out test under unidirectional and reverse cyclic loading and proposed mathematical equation for the same. The proposed equation for reverse cyclic loading is,

$$\log_{10}(\Delta s) = -4.41 + 0.0119\,P_{max.} \qquad (2\text{-}13)$$

and for unidirectional cyclic loading is,

$$\log_{10}\Delta s = -5.29 + 0.0130\,P_{max.} \qquad (2\text{-}14)$$

where, Δs is the slip growth in mm/cycle and $P_{max.}$ is the peak load or maximum load applied per cycle in kN.

Naithani et al. (1988) proposed a modified push-out test method (L-shaped concrete and steel sections connected with vertical edges) for composite specimen with headed stud connectors and conducted an experimental study under fatigue loading. On the basis of experiments, a relationship between number of cycles and the range of shear stress, as under, was proposed

$$\log(N) = A_o + B_o\,S_r \qquad (2-15)$$

where, N is the number of cycles up to failure, A_o and B_o are empirical constants having values of 7.597 and 0.02827 respectively, and S_r is the range of shear stress $(s_{max.} - s_{min.})$ in N/mm^2.

An equation to estimate the load-slip behaviour of normal and high strength concrete, under cyclic loading was proposed by An and Cederwall (1996). The mathematical relationship to estimate the load-slip behaviour for normal strength concrete is given by

$$\left(\frac{P}{P_u}\right) = \frac{2.24(s-0.58)}{1+1.98(s-0.058)} \qquad (2-16)$$

while for high strength concrete, it is,

$$\left(\frac{P}{P_u}\right)=\frac{4.44(s-0.31)}{1+4.2(s-0.032)} \qquad (2-17)$$

where, P and P_u are the loads in kN and s is the relative slip at interface in mm.

The fatigue strength of composite connections with headed stud connectors was analytically evaluated by Hanswille et al. (2007). A mathematical equation to estimate the reduction in strength due to cyclic loading was also proposed. The reduced static strength of connection after (N) number of cycles is,

$$\frac{P_{u,N}}{P_{u,0}}=0.74\left(\frac{P_{\max.}}{P_{u,0}}\right)\left(1-\frac{\Delta P}{P_{\max.}}\right)+0.54-0.04\ ln\left(\frac{\frac{N_i}{1-\frac{P_{\max.}}{P_{u,0}}}}{10^{0.1267-0.1344\frac{P_{\max.}}{P_{u,0}}\left(1-\frac{\Delta P}{2P_{\max.}}\right)}-N_i}\right) \qquad (2-18)$$

where, $P_{u,\mathrm{N}}$ is the reduced static load of stud after N cycles (kN), $P_{u,0}$ is the capacity of stud shear connector (kN), $P_{\max.}$ is the peak of cyclic loading (kN), ΔP is the range of cyclic loading (kN) and N_i number of cycle corresponding to the i^{th} block of constant loading in a loading sequence.

The capacity of mild steel fabricated headed stud connecters under static push out test, based on working stress method, as per IRC 22 (1986) for height to diameter $\left(h_s/d_s\right)$ ratio less than 4.2, is,

$$Q_u=1.49\,h_s\,d_s\sqrt{f_c^{'}} \qquad (2-19)$$

while, for $\left(h_s/d_s\right)$ ratio more than 4.2, is,

$$Q_u=6.08\left(d_s\right)^2\sqrt{f_c^{'}} \qquad (2-20)$$

where, Q_u is the shear resistance of connector (kN), h_s is the height of connector (mm), d_s is the diameter of connector (mm), and $f_c^{'}$ is the characteristic compressive strength of concrete cylinder at 28 days (MPa) or 0.8 f_{ck} is the characteristic compressive strength of concrete cube at 28 days (MPa).

The equations (*2-19*) and (*2-20*) are based on working loads and are valid for studs having an ultimate tensile strength and yield strength less than 460 MPa and 350 MPa, respectively, with an elongation of about 20 percent. In subsequent

revisions of the design specifications IRC 22 (2015)and EC4 (2004), the design approach has been modified to limit state method, to incorporate the uncertainty in material behaviour. The primary modification was to determine the shear strength of the connection on the basis of either headed stud failure equation (*2-21*) or concrete crushing equation (*2-22*). The capacity of the connection design is the lower of two values.

$$Q_u = 0.8\, f_u\, A_s, \qquad \forall f_u < 500 \tag{2-21}$$

$$Q_u = 0.29\,\alpha\,(d_s)^2\left(\sqrt{f_c^{'}\,E_c}\right) \tag{2-22}$$

$$\alpha = 0.2\left(\frac{h_s}{d_s}+1\right) \qquad \forall 3 \le \frac{h_s}{d_s} \le 4$$

$$\alpha = 1 \qquad \forall \frac{h_s}{d_s} \ge 4$$

where, Q_u is the shear resistance of the connector in kN, h_s is the height of connector (mm), d_s is the diameter of connector (mm), and $f_c^{'}$ is the characteristic compressive strength of concrete cylinder at 28 days (MPa) or 0.8 f_{ck} is the characteristic compressive strength of concrete cube at 28 days (MPa), and E_c is the Young's modulus of elasticity of concrete. A partial safety factor γ_v may also be introduced, equal to 1.25 to estimate the design resistance of stud connector.

The equations to estimate the shear strength of composite connections with headed studs have been modified several times with enhancement in understanding of their behaviour. The American design provisions AISC-ANSI 360 (2010) recommends the following equation to estimate the strength of shear connectors embedded in concrete as,

$$Q_u = 0.5\, A_s\left(\sqrt{f_c^{'}\,E_c}\right) \le A_s\, f_u \tag{2-23}$$

where, Q_u is the shear resistance of the connector in kN, A_s is the cross-section area of headed stud connector in $(mm)^2$, $f_c^{'}$ is the characteristic compressive strength of concrete cylinder at 28 days (MPa), E_c is the Young's modulus of elasticity of concrete, and f_u is the tensile strength of headed stud connector (MPa).

The relationship is valid for certain maximum dimensions of the connectors and properties of surrounding concrete. However, the capacity of shear connectors

depends on several other factors than those considered in equation (*2-23*), such as, dimensions of concrete slab, height and diameter of stud, spacing between stud connectors, amount and reinforcement etc. Thus, it is generally recommended that experimental push-out test shall be conducted to correctly estimate the bearing capacity of a particular type of connector.

An analytical finite element study on the effect of temperature variation on steel-concrete composite push out test specimens demonstrated that at temperatures (*-60°C*) below the room temperature (*30°C*) the capacity of connection increases (30% increase) (Noel et al. 2016).

2.3.2.1 Strength and Density of Concrete

The strength of concrete slab is a critical parameter that ensures a desirable performance of a steel-concrete composite member. One of the most commonly observed modes of failure of a composite connection is the crushing of concrete in the region around the headed stud connector. The failure of concrete before the ultimate strength of connectors is developed has been reported widely, throughout the literature. The initial recommendation on the strength of concrete was put forth by Slutter and Driscoll Jr (1961). The authors suggested that the minimum concrete strength required for the development of full connection capacity in steel-concrete composite members is 20 MPa. In another study, the authors Slutter and Driscoll Jr (1963) experimentally confirmed the proposition that the concrete strength below 20 MPa is insufficient for the development of full plastic capacity of connector. It was also reported that in cases, where the concrete slab has strength in access of 20 MPa, the effect of properties of concrete on strength of connections is insignificant. The influence of density of concrete on connector strength under push out test was studied by Ollgaard et al. (1971). It was suggested that the density, and thus modulus of elasticity, of concrete is a critical parameter that governs the strength of connection. The authors recommended an additional factor of $(E_c)^{0.44}$, obtained through detailed regression analysis, to be used while estimating the design strength of connector (equation *2-10*).

The literature suggest that the strength of concrete has a significant influence on connection strength in case of steel-concrete composite connections. Push out tests on steel-concrete composite specimens, connected using headed shear studs, on normal and high strength concrete were conducted by An and Cederwall (1996). It was reported that with an increase in concrete strength (from 30 MPa to 80 MPa), the connection strength increased by about 34%. However, the connection ductility in the negative stiffness region was observed to decrease with an increase in strength of concrete.

The behaviour of profile sheeted composite members, in light of the location of headed studs in the steel slab was experimentally investigated by Easterling et al. (1993), using full scale beams and push out specimens. It was reported that the connection strength depends on the strength of concrete only when the stud connectors are placed in strong position of profile deck.

The influence of variation in concrete strength on the failure pattern on push out test specimens was investigated by Lam and El-Lobody (2005). It was observed that, in specimens with lower concrete strength the mode of failure is conical failure (at 45^0) in concrete (≤ 20 MPa), while the connectors remain elastic. However, in case of specimens with high strength concrete (≥ 50 MPa), the primary mode of failure is the yielding of headed stud. Also, for specimens having concrete strength of around 30 MPa, a mixed mode of failure of connection was reported, i.e., concrete crushing with stud yielding (Lam 2007). Nonetheless, in case of specimens with hollow concrete slab having strength of 30 MPa, crushing of concrete was the only reported mode of failure. Also, concrete cone failure was observed in case of concrete having strength lesser than 40 MPa (Qureshi et al. 2011).

2.3.2.2 Geometry of Headed Stud

The geometry of headed studs critically governs the behaviour of composite connections. The behaviour of headed stud connectors, under static and fatigue loading was investigated by Viest (1956), Thurlimann (1958) and Thurlimann (1959). The literature suggests that the height, diameter and height to diameter

(h_s/d_s) ratio of headed stud connectors significantly influence the connection strength. The experimental investigations carried out by Slutter and Driscoll Jr (1961) and Ollgaard et al. (1971) suggested that the studs having (h_s/d_s) ratio more than 4.2 fails in tension rather than shear, while, those having (h_s/d_s) ratio less than 4.2, fracture of the connector governs the failure. It was reported that, in case of long headed stud connectors, subjected to tensile forces, the tensile strength of connectors has significant influence on connector capacity. Another investigation, to understand the fatigue behaviour of headed stud connectors of different diameters, ranging from 0.5 to 0.875 inches, was carried out by Slutter and Fisher (1966). Push out tests were conducted to estimate the relation between the fatigue strength and diameter of studs (Lee et al. 2005). The fatigue strength was found to bear a decremental direct relationship with increase in diameter of stud. The studs having the diameters of 0.75 and 0.875 inches exhibited insignificant variation in fatigue strength. It was also suggested that, for connectors having diameter greater than 25 mm, the studs have only marginal contribution towards the shear strength of connections, owing to splitting of concrete (Mattock 1977).

The strength of headed stud connectors having large diameters was analytically compared with the design strengths of connecters prescribed in EC4 (2004) and AISC-ANSI 360 (1978) specifications by Nguyen and Kim (2009), using finite element software ABAQUS (HKS, 2013). The study reported that AISC-ANSI 360 (1978) overestimates the strengths of connectors by up to 27%, while EC4 (2004) overestimates the capacity of stud in case of 30 mm diameter of stud by 8.7%. However, EC4 (2004) was found to give a conservative estimate in cases of studs having diameters of 22 mm, 25 mm and 27 mm. The capacity of headed stud up to diameter 30 mm is safely predicted by EC4 (2004) but an additional safety factor may be required in case of AISC-ANSI 360 (1978) specifications (Lee et al. 2005).

The effect of thickness of concrete slab on the failure mode of composite connections was investigated by Lam (2007) and de Lima Araújo et al. (2016). The study suggested that the minimum thickness of concrete slab required to avoid premature failure in concrete slab is 35 mm more than the overall height of studs.

In another study de Lima Araújo et al. (2016) established a relationship between the depth of slab and connector strength and suggested that the concrete cover of more than 40mm above head of the stud has no effect on the connection strength. Effect of layout of the headed studs on the behaviour of profile sheeted composite push out test specimens was evaluated by Qureshi et al. (2011). The capacity of stud shear connectors is significantly influenced by the layout of shear connectors and the spacing between adjacent connectors and their position. The capacity of connectors in a group exhibits only 71% of the capacity of individual connector. The connector resistance remains unaffected, in case of connectors spaced below 80 mm and above 200 mm. However, when the studs are placed in a strong position, the capacity of stud is 94% and 86% of single connector, for both inline and staggered arrangement of connectors respectively.

The strength of connections was observed to vary in proportion with the cross-sectional area of the connectors, i.e., the strength of connection increases proportionately with the diameter of connectors in a composite member (Badie et al. 2002). Also, the number of connectors required to attain the desired strength of connection, decreases with an increase in the diameter of connectors. However, the increase in diameter of stud from 22.2 mm to 31.8 mm reduces the slip at failure by about 30%. Another critical observation was related to the effect of removal of head of alternate studs in a composite connection. It was reported that the strength of aforementioned connection reduces by 17% of that of the normal connection. In the same study, it was also reported that thickness of top flange of steel element of the composite connections must be at least 0.4 times the diameter of stud, to avoid flange failure. Another conclusion of this study was that, under fatigue loading, the engendered slip was observed to be more in case of connections with headed studs having large diameter. The load slip behaviour of connections with headed stud connectors was also observed to be dependent on the location of headed studs in a profile sheeted composite members. If the studs are located at the strong position, they exhibit higher strength and lesser ductility than the connections with connectors located in weaker position (Easterling et al. 1993).

The effects of degree of connection was analytically evaluated through finite element analysis by Queiroz et al. (2007). The degree of connection was made to vary between 47% to 136% and the variation in strength, stiffness and flexibility of composite connections subjected to concentrated and uniformly distributed loads was observed. It was observed that the degree of connection above 100% in beam under point load, and above 118% in beam under UDL, has no significant effect on the behaviour of the beam. The failure in such beams occur due to crushing of concrete. At a particular degree of connection (118% in beam subjected to UDL and 100% in beam subjected to point load), the observed failure mode was combined crushing of concrete and yielding of studs. The yielding of studs was reported as the primary mode of failure in cases of degree on interaction lesser than those specified above.

Another similar investigation to study the effect of lower degrees in connection (83%, 50% and 33%) on beams subjected to hogging moment was carried out by Loh et al. (2004). It was reported that the initial as well as ultimate behaviour of the beams varies marginally with a maximum reduction of only 7.4%. While the deflection increases with a reduction in degree of connection, the possibility of local buckling reduces with reduction in degree of connection. With an increase in degree of shear connection, there is increase in the shear, which increases the required thickness of concrete slab (Liang et al. 2004).

2.3.2.3 Reinforcement Position and Amount

The contribution of concrete strength in the hogging region of slab is generally ignored during the design of beams, thereby making the reinforcement an important component governing the behaviour of concrete element. Thus, the flexural strength of composite beams is critically influenced by the properties of steel section and tensile reinforcement of slab. The initial experimental studies on continuous composite beams were conducted by Siess and Viest (1952) and Viest et al. (1958). It was observed that the use of shear connectors governs the effectiveness of reinforcement in hogging region of beams, i.e., the effective utilisation of reinforcement can be achieved only when the shear connectors are provided in the hogging region. The earliest proposal for the inclusion of tensile

strength of longitudinal reinforcement in the design of composite beams was made by Daniels and Fisher (1967).

The contribution of longitudinal reinforcement towards the prevention of local buckling of the top flange and web of steel element was investigated by Davison and Longworth (1969). The increase in longitudinal reinforcement leads to an upward shift of neutral axis was also reported with increase in amount of longitudinal reinforcement. This upward shift of neutral axis increases the negative moment capacity and reduce the rotation capacity of negative plastic hinge. However, the increase in longitudinal reinforcement increases the probability of premature failure (local buckling of top flange and web) of steel element (Loh et al. 2004). This reduces the ratio of moment capacity $\left(M_{ultimate}/M_{plastic}\right)$ from 1.42 to 1.20 for steel-concrete composite beams. Hamada and Longworth (1973) reported that the probability of premature failure (local flange buckling of steel beam) or ratio of local flange buckling moment to plastic moment capacity decreases with increase in amount of longitudinal reinforcement. Also, with increase in amount of reinforcement, the increase in flange width to thickness ratio of steel beam reduces significantly, with a considerable reduction in overall deflection. The failure mode changes with the change in amount of longitudinal reinforcement.

Garcia and Daniels (1972) reported that the composite beam subjected to hogging moment has significant influence of reinforcement on the behaviour. It was observed that the change in reinforcement amount from 0.89% to 1.02% reduces the crack width by almost half. The effect of reinforcement position and its confinement, on split tensile strength of concrete and dowel strength of connection was investigated by Oehlers (1989). It was reported that the confining reinforcement around the base of stud connectors develops a complex triaxial state of compression in the region. This complex sate of stresses leads to an increase in connector strength after splitting of concrete along with an increase in dowel strength of connector. However, in case of unconfined reinforcement only a slight increase in strength was observed with the failure occurring just after splitting of concrete.

Effect of reinforcement layers on the strength of connections under push out tests was investigated by An and Cederwall (1996). The effect of change in reinforcement from single layer to double layer reinforcement on normal and high strength concrete was reported, and the increase was observed to be 6% and 2% in case of normal and high strength concrete, respectively. The cracking pattern for single and double layer reinforcement was also observed to be different. For a single layer of reinforcement, the cracks develop at the top and run around the stud, while for double layer of reinforcement, the cracks develop at top and run parallel to long edge.

The ductility of connection in composite push out test specimen was also observed to increase with increase in amount of reinforcement. The transverse reinforcement was recommended for placing below the head of studs (Lam 2007). In case of profile sheeted composite beams with headed stud connectors, the location of reinforcement is observed to induce a variation of up to 31% Also, in case of hollow core slabs subjected to push out test, the behaviour of connections, in terms of shear capacity and induced slip, was found to be significantly influenced by the transverse reinforcement (de Lima Araújo et al. 2016).

2.3.2.4 Loading Condition

The performance of composite members subjected to static and impact loading has also been an area of investigation. The dynamic behaviour of eccentric composite connections with headed studs was observed to be similar to the static behaviour in lieu of shear strength of connections (Louw et al. 1970). The effect of induced stresses in the connectors due to dynamic loading was observed to be less owing to the time lag between the applied load and engendered reaction. The effects of high frequency eccentric dynamic loading $\left(>10^5\ MPa/\sec\right)$ were observed to be similar to that of a static axial force on the specimen, as the concrete remains ineffective dynamically at higher loading rates. The effect of pre-stressing force on the behaviour of continuous composite beam was investigated by Sarnes Jr (1975). The primary observation was a reduced cracking potential in the negative moment region of the beam due to the presence of pre-stressing force. However, it was

recommended that the pre-stressing must be performed before placing shear connectors, so as to increase the initial compressive strength; this leads to a delayed crack initiation.

The effect of incremental loading on engendered slip at various load levels, under push out tests was studied by Taplin and Grundy (1997). It was observed that the reverse cyclic loading induces larger relative slip as compared to unidirectional cyclic loading. Also, at any load level, the induced slip was observed to bear a linear relationship with number of cycles.

The influence of type of loading on the stiffness of connectors has also been investigated and it was reported that the shear stiffness of connectors, in case of cyclic loading is almost three times (2.8) greater than the static stiffness of connectors (Oehlers and Coughlan 1986). The behaviour of connectors under push-out test and full scale beam test was studied by Lee et al. (2005). The strength of connectors in composite beams with degree of connection 0.38 was found to be 1.59 times (almost 60%) higher than that of push out test specimen.

The performance of composite push out test specimens subjected to shear and axial loading was investigated by Mirza and Uy (2010). It was reported that the axial load has a significant impact on connector resistance. The behaviour of connections in case of profile sheeted slab was found to be opposite to that in case of solid concrete slab. The shear resistance of solid concrete slab was found to increases with an increase in thickness of slab; however, a decrease in axial tensile capacity was also observed. In case of profile sheeted composite specimen both the shear resistance and axial tensile capacity were reported to increase with increase in thickness of slab. In another study, a degradation in static strength was reported in push out test specimens after a fatigue life of 10% - 20%, when subjected to high cyclic fatigue loadings (Hanswille et al. 2007).

2.3.3 Demountable Shear Connector

The rapid popularity of headed stud connectors owing to the uniform circular geometry providing equal section modulus in all directions encouraged the researchers to explore the similar forms of connectors further. During the late-

1960s, the damages sustained by various composite bridge decks due to poor strength of concrete slabs posed the demand for development of demountable shear connectors (Dallam 1968; Dallam and Harpster 1968; Dedic and Klaiber 1984; Henderson et al. 2015; Moynihan and Allwood 2014). These connectors were supposed to provide flexibility of replacing the connected elements based on requirement, with minimum installation cost. The better seismic resistance offered by these connectors, owing to dissipation of energy through friction initially, has provided another advantage in their behaviour.

The initial investigations on the behaviour of friction grip bolts as connectors were carried out by Dallam (1968) and Dallam and Harpster (1968). They conducted push out tests and full scale beam tests, to observe that at service load, no slip occurs at the interface. It was also observed that at failure, the strength is twice of that of the welded connector having same geometry. The suitability of demountable shear connector was further validated through the results of flexural strength tests. The effect of various connection strength influencing parameters such as concrete strength, cast in-situ and pre-cast concrete effect was studied by Marshall et al. (1971).

The effect of static and fatigue loading on the behaviour of shear connectors was studied by Kwon et al. (2010a). They suggested that the effective shear area of threaded demountable connector is about 80% of the gross cross-section area. The fatigue strength of post installed shear connectors is significantly higher than that of the conventional stud shear connectors, as suggested by AASHTO-LRFD (2007). An empirical relation was proposed by Kwon et al. (2010a) to find ultimate strength Q_u of post installed connectors under static loading

$$Q_u = 0.5 A_{ds} f_u \qquad (2-24)$$

where, A_{ds} is the effective area of cross section of stud (80% of gross area) and f_u is the ultimate tensile strength of connecter.

Later, the behaviour of composite beam retrofitted using demountable shear connectors was studied by Kwon et al. (2010b). It was observed that the strength of retrofitted beam was 65% higher than that of the original composite beam. It was also observed that when retrofitted with demountable connectors,

even at low degree of interaction (30%), the beam strength increases by about 40-50% as compared to the non-composite beam (Pathirana et al. 2015). The ductility of beam also increases with the installation of shear connectors at the beam ends (zero moment regions).

The load-slip behaviour of high strength friction grip bolts with headed stud, through static push-out tests, was investigated by Ataei et al. (2014). The load-slip curve, as observed, exhibited an approximately trilinear behaviour, signifying zero, partial and full interaction. The load-slip behaviour of demountable shear connectors was found to be considerably different from that of, headed stud connectors, which exhibit an almost bilinear behaviour representing zero and full interaction. Apart from the structural analysis, the sustainability aspect of demountable shear connectors were analysed by Moynihan and Allwood (2014). An experimental study on profiled steel decking composite beams having various spans was conducted to demonstrate the superiority of demountable shear connectors over the conventional welded stud connectors. It was also observed that the overall strength of beam reassembled after application of service load was higher than that prescribed in EC4 (2004).

The effects of variation in concrete strength and stud collar diameter on the behaviour of group of demountable connectors under push-out test were investigated by Dai et al. (2015). They concluded that the effect of increase in strength of concrete has marginal influence on load carrying capacity of connectors, that too only up to the concrete strength of 30 MPa, beyond which, the effect is negligible. However, the stiffness varies considerably with variation in strength of concrete (Pathirana et al. 2016a). It was also noted that the reduction in connector collar diameter significantly reduced the connection strength. The dynamic behaviour of demountable shear connectors under in push-out test and beam test was studied by Henderson et al. (2015). The observations suggested that the dynamic behaviour of demountable shear connectors is having close correspondence with that of welded stud connectors. The failure mode was observed to change from shearing failure of bolts to the intrusion of bolts into concrete with change in stud geometry. The long term behaviour has been found

to be favourable for demountable shear connectors in composite beams, owing to the lesser overall deflection (Ban et al. 2015).

In an experimental investigation to determine the post yield behaviour of demountable stud connectors, push-out test was conducted. The results of the study suggested that in case of welded stud connectors, major slip (85% of total) occurs after the yielding of connectors (Pathirana et al. 2015), while, in case of demountable shear connectors much of the slip occurs due to shear transformation of bolts, before their yielding(Pathirana et al. 2016b). It was also noted that the friction between the steel element and nut of demountable connectors offers additional resistance to the applied force, thereby increasing the ultimate strength and deformability (Pathirana et al. 2015). In another study Pathirana et al. (2015) compared the behaviour of composite beams, retrofitted using headed stud connectors and demountable stud connectors. It was observed that the overall behaviour (strength and ductility) of composite beam retrofitted with demountable studs is almost similar to that of the original beam, whereas, the composite beam retrofitted using welded connectors exhibited very low strength. It was also observed that the influence of the diameter of grout hole, surrounding the connectors is insignificant (of the order of only 4%). However, the geometry of the bolted connector has significant influence on the degree of connection. The results of the study also suggested that the bolted connectors, with additional nut and collapsible washer embedded in concrete slab, exhibit higher degree of connection as compared to welded stud connectors. The degree of connection affects the failure mode, stiffness, ultimate strength, deformability and position of the neutral axis (Ataei et al. 2016). In a similar study, Pathirana et al. (2016a) concluded that the bolt with rubber washer has highest stiffness among various mechanical connectors (welded stud and bolts with collapsible washer) examined in the study. The bolted connectors with rubber washer does not exhibit any sign of yielding up to service load and was able to be reused, up to the service load (40%of the load capacity). It was also suggested that even at lower degrees of connection (<25%), the ultimate strength of composite beam increases by approximately 40% as compared to the non-composite beam. Pathirana et al.

(2016b) proposed an empirical relation to predict the ultimate load capacity Q_u (kN) of grouted bolted connectors under static loading

$$Q_u = 0.07\, A_{ds}\, h_s \sqrt{f_c^{'}\, E_c} \qquad (2-25)$$

where, A_{ds} is the cross-sectional area of demountable stud in (mm)^2, h_s is height of the connector in mm, f_c' is the compressive strength of concrete cylinder at 28 days (MPa) and E_c is the Young's modulus of concrete (MPa).

Rehman et al. (2016) also compared the behaviour of welded stud connectors with demountable stud connectors, through push out tests. It was observed that the ultimate resistance offered by a single connector per trough was significantly higher than that offered by the same connector in a group of connectors per trough. However, a group (two) of connectors per trough exhibited better ductility than a single connector. The aptness of the design guidelines, based on serviceability limit state, as prescribed by AISC-ANSI 360 (2010) and ACI 318 (1977) was underscored. The strength of connectors as determined using the specifications of EC4 (2004) was also discussed.

Despite all the aforementioned advantages, the use of demountable shear stud connectors remains limited, owing to certain limitations of these connectors. The first limitation is the reduction in shear strength of connectors, owing to the reduction in its cross-sectional area due to threading (Kwon et al. 2010a). This reduction further leads to other second order limitations such as the shear transformation of the bolts due to their larger diameter holes as compared to the bolts and unevenness in the torque applied for tightening the bolts. This difference in diameters of bolt and bolt hole leads to pinching of force deformation behaviour of the composite member, especially under reverse cyclic loading. Another major limitation of demountable shear connectors is the more requirement of steel means with significantly thicker top flange to prevent the possibility of local flange buckling and shear lag. The provisions of bolt holes in the top flange of steel beam also reduces the effective cross-sectional area of the beam at the bolt hole location, leading to reduced section modulus. Also, the abundance of the forms of demountable connectors, along with the insufficient design guidelines, further complicates the design of such connectors.

2.3.4 Perfobond Shear Connector

During the later half of 1980s, the quest for better connectors to establish effective steel-concrete composite connections led to the discovery of perfobond connectors. Apart from the effective transfer of stresses between the connected elements, these connectors ensure minimal slip at service loads, and provide enhanced stiffness with improved fatigue life at a lesser cost (Kim and Jeong 2006).

The initial experimental studies, which led to the development of perfobond connectors, were conducted by Zellner (1987). The objective was to compare the performance of a perfobond rib connector (perforated steel plate) with that of the various other commonly used forms of mechanical connectors. It was observed that a single one meter long perfobond rib connector performs similar to 24 headed shear studs of 19 mm diameter, and 18 headed shear studs of 22 mm diameter. The similarity was however limited to the strength, while the deformability of these connectors was significantly lesser than that of headed stud connectors. The various shapes of perfobond shear connectors have been shown in *Fig. 2-4*.

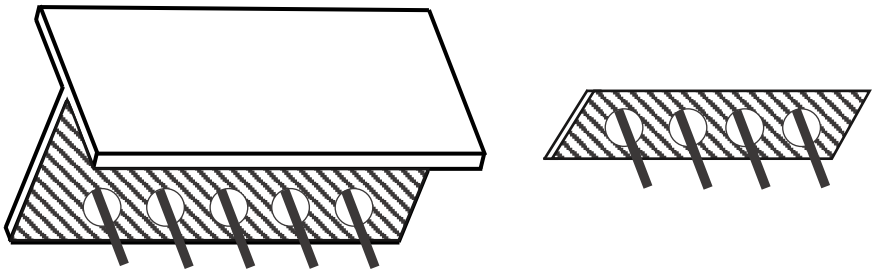

Fig. 2-4: Various shapes of perfobond shear connector; T-perfobond and perfobond rib

Further experimental investigations to determine the feasibility of perfobond rib shear connector in steel-concrete composite beam with ribbed metal deck was investigated by Veldanda and Hosain (1992). The failure pattern observed was owing to the crushing and splitting of the concrete slab in longitudinal direction (Valente and Cruz 2004). The results of push-out tests, to compare the performances of specimens with perfobond connectors and headed stud connectors suggested that the ductility capacity of the former is significantly lesser owing to their higher stiffness and friction (Oguejiofor and Hosain 1992; Oguejiofor and Hosain 1994; Vianna et al. 2008). The observed load resistance -slip

behaviours of test specimens depicted a better redistribution of stresses in concrete block owing to enhanced friction between concrete and connector. The perfobond shear connector was thus deemed as an effective alternative of headed stud, when placed parallel to steel beams.

The applicability of perfobond connectors in full scale composite beams was studied by Oguejiofor and Hosain (1992). They suggested that the increase in number of perfobond connectors, maintaining required resistance (length), reduces the stress concentration in concrete element. The reduction in strength with ribbed metal deck was found to be less in perfobond connector compared to headed stud. In another study, Oguejiofor and Hosain (1994) conducted a parametric study on perfobond rib connectors and observed that an increase in concrete strength, increases the connection capacity linearly, with a factor of half (Vianna et al. 2008). It was also observed that the connection strength increases linearly with the number of holes in the perfobond connector, but only up to three holes. This conclusion was invalidated through another experimental study conducted by Vianna et al. (2008). It was suggested that increasing the number of rib holes from two to four exhibits negligible change in strength. However, the conclusion was noted to hold good only if the centre to centre distance between two rib holes is at-least 2.25 times the hole diameter. An empirical relation to estimate the ultimate strength Q_u (N) of a perfobond connector was proposed by Oguejiofor and Hosain (1994) as,

$$Q_u = 0.590 A_{spc} \sqrt{f_c'} + 1.233 A_{tr} f_{yr} + 2.871 n_p \left(d_{pc}\right)^2 \sqrt{f_c'} \qquad (2-26)$$

where, A_{spc} is the shear area of perfobond connector in (mm)^2, A_{tr} is the total area of transverse reinforcement in mm^2, f_{yr} is the yield strength of reinforcement in MPa, n_p is the number of rib holes and d_{pc} is the diameter of rib holes in (mm).

In an attempt to effectively simulate the results of experimental study, a finite element analysis of push-out test composite specimen with perfobond connectors was carried out using finite element (FE) software ANSYS by Oguejiofor and Hosain (1997). It was observed that the difference in ultimate strength, estimated through FE analysis and obtained through experiments, is of

the order of approximately 17%, the numerical simulation being more conservative. On the basis of the results obtained, the empirical relation for estimation of ultimate strength Q_u was modified to,

$$Q_u = 4.5\, h_{pc}\, t_{pc}\, f_c^{'} + 3.31 n_p \left(d_{pc}\right)^2 \sqrt{f_c^{'}} + 0.91 A_{tr}\, f_{yr} \qquad (2-27)$$

where, h_{pc} is the height of perfobond rib connector in mm, and t_{pc} is the thickness of perfobond rib connector in mm.

The literature also suggests that the strength of perfobond connectors depends on the strength of concrete, friction between steel plate and concrete element, number and diameter of holes in perfobond connector, number of reinforcing bars and amount of transverse reinforcement (Klaiber and Wipf 2000; Oguejiofor and Hosain 1994; Oguejiofor and Hosain 1997).

It was later suggested that the effect of spacing of holes in the perfobond connector is negligible beyond a minimum spacing of 1.6 times the diameter of holes (Klaiber and Wipf 2000). It was thus concluded that the equation (*2-26*), as proposed by Oguejiofor and Hosain (1994) was conservative for connectors with web thickness greater than 10 mm.

During the last decade, the application of perfobond connectors with lightweight concrete was experimentally studied by Valente and Cruz (2004). The induced slip and ultimate strength of specimens with lightweight concrete was observed to be significantly different from those of normal strength concrete as reported in literature. The induced slip was approximately 2 mm lesser than that reported for corresponding normal strength concrete specimens, while the ultimate strength was observed to be 0.8 times of the strength predicted using equation (*2-27*) suggested by Oguejiofor and Hosain (1997).

Subsequently, experimental studies on full scale beam specimens along with push-out tests on conventional solid slab and metal deck composite specimens, with perfobond connectors were carried out by Kim and Jeong (2006). It was reported that the metal deck slabs with lesser wavelengths offer higher resistance. It was also observed that in order to achieve the maximum shear resistance, the spacing of holes in the perfobond connector should be between 2 and 2.5 times the diameter of hole. The superiority of metal deck slab over the

conventional solid slab was underscored by concluding that the strength of metal deck slab is higher than that of solid slab by approximately 100%. Later, the efficient utilization of the perfobond/T-perfobond rib shear connector in semi rigid portal frame was demonstrated by An study on T-perfobond connections by De Andrade et al. (2007) demonstrated the efficiency of these connectors in transmitting the stresses from concrete slab reinforcement bars to the flange of steel column. In another comparative study in perfobond and T-perfobond connectors, Vianna et al. (2008) observed the effects of the orientation of connector (flange towards concrete bearing end), variation in concrete slab thickness, variation in number of holes and variation in connector height on the degree of connection. It was observed that the induced slip increases with increase in slab thickness, number of holes and connector height. In another similar study, Vianna et al. (2009) observed that T-perfobond connectors exhibits higher strength and stiffness than normal perfobond connectors.

The effect of increase in number of perfobond connectors was investigated by Cândido-Martins et al. (2010). It was observed that the shear resistance offered by single connector is approximately 1.25 times higher than the resistance per connector in a group of connectors (Ahn et al. 2010). The ductility of connection with a group of connectors is significantly lesser than that with a single connector. The contribution of holes in the strength of perfobond connectors, as estimated using the equation proposed by Yoshitaka et al. (2001), was also found to be over-estimated by approximately 6.5 times. The authors proposed a modification in the empirical equation, proposed by Oguejiofor and Hosain (1997), to estimate the ultimate strength of perfobond connectors as

For single perfobond connector

$$Q_u = 3.14 h_{pc}\, t_{pc}\, f_c^{'} + 3.79\, n\pi \left({d_{pc}}/{2} \right)^2 \sqrt{f_c^{'}} + 1.21 A_{tr}\, f_{yr} \qquad (2-28)$$

For twin perfobond connect is

$$Q_u = 2.76\, h_{pc}\, t_{pc}\, f_c^{'} + 3.32\, n\pi \left({d_{pc}}/{2} \right)^2 \sqrt{f_c^{'}} + 1.06\, A_{tr}\, f_{yr} \qquad (2-29)$$

where, Q_u is the shear capacity of perfobond connector (N), f_c' is the compressive strength of concrete cylinder at 28 days (MPa), A_{tr} is the total area of transverse reinforcement in mm², f_{yr} is the yield strength of reinforcement in MPa, n_p is the number of rib holes, d_{pc} is the diameter of rib holes in mm, h_{pc} is the height of perfobond rib connector in mm, and t_{pc} is the thickness of perfobond rib connector in mm.

The behaviour of perfobond shear connector connected push-out test specimen under elevated temperature was studied by Rodrigues and Laím (2011). It was noted that at elevated temperatures, the connectors with holes exhibits higher reduction in strength compared to connectors without holes. The study also suggested that the specimen having connector with single hole and without any reinforcement perform better among all the specimen with connectors having holes. Nevertheless, the performance of specimens with a group of connectors exhibited poorest performance at elevated temperatures.

The basic philosophy of perfobond connectors is to improve the stiffness and strength of pre-existent forms of connectors by introducing holes to ensure better shear resistance through dowel action. This increase in stiffness, in turn resulted in brittle connections between steel and concrete elements of a composite member. Apart from the lesser ductility, another limitation of the perfobond connections is the practical complexity in achieving the dowel action by passing the reinforcements of concrete slab through the holes of connectors. This makes the perfobond connectors a less preferable practical method to achieve composite action in general.

2.3.5 Structural Adhesive

Structural adhesives contribute substantially to the integrity of the component or the product being prepared. Structural adhesives mainly find their use in the construction industry for repairing, strengthening and reinforcing existing structures, connecting two similar or dissimilar materials and resisting mechanical and environmental loads. Earlier, these structural adhesives were used to fill the gaps between precast members. Homo-polymer Polyvinyl Acetate (PVAC) is

among the first constructional adhesives used as filler in the gaps between precast members. However, owing to its poor resistance against environmental action, its use has been limited to internal applications (BS 1989). The chemical composition of structural adhesives usually consists of polymeric chains of epoxy, polyurethane or acrylic based groups.

Various enhancements in existing structural adhesives and the development of new adhesives have increased their applicability in various areas such as retrofitting of existing structures and structural connection. In comparison to the conventional mechanical connectors, structural adhesives offer increased homogeneity in stress distribution, along with a reduced formwork, accelerated construction speed, quality assurance and improved fatigue life of members. Structural adhesives can also be used to join members having thin cross-sectional elements. They act as binding materials and provide better resistance to corrosion and water percolation (Mays and Hutchinson 2005; Shaw 1990; Täljsten 2006; Tremper 1960) .

With time, any structure deteriorates, irrespective of the construction material used. This deterioration usually leads to reduced stiffness and strength of members and structure. In the case of cement concrete (CC) and RCC structures, cracking, spalling and collapse of large concrete masses are common reasons for the deterioration of concrete in any structure/member. The selection of an appropriate repairing/retrofitting method for deteriorated structures is imperative (Kalyanasundaram et al. 1990), and the use of structural adhesives is among the most common and efficient techniques to prevent structural deterioration (Chand 1979; Johnson 1965; Shash 2005).

Steel-concrete composite constructions have numerous advantages over non-composite constructions such as a higher strength to weight ratio, more flexural strength and stiffness, speedier and more flexible construction, ease in retrofitting and repair, higher durability and better aesthetics (Bouazaoui et al. 2007; Ekenel et al. 2006; Ellobody 2014; Souici et al. 2013; Yu-Hang et al. 2014). Conventionally, mechanical connectors are used in steel-concrete composite constructions, but they cause stress concentration and have poor fatigue life

(Bouazaoui et al. 2007; Souici et al. 2013). Another shortcoming of such connections is their inability to provide high degree of interaction. Also, the higher density of mechanical connectors may result in improper placement of concrete. To overcome the shortcomings of mechanical connectors, the efficacy of structural adhesives has been thoroughly researched. The new age design requirements with light weight and multi-material approach can be effectively met with structural adhesives (Mette et al. 2016). *Fig. 2-5* shows a schematic view of an adhesive bonded steel-concrete composite member.

Fig. 2-5: Schematic view of adhesive bonded steel-concrete composite member

2.3.5.1 Repair and Strengthening of Existing Structures

The repair of CC or RCC members and their joints is commonly done using low viscosity epoxy resin because adhesives penetrate well, fill the cracks efficiently, and are capable of restoring the lateral load capacity (Chung 1981; Ellobody 2014; Mette et al. 2016; Pan and Moehle 1992; Robertson and Johnson 2004; Tremper 1960).

Thanoon et al. (2005) noted that the load carrying capacity of RCC slab, repaired using structural adhesive, was found to increase considerably, with the deflection and stiffness approximately similar to those of the control slab. The deflection and stiffness of the precast RCC slab repaired using epoxy were almost

the same as those of the control slab. *Fig. 2-6* shows a schematic view of a repaired precast RCC slab, which has two cracks. The stiffening of hardened concrete may arrest the cracking in structures and may also facilitate the correction of errors in design and defects in construction. The adhesive bonded structures are capable of resisting more loads and exhibit slightly increased stiffness (MacDonald and Calder 1982).

The repaired flat-slabs and columns may sometimes fail below the load carrying capacity of the original members, and may also exhibit a reduction in stiffness. However, the lateral drift capacity of repaired members is nearly equal to that of the original members (Pan and Moehle 1992). Another parameter that affects the strength of a repaired member is the pressure with which epoxy is injected into the member; the member strength is directly proportional to the injection pressure of the epoxy (Farhey et al. 1995).

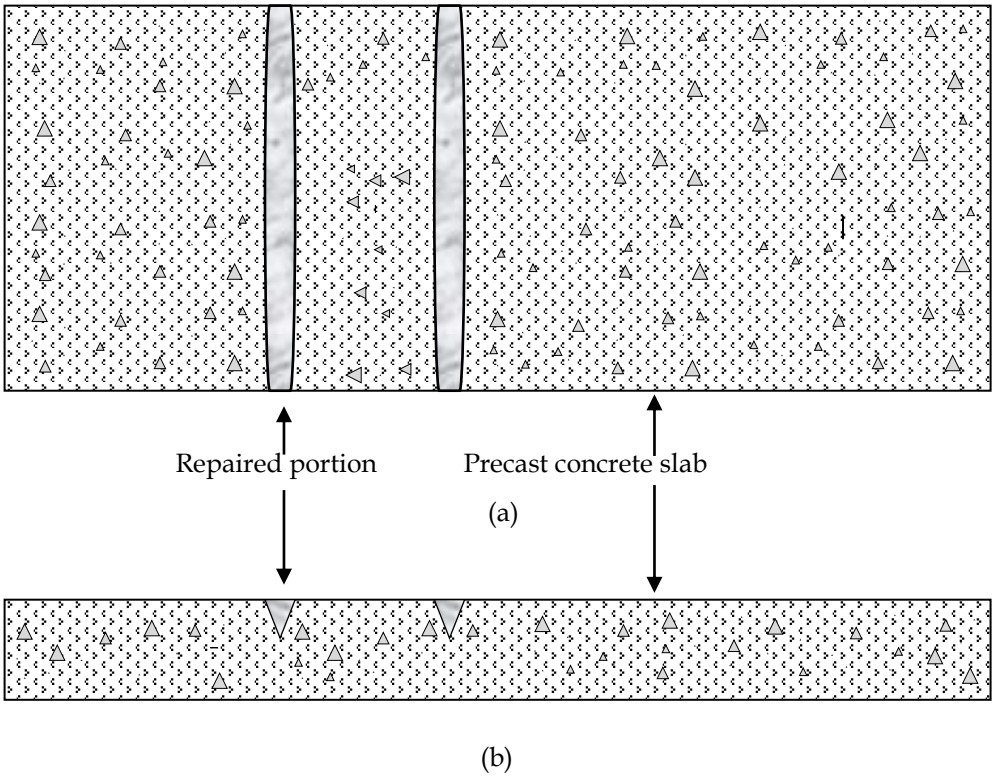

Fig. 2-6: Crack repaired using low viscosity adhesive; (a) top view and (b) side view

Systematic studies on the strengthening of RCC structures using adhesives were started during the 1970s. Various researchers, including (MacDonald and Calder (1982); Mays and Vardy (1982); Tilly (1985); Van Gemert and Maesschalck

(1983); Wake (1978)), carried out studies on strengthening of precast RCC members. The strengthening of beam elements in tension, compression and shear zones has recently become a common practice (Ali et al. 2000; Ali et al. 2005; Oehlers et al. 2003). The primary modes of failure of such strengthened beams are plate end debonding, critical diagonal cracks and intermediate cracks (Chen and Teng 2003). However, on beams bonded using polymer, a premature failure of connections in the tension zone has been observedAli et al. (2005). Similar studies also show that externally bonded steel plates at the bottom and side/web faces of precast RCC members act as additional reinforcement for the member. *Fig. 2-7* shows a schematic view of a precast RCC beam member strengthened with adhesive bonded external steel plates. *Fig. 2-7(a)* depicts the cross-sectional and side views of a shear strengthened precast RCC beam (structural adhesive is used to connect the steel plates and a precast RCC beam member). *Fig. 2-7(b)* shows a flexurally strengthened precast RCC member, wherein a steel plate is provided at the bottom face of the precast RCC member, along the length of the beam.

The effect of strengthening on the flexural strength, shear strength and stiffness of a member has been thoroughly investigated by various researchers (Adhikary and Mutsuyoshi 2002; Adhikary et al. 2000; Ali et al. 2005; Barnes and Mays 2006; Barnes and Mays 2006; MacDonald and Calder 1982; Oehlers et al. 2003; Oehlers 2001). The strengthened members exhibit a higher enhancement (as high as three times) in stiffness, compared to the original member. However, this enhanced stiffness is elastic, and the failure of a member strengthened using adhesive is brittle in nature (Chung 1981; Ekenel and Myers 2007; Ekenel et al. 2006; Farhey et al. 1995). Also, it has been reported that the flexural strength of members, strengthened using epoxy resin is higher than that for the control specimen (Ekenel et al. 2006; Thanoon et al. 2005).

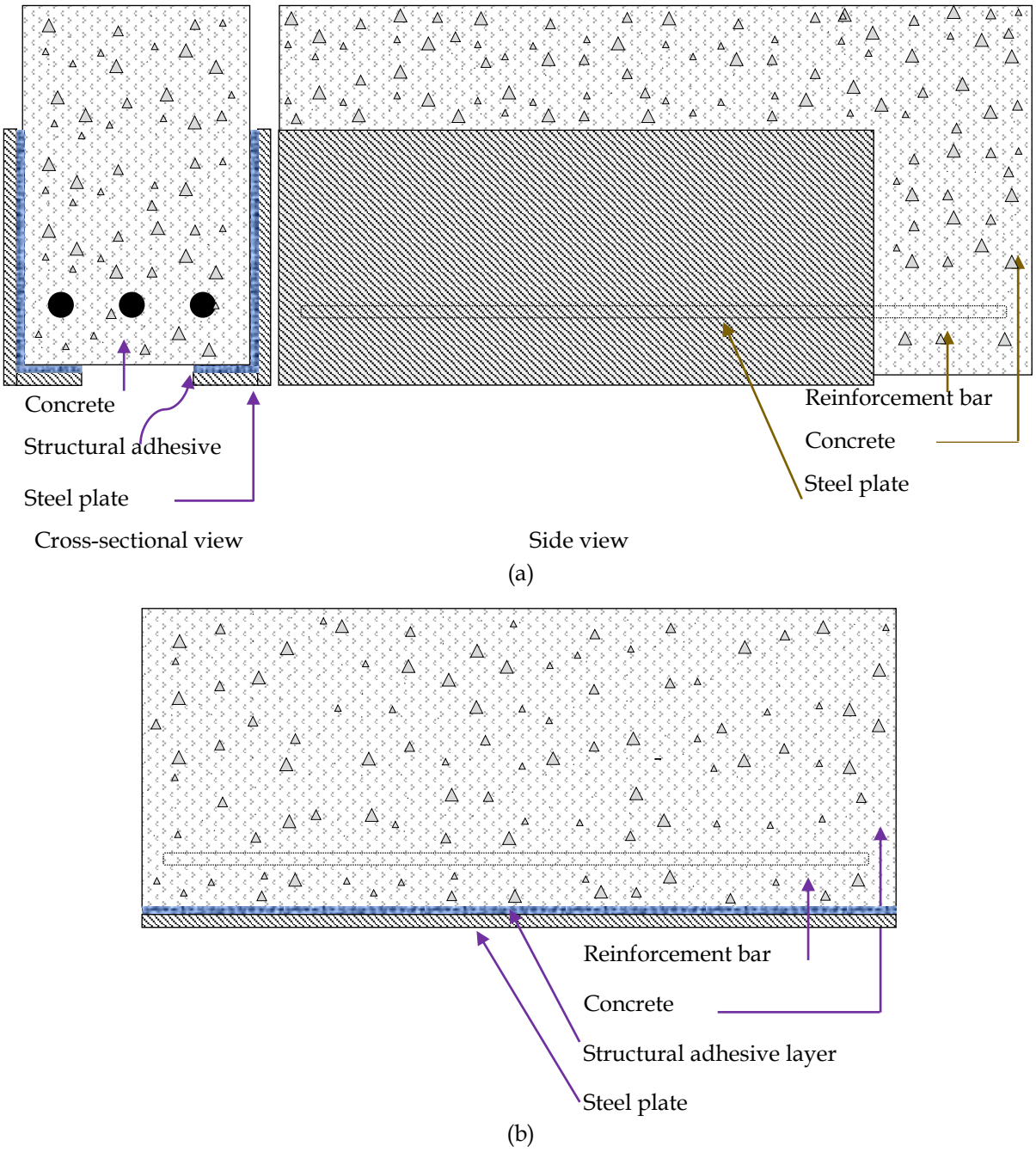

Fig. 2-7: RCC beam member strengthened with adhesively bonded external steel plates; (a) cross-sectional and side view of shear strengthened RCC member using steel plates and (b) side view of flexural strengthened RCC member

The effect of strengthening on precast beams has been investigated by Ali et al. (2005). It has been observed that the shear strength at the compression face is notably higher than that at the tension face, while the strengthening of the compression face is independent of the thickness of the steel plate. It has also been observed that due to the enhanced flexibility of the strengthened beam, the shear

strength of the retrofitted beam varies inversely with the modulus of elasticity of the strengthening material (Ali et al. 2000). Adhikary et al. (2000) conducted an experimental study on precast RCC beams, strengthened using bonded steel plate and found that the shear strength of web, strengthened with thicker plates is higher than that of unstrengthened (control) web.

Adhikary and Mutsuyoshi (2002) observed that the flexural strengthening with thick plate increases the probability of debonding failure at the beam ends. The use of deeper steel plates instead of thicker plates has been recommended in order to facilitate the maximum shear contribution for identical cross-sections by Adhikary and Mutsuyoshi (2006).

Another experimental study, conducted using externally bonded steel plates on precast RCC beams validates the efficiency of such configurations in achieving a high degree of crack control. Crushing failure happens in such beams (Adhikary et al. 2000). Along with an increase in the thickness and width of the web strengthening plates the ultimate shear strength of the beams increases. The effectiveness of web strengthening, in terms of the increased shear capacity of rectangular and T-cross-sectioned RCC beams, is validated through the close compliance of experimental results with BS 8110 (Barnes and Mays 2006; Barnes and Mays 2006; British Standard 1997).

The flexural strengthening of precast RCC beams has also been thoroughly investigated. Changes in the failure modes of such beams, with the thickness of strengthening plates, the position of plate curtailment and support conditions, have been reported by MacDonald and Calder (1982). They recommend the use of bond plates, having a minimum width to thickness ratio of sixty, to achieve maximum flexural capacity of a member. The durability of epoxy adhesives through a comparative experimental study has been reported by . Two sets of similar specimens showing cracks were strengthened using epoxy; one set was exposed to environmental conditions, while the other was monitored in the controlled atmosphere of a laboratory. The results of the study suggested that the environmental exposure led to about 15% reduction in strength of the retrofitted specimens.

The behaviour of adhesive bonded anchor rods embedded in concrete has been investigated by numerous researchers (Barnaf et al. 2012; El-Hawary 1999; Omar et al. 2016; Upadhyaya and Kumar 2015; Wang et al. 2015; Wang et al. 2016; Yilmaz et al. 2013). The effect of epoxy coated and uncoated bars, embedded axially in concrete cylinders and exposed to a marine environment, on the bond strength, was investigated through pull out tests by El-Hawary (1999). The results of the study suggest that there is no effect of the epoxy coat on the behaviour of bond. Another similar study on steel rods embedded in low strength concrete, was performed by Yilmaz et al. (2013), in which the effects of the concrete strength, embedded length, diameter of the anchor bar and edge distance were analysed. The authors concluded that with an increase in diameter of the anchor bars, the failure mode of connection changes from ductile to brittle. The study also concluded that both the embedment depth and edge distance should be at least fifteen times the anchor bar diameter for an efficient and economic design. Similar tests were conducted by Barnaf et al. (2012) to determine the bond strength of chemically bonded anchors in high strength concrete. It was noted that the behaviour and failure of the specimen depends on the characteristics of the adhesive. The changes in the failure pattern, with respect to the diameter of the steel rod, in a pull out test were studied by Wang et al. (2015). The study indicated that with an increase in the diameter of anchor bar, the failure mode changes from steel bar pull out to mixed cone damage of the concrete with pull out of the rod. The failure mode of connection also depends on the surface treatment of the anchor bar. Wang et al. (2016) indicated that the grooving in the anchor bar increases the bonded area and thereby, improves the mechanical interlocking force. Upadhyaya and Kumar (2015) proposed an analytical method to predict the pull out capacity of adhesive bonded anchors in concrete, on the basis of stress intensity. The strength of connections was found to be independent of the boundary conditions of embedded anchors.

Epackachi et al. (2015) investigated the tensile and shear behaviour of post installed anchors in high strength concrete, using the pull out tests. It was observed that for a single anchor subjected to tensile force, fracture of the steel rod is the

primary mode of failure, while for a group of anchors, the failure mode was dominated by concrete core splitting. The fracture of steel anchor was observed to be the mode of failure in a specimen subjected to shear forces. The authors concluded that the spacing of anchors has a significant effect on the tensile behaviour of the specimen. Mahrenholtz and Eligehausen (2015) reported a similar behaviour of anchors in shear and tensile loading for normal strength concrete. (Ashour and Alqedra (2005); Sakla and Ashour (2005)) observed that the pull off strength, of cast in concrete and post installed adhesive bonded anchors, under tension, in concrete is proportional to the anchor diameter, embedded length, concrete strength and type of resin. A similar study carried out by Alqedra and Ashour (2005) noted that the strength of an adhesive bonded anchor in shear is not significantly influenced by the anchor diameter, embedment length and concrete strength.

2.3.5.2 Structural Adhesive as Connector at Steel-Concrete Composite Interface

The adhesive connection at the steel-concrete interface is still an evolving concept for the structural engineering/construction industry. The connection at the interface of two members is capable of effectively resisting and transferring the stress/force between the members with adequate rigidity. In structural engineering applications, adhesives primarily act as shear connections in beams, floor systems, bridge deck slabs and beam-column connections. The composite behaviour of bonded connections in steel-concrete composite members has been studied by many researchers (Aboobucker et al. 2009; Berthet et al. 2011; Bouazaoui et al. 2008; Bouazaoui et al. 2007; Jurkiewiez et al. 2011; Larbi et al. 2007; Luo et al. 2012; Souici et al. 2013; Zhao and Li 2008).

Generally, for connection purposes, two types of adhesives are used as connection mediums, namely, epoxy resin based adhesives and polyurethane based adhesives. The type of adhesives used for composite connections determines the behaviour of such members. The epoxy adhesives show brittle behaviour with perfect interaction (full interaction), while polyurethane adhesives exhibit flexible (ductile) behaviour with partial interaction (Bouazaoui et al. 2007; Larbi et al. 2007). The degree of interaction is decided by the stiffness and strength of the connection;

an increase in the connection strength might increase the stiffness of connection (Oehlers and Bradford 1999). The stiffness of bonded connections is reported to be five to fifteen times higher than that of mechanical connections (Larbi et al. 2007; Meaud et al. 2014).

Souici et al. (2013) compared the behaviour of adhesive bonded and mechanical stud connected steel-concrete composite beams, and found that the adhesively bonded connection facilitates a continuous transfer of shear force between the steel and concrete, whereas a perfect connection is not ensured at the interface by mechanical stud connectors. Another study by Jurkiewiez et al. (2011) suggested that the composite behaviour in both mechanically connected and adhesive bonded connections is almost identical. It has also been observed that the primary mode of failure of adhesive bonded composite flexural members is crushing of concrete instead of failure of connections (Bouazaoui et al. 2007).

The variation in shear strength along the longitudinal span of a steel-concrete composite beam bonded with adhesive is almost insignificant, with a marginally higher concentration at discontinuous edges. However, the peeling stress is highly concentrated at the connection edges (Bouazaoui et al. 2008). Zhao and Li (2008) developed a numerical model for an adhesive bonded composite beam, tested by . The composite behaviour of the 3.5 m long beam was observed to be similar for both numerical (FE) simulations and the experimental study. Finite element simulations and the nonlinear beam model developed by Zhao and Li (2008) corroborated the observed experimental behaviour of the composite beam (Bouazaoui et al. 2007; Zhao and Li 2008).

Ernst et al. (2010) demonstrated that the behaviour of push-out test specimens exhibits a very similar behaviour to the full-scale composite beams. The push-out tests are able to predict the performance of shear connections accurately. The shear strength, effective bond length, failure mode and the force transfer mechanism of steel-concrete composite beams can be efficiently predicted through push-out tests.

The strength of steel-concrete composite specimen depends significantly on the bonded area geometry of the connection, whereas the specimen geometry has

a negligible effect on its bond strength (Berthet et al. 2011). Berthet et al. (2011) developed an analytical model for push-out tests, which was capable of predicting the strain variation at the bonded interface of composite specimen. It can be clearly established that the stress variation profile always depends on the bond length and magnitude of load, in the direction of loading. The use of structural adhesives as shear connectors in steel-concrete composite member interface has been discussed in *Table 2-1*. Scientific research on bonded interfacial connections started in the 2000s. Only a few studies were conducted on structural adhesives as the shear connection between the steel-concrete composite interfaces. The effect of different parameters such as the bond layer thickness of adhesive, concrete strength, the surface treatment of the adherend, shear stress and strain variation along the longitudinal span and cross-sections have been studied.

Table 2-1: Summary of studies carried out on structural adhesives as shear connector at the steel-concrete composite interface

Reference	Structural adhesive	Filler*	Nature of studies	Mechanical properties considered	Parameters/Variables studied
Bouazaoui et al. (2007)	Epoxy resin, polyurethane	No	Three point bending test on composite beam	Ultimate load capacity, deflection, strain, slip, neutral axis position	Adhesive nature, irregular thickness in longitudinal and transverse direction, cross-section strain variation
Larbi et al. (2007)	Epoxy resin, polyurethane	Silica	Experimental push-out test, numerical [FE] and analytical study on composite beam	Ultimate bond strength, shear stress, peeling stress, tangent stiffness, deflection, slip, stress	Surface treatment, adhesive bond thickness, shear connector spacing effect
Zhao and Li (2008)	Epoxy resin	No	Numerical study on composite beam	Ultimate load, longitudinal shear strain and stress variation along the longitudinal and transverse axis, neutral axis, crack position and propagation, principal stresses, collapse position	--
Bouazaoui et al. (2008)	Epoxy resin	Silica	Three point bending test on beam, analytical modelling [beam and slipping model]	Ultimate load, strain distribution, deflection, slip variation, neutral axis position, shear stress, peeling stress	Deviation in results of simple beam, improved beam, finite element model and experimental results
Bouazaoui and Li (2008)	Epoxy resin	No	Pull out test, theoretical model	Ultimate capacity, shear stress, crack initiation stress	Diameter of reinforcement bar, embedded length of bar, area of embedded portion
Aboobucker et al. (2009)	Epoxy resin	No	Push-out test	Direct shear bond strength	Adhesive application time, demoulding time, type and weight of concrete, type of epoxy, water content, super plasticizer dose, surface preparation of steel, pressure during curing
Berthet et al. (2011)	Epoxy resin	No	Push-out test, analytical study [beam model]	Ultimate load of bond, shear strain and stress variation with loading height.	Connection type, test specimen geometry, surface preparation
Jurkiewiez et al. (2011)	Epoxy resin	Silica	Push-out test, three point bending test, analytical study [beam model and FE model]	Ultimate bond strength, stress-slip behaviour, beam test: ultimate load, deflection, maximum strain and strain variation in cross sections, load-deflection for beam	Concrete strength, surface preparation, section geometry
(Luo et al. (2012))	Epoxy resin, polyurethane	No	Push-out test, numerical [FE] analysis of beam	Shear bond strength, load-slip behaviour, ultimate load capacity and deflection of beam	Surface preparation, adhesive nature, adhesive layer thickness, concrete strength, bonding area, bonding strength, elastic modulus
Souici et al. (2013)	Mechanical shear stud, epoxy resin	No	Four point bending test	Failure mode, ultimate load capacity, maximum deflection, strain distribution, slip, neutral axis position.	Degree of interaction, nature of connection
Meaud et al. (2014)	Epoxy resin	Silica	Push-out test, numerical modelling, FE analysis	Shear stress, peeling stress, strain distribution, average ultimate shear stress.	Specimen size, connection geometry, influence of bonded area, bottom edge or base friction effect
Jurkiewiez et al. (2014)	Epoxy resin	Silica	Three point bending test, multi-layer beam theory, numerical [FE] analysis	Ultimate load, mid span deflection, shear stress, strain variation along the cross-section	Concrete strength, cross section profile and area of concrete and steel, reinforcement

* *fillers are added at the time of adhesive application*.

2.3.5.2.1Thickness of connection

The bond thickness significantly affects the strength and failure mechanism of a connection. The effect of adhesive thickness is more dominant when the bond length is relatively shorter, the thickness of the adherend is high and the nature of the adhesive is brittle (Da Silva et al. 2009a). The traction deformation relation does not depend on the thickness of adherends (Leffler et al. 2007). There is no unequivocal opinion on the effect of the adhesive layer thickness on the strength of connections. Some researchers (Da Silva et al. 2009b; Derewonko et al. 2008) reported that an increment in thickness causes an enhancement in strength, while some suggested that an increase in thickness decreases the strength (Colak 2001; Çolak et al. 2009; Kahraman et al. 2008; Mette et al. 2016). Colak (2001) studied the bond strength of steel–concrete composite connections subjected to pull-out tests and found that the connections' bond strength increased up to a bond thickness of 2 mm and then started to decrease beyond it.

Da Silva et al. (2009b) reported that a thin layer of bonded adhesive fails at relatively lower load levels, owing to the high concentration of shear stresses. Thus, the ultimate state of strain at the bond level is attained before stress dispersion can initiate. The shear and peeling stresses in the bonded adhesive at the edges of the bonded joint are also affected by the adhesive thickness itself (Schnerch et al. 2007). At the same load level, higher shear stresses were observed for lower bond thicknesses (Derewonko et al. 2008).

The thickness of the adhesive layer also affects the modes of failure (Buyukozturk and Hearing 1998). The adhesive thickness in lower strength concrete does not affect the bond strength significantly, while, in higher strength concrete, it leads to a drastic change in the failure mode (López-González et al. 2012). The filler particle size also affects the thixotropy of adhesives (Mays and Vardy 1982). An increase in the thickness of the adhesive layer in a bonded assembly generally decreases the connection efficiency. Therefore, joints with a less thick adhesive layer show a positive influence on bond strength (Cognard et al. 2005; Frigione et al. 2006), along with an increase

in rigidity (Jurkiewiez et al. 2011). The compliance (flexibility) also increases proportionally with increase in the adhesive bond thickness (Stigh et al. 2014).

Martiny et al. (2012) reported that with an increase in thickness of the adhesive layers the fracture energy of a bond increases. Cooper et al. (2012) reported that the fracture energy of a connection increases up to a certain value of bond layer thickness and attains a constant value beyond that. The authors also stated that the maximum adhesive fracture energy is obtained when the thickness of the bonded layer (h_a) and the plastic zone diameter are almost equal ($2r_y$).

$$t_a = 2r_y = \frac{1}{\pi}\frac{E_a G_{IC(bulk)}}{\left(\sigma_{ya}\right)^2} \qquad (2-30)$$

where, t_a is the thickness of the adhesive in mm, r_y is the first order plastic zone size under plane stress conditions mm, E_a is the adhesive's Young's modulus in MPa, $G_{IC(bulk)}$ is the Mode I fracture energy of the bulk specimen in N-mm; σ_{ya} is the uniaxial yield strength of the adhesive in MPa.

Carlberger and Stigh (2010) stated that the fracture energy in peel (Mode I) increases with an increase in adhesive thickness up to a certain level beyond which the peel (Mode I) fracture energy decreases. The same pattern appears in shear (Mode II) fracture energy.

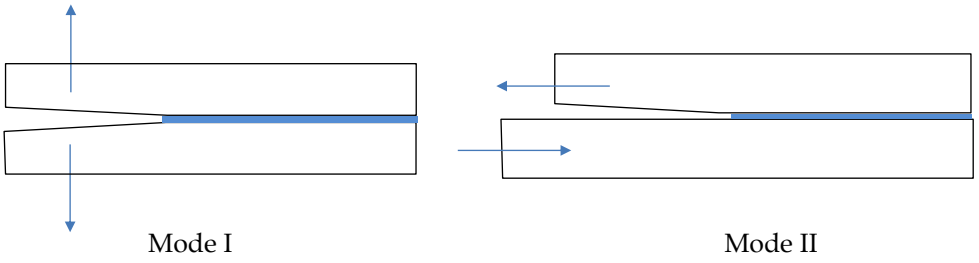

Fig. 2-8: Representation of Mode I and Mode II subjected specimen

Fig. 2-8 represents a schematic view of specimens subjected to simplified Mode I and Mode II loading. Simplified equations to determine the connection fracture energies in tensile and shear mode have also been proposed. The Mode I and Mode II fracture energies are

$$G_{IC} = \frac{4P_u}{E_a \left(b_{ad}\right)^2} \left(\frac{3a^2}{\left(h_{ad}\right)^3} + \frac{1}{h_{ad}} \right) \qquad (2-31)$$

and

$$G_{IIC} = \frac{\tau_v^2 t_a}{2G_a} \qquad (2-32)$$

where, G_{IC} and G_{IIC} are the fracture energy in Mode I and Mode II, respectively. P_u is the maximum load in N, b_{ad} is the width of the adherend in mm, a is the opening distance in mm, h_{ad} is the height of the adherends in mm, τ_v is shear stress in MPa, t_a is the thickness of the adhesive layer in mm, G_a is the shear modulus of the adhesive in MPa.

Zhao and Zhang (2007) reported that the crack development pattern also changes significantly beyond a certain (one mm) adhesive layer thickness in metallic connections. The failure mode changes from cohesive mode to slant mode and the failure pattern varies with the changing thickness of the connections.

2.3.5.2.2 Bond geometry

The bond geometry of the connection area and the adherend geometry significantly affect the bond strength of connections. These aspects play a key role in defining the performance of the connection. Custódio et al. (2009) and Kang et al. (2012) chronicle the research on joint selection and its effect on connection performance. The authors discussed the effect of the joint geometry on the stress intensity at the bond line, the type of stresses induced, the effectiveness of the connection and the fracture energy of the connections. Kang et al. (2012) described the various models available to determine the bond length and strength of a connection. It has also been stated that the bond performance depends on the joint configuration and bond length of the connection. Single and double lap shear tests (*Fig. 2-9*)are common, and suffice for assessing the effectiveness of a connection. ASTM D1002-98 (2010) proposes a simplified equation to determine the maximum permissible bond length of connection for a single shear test:

$$L_b = \frac{\sigma_{y\,ad}\, t_{ad}}{\tau_{avg}} \qquad (2-33)$$

and for a double shear test:

$$L_b = \frac{\sigma_{y\,ad}\, t_{ad}}{2\tau_{avg}} \qquad (2-34)$$

where, L_b is the bonded length of connection in mm, $\sigma_{y\,ad}$ is the yield strength of the adherend in MPa, t_{ad} is the thickness of the adherend in mm, τ_{avg} is the average shear stress in MPa.

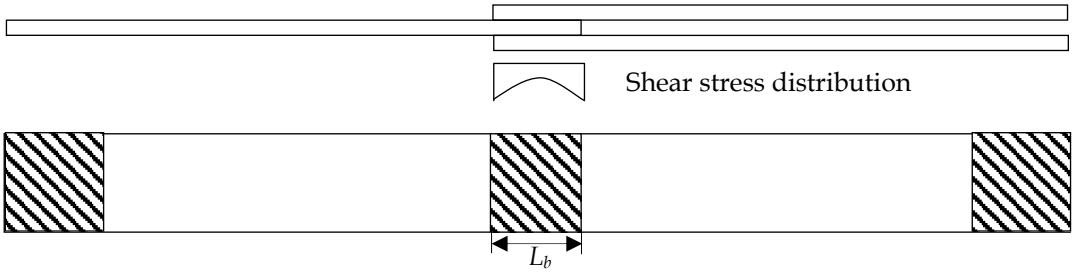

Fig. 2-9: Double shear test assembly with shear stress distribution

If the bond length and bond area of the connection are sufficient to ensure the effective distribution and transfer of stresses in the adhesive layer, the connection performance then depends on factors such as the type of adhesive and adherends, surface preparation and environmental factors. Yao et al. (2005) reported that the bond length of a connection is a function of the corresponding load level. Any increment in bond length beyond a certain value does not affect the ultimate strength of the connection. Bizindavyi and Neale (1999) observed that, at an initial load level (up to the cracking load), the strain decreases exponentially along the bond length up to a certain length, and thereafter it follows a linear path in the direction of load application. Volnyy and Pantelides (1999) concluded that, after crack initiation, the stress region is transferred towards the unloaded end. The distribution of shear stress depends on the mechanical properties of the adhesive and follows a triangular path. The shear strength of the adhesive layer also affects the bond length. If the adherend

is stronger than the adhesive, the connection may fail due to shear strain as it reaches its ultimate value (Nozaka et al. 2005).

Branco et al. (2003) observed that the strength of bonding is not only a function of the bonded area, but is also dependent on the width of the bonded area. For the same bonded area the bond strength increases with an increase in bond width. For high strength concrete, the bond width has an even higher influence, compared to that for normal strength concrete. The normal stress concentration along the concrete edge line in an adhesive bonded specimen is very high. At elevated temperatures, the effect of the bond geometry on the shear strength of the connection is negligible. A bond width to length ratio of 2.4 or 0.4 offers the maximum shear strength. If specimens were bonded leaving a certain distance from the concrete edge, a significant reduction in normal stress concentration was observed, with a sharp increase in peeling stress (Tadeu and Branco 2000).

Bizindavyi and Neale (1999) demonstrated that the three-dimensional mode of failure would be prevented by rounding off the bearing section of the concrete block and by starting the bond line away from the bearing section. Coronado and Lopez (2008) concluded that prisms are more sensitive to the bond width to specimen size ratio, compared to cylinders. The width of the bearing strip affects the tensile strength of the connection after a width (of bearing strip) to specimen size ratio of 0.1. However, for this study, the width of the specimen was kept constant in order to ignore the effect of crack patterns. The specimen size to bearing strip ratio was varied from 4% to 20%, and the formation of primary cracks was observed up to a limit of 10%, and thereafter both primary and secondary cracks were observed. It was advised that, if the specimens are subjected to pure tensile stresses, this ratio must remain less than or equal to 0.1.

2.3.5.2.3 Surface preparation

The purpose of surface preparation is to remove the weak and unclean layer from the adherend's surfaces. The surface preparation of the adherend or surface pre-treatment before the application of adhesive improves the

connection/ bond performance. The surface roughness depends on the strength of the material, the cleaning method of the interfacial surfaces, the order and magnitude of cleaning and the size of the elements (Siewczyńska 2012). The roughness of the concrete substrate has a significant influence on the bond strength of the interface (Horgnies et al. 2011). Several techniques can be used for surface preparations, such as sand blasting, mechanical grinding, wire brushing, water jetting, jack hammering and chemical cleaning. The technique of hammering damages the interfacial surface and leads to the development of micro-cracks. These micro-cracks reduce the interfacial connection bond strength (Hindo 1990; Julio et al. 2004). Horgnies et al. (2011) reported that the mould material used for high strength concrete casting affects the bond strength, due to a change in the associated surface energy. During demoulding, the surface of the concrete sticks out from the interface and increases its porosity. This may result in an increase in the roughness of the connection and also in the fracture energy of the interface. The failure bond strength is a function of the roughening material, concrete strength, texture depth, shape factor and the plot ratio of the adherend (Wang et al. 2014).

Tensile strength tests on butt jointed steel to steel were performed by Mays and Vardy (1982) for many adhesives. The surface preparation was found to have a significant effect (more than 150%) on the tensile strength of some adhesives. It was concluded that the strength of an interfacial connection depends more on the surface energy of the adherend than on the surface energy of the adhesive. Surface preparation done using grit-blasting with large diameter aggregates gave rougher surfaces, which in turn affected the bonding, due to the increased bond area. Fernando et al. (2013) could not observe any significant effect of the chemical composition of the bonded surface on the bond strength. Ekenel and Myers (2007) conducted tests and reported that surface roughness combined with crack injections significantly increased the flexural capacity of specimens and reduced the crack width openings, as compared to other carbon fiber reinforced plastic (CFRP) strengthened specimens.

Julio et al. (2006) used five roughness techniques, namely, casting against steel formwork, wire brushing, partially chipped, partially chipped and pre-wetted, and sand blasting on the concrete interface. The sand blasting technique gave the highest strength in shear and tension. Benzarti et al. (2011) reported that for fiber reinforced plastic FRP–concrete bonds, the sandblasting gives greater bond strength than hand grinding. Santos and Julio (2007) used three surface techniques, namely, casting in steel against steel formwork, wire brushing and sand blasting, to analyse the effect of surface roughness on bond strength in a specimen subjected to shear and tension. It was observed that the bond strength is a function of surface roughness. These aforementioned surface techniques were employed to connect hard to hard or hard to fresh concrete. It was observed that the bond strength in shear loading, at the bonding interface of concrete, is significantly affected by substrate moisture and roughness. The surface roughness changes the failure modes from adhesive to cohesive or mixed.

According to Santos et al. (2012), the bond strength of a composite specimen is influenced by the surface roughness and moisture content of the substrate. In the case of the specimen consisting of dry hardened substrate and fresh concrete, the bond strength is significantly influenced by the surface preparation/roughness of the hardened substrate. However, in the case of a saturated hardened substrate with fresh concrete, the bond strength decreases with an increase in surface moisture content. They also observed that the specimen with a saturated substrate attained lower bond strength, compared to the composite specimen with dry substrate. At the same shear stress level, the higher roughness (peak to valley height) stores more load (Papastergiou and Lebet 2014).

2.4 Need of the Study

The comparative behaviour of mechanical headed stud connected and adhesive bonded connected steel-concrete composite connections under monotonic as well as extreme loading has not been investigated in detail under push-out

specimens as well as beam specimens. The effect of amount and position of reinforcement on dowel strength of mechanical headed stud connectors have not been considered in design. The design strength of adhesive bonded steel-concrete composite connections has not been fairly proposed. The connection strength influencing factors has also not been considered in any design.

2.5 Objectives

On the basis of comprehensive review of the literature and need of the study, the following objectives based on state of the art have been identified:

- To study the behaviour of both mechanically connected and adhesive bonded steel-concrete composite members, and to evaluate the performance of connections strategy under monotonic and impact loading.
- To study the effects of variation in concrete strength, confining reinforcement arrangement and density on the behaviour of steel-concrete composite members using shear stud.
- To study the effect of variation in thickness of adhesive layer on the failure mechanism of a steel-concrete composite member, and to determine the optimum thickness of adhesive layer on the basis of desirable consequent failure mechanism, and connection strength.
- To study and compare the behaviour of steel-concrete composite beams connected using mechanical shear studs arranged in in-line and staggered pattern with that of adhesive bonded steel-concrete composite beam.

Chapter: 3

Materials and Methodology

3.1 Overview

The inherent characteristics of constituent materials, significantly affects the performance of composite members. The selection of the grades of the materials to obtain a composite member shall be based on the function of the member and the anticipated loads that the member is supposed to resist. Literature suggests that with the change in connecting material from headed stud connector to adhesive, the performance of steel-concrete composite member changes from ductile to brittle. Therefore, the suitability of a connecting material is determined based on the expected demands on interfacial connections. This chapter presents the details of the physical and mechanical properties of the materials used in the study, namely, steel, concrete, reinforcement bar, headed stud and structural adhesive along with their mathematical (FE) models.

The comparative behaviour of steel-concrete composite push-out specimens and full-scale steel-concrete composite beam members has been experimentally investigated. Instantaneous properties of connections have been examined by performing the push-out tests on standard steel-concrete composite specimens. The behaviour of composite push out test specimen under impact loading in terms of energy absorbance capacity has also been evaluated along with the flexural behaviour of full-scale composite beams for both mechanical headed shear stud connected and adhesive bonded. The results of experimental investigation of the steel-concrete composite push-out specimen have been validated through the finite element analysis using ABAQUS (HKS, 2013) software package.

The present chapter provides detailed descriptions on the material properties and methodology adopted for the various experiments and numerical models discussed.

3.2 Materials

The physical, chemical and microstructural properties of materials used and the connecting interface have been discussed in detail, along with their mathematical models for finite element analysis.

3.2.1 Concrete

The performance of steel-concrete composite members depends on the properties of the concrete slab. One of the objectives of this study is the evaluation of influence of the various concrete grades on the behaviour of composite members. To achieve this, slabs have been prepared using different normal and high strength concretes. Concrete mix proportioning has been carried out in accordance with the BIS 10262 (2009) and ACI 211 (2008) specifications. The concrete for all the slabs has been prepared using PPC cement with 10 mm and 20 mm aggregates, along with *Zone II* sand as specified in the BIS 383 (2016), tap water and superplasticizer. Ratio of ingredients for concrete mix proportioning and quantity of ingredients per cubic meter have been shown in *Table 3-1*.

Table 3-1: Ratio of ingredients for concrete mix proportioning

	Cement	Sand	Aggregate		Water	Plasticizer
			10 mm	20 mm		
Ratio (C_1)	1.00	1.57	1.95	1.70	0.48	0.0
(kg/m^3)	361.00	567.00	704.00	614.00	174.00	0.00
Ratio (C_2)	1.00	1.77	1.81	1.21	0.45	0.00
(kg/m^3)	385.00	702.10	718.31	478.88	173.8	0.00
Ratio (C_3)	1.00	1.58	1.67	1.2	0.38	0.60
(kg/m^3)	417.00	658.86	696.39	500.4	158.46	2.502
Ratio (C_4)	1.00	1.54	1.62	1.17	0.35	0.900
(kg/m^3)	432.00	665.28	699.84	505.44	151.2	3.89
Ratio (C_5)	1.00	1.14	1.81	1.20	0.32	1.51
(kg/m^3)	457.00	521.89	823.34	550.23	146.24	6.86

3.2.1.1 Compressive Strength Test

The compressive strength test has been performed on 150 mm size cubes, for all concretes grades. The average compressive strength$\left(f_{ck} \right)$ of concrete cubes at 7 days and at 28 days, as observed, have been reported in *Table 3-2*.

Table 3-2: Compressive strength of concrete cubes after 7 and 28 days

Designation	C_1	C_2	C_3	C_4	C_5
IS Designation	M 25	M 30	M 40	M 50	M 60
Compressive strength (MPa) (7 days)	26.27	32.01	37.25	73.95	61.33
Compressive strength (MPa) (28 days)	32.50	38.55	46.50	57.71	73.46

3.2.1.2 Flexural Strength Test

The flexural strength test has been performed on 100 mm × 100 mm × 500 mm size beams. The average flexural strength$\left(f_{ct}\right)$ of concrete beams at 7 days and at 28 days, as observed, have been reported in *Table 3-3*.

Table 3-3: Flexural strength of concrete beams after 7 and 28 days

Designation	C_1	C_2	C_3	C_4	C_5
IS Designation	M 25	M 30	M 40	M 50	M 60
Flexural strength (MPa) (7 days)	3.64	3.88	4.12	5.18	5.39
Flexural strength (MPa) (28 days)	4.02	4.14	4.29	5.32	5.64

3.2.1.3 Modulus of Elasticity

The modulus of elasticity for all thee prepared grades of concrete has been evaluated by conducting compression test on 150 mm × 300 mm standard specimens, as prescribed in ASTM C469/C469M (2014). The deformation in concrete specimens has been measured using one compressometer in longitudinal direction and one extensometer in lateral direction. The stress dependent loading rate of (0.241 ± 0.034 MPa/sec) has been maintained during the entire testing process. The applied load and the corresponding strain (longitudinal and lateral) has been measured (*i*) at the longitudinal strain of 0.00005, and (*ii*) at the load of 40% of the ultimate load. The modulus of elasticity has been calculated using equation (*3-1*) suggested by ASTM C469/C469M (2014), as given below,

$$E_c = \frac{\left(\sigma_{c2} - \sigma_{c1}\right)}{\left(\varepsilon_2 - 0.00005\right)} \qquad (3-1)$$

where, σ_{c1} is the stress corresponding to longitudinal strain ε_1 of 0.00005, and

σ_{c2} & ε_2 are stress and strain corresponding to a load level of 40% of the ultimate load. The elastic modulus obtained using equation (*3-1*) has been reported in *Table 3-4*.

Table 3-4: Elastic modulus of concrete along with concrete grades

Designation	C_1	C_2	C_3	C_4	C_5
IS Designation	M 25	M 30	M 40	M 50	M 60
Elastic Modulus (MPa)	25149	27556	31029	33849	38981

3.2.1.4 Analytical Model

The effective finite element simulation of concrete requires adequate estimation of linear and non-linear behaviour of material in terms of mathematical model. Several standard material models exist to capture the behaviour of concrete, such as, Drucker-Prager model, Mohr- Coulomb Plasticity model, Smeared Cracking model, Concrete Damaged Plasticity model. The present study requires adequate estimation of compressive and tensile behaviour of concrete. Concrete, as a material, exhibits entirely different properties in compression and tension. The propagation of cracks along with the post-cracking behaviour of concrete is a critical parameter that governs the selection of appropriate analytical model.

3.2.1.4.1.Elastic behaviour

The elastic behaviour of concrete has been modelled in ABAQUS (HKS, 2013) as a linear elastic material model with isotropic hysteretic properties. The value of density, elastic modulus and Poisson's ratio have been assigned, as obtained through the tests carried out on the material specimens. The mathematical expression governing the elastic behaviour of concrete is,

$$\sigma_{cc} = \varepsilon_{cc} E_c \qquad (3-2)$$

where, σ_{cc} is the stress in concrete at any instance, ε_{cc} is the strain in concrete at corresponding stress level, E_c is the Young's modulus of concrete.

3.2.1.4.2.Plastic behaviour

The plastic behaviour of concrete in the present study is simulated using the Concrete Damaged Plasticity (CDP) model. The model uses the concepts of

isotropic damaged elasticity in combination with isotropic plasticity (tensile and compressive) to incorporate the inelastic behaviour of concrete. The complete definition of CDP model in ABAQUS (HKS, 2013) requires the following obligatory parameters:

Dilation Angle - to incorporate the amount of plastic volumetric strain developed during plastic shearing. A default value of *36°* has been used during the entire plastic yielding.

Eccentricity - is the rate at which the function approaches the asymptote (the flow potential tends to a straight line as the eccentricity tends to zero). The default flow potential eccentricity (*0.1*) has been assigned, which implies that the material has almost the same dilation angle over a wide range of confining pressure stresses.

f_{b_0}/f_{c_0} - is the ratio of ultimate biaxial compressive stress to the ultimate uniaxial compressive stress. A default value of *1.16* has been adopted in this study.

K_c *(shape factor)* - is the ratio of the second stress invariant on the tensile meridian, to that on the compressive meridian, at initial yield for any given value of the pressure invariant *p* such that the maximum principal stress is negative. The value of shape factor must lie in the range of $0.5 \le K_c \le 1$. A default value of *0.667* has been used.

Viscosity Parameter - is the relaxation time of the viscoelastic system. Using the viscoplastic regularisation with a small value for the viscosity parameter (small compared to the characteristic time increment) usually helps in improving the rate of convergence of the model in the softening regime, without compromising the results. The default value of viscosity parameter is adopted as *0.00001* in this study.

The concrete damaged plasticity model assumes that the two main failure mechanisms in concrete are the compressive crushing and the tensile cracking.

3.2.1.4.3.Numerical model for compressive behaviour

The compressive behaviour of concrete, in the inelastic region, has been incorporated in CDP model using the equation (*3-2*), suggested by Carreira and Chu (1985).

$$\sigma_{cc} = \frac{\sigma_{cc}^{'} \gamma_m \left(\varepsilon_c / \varepsilon_c^{'} \right)}{\gamma_m - 1 + \left(\varepsilon_c / \varepsilon_c^{'} \right)^{\gamma_m}} \qquad (3-2)$$

where, σ_{cc} is the compressive stress in concrete (MPa), ε_c is the strain in concrete, $\sigma_{cc}^{'}$ is the ultimate compressive strength of concrete (MPa), $\varepsilon_c^{'}$ is the strain corresponding to $\sigma_{cc}^{'}$,

$$\varepsilon_c^{'} = \left(0.71 \times f_c^{'} + 168 \right) \times 10^{-5} \qquad (3-3)$$

where, $f_c^{'}$ is the characteristic strength of concrete cylinder at 28 days (applicable for compressive strength more than 20.7 MPa), γ_m is a material parameter and function of initial tangent modulus E_c, and is defined as

$$\gamma_m = \frac{1}{1 - \left(\sigma_{cc}^{'} / \varepsilon_c^{'} E_c \right)} \qquad (3-4)$$

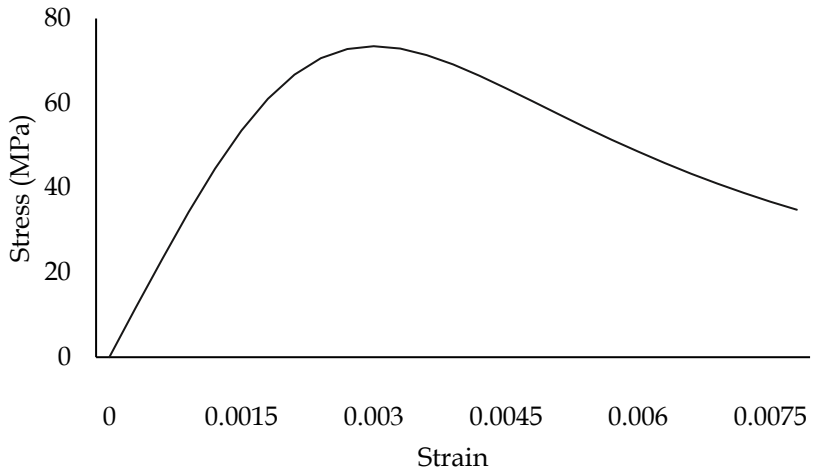

Fig. 3-1: Stress-strain curve for plain concrete in compression for M 60 (C_5) concrete

3.2.1.4.4.Numerical model for tensile behaviour

Under uniaxial tension, the stress-strain response of concrete remains linear in the elastic range followed by a brittle yield at failure stress, beyond which, microcracking in concrete initiates. This microcracking leads to strain localization at the section, that is mathematically represented by softening response in the

stress-strain relationship. The tensile behaviour of concrete given in equation (*3-5*), as suggested by Carreira and Chu (1986) has been employed to model the elasto-plastic material characteristics,

$$\left(\frac{\sigma_{ct}}{\sigma_{ct}^{'}}\right)=\frac{\gamma_m\left(\varepsilon/\varepsilon_t^{'}\right)}{\gamma_m-1+\left(\varepsilon/\varepsilon_t^{'}\right)^{\gamma_m}} \qquad (3-5)$$

where, σ_{ct} is the maximum tensile stress for concrete in MPa, and has been obtained as (Carreira and Chu 1986), $\varepsilon_t^{'}$ is the strain corresponding to with the maximum stress (unitless).

$$\sigma_t = 0.45\sqrt{\sigma_c} \qquad (3-6)$$

The tensile behaviour of concrete for finite element analysis has been defined by GFI type model. *Fig. 3-2(a)* shows the stress-strain behaviour of concrete under tension. The fracture energy has been used to define post cracking stress-displacement response of the brittle concrete material, and is shown in *Fig. 3-2(b)* The fracture energy G_f has been estimated using equation (*3-7*), suggested by Phillips and Binsheng (1993),

$$G_f = 30.5 + 6.64\left(f_t\right)^2 \qquad (3-7)$$

where, G_f is the fracture energy in N-m and f_t is the maximum tensile strength in MPa. If compressive strength of concrete f_{ck} is given, fracture energy is expressed, as,

$$G_f = 43.2 + 1.13 f_{ck} \qquad (3-8)$$

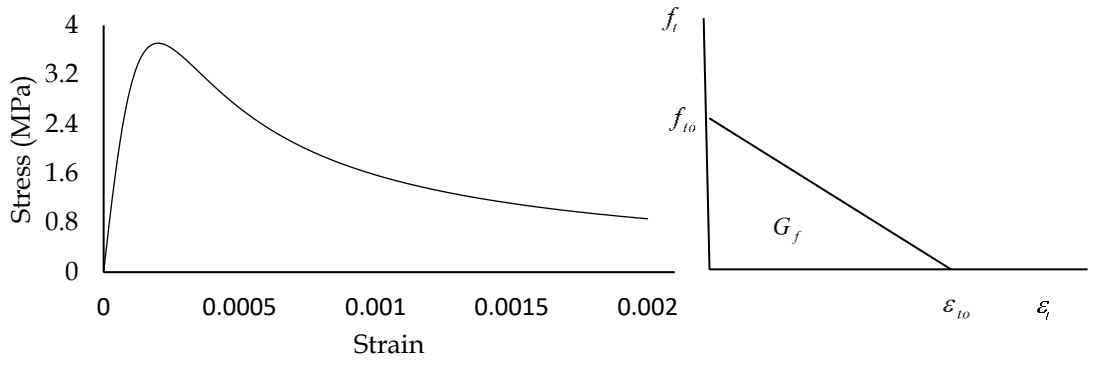

Fig. 3-2: Tensile stress-strain curve and fracture energy; (a) tensile stress-strain curve for concrete and (b) post failure idealization of stress-strain curve

3.2.2 Structural Steel

The mechanical properties of steel have been obtained by conducting tests on coupons taken from the sections used in this study.

3.2.2.1 Tensile Strength Test

The tensile strength tests have been carried out on coupons cut from steel flange and web of steel sections. The tensile test specimens, with circular cross-section, have been prepared in accordance with the BIS 1608 (2005). The schematic geometry and dimensional details of mild steel coupon have been shown in *Fig. 3-3*. A strain dependent loading rate of 70 μm/s has been maintained for the entire testing process. The yielded coupon has been shown in *Fig. 3-4*, a standard failure mechanism has been observed with the formation of the neck near the middle portion/ gauge length. For all the coupons, a cup-cone type failure has been observed. *Table 3-5* presents the mechanical properties (average) of tested coupons. The tested coupons have an average yield (0.2% offset) strength of 262.83 MPa and an ultimate strength of 423.67 MPa. Also, the tensile strain at initiation of elongation and ultimate failure have been obtained as 0.0136 and 0.319 respectively. *Fig. 3.5* shows applied load elongation curve of tensile test coupon.

Table 3-5: Tensile properties of coupons obtained from steel sections

Elastic modulus	Yield Stress	Yield strain	Ultimate stress	Ultimate strain	Failure strain	Elongation
(MPa)	(MPa)		(MPa)			(mm)
2002263.05	262.83	0.0136	423.67	0.189	0.319	8.93

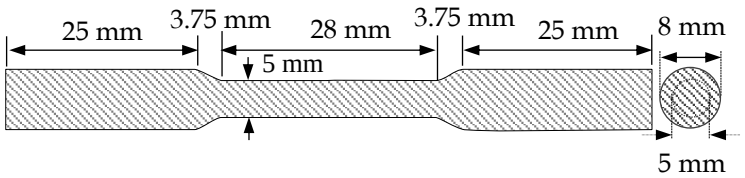

Fig. 3-3: Side view and cross-sectional view of circular tensile test coupon

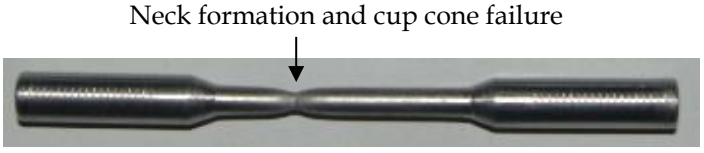

Fig. 3-4: Tensile test coupon after failure

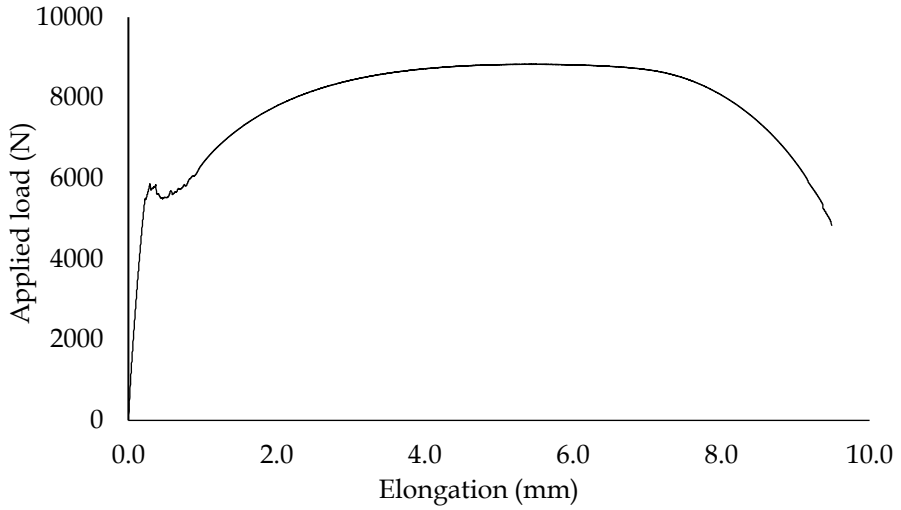

Fig. 3-5: Applied load-elongation curve for steel coupon under tensile loading

3.2.3 Reinforcement Bar

This section presents the details of the tests carried out to determine the mechanical properties of reinforcement bars.

3.2.3.1 Tensile Strength Test

The tensile properties of reinforcement bars, used to prepare the push out test specimens, are reported in this section. The tensile tests have been performed on 10 mm diameter reinforcement bar specimens of one meter length. The standard gauge length of $5.65\sqrt{d_r}$, where, d_r is the diameter of reinforcement bar, i.e. 50 mm was marked on each specimen in accordance with BIS 1786 (2008). Five identical reinforcement bar specimens have been subjected to tensile test on a universal testing machine of 1000 kN capacity. The tested bar specimens have an average yield strength of 500.44 MPa and ultimate tensile strength of 583.22 MPa at 23.04% elongation. The average load-elongation curve obtained from specimens (reinforcement bars) has been shown in *Fig. 3-6*.

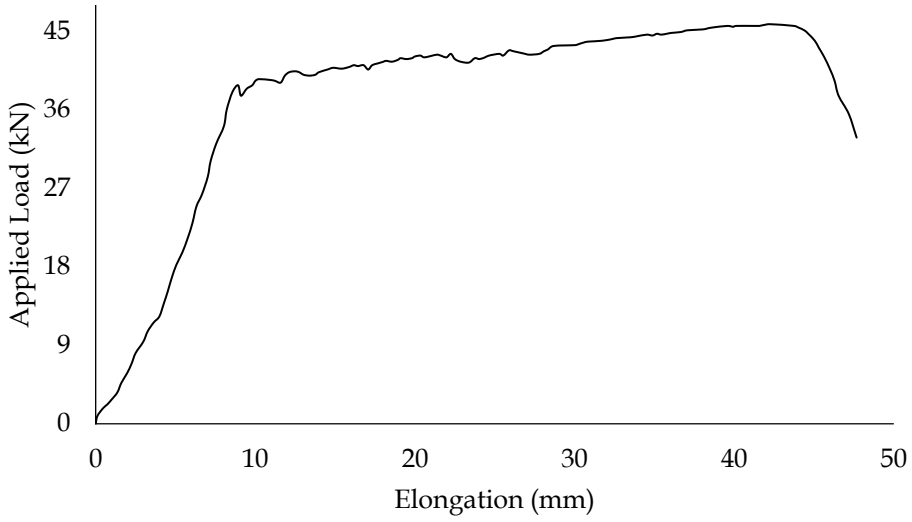

Fig. 3-6: Applied load-elongation curve for 10 mm diameter reinforcement bars

3.2.4 Mechanical Headed Stud

The strength of mechanically connected composite members depend on the mechanical properties of headed stud connectors and the properties of the weld between connector and steel section. This section presents the details and results of tests carried out to assess the mechanical properties of studs and welds, used in present study.

3.2.4.1 Tensile Strength Test

Tensile tests on stud shear connectors have been performed in accordance with BIS 1608 (2005) specifications. Circular coupons have been cut from the headed stud connectors to perform tensile tests. The rate of loading has been maintained at 70 μm/second for the entire testing process. *Fig. 3-3* shows the schematic geometry and dimensional details of circular mild steel coupons. Material characteristic properties obtained from tensile loading test have been reported in *Table 3-6*. The coupons have average yield (0.2% offset) strength of 321.97 MPa and ultimate strength of 517.04 MPa. The obtained tensile strain at initiation of elongation and ultimate failure strains are 0.0133 and 0.182 respectively.

Table 3-6: Tensile properties of headed stud connector specimens

Elastic modulus	Yield Stress	Yield strain	Ultimate stress	Ultimate strain	Failure strain	Elongation
(MPa)	(MPa)		(MPa)			(mm)
209187.15	321.97	0.01332	517.04	0.0668	0.182	5.113

3.2.4.2 Bend Test

Bend test is performed to assure the quality of welding used to connect the stud to the flange of the steel section. The test uses a benchmark behaviour to examine the quality of a selected welding technique. In this test the welded component is subjected to bending, such that, the component makes an angle of 45 degree with the horizontal after deformation, as suggested by BS EN ISO 14555 (2014). *Fig. 3-7* shows a deformed headed stud after the performance of weld test. Samples of headed studs, welded using two different welding processes (electrode welding and metal inert gas welding), have been tested. The metal inert gas welding technique has been found to be more suitable for welding of headed stud connectors.

Fig. 3-7: Deformed headed stud connector after bend test

3.2.4.3 Analytical Model

The accuracy of finite element analysis depends on adequate modelling of the material behaviour. The steel-concrete composite specimens consists of three independent steel elements, namely, reinforcement bars, headed studs and beam/column sections. A similar material model to structural steel has been

defined to effectively simulate the behaviour of steel elements in composite specimens. An elasto-plastic strain hardening model has been employed, with values obtained through coupon tests, to capture the material behaviour.

3.2.4.3.1 Elastic behaviour

The elastic part of the material model has been defined as linear with isotropic hysteretic properties. The value of density, elastic modulus and Poisson's ratio have been assigned, as obtained through the tests carried out on the individual material specimens. The elastic behaviour of steel has been defined to be governed by equation (*3-2*).

3.2.4.3.2 Inelastic behaviour

The inelastic or post-yield material behaviour has been defined using a bi-linear model, constituting a plastic region (represented by a strength plateau), followed by a strain hardening region (increasing strength with a gentle slope), upto the ultimate strain. The stress-strain curve for the tested structural steel coupon (refer *Table 3-5*), having the yield and ultimate strains of 0.0136 and 0.189 respectively, has been shown in *Fig. 3-8*.

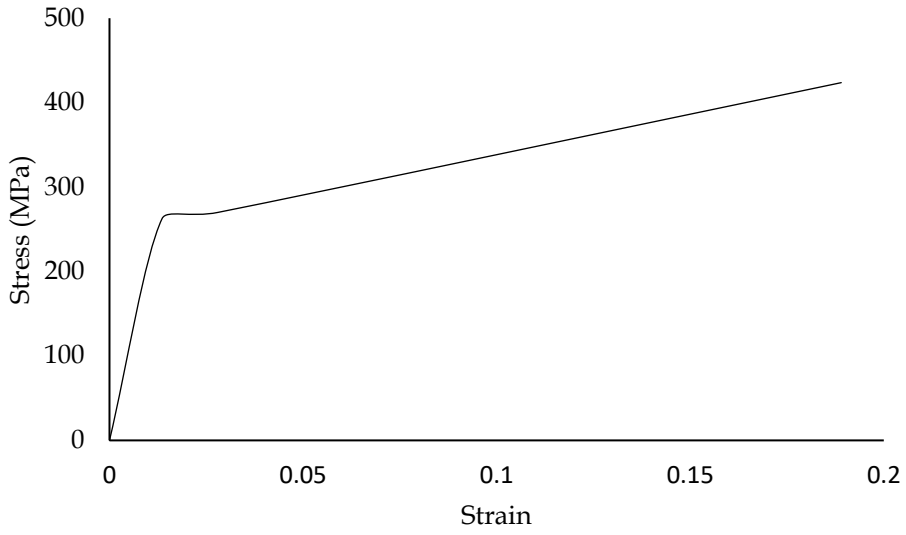

Fig. 3-8: Idealised tri-linear stress-strain curve for structural steel coupon

3.2.5 Structural Adhesive

3.2.5.1 Selection of Suitable Adhesive

Steel-concrete composite members require efficient connection between the elements, to ensure desirable performance with adequate strength. Structural adhesives are being used, rapidly, to establish strong and stiff connections between the elements of a composite member. A wide range of structural adhesives are available commercially, having distinct properties to serve different purposes. The most common of structural adhesives are, polyurethane based, polypropylene based and epoxy based. Selection of a particular adhesive for a composite member, depends on various factors, the most important being the connection strength and interfacial slip. In this study, an adhesive bonded composite connection has to be prepared. In order to select a particular type of adhesive to achieve the desired connection, a preliminary study has been conducted.

In the preliminary study, push-out tests on eighteen composite specimens, using six different type of adhesives (three identical specimens of each adhesive) have been carried out. Six types of adhesives, A, B, C, D, E and F (*Table 3-7*) have been selected for the preliminary study. The variations in total applied load with respect to the observed maximum relative slips, on log scale for all adhesives, have been shown in *Fig. 3-9*. *Table 3-7* presents the average ultimate strength and relative slip for three tested specimens, of each adhesive type. The results of the push-out tests indicate that adhesives A and B, which are polyurethane based adhesives, depict very low bond strength with high relative slip. However, epoxy based adhesives (adhesive C, D, E and F) show considerably higher ultimate strength with lesser slip. Among the tested epoxy based adhesives, adhesive C exhibited significantly higher relative slip at considerably lower strength, and has therefore been considered unsuitable for connection purposes. While, the adhesives D, E and F exhibit almost similar ultimate relative slip, also the ultimate strength in case of all adhesives varies significantly. This renders the ultimate bond strength as the deciding parameter for selection of adhesive type, thereby substantiating the use of Adhesive F as the bonding agent between steel and concrete, to ensure stiff and strong connection at the interface. Adhesive F is ASTM Type IV (load bearing)

epoxy resin based bonding system as per ASTM C881 (2010).

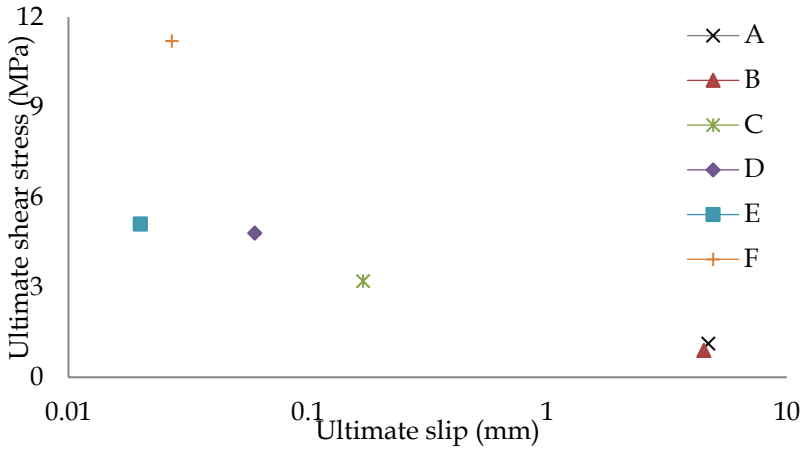

Fig. 3-9: Ultimate shear stress and corresponding relative slip for different adhesives

Table 3-7: Preliminary test results of structural adhesives under push out test

Adhesive	Material	Ultimate load (N)	Ultimate stress (MPa)	Ultimate slip (mm)
Adhesive-A	Polyurethane	8910	1.12	4.700
Adhesive-B	Polyurethane	7210	0.89	4.500
Adhesive-C	Epoxy	25920	3.2	0.37
Adhesive-D	Epoxy	41310	5.1*	0.02
Adhesive-E	Epoxy	38880	4.8	0.06
Adhesive-F	Epoxy	82620	10.2	0.027

**Not fully bonded due to low viscosity*

3.2.5.2 Properties of Selected Adhesive

Standard tests have been carried out to determine the various physical and mechanical properties of selected structural adhesive. The details of the same have been presented in this section.

3.2.5.3 Tensile Strength Test

Tensile strength tests on bulk epoxy specimens have been carried out as per ASTM D638 (2010) using prismatic coupons. The geometric details of rigid adhesive coupon for tensile test have been shown in *Fig. 3-10*. Strain based tensile load has been applied on the specimen at a constant rate of 17 µm/s. *Figs. 3-11(a)* and *(b)* shows the photographs of the specimen during the test, and after failure. *Fig. 3-12* shows the obtained stress-strain curve for bulk epoxy adhesive. The curve shows that the stress-strain relationship of bulk epoxy follows an almost linear path up

to failure. The behaviour of epoxy adhesive under tensile loading is unyielding (inflexible). The results of tensile test of bulk epoxy specimens, as reported in *Table 3-8.*

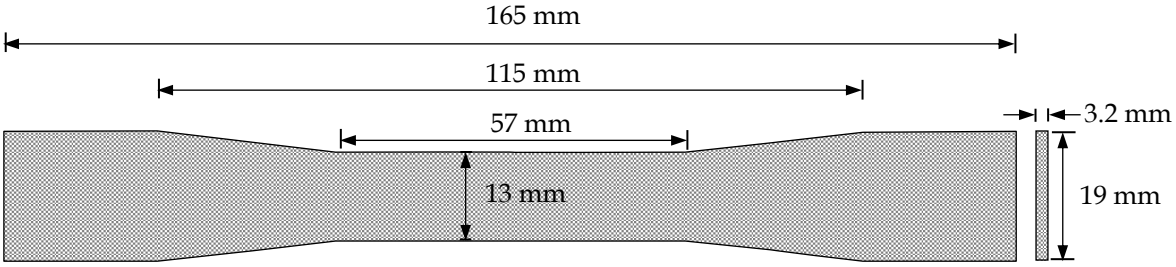

Fig. 3-10: Geometric details and shape of bulk epoxy adhesive specimen for tensile test

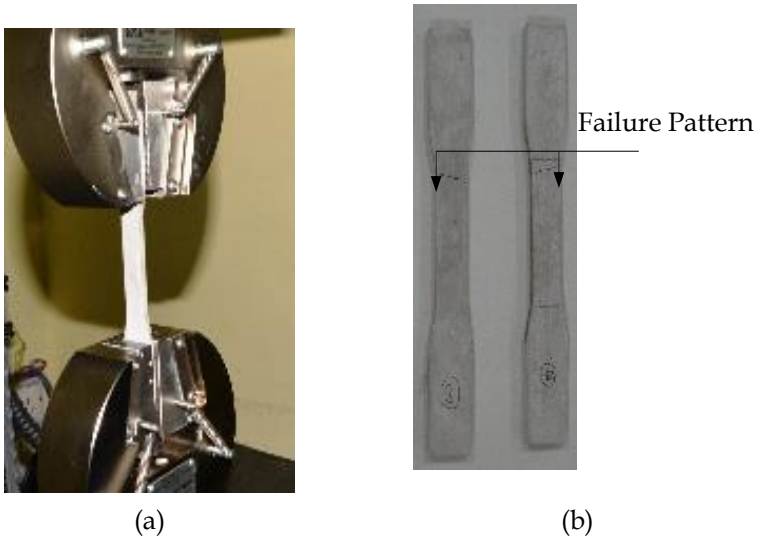

Fig. 3-11: Bulk epoxy specimen subjected under tensile loading in servo control universal testing machine and failed specimen, (a) epoxy specimen subjected under tensile loading in UTM and (b) epoxy specimen after tensile failure

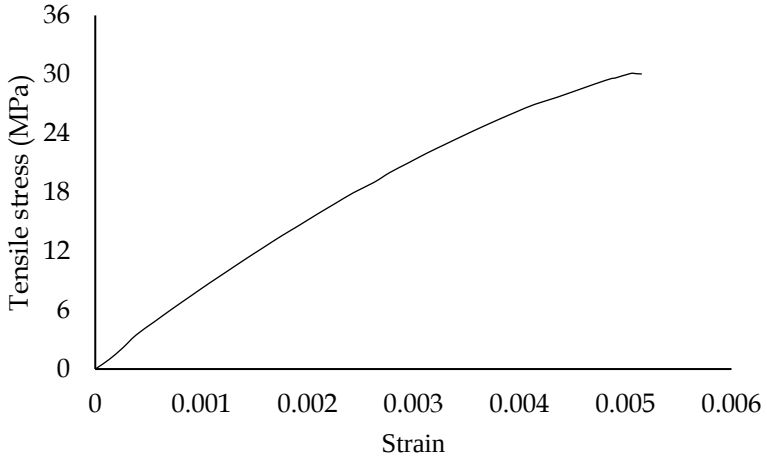

Fig. 3-12: Load-elongation curve for bulk epoxy adhesive specimen under tensile loading

Table 3-8: Tensile test results of bulk epoxy specimen

Yield stress	Yield strain	Ultimate stress	Ultimate strain	Failure strain	Elastic modulus
(MPa)	(mm/mm)	(MPa)	(mm/mm)	(mm/mm)	(MPa)
-	-	30.08	0.00496	0.00515	7551.88

3.2.5.4 Compressive Strength Test

Compressive strength tests on bulk epoxy specimens have been performed as per ASTM D695 (2015) specifications. Five identical cylindrical specimens of diameter 12.7 mm and height 25.4 mm have been subjected to compressive load in universal testing machine (UTM). A constant strain rate of 17 μm/s has been applied. *Fig. 3-13(a)* shows a schematic view of bulk epoxy cylindrical specimen, along with the geometric details. *Figs. 3-13(b)* and *3-13(c)* show the epoxy specimen subjected to compressive loading and the brittle failure of the specimen respectively. It can be observed that the failure plane is inclined at an angle of 45° from load bearing (horizontal) face representing shearing failure. The results of the compressive tests have been presented in *Table 3-9* and the stress-strain behaviour of epoxy specimen has been shown in *Fig. 3-14*.

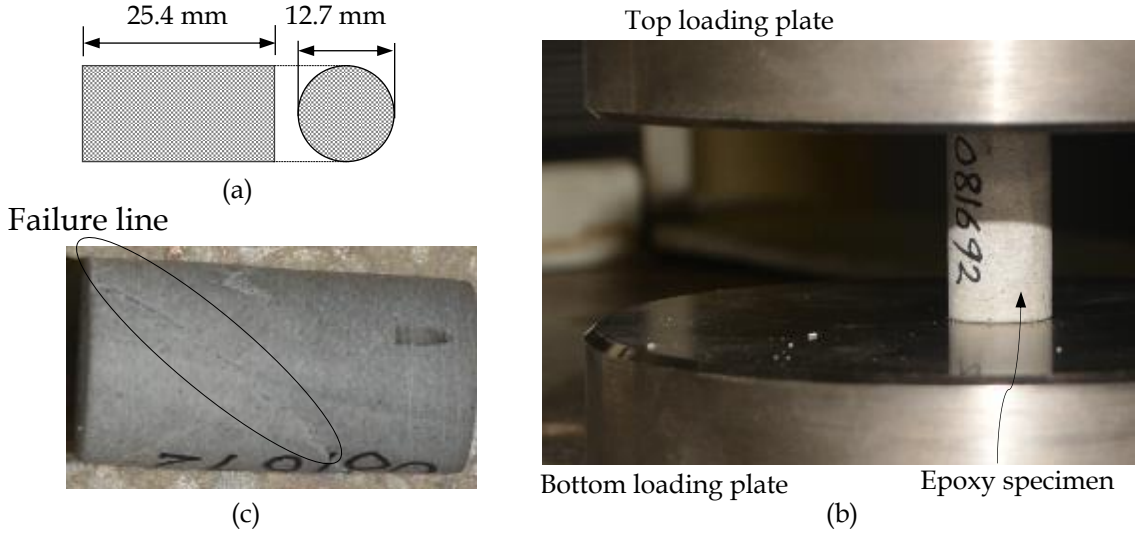

Fig. 3-13: Compressive testing; (a) side and cross-sectional view of circular compressive test specimen (b) specimen subjected under compressive loading and (c) specimen after failure

Table 3-9: Compressive test results of bulk epoxy specimen

Yield stress (MPa)	Yield strain (mm/mm)	Ultimate stress (MPa)	Ultimate strain (mm/mm)	Failure strain (mm/mm)	Elastic modulus (MPa)
73.94	0.0129	82.073	0.0228	0.0517	7537.78

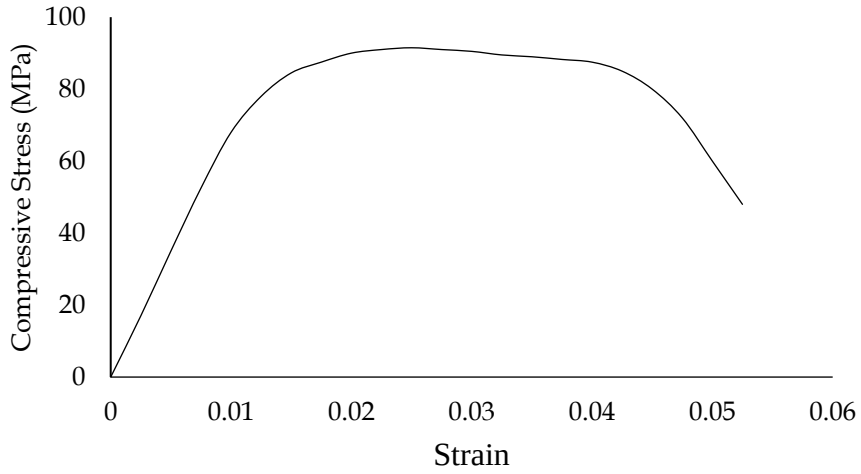

Fig. 3-14: Compressive stress-strain curve for bulk epoxy adhesive specimen under compressive loading

3.2.5.5 Dynamic Mechanical Analysis

To investigate the detailed physical properties, dynamic mechanical analysis (DMA) on bulk epoxy adhesive specimens has been carried out. The parameters of interest, estimated using DMA are storage modulus (E'), damping factor $(\tan\delta)$ and glass transition temperature (T_g) The effect of temperature variation has been studied by varying the temperature in the range of -10°C to 110°C, at a constant rate of 2°C/minute. Liquid nitrogen has been used to reduce the temperature below ambient temperature. The specimen has been subjected to a dynamic three-point bending load (*Fig. 3-15*), varying at a frequency of 1.0 Hz. *Fig. 3-16(a)* shows the variation of storage modulus, in terms of stiffness, with respect to temperature. It can be observed that the storage modulus remains constant up to a temperature of 57.5°C, beyond which it decreases linearly. *Fig. 3-16(b)* shows the change in damping factor $(\tan\delta)$ with temperature. The energy dissipation along with the glass transition temperature of adhesive specimen has been estimated through *Fig.*

3-16(b). The temperature at which the damping factor $(\tan\delta)$ vs temperature curve changes its direction is termed as the glass transition temperature.

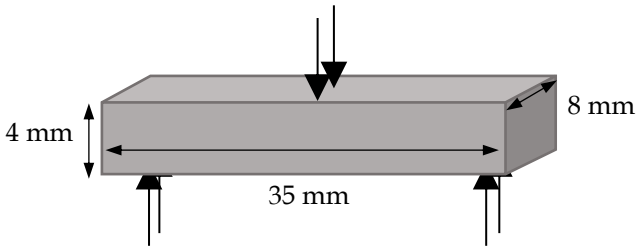

Fig. 3-15: Three point bending sample for dynamic mechanical analysis

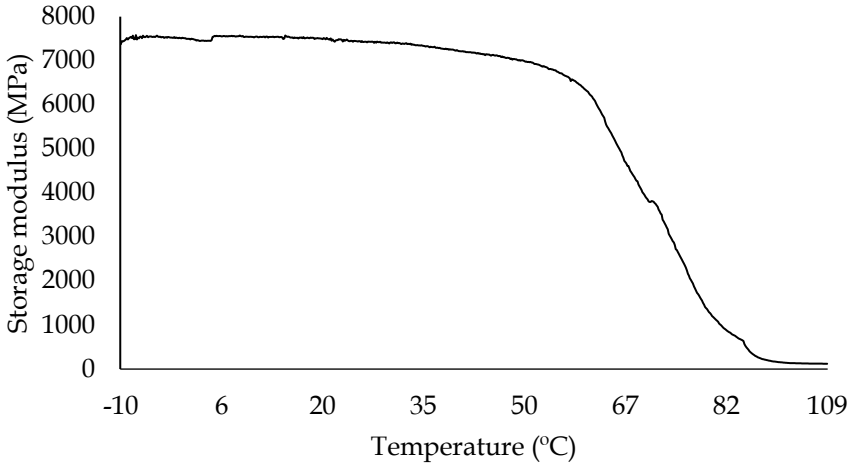

(a)

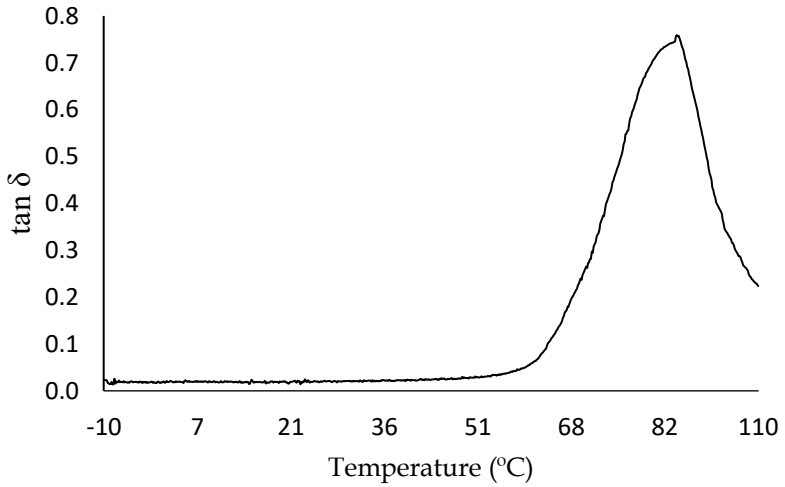

(b)

Fig. 3-16: Change in storage modulus and damping factor (tan δ) plot with temperature; (a) change in storage modulus with temperature curve and (b) change in damping parameter with temperature curve

It can be observed from *Fig. 3-16(b)* that there is no significant energy dissipation in adhesive specimen up to a temperature of 57.5°C, while the glass

transition temperature of epoxy adhesive has been observed to be 84.5°C. Beyond the glass transition temperature, the state of amorphous epoxy adhesive changes from solid to rubbery, along with a rapid decrement in damping ratio $(\tan\delta)$. The results of DMA analysis suggests that adhesive F (epoxy based) is a suitable material for bonding purposes in the temperature range from -10°C to 60°C without any noticeable deterioration.

3.2.5.6 Finite Element Modelling

The simulation of behaviour of epoxy adhesive in finite element analysis has been carried out using linear Drucker-Prager model. The use of von-Mises yield criteria along with hydrostatic stress sensitivity in the linear Druker-Prager model effectively captures the mechanical behaviour of epoxy adhesive. The material properties of adhesive defined for FE analysis purposes are obtained through tests on adhesive specimen as reported in *section 3.1.2*. The Linear Druker-Prager model criteria has been defined through equation (*3-9*), as,

$$\sigma_{ae} = \sigma_{ao} - \mu\sigma_m \qquad (3-9)$$

where, σ_{ae} is the effective stress induced in the adhesive; σ_{ao} is the yield stress of adhesive, defined as,

$$\sigma_{ao} = \sqrt{3}(\sigma_{as}) \qquad (3-10)$$

where, σ_{as} is the shear stress, and σ_m is the hydrostatic stress, defined as.

$$\sigma_m = \frac{1}{3}(\sigma_1 + \sigma_2 + \sigma_3) \qquad (3-11)$$

where, σ_1 , σ_2 and σ_3 are the normal stresses in X, Y and Z directions respectively.

Owing to the low shear strength of epoxy as compared to the tensile and compressive strengths, the linear Druker-Prager shear behaviour of adhesive has been considered in the modelling. The model requires the specification of certain parameters to simulate the behaviour of adhesive, namely, angle of internal friction (β), flow stress ratio (*K*), dilation angle (ψ) and flow potential eccentricity. Chiang and Herzl (1994) proposed a mathematical relation to estimate the values of angle of friction and flow stress ratio *(K)*, which is given as,

$$K = \left(\frac{2+\lambda}{2\lambda+1} \right) \qquad (3-12)$$

where, λ is the ratio of yield stress in uniaxial compression to uniaxial tension, which is 2.458 for epoxy based adhesive F (*section 3.2.5.2*). The value of flow stress ratio (K), as obtained using equation (*3-12*) is 0.753.

The value of arbitrary parameter μ depends on the properties of adhesive material and represents the sensitivity of yielding of adhesive material under hydrostatic stress $(\mu = \tan\beta)$. However, the angle of internal friction (β) is also a function of λ and is given as,

$$\beta = \tan^{-1}\left(\frac{3(\lambda-1)}{\lambda+2} \right) \qquad (3-13)$$

This gives an angle of internal friction (β) as 44.45°.

The associated flow behaviour (resultant of the strain increment during flow directed normal to the yield surface) has been assumed owing to the brittle nature of adhesives. Thus, the dilation angle (ψ) will be same as the angle of friction $(\beta = \psi)$. The default value of flow potential eccentricity (0.1) has been used for analysis purposes.

3.2.6 Microstructural Study on Composite Interface

The integrity of interfacial connection depends on the adequate bonding at the microstructural level. This section presents the evaluation of chemical bonding and microstructural properties at concrete-epoxy interface. On the basis of the tests described in the previous sections, epoxy based adhesive has been selected as the most appropriate binding agent at the steel-concrete composite interface. The extent of chemical bonding at the concrete-epoxy interface has been evaluated through Fourier Transform Infrared Spectroscopy test and microstructural surficial analysis.

3.2.6.1 Fourier Transform Infrared Spectroscopy (Spectrometry) Test

The bonding properties of concrete, epoxy and composite interface, have been investigated through Fourier transform infrared spectrometry (FT-IR). The

spectrometry provides an insight on the chemical bonds in concrete, epoxy and at their interface. The variations in absorbance with the wave number, obtained by FT-IR, have been shown in *Fig. 3-17*. The chemical bonds, developed in the materials have been distinguished through intensity peaks present at a certain wave number.

The relative shifts of the intensity peaks explicitly represent the characteristies and composition of bonding behaviour at the concrete-epoxy composite interface. The spectral data shown in *Fig. 3-17* illustrates the presence of –OH bond in the concrete and concrete-epoxy interface at wave number 3602.78 cm^{-1} and 3484.61cm^{-1} respectively. A slight decrease in the wave number of the interface sample can be clearly observed, which represents the desolation of –OH bond. A band of $–CH_2$ bond can also be observed at wave numbers 2925.38 cm^{-1} and 2867.14 cm^{-1} for the epoxy adhesive and composite interface, respectively. The relative shift of −58.24 cm^{-1} is evident in the case of the concrete-epoxy interface for the $-CH_2$ band bond. The shifting of intensity peaks towards lower wave numbers represents an increase in bond length, which signifies weaker bonds at the interface.

Wave numbers 1414.50 cm^{-1}, 1430.18 cm^{-1} and 1435.06 cm^{-1} represent the peaks for the concrete (-CO), epoxy and concrete-epoxy composite interface (-CH) respectively. However, the relative shift in the composite interface wave number is not significant. It can be concluded that this chemical bond band has a minor influence on the bond strength.

The formation of –SiO and -CH bond bands has been observed at wave numbers 990.06 cm^{-1} and 1081.33 cm^{-1} for concrete and epoxy respectively. For the composite interface, a bond band at wave number 1008.95 cm^{-1} has been observed. This chemical bond at composite interface, leads to the development of bond strength at the epoxy-concrete composite interface.

In addition to the above mentioned bond bands, the presence of -POC, -COC, and benzene ring in the epoxy adhesive and –Si-O-Si bond in the concrete element have also been observed. The peaks at the composite interface have similar intensity and wave number as those observed in the concrete and epoxy adhesive.

The comparable characteristics of the peaks show that, the bond bands have certain influence on the reaction mechanism, leading to enhanced bond strength at the composite interface.

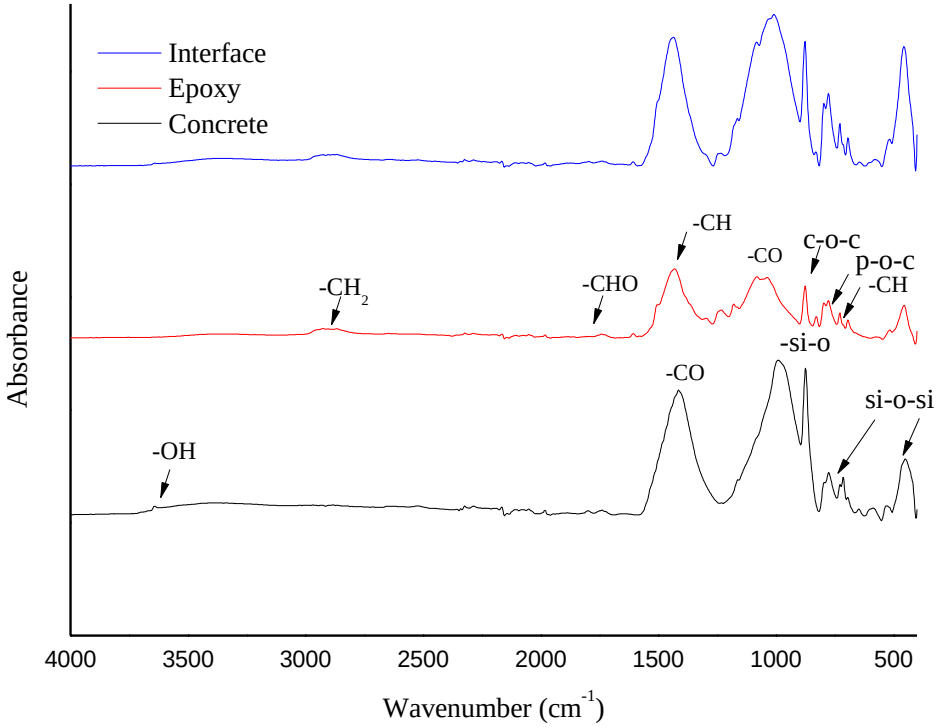

Fig. 3-17: FT-IR spectroscopy of concrete, epoxy and concrete-epoxy interface

3.2.6.2 Scanning Electron Microscopy

Scanning electron microscopy (back scattered electron technique) has been employed to analyse the concrete-epoxy interface at micro level. The interface has been analysed at different magnification levels to efficiently examine the interface bonding. *Fig. 3-18* shows the interface at the magnification levels of 150×, 1000× and 5000×. The interface layers can be clearly distinguished as concrete and epoxy, at higher magnification levels. The brighter area observed in the 150× image represents concrete, while the dark area corresponds to epoxy adhesive layer. Another observation drawn from the image is the near perfect bonding (absence of voids and cracks) between the concrete element and the adhesive layer. At 5000× level, the bonding due to the chemical reaction, between the concrete element and epoxy adhesive layer, is clearly visible.

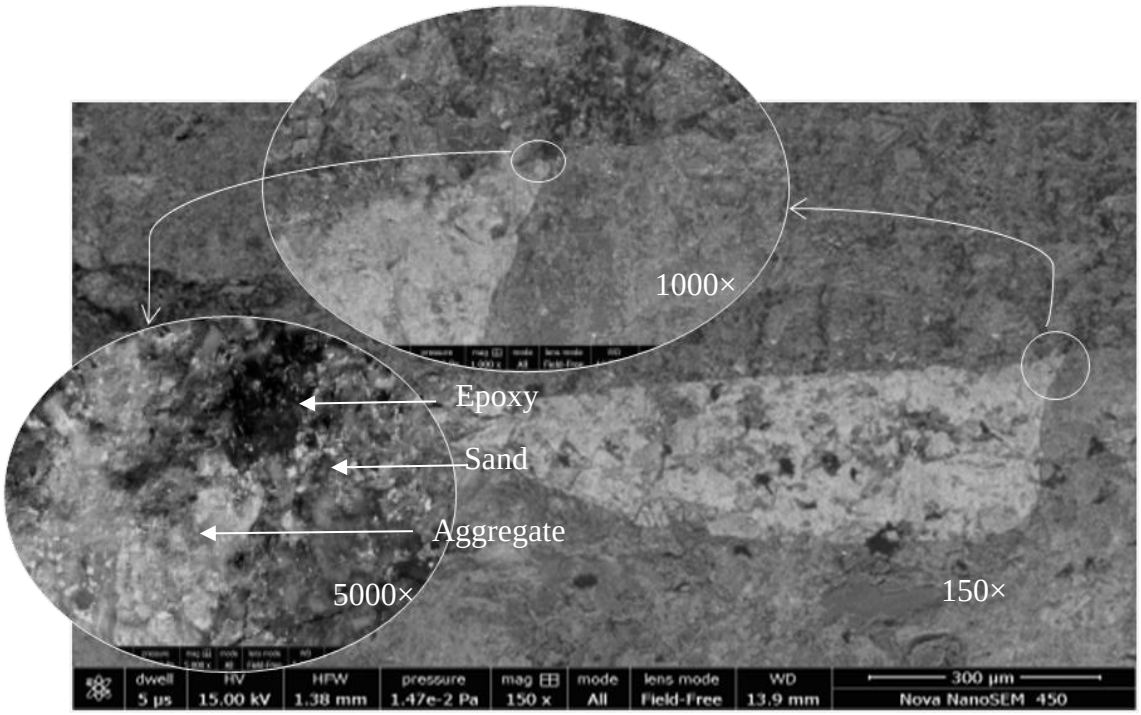

Fig. 3-18: Back scattered electron image of concrete-epoxy composite interface

3.3 Push-Out Test

The behaviour of steel-concrete composite specimens under direct shear has been evaluated using push-out test. For this purpose small-scale composite specimens have been prepared in the laboratory, and subjected to vertical push (compressive shear) such that the shear forces are introduced at the connecting interfaces, and consequently transferred from one element to another element through the connection. With the application of load, a relative slip is induced between the steel and concrete elements. The behaviour of composite specimens has been obtained in terms of applied load-engendered slip curves, and analyse to determine the connection properties, such as stiffness, ductility, strength capacity and relative slip. The push-out test specimens can be performed by two different methods, namely, *(i)* horizontal push out test, in accordance with BIS 11384 (1985, 2003) and *(ii)* vertical push out test in accordance with BS 5400 (2005), EC4 (2004) and IRC 22 (2015). In the present study, vertical push out tests have been carried out to determine the connection behaviour.

3.3.1 Vertical Push-Out Test

The vertical push-out test specimens consist of a steel beam of suitable size having welded mechanical shear connectors/bonded structural adhesive on both the flanges. The mechanical shear connectors have been embedded in concrete, by casting slabs of desired size and strength around them. Although, structural adhesive has been applied over area, as prepared for bonded between steel and concrete elements. The EC4 (2004) recommends that the concrete slabs, on either side of the steel flange, must be cast in horizontal position, so that the site conditions during composite deck construction at a site can be effectively simulated. The concrete slabs have been reinforced with 10 mm diameter reinforcement, in both longitudinal and transverse directions. The standard arrangement of a push-out test specimen as per EC4 (2004) has been shown in the *Fig. 3-19.*

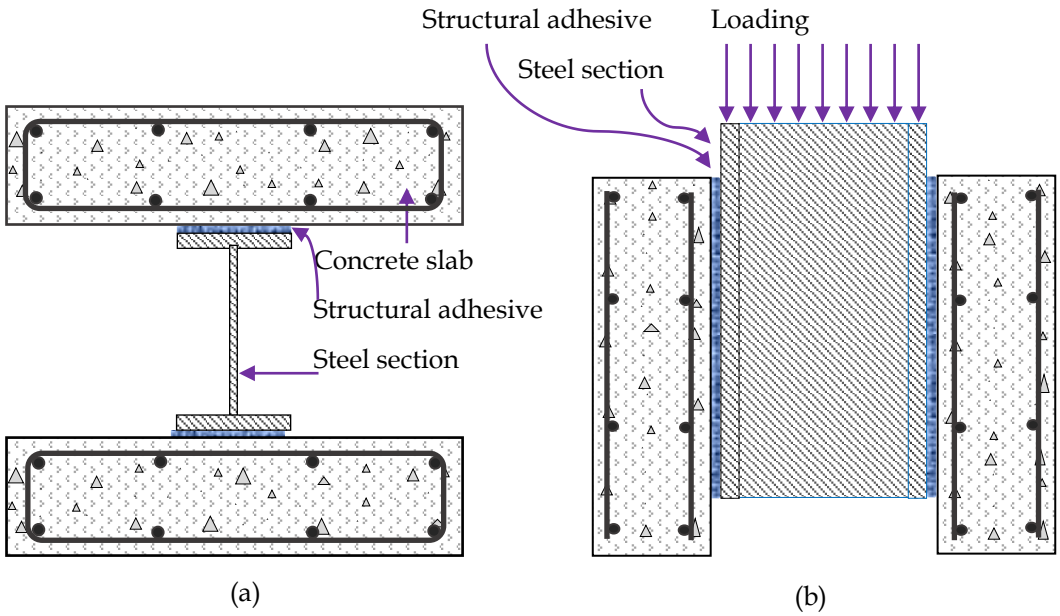

Fig. 3-19: Steel-concrete composite vertical push-out specimen bonded with adhesive as per EC4 (2004); (a) top view and (b) side view

As per the codal recommendations, the relative dimensions of the specimens, along with slab reinforcement have been adjusted according to the beam for which the test is being performed. The interfacial surface of the specimen has been thoroughly greased, to avoid the frictional resistance between steel and concrete. Four compression test concrete cubes or cylinders have been prepared

and cured along with the push-out test specimens, to obtain the compressive strength of concrete at the time of testing. The other mechanical properties such as Young's modulus, tensile strength and elongation etc. of shear connector, steel section and concrete material have also been measured by performing relevant tests.

The prepared specimens have been subjected to vertical compressive load. The specimens have been secured against any sudden lateral separation between steel and concrete by providing suitable restraining arrangement. As recommended by the code, initially the load has been applied in 25 steps of incremental vertical load, from 5% to 40% of the expected ultimate strength of connection, such that the occurrence of premature failure of the specimen has been eliminated. The longitudinal slip at the interface has been measured throughout the application of the incremental load to obtain the applied load vs. relative slip curve.

The code recommends that atleast three identical specimens should be tested, and the results of each test must not vary by more than 10% of the mean results. Further, the characteristic strength of the connection (Q_u), should be taken as 90% of the minimum failure load, while the ultimate slip (s_u) should be the maximum slip observed at the characteristic load level. Although, the values of corresponding slip should be taken as only 90% of the ultimate slip. The experimentally obtained applied load-relative slip curve shall also be used to evaluate the stiffness of the connection, as the secant of line joining the origin to the point on curve corresponding to 50% of characteristic load (as suggested in EC4 (2004)). The push out tests, reported in the subsequent chapters, have been carried out as per the described procedure.

3.4 Impact Test

Steel-concrete composites most commonly find their use in bridge structures. These are subjected to impact loading, often owing to vehicular impact, ship impact, aircraft impact etc. Impact loading is generally a concentrated loading, which usually has a frequency of 10^1 s^{-1}. Behaviour of composite members under

impact loading is significantly different from the behaviour under monotonic loading. The impact strength of a composite member depends on both structural resistance and energy absorption capacity of the member. Impact test comprises of two different loading schemes: large mass with low velocity or small mass with high velocity. Large mass with low velocity include tests like drop-weight, Charpy test and Izod test. The drop-weight test is preferred over other methods of impact testing as it offers highest flexibility in terms of specimen geometry. ACI 544 (2009) recommends drop-weight impact test on conventionally mixed and placed fibre reinforced concrete (FRC) or fibre reinforced shotcrete (FRS) using steel, glass, polymeric, and natural fibres.

Impact resistance of steel-concrete composite connections has been obtained by carring out experimental investigations. Static capacity of adhesive bonded and mechanical connected connection has been determined by push out test. Push out tests have been conducted to ensure that both type of connections have the same shear capacity. Subsequently drop-weight impact test has been performed to find absorbed energy by the composite connections.

Drop weight impact test has been carried out using the standard assembly of drop-weight impact test apparatus as shown in *Fig. 3-20*. 28 days cured composite specimens have been tested by the drop-weight impact testing assembly. All specimens have been subjected to impact at the centre by using hardened steel ball. The specifications provided by the ACI 544 (2009) have been used. The verticality of drop has been ensured by confining a vertical inclined pipe. The guide assembly for vertical drop was fixed to a column by clamping through the projection strips.

(a) (b)

Fig. 3-20: Drop-weight impact test apparatus; (a) guiding assembly and (b) impacter

Impact energy required for crack initiation $E_{dw,i}$ and for final failure $E_{dw,f}$ have been calculated by the equation (*3-14*) and equation (*3-15*) as given below:

$$E_{dw,i} = N_1 mgh_{dw} \qquad (3-14)$$

$$E_{dw,f} = N_2 mgh_{dw} \qquad (3-15)$$

where, N_1 and N_2 are the number of blows at crack initiation and final failure level, m is the mass of impacter, g is earth gravitational acceleration (9.81 m/s^2) and h_{dw} is the releasing height of impacter.

3.5 Flexural (Bending) Test

The flexural behaviour of steel-concrete composite specimens has been investigated by carrying out two point flexural test on full-scale beams. The discontinuous lateral ends of composite beam supported in simply supported condition. The distributed loading has been applied at two different point of composite beam on beam. The general schematic assembly of loaded composite beam has been shown in *Fig. 3-21*. The comparative behaviour of all three (mechanical headed stud connectors connected and adhesive bonded) kind of beam specimens has been studied. The load-deformation curves at different span positions and load-slip curves at the end positions have been obtained to compare the composite behaviour.

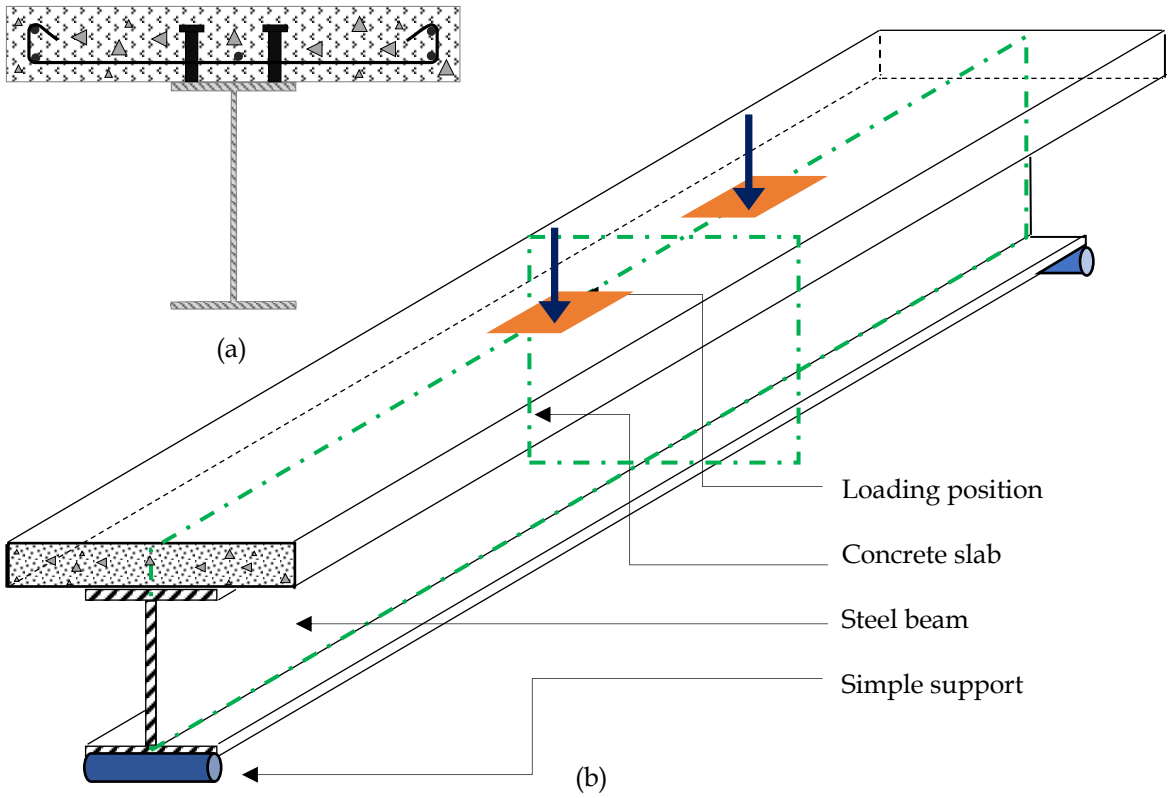

Fig. 3-21: Mechanical headed stud connected steel-concrete composite simply supported beam; (a) cross-sectional view and (b) isometric view

3.6 Conclusions

Physical, mechanical, chemical and microstructural properties of materials used in in the present study are necessary to understand the behaviour of composite member. Experiments have been carried out to understand the elementary behaviour of concrete, structural steel, reinforcement bar, headed stud and adhesive. The conclusions drawn from the observations are as follows:

- The mix design of concrete followed in this study established a good relation between compressive strength and modulus of elasticity. An increase in the value of empirical constant $\left(E_c/\sqrt{f_{ck}}\right)$ has been observed with increase in compressive strength from C_1 to C_5.
- The steel utilised in present study shows typical load-elongation pattern under tensile loading. The yield and ultimate strength values for structural steel are 262.83 MPa and 423.67 MPa, respectively. However, the values for headed stud observed are 321.04 MPa and 517.04 MPa, respectively. The

ultimate failure strains for structural steel and headed stud are 0.319 and 0.182, respectively.

- The quality of welding to connect structural steel and headed stud has been ensured by Bend test. Metal inert gas type welding has been found to be suitable for the present study.
- The epoxy resin based structural adhesive has been selected based on preliminary study. The adhesive has exhibited brittle behaviour under tensile loading with ultimate strength of 30.08 MPa. The failure strain of 0.00515 is observed without clear yield point.
- The bond behaviour at concrete and adhesive interface has been ensured by chemical and microstructural analysis.
- The chemical bond behaviour studied through FT-IR demonstrates that the composite interface has stronger bond band than concrete and slightly weaker than epoxy. The interfacial strength influencing bond band has been observed at 990.06 cm^{-1} for concrete, 1081.33 cm^{-1} for epoxy, 1008.95 cm^{-1} at composite interface.
- The microstructural investigation (BSE imaging) reveals a near perfect bonding behaviour between concrete and adhesive layer.
- Dynamic mechanical analysis of selected epoxy adhesive suggests the applicability in structural operating range for temperatures in steel-concrete composite construction.

Chapter: 4

Comparative Behaviour of Mechanically Connected and Adhesive Bonded Connections

4.1 Overview

The type of connection employed, determines the behaviour as well as failure mechanism of a steel-concrete composite connection. In this chapter, two types of connections, namely, mechanical headed studs and structural adhesive, have been analysed. The composite behaviour of connections, using each of the two techniques, have been critically evaluated by conducting push-out test. The behaviour of composite push-out test specimens under monotonic as well as impact loading have been compared. The push-out tests have been conducted on steel-concrete composite specimens, as per the monotonic loading procedure suggested in EC4 (2004). The applied load-relative slip behaviour of composite connections, connected with mechanically headed stud and structural adhesive has been compared. The behaviour has been compared in terms of connection strength capacity, maximum relative slip, stiffness and connection influence area.

The effect of impact loading on the behaviour of connections has been evaluated through Drop Weight Impact Test. The drop weight impact test has been performed as per ACI recommendations (ACI 544 2009). The energy absorption capacity of individual connection strategy has been adopted as a criteria to estimate the impact resistance.

4.2 Materials Used

4.2.1 Concrete

For the present study, the steel-concrete composite push-out test specimens have been prepared using the normal strength concrete (C_1) (*Table 3-2*). The 28 days compressive strength of cured concrete cube is 32.50 MPa.

4.2.2 Steel Section

Universal steel column sections have been used to prepare the steel-concrete composite specimens. Two types of specimens have been prepared, namely,

mechanical connected and adhesive bonded. The mechanical headed studs connected specimens have been prepared using the Universal Column section (UC) 203@46 kg/m (400 mm length), while the adhesive bonded specimens have been prepared using the UC 152 @37 kg/m section, cut to the length of 350 mm. The geometric details of both steel colum sections have been detailed in *Table 4-1*. *Fig. 4-1* shows a schematic view of structurl steel section (UC 203@46 kg/m).

Table 4-1: Geometric details of structural steel sections

Description	Sectional weight	Total depth	Flange width	Thickness of web	Thickness of flange	Area
	(kg/m)	(mm)	(mm)	(mm)	(mm)	(mm^2)
UC 203 × 203 × 46	46.1	203.2	203.6	7.2	11	5872
UC 152 × 152 × 37	37.0	161.8	154.4	8.0	11.5	4711

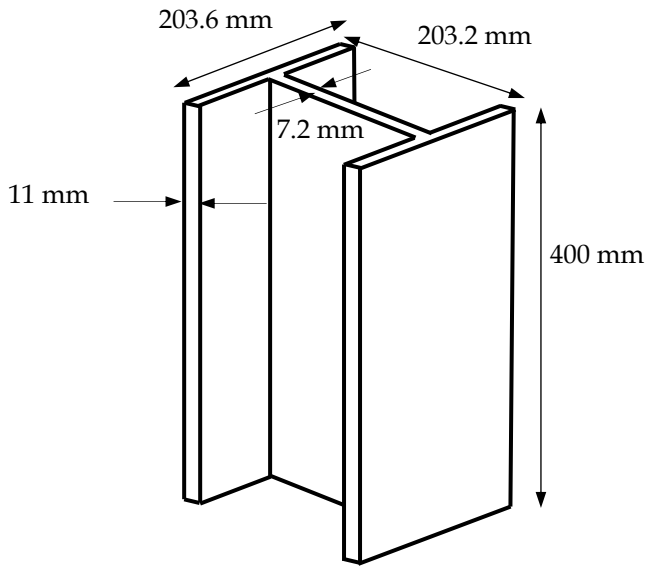

Fig. 4-1: Geometric details of structural steel section (UC 203@46 kg/m)

4.2.3 Headed Stud

In case of steel-concrete joints with mechanical headed studs, the composite specimens have been prepared using headed shear stud manufactured by Nelson®. The present study employs the headed studs of diameter 19 mm and height 100 mm for the mechanically connected specimens. The geometrical properties of a headed stud shear connector used have been shown in *Fig. 4-2*. The assembly of

headed studs, welded on the both flanges of the steel section, at a distance of 200 mm from the loading side, has been shown in *Figs. 4-3*(*a*), (*b*) and (*c*).

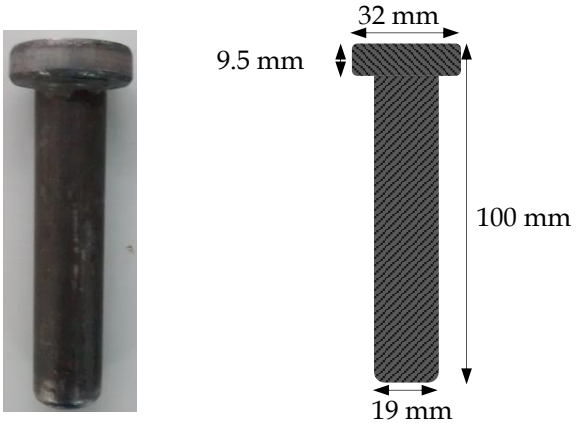

Fig. 4-2: Detailed geometry of headed stud connector

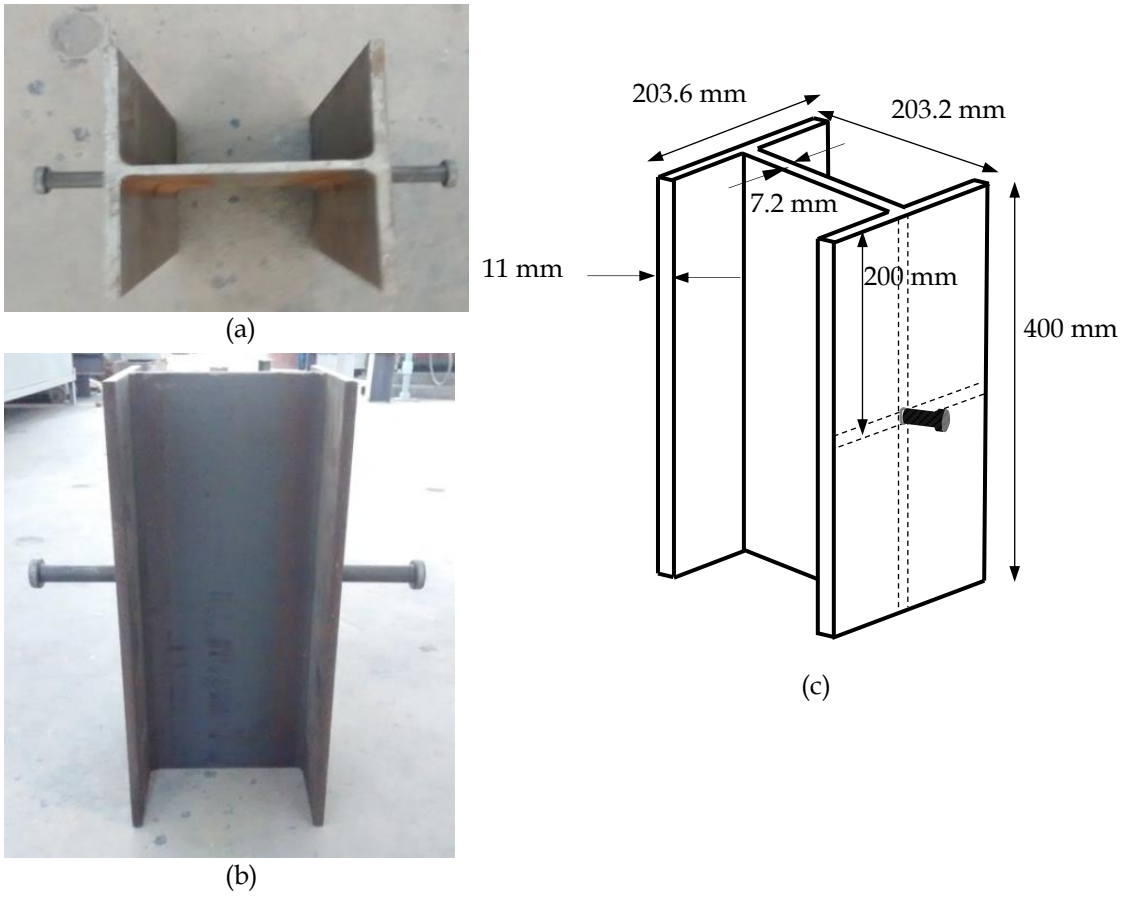

Fig. 4-3: Headed stud connector welded steel section; (a) top view, (b) front view and (c) isometric view

4.2.4 Structural Adhesive

The epoxy based structural adhesive, selected on the basis of a preliminary study, as discussed in *section 3.2.5.1*, has been used. The physical, mechanical, chemical and microstructural properties of selected adhesive have been discussed in detail in the previous Chapter (*section 3.2.5.2*). The adhesive bonded specimens have been prepared by keeping the aspect ratio of the bonded area to be unity. *Fig. 4-4(a)* shows the outline of the bonded area on the concrete surface of the prepared specimens. A schematic representation showing the geometry of bonded area on steel surface has been shown in *Fig. 4-4(b)*.

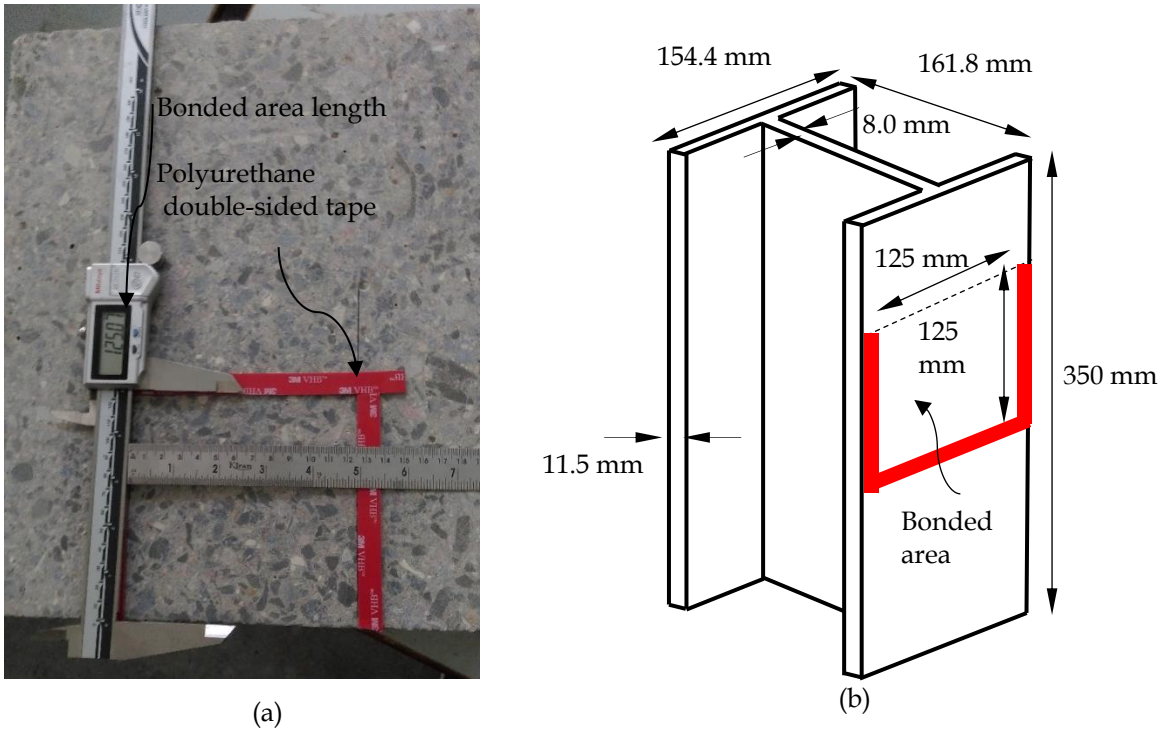

Fig. 4-4: Adhesive bonded steel section, (a) prepared area for adhesive application in concrete specimen and (b) prepared steel section for adhesive application

4.3 Experimental Procedure

The experimental studies on steel-concrete composite push-out test specimens, for monotonic as well as impact loading, have been carried out. The adopted procedure is discussed in details, in this section.

4.3.1 Static Push-Out Test Procedure

The vertical push-out tests have been performed in accordance with EC4 (2004).

The monotonic loading procedure, adopted to obtain the connection properties under incremental loading, such as, strength of connection, relative slip, stiffness etc., has already been discussed in Chapter three (*section 3.3.1*). The geometric details of individual elements, used for preparation of composite specimens, have also been discussed in *section 4.2*. The geometrical details of both (mechanically connected and adhesive boned) push-out test specimens have been shown in *Fig. 4-5*. A constant stress based loading (0.14 kN/sec) has been applied on the specimens during the testing procedure.

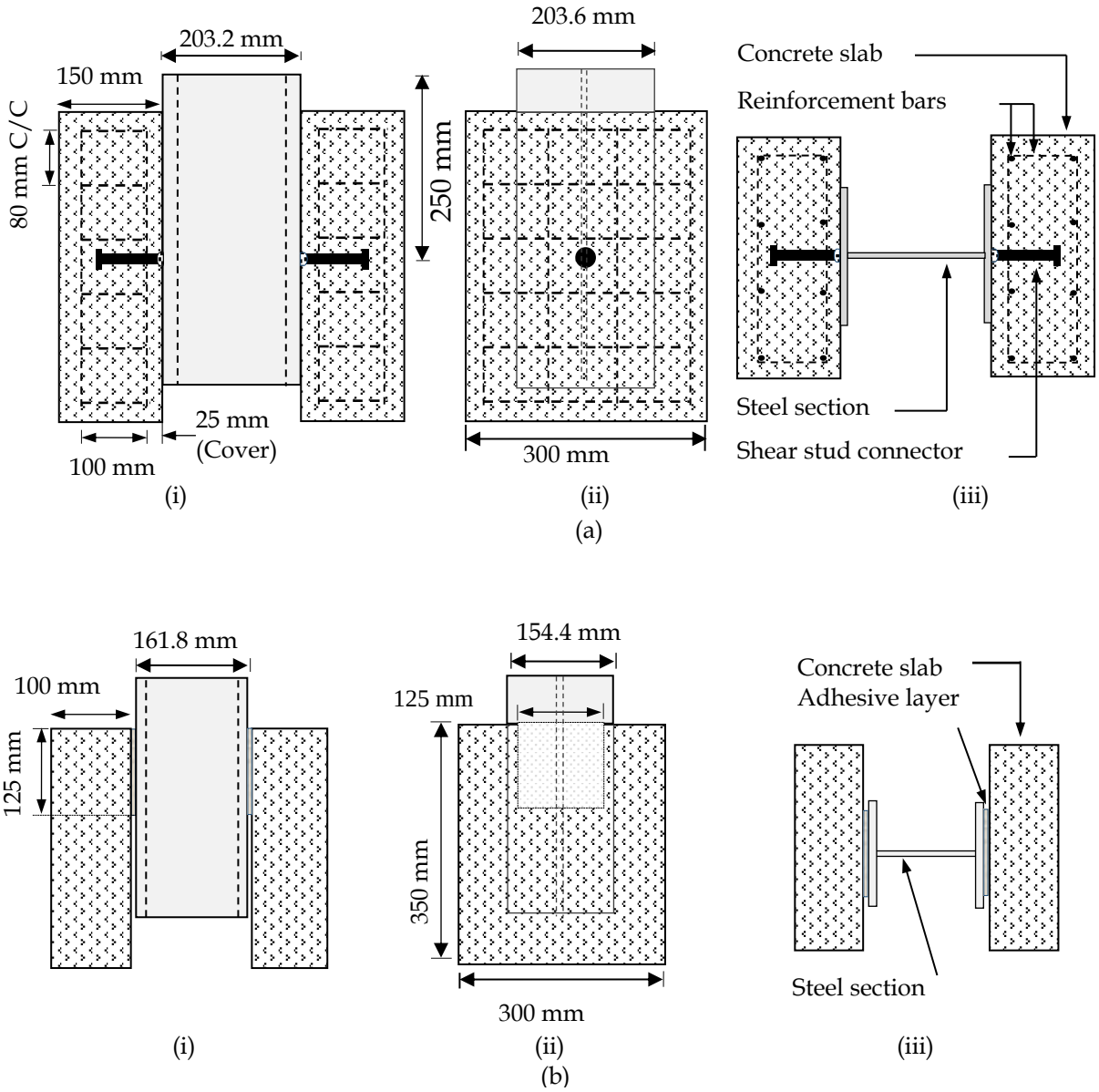

Fig. 4-5: Vertical Push-out test specimen; (a) headed stud connected steel-concrete composite specimen; (i) front view, (ii) side view and (iii) top view, and (b) adhesive bonded steel-concrete composite specimen; (i) front view, (ii) side view and (iii) top view

Two Linear Variable Differential Transformers (LVDTs) have been mounted on the both sides of steel section, to capture the relative slip at steel-concrete interface. The relative slip has been measured in the direction of loading, at the mid-height of bonded area in case of adhesive bonded specimens, and at the location of headed studs in case of mechanically connected specimens. A load cell has been mounted at the top of the steel section to capture the load, concurrently. A data logger has been used to log the data of the applied load and the induced relative slip at steel-concrete interface. The detailed test set-up, along with the arrangement of LVDTs has been shown in *Fig. 4-6*. To avoid the possibility of any accident during testing, an outer horizontal assembly, as shown in *Fig. 4-7* has been provided. Non participation of the holding assembly on the load path has been ensured by maintaining a clear gap of 10 - 20 mm, between the holding assembly and the concrete slabs, throughout the length and width of concrete slabs. The holding assembly has been placed over the loading platform as evident through the figure.

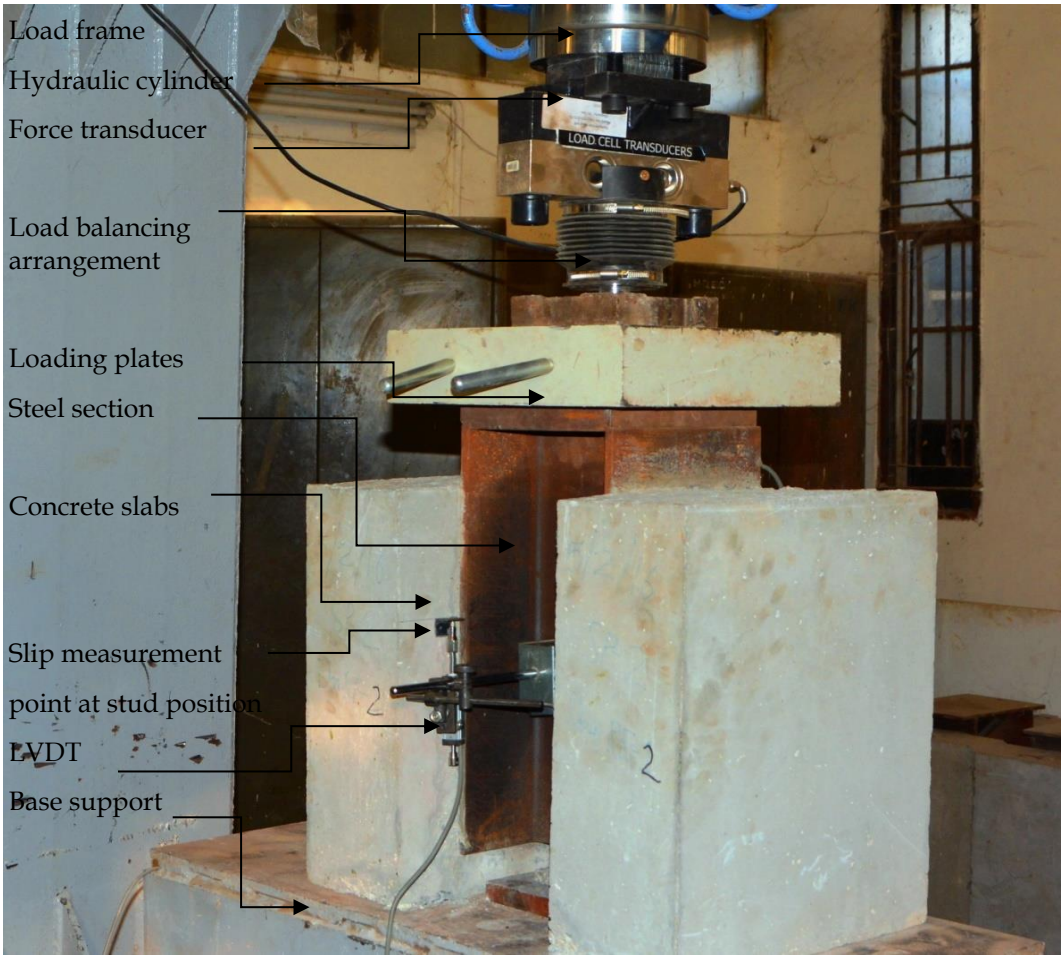

Fig. 4-6: Arrangement of Push out test assembly with loading arrangement for load-slip

Fig. 4-7: Holding assembly for composite specimen to prevent accidental damage

The maximum shear stress (for adhesive bonded connection) $S_{\max.}$ (MPa) is obtained using equation (*4-1*), as,

$$S_{\max.} = \frac{1}{2}\left(\frac{Q_u}{A_{bc}}\right) \qquad (4-1)$$

where, Q_u is the maximum load resistance of composite connection (kN) and A_{bc} is the bonded area (mm^2) of concrete (or steel) element, on one side. Steel-concrete composite specimen has two shearing faces on either side of the steel section. Therefore, a coefficient $(1/2)$ is applied in equation (*4-1*).

The maximum shear resistance (for mechanical headed stud connection) Q_u is obtained using equation (*4-2*), as,

$$Q_u = \left(\frac{P_u}{N_s}\right) \qquad (4-2)$$

where, P_u is the total applied load in kN, N_s is the total number of connectors in a composite specimen.

The performance of composite connections depend on their shear stiffness and the degree of interaction. The shear stiffness is generally estimated on the basis of either the slope of shear resistance-relative slip curve or shear capacity of the

composite connections. Researchers (Johnson and May 1975; Oehlers and Coughlan 1986; Wang 1998) have suggested different methods to determine the shear stiffness of connections. The methods based on the shear capacity of connection include some empirical coefficients, that can be applied only for that particular type of shear connector. While, on the basis of the load-slip behaviour, the stiffness of any connection is defined using the secant modulus within the elastic range. Oehlers and Bradford (2013) reported that the slope of total applied load-relative slip curve follows a linear path for a substantial range of loading, and the ratio of total applied load and corresponding deformation in this range is known as initial shear stiffness (*Fig. 2-1*). According to EC4 (2004), shear stiffness is the ratio of 70% of the maximum shear resistance of connection and the corresponding slip at composite interace. Thus, the initial shear stiffness k_i is estimated using equation (4-3), as,

$$k_i = (0.7)\frac{(Q_u)}{s} \qquad (4-3)$$

where, Q_u is the maximum shear resistanceof the composite connection and s is the relative slip corresponding to a load level of $0.7Q_u$. As the relative slip at each interface is due to the shear force experienced by each bonded interface (which inturn is half of the total applied force), the shear stiffness is estimated on the basis of the force experienced by each interface. However, for correct estimation of shear stiffness, the relative slip corresponding to the load level of $0.7Q_u$ has been considered.

4.3.2 Drop Weight Impact Test Procedure

The behaviour of the composite specimens under impact loading has been observed using drop-weight impact test apparatus, as shown in *Fig. 4-8*. Composite specimens, prepared using mechanically connected headed studs as well as with adhesive bonds, have been subjected to impact along the centroidal axis of steel section, using a mild steel ball weighing 4.54 kg. The specification prescribed in the ACI Committee 544 report (ACI 544 2009) recommending a drop height of 457 mm, has been adopted for testing the first specimen. However, no

crack initiation has been observed for this drop height, even after 750 blows. Hence, an increased drop height of 1500 mm has been used to test the impact behaviour of later specimens. The guide assembly for vertical drop has been clamped to a column using projection strips. *Fig. 4-8(a)* shows a push out test specimen prepared for Drop Weight Impact test, and *Fig. 4-8(b)* shows whole assembly of Drop Weight Impact Test, along with the specimen.

(a) (b)

Fig. 4-8: (a) steel-concrete composite specimen prepared for drop weight impact test and (b) testing arrangement with specimen

4.4 Connection Behaviour under Static Loading

The behaviours of mechanical shear stud connected and epoxy adhesive bonded composite specimens, under static loading, have been evaluated and compared in this section. *Fig. 4-9* shows the total applied load - relative slip curves for adhesive bonded (3 mm thick adhesive layer) and mechanical headed stud connected (diameter 19 mm and height 100 mm) specimens, underlining the comparative performance of both the connections. The comparision of applied load - relative slip curves (*Fig. 4-9*), demonstrates that the adhesive bonded specimens exhibits higher degree of connection as compared to that exhibited by mechanical headed studed connected specimens.

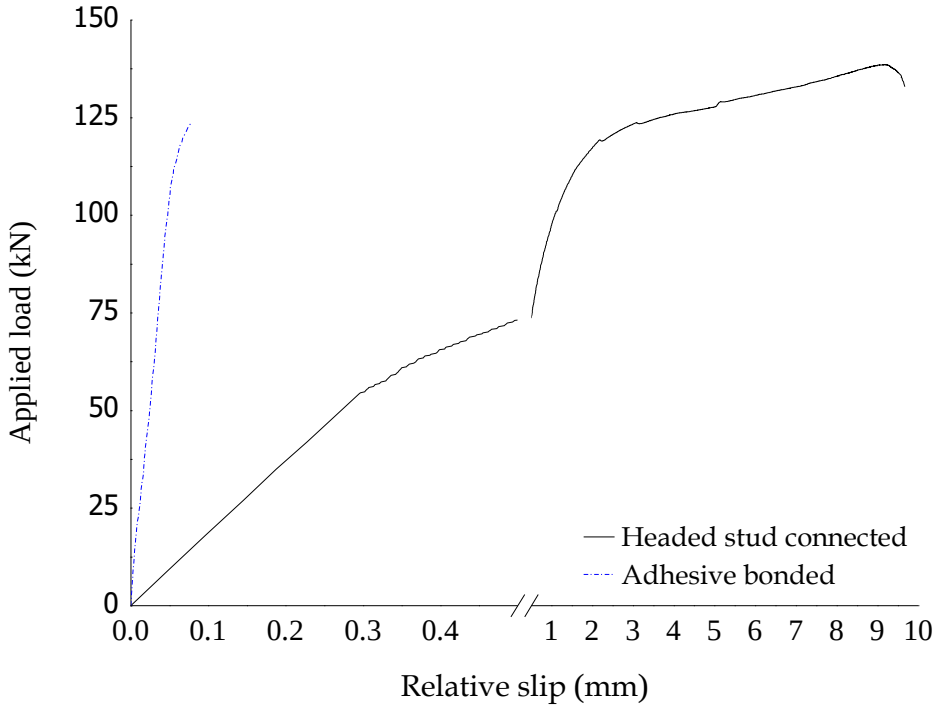

Fig. 4-9: Total applied load-relative slip plot for mechanical stud shear connector and adhesive bonded steel-concrete composite connections

4.4.1 Shear Resistance and Relative Slip

The shear resistance and the induced relative slip at the composite interface, observed for the specimens with headed stud connectors and epoxy adhesive bond, have been listed in *Table 4-2*. The difference in strength and ductility, for both the connection schemes has also been presented. Based on the observed values, it can be concluded that the connections with adhesive bonds exhibits almost negligible flexibility, when compared to the significantly ductile connections achieved through mechanical headed studs. An almost similar strength of the two connection strategies can also be noted through the results obtained.

Table 4-2: Applied load, shear resistance and ultimate slip for headed stud connected and adhesive bonded composite specimen

Connector category	Ultimate applied load (kN)	Shear resistance (MPa)	Ultimate relative slip (mm)
Headed stud connector-(19 mm× 100 mm)	277.16	8.65	9.67
Bonded specimen-(125 mm× 125 mm)	247.04	7.90	0.78
% Difference	10.86%	8.67%	99.19%

4.4.2 Area of Influence

The interfacial connections in a composite member are predominantly subjected to shear forces. The efficiency of a connection scheme therefore depends on the area of influence. The increase in influence area reduces the shear stresses, thereby reducing the demand on the connection. Although, the characteristics and behaviour of the connection changes significantly with a change in connection scheme, the influence area of the connections plays a crucial role in determining its overall performance. An effective comparison of the characteristics of both the connection strategies requires a comparison of the influence areas, along with strength and deformability. In case of mechanical headed stud connectors, the influence area is generally marked using a conical failure shape, having a vertex area of 110° at the top of effective height of stud as per ACI 349 recommendations (ACI 349 2001). While, the effective influence area in case of adhesive bonded connections is same as the bonded area of the connections. In the present study, the effective influence area for the mechanical headed stud connector, having a height of 100 mm and shank diameter of 19 mm, has been calculated as,

$$A_{eff} = \frac{1}{4}\left(\frac{\pi}{4}\left(d_{ia}\right)^2\right) \qquad (4-4)$$

where, d_{ia} is the effective width of the influence area calculated, as,

$$d_{ia} = 2\times\left(100\times\tan(55^\circ)\right) = 285.62\,\text{mm}$$

Thus, the effective influence area of headed stud connector is 16017.95 mm^2 or 126.55 mm × 126.55 mm. *Fig. 4-10* shows the effective influence area of the headed

stud connector considered in the present study. The area of influence for epoxy adhesive bonded specimen has been calculated as 125 mm × 125 mm (= 15625 mm^2). It is interesting to note that the difference between the area of influence of adhesive bonded (15625 mm^2) and headed stud connector (16017.95 mm^2) is approximately 2.51%, and thus to be considered as quite marginal.

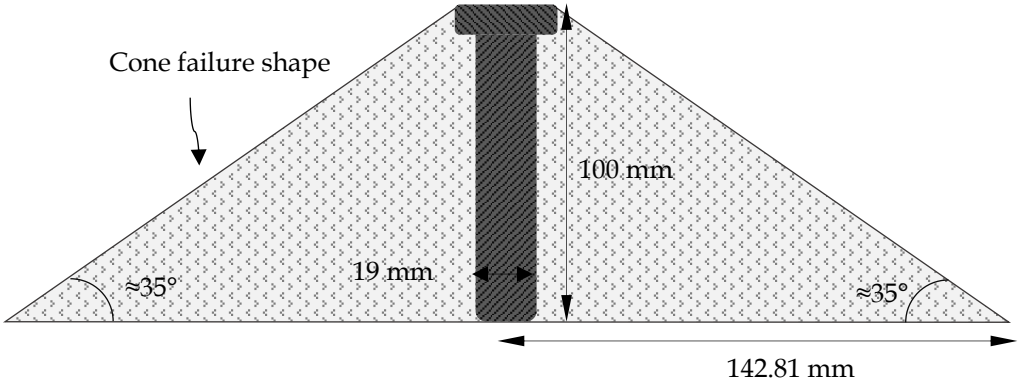

Fig. 4-10: Possible shape of concrete cone failure in concrete breakout condition

4.4.3 Shear Stiffness

Shear stiffness of a connection is another inflencing parameter, governing the performance of a connection under static loading. As per the procedure described in section 3.2.1, the shear stiffness of both connection stratgies has been evaluated, and reported in *Table 4-3*. The shear stiffness of mechanical headed stud connected and adhesive bonded connections has been obtained to be 97.88 kN/mm and 2194.42 kN/mm, respectively. It can be noted that the shear stiffness of adhesive bonded connection is almost twenty two (22.42) times higher than that of mechanical headed stud connected specimens. Also, the failure in adhesive bonded connections has been observed to be brittle, while for mechanical headed stud connections, a ductile behaviour has been observed.

Table 4-3: Shear stiffness of mechanical headed stud connected and adhesive bonded composite connection

Connector category	Applied Load ($P_{u)}$	$(0.7\ P_u)/2$	Relative Slip at $(0.7\ P_u)/2$	Shear stiffness (k_i)
	(kN)	(kN)	(mm)	(kN/mm)
headed stud 19 mm× 100 mm	277.16	97.01	0.99	97.88
Bonded specimen 125 mm× 125 mm	247.04	86.46	0.0394	2194.42
Difference (%)	10.86	10.86	96.02	2141.52 (-)

4.5 Connection Behaviour under Impact Loading

The impact behaviour of both the composite connections has been compared in terms of the energy absorption capacity of the specimens, when subjected to the drop weight test.

4.5.1 Specimens with Mechanical Headed Stud Connecters

This section deals with the behaviour of composite specimens connected using mechanical headed studs, under impact loading. A relative slip of 3 mm has been considered as the serviceability limit. The surficial cracking of the concrete surface in composite specimens has not been considered as a deciding criterion, as the occurrence of surficial cracks is preceded by significant damage in terms of connection yielding and strength loss. The initiation of failure of headed stud connected specimens is characterized by the rotation of steel element of the specimen about the axis of the headed stud. The drop weight testing specifications for headed stud connected specimens suggest that the energy required to initiate the failure of the composite specimen ($E_{dw,i}$) is,

$$E_{dw,i} = N_1 mgh_{dw} \qquad (4-5)$$

while the impact energy required for failure ($E_{dw,\mathrm{f}}$) is given as

$$E_{dw,\mathrm{f}} = N_2 mgh_{dw} \qquad (4-6)$$

where, N_1 is the number of blows required to induce the minimum observable rotation in the steel element of the specimen, and N_2, is the number of blows required to induce a relative slip of 3 mm between the elements of the specimen. *Fig. 4-11* shows the photographs of the headed stud connected specimens after conducting the drop weight impact tests. *Fig. 4-11(a)* shows the separation of concrete and steel elements of the specimen resulting from the relative rotation of the steel section due to yielding of headed stud. The cracking and crushing of concrete around the headed stud has also been observed, as shown in *Fig. 4-11(b)*. A significant deformation of stud, when subjected to impact loading, is evident from the distorted cavity shown in *Fig. 4-11(c)*. Another broad conclusion drawn from *Fig. 4-11* is that the failure of headed stud connection under impact loading is localized near the stud, and is owing to the high (shear) stress concentration in

that region. *Table 4-4* shows number of blows and associated energy absorbed by the connections with headed stud. The ratio of number of blows required to initiate the cracking to those required to cause failure of connection varies between 1.75 and 2.44. This observation underscores the conclusion that the composite connections with headed studs exhibits good ductility.

(a) (b) (c)

Fig. 4-11: Failure of mechanically shear stud connected composite specimen by concrete crushing around stud and slip in shear stud; (a) shift of I section indicated by the mark, (b) cracking in concrete surrounding the stud and (c) slip near root of stud

Table 4-4: Impact resistance results of mechanically connected composite specimen under drop-weight impact test

Specimen No.	N_1	N_2	N_2-N_1	Impact Energy (E)		N_2/N_1
				Crack Initiation	Ultimate Failure	
1	28	67	39	1870.57	4476.01	2.39
2	29	60	31	1937.37	4008.37	2.07
3	25	61	36	1670.15	4075.17	2.44
4	33	58	25	2204.6	3874.75	1.75
5	24	54	30	1603.34	3607.53	2.25
	Mean= 27.8 SD= 3.19 COV=11.47%	Mean= 60 SD= 4.24 COV=7.07%				

4.5.2 Specimens with Adhesive Bond

The assessment of impact behavior of adhesive bonded composite connections is significantly different than that of headed stud connections. The impact energy imparted, during the drop weight testing of adhesive bonded composite specimens, is dissipated in the form of cracking of the connection layer at the steel-concrete interface. The drop weight test on adhesive bonded specimens causes

progressive cracking of concrete, ultimately leading to separation of the bonded elements. The ratio of number of blows required to cause crack initiation (N_1) and the number of blows required to cause separation (N_2), depicts the ductility of the connection. The failure of adhesive bonded specimens under impact testing has been shown in *Fig. 4-12*. *Fig. 4-12(a)* shows the initiation of cracking in the composite specimen, depicting the formation of a distinct crack in the concrete element in the vicinity of the adhesive layer. The separation of the two elements, due to increased crack width has been shown in *Fig. 4-12(b)*. The surfaces of two elements of the failed specimen have been shown in *Figs. 4-12(c)* and *4-12(d)*, respectively. The separation of a thick layer of concrete along with the epoxy interface on the steel element (*Fig. 4-12(c)*) has been primarily owing to the strong adhesion between steel and epoxy, than the weaker cohesion in concrete.

(a) (b) (c) (d)

Fig. 4-12: Adhesive bonded steel-concrete composite specimen connection interface failure; (a) crack initiation near the epoxy-concrete interface, (b) crack leading to final failure and the consequent separation near the interface and (c) concrete layer separation at the interface

Table 4-5 shows the number of blows (N_1 and N_2) and energy associated with epoxy adhesive bonded connections. It has been noted that the energy absorbed between crack initiation and ultimate failure is only 27%, which is significantly less than that for connections with headed stud. Comparison between the results of drop weight tests for specimens connected with mechanical headed stud and adhesive (*Table 4-4* and *4-5*) also show that energy required for crack initiation is relatively less in case of mechanically connected rather than adhesive bonded connections, while the energy required for final failure in case of mechanical connection is high compared to bonded connection.

Table 4-5: Impact resistance results of adhesive bonded composite specimen under drop-weight impact test

Specimen No.	N_1	N_2	N_2-N_1	Impact Energy (E)		N_2/N_1
				First Crack	Ultimate Failure	
1	40	43	3	2672.24	2872.66	1.05
2	33	42	9	2204.6	2805.86	1.27
3	49	51	2	3273.5	3407.11	1.04
4	38	41	3	2538.6	2739	1.07
5	36	41	5	2405.02	2739	1.14
	Mean= 39.2 SD= 5.42 COV=13.82%	Mean= 43.6 SD= 3.77 COV=8.64%				

4.6 Conclusions

In this chapter, a comparative study between the steel concrete composite specimens connected using two different connection strategies, namely mechanical headed stud and adhesive, has been carried out. The behaviour of both the connections under static and impact loading has been experimentally evaluated, and presented. On the basis of the experimental study, following broad conclusions can be drawn:

- The area of influence for mechanically connected and adhesive bonded specimens has been choosen to be identical for the present study.
- The static strength capacity for both connection strategies differ by 10.88% with respect to mechanically headed stud connected specimen. Although, the variation in effective area is 2.51%.
- The initial shear stiffness of specimen having bonded connection is twenty two times higher than the stiffness of mechanical headed stud connector connected specimen.
- The overall dutility of adhesive bonded connection is almost negligible, while mechanically headed stud connected connections are ductile in nature.
- The number of blows required for crack initiation in adhesive bonded composite specimens are 1.4 times higher than that required for crack initiation in mechanical stud connected specimens.

- The number of blows required for the final failure of adhesively bonded composite specimens are 0.72 times (significantly less) than that required for causing a serveciability failure (slip of 3 mm) in mechanically connected specimens.
- The ultimate failure of adhesively bonded composite specimen is brittle in nature and failure of concrete is observed under the action of impact load.

Chapter: 5

Effect of Concrete Strength and Reinforcement Detailing on Performance of Composite Connections with Headed Studs

5.1 Overview

The effectiveness of a composite connection lies in the adequate transfer of forces between the steel and concrete elements. The connection strategy adopted, determines the behavior of connection. This behaviour of composite specimens connected using headed studs depends on various factors, such as, cross-sectional area and dimensions of shear connectors, material properties of connectors, grade of concrete, type of loads acting on the members and quantity and location of reinforcement in concrete slab. Literature suggest that the dowel strength of headed stud connector, under push-out test, is a function of various parameters, and is given as,

$$Q_u = f(E_c / E_s, f_c, f_u, A_{sh}, \mathrm{A}_r) \qquad (5-1)$$

where, Q_u is maximum dowel strength of connection, E_c is elastic modulus of concrete,E_s is elastic modulus of steel, f_c is the compressive strength of concrete of slab, f_u is the ultimate tensile strength of shear stud connector and A_{sh} is cross section area of shear stud connector.

The ultimate strength and modulus of elasticity of shear stud connectors depend on the material properties. The selection of adequate geometry of concrete slab can reduces the chances of concrete cracking. Certain other parameters, that affect the dowel strength of headed stud connectors, are cross-sectional area of shear studs, confinement of concrete due to transverse reinforcement and compressive strength of concrete.

In this chapter, the effects of strength of concrete and confinement of concrete slab, on the behaviour of connection have been investigated. The effects of variation in strength have been studied by varying the grade of concrete in the specimens, while the effects of confinement of concrete have been studied by altering the quantity and location of reinforcement. The behavior of connection has been investigated in terms of its bearing capacity, ductility and shear stiffness.

Four different groups of push out test specimens have been cast having unreinforced, singly reinforced, doubly reinforced and triply reinforced concrete slabs. The spacing of reinforcement layer(s), from the root of stud (and between the layers), has been varied in case of singly and doubly reinforced specimens. This has been done to investigate the effect of reinforcement detailing on the behaviour of the push out test specimens. The chapter also presents an experimental verification of the EC4 (2004) and BS 5400 (2005) codal specifications related to the bearing capacity of headed stud connectors.

5.2 Material Used

5.2.1 Concrete

The normal strength concrete mixes have been used to prepare concrete elements for steel-concrete composite push-out specimens. Concrete slabs with five different grades (C_1, C_2, C_3, C_4, and C_5 concrete) (detailed in *Table 3-1* of Chapter three) have been considered in the present study. The average compressive strengths of cubes at 28 days have been found to be 32.50 MPa for C_1 concrete, 38.55 MPa for C_2 concrete, 46.50 MPa for C_3 concrete, 57.71 MPa for C_4 concrete, and 73.46 MPa for C_5 concrete.

5.2.2 Structural Steel

Hot rolled steel column sections have been procured and cut in 450 mm length to prepare composite push-out specimens. The geometric details of selected section have been shown in *Table 5-1*. The mechanical properties of structural steel have already been discussed in Chapter three (*section 3.2.2*).

Table 5-1: Geometric details of universal column (UC) steel-section

Description	Total depth	Flange width	Web thickness	Flange thickness	Root radius	Area
	(mm)	(mm)	(mm)	(mm)	(mm)	(mm^2)
UC 203 × 203 × 46	203.2	203.6	7.2	11	10.2	5872

5.2.3 Headed Stud Connectors

Mechanical headed stud connectors of diameter 19 mm and height 100 mm have been used in the present study. The properties of headed studs have already been discussed in Chapter three (*section 3.2.4*). Also, the dimensional details of connectors have been discussed in Chapter four (*section 4.2.3*, *Fig. 4-2*).

5.2.4 Reinforcement

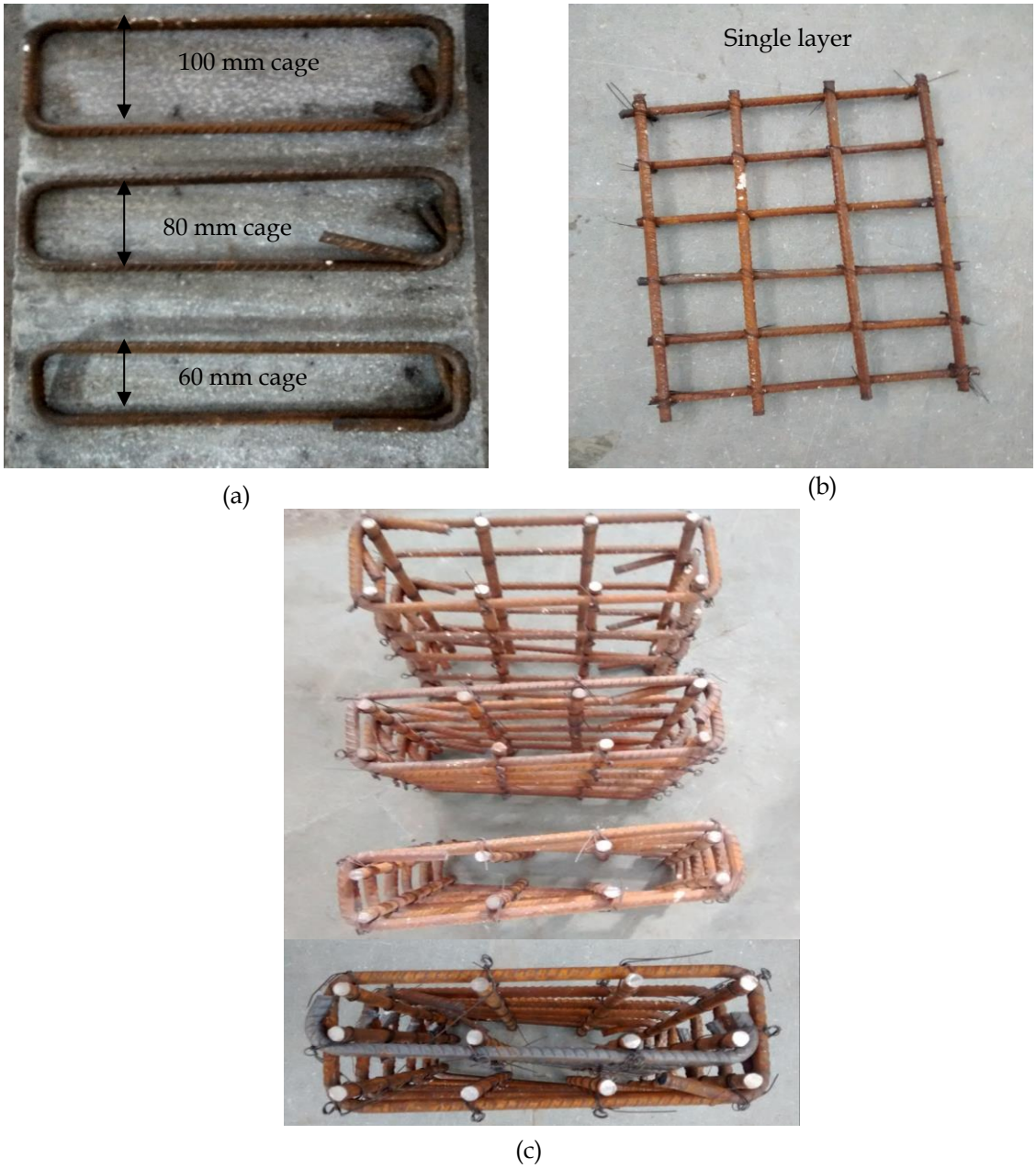

Fig. 5-1: Geometry of reinforcement bars; (a) shear stirrups for 100 mm, 80 mm and 60 mm cages, (b) single layer reinforcement cage and (c) double layer (100 mm, 80 mm and 60 mm cages) and triple layer reinforcement cage

Reinforcement bars of 10 mm diameter have been used in the concrete elements of the push-out test specimens. The tensile properties of reinforcement bars have already been discussed, in detail in Chapter three (*section 3.2.3*). Different combinations of reinforcement bars have been used to investigate the confinement and amount effect. The various reinforcement cages prepared have been shown in *Figs. 5-1(a), (b)* and *(c)*.

5.3 Experimental Program

To achieve the desired objectives, an experimental program has been designed. A total of sixty nine push-out test specimens have been cast, tested and investigated during this study. The experimental program can be subdivided into following parts, based on their broad objectives:

5.3.1 Effects of Strength of Concrete Elements

Fifteen specimens have been tested to investigate the effects of variation in concrete strength. Three identical composite push-out test specimens for each concrete C_1, C_2, C_3, C_4 and C_5 have been prepared. Push out tests have been conducted on the prepared specimen as per the procedure described in Chapter three (*section 3.2.5*). The average applied load-relative slip curves for composite push out test specimens with concretes of different strengths (C_1, C_2, C_3, C_4 and C_5) have been plotted. These curves have been used to estimate the shear stiffness of each composite specimen, and the results have been reported. The effective estimate of the initial shear stiffness and post yield stiffness of the composite connections has been obtained by equating the energy under the observed load-slip curve and the idealized behaviour. Also, the observed failure of each composite specimen has been discussed.

5.3.2 Effects of Detailing of Confining Reinforcement

The effects of the quantity and distribution of the confining reinforcement, on the connection behaviour have been investigated through sixty push out specimens. The investigation has been carried out for specimens having strength of concrete elements defined by C_1 and C_2. The study has been carried out by dividing the total

number of specimens into four groups *(G-1, G-2, G-3* and *G-4)*. *G-1* comprises of specimens with concrete elements having no reinforcement and *G-2* consists of specimens with concrete elements having single layer of reinforcement, while *G-3* and *G-4* have specimens with concrete elements having two layers and three layers of reinforcement, respectively. Group *G-2* has some additional specimens with C_3, C_4 and C_5 concrete to investigate the effect of variation in concrete strength. The push out test specimens with detailed geometric details have been shown in *Figs. 5-2* to *5-5*. *Fig. 5-2* shows the unreinforced steel-concrete composite specimen with geometric details. The steel-concrete composite specimens with single layer of reinforcement at 25 mm, 50 mm, 75 mm and 100 mm from root of studs have been shown in *Fig. 5-3*. The composite specimens with two layers of reinforcements have been shown in *Fig. 5-4*. *Fig. 5-4(a)* shows the specimen, confined with shear stirrups, in 100 mm cage at 25 mm from root of stud. Similarly, *Fig. 5-4(b)* shows the specimen with 80 mm cage at 25 mm from root of stud. Further, *Figs. 5-4(c)* and *(d)* show specimens with 60 mm cage at 25 mm from root of studs and 50 mm from root of studs, respectively. The geometric details of composite specimen with concrete element having triple layer of reinforcement have been shown in *Fig. 5-5*.

A brief detail of test groups has been presented in *Table 5-2*. To identify an individual specimen, a generalized nomenclature method for specimens has been adopted. The specimens have been designated as *MAXRLYSZ*,

where,

M stands for concrete mix used in slabs *(C_1, C_2, C_3, C_4* or *C_5);*

A is an alphabet *(a, b or c)* used for one of the three identical specimens in a group;

X denotes the number of reinforcement layers *(1, 2* or *3);*

RL stands for Reinforcement Layers, following *X;*

Y denotes the center-to-center distance between two successive reinforcement layers *(*in mm*)*;

S denotes effective cover (from root of headed stud to distance of first layer); and

Z stands for clear cover from root of shear stud to reinforcement bar (in mm).

Table 5-2: Summary of the prepared push-out test specimens

Reinforcement Detailing			
Group-1 (G-1)	Group-2 (G-2)	Group-3 (G-3)	Group-4 (G-4)
No reinforcement	Single layer	Double layer	Triple layer
C_1(and C_2)a0RL0S0,	*C_1(and C_2)a1RL0S25*	*C_1(and $C_{2\text{-}5}$)a2RL100S25,*	*C_1(and C_2)a3RL50S25,*
C_1(and C_2)b0RL0S0,	*C_1(and C_2)b1RL0S25*	*C_1(and $C_{2\text{-}5}$)b2RL100S25,*	*C_1(and C_2)b3RL50S25,*
C_1(and C_2)c0RL0S0	*C_1(and C_2)c1RL0S25*	*C_1(and $C_{2\text{-}5}$)c2RL100S25*	*C_1(and C_2)c3RL50S25*
	C_1(and C_2)a1RL0S50,	*C_1(and C_2)a2RL80S25,*	
	C_1(and C_2)b1RL0S50,	*C_1(and C_2)b2RL80S25,*	
	C_1(and C_2)c1RL0S50	*C_1(and C_2)c2RL80S25*	
	C_1(and C_2)a1RL0S75,	*C_1(and C_2)a2RL60S25,*	
	C_1(and C_2)b1RL0S75,	*C_1(and C_2)b2RL60S25,*	
	C_1(and C_2)c1RL0S75	*C_1(and C_2)c1RL0S75*	
	C_1(and C_2)a1RL0S100,	*C_1(and C_2)a2RL60S50,*	
	C_1(and C_2)b1RL0S100,	*C_1(and C_2)b2RL60S50,*	
	C_1(and C_2)c1RL0S100	*C_1(and C_2)c2RL60S50*	
6	*24*	*33*	*6*
		Total specimens	*69*

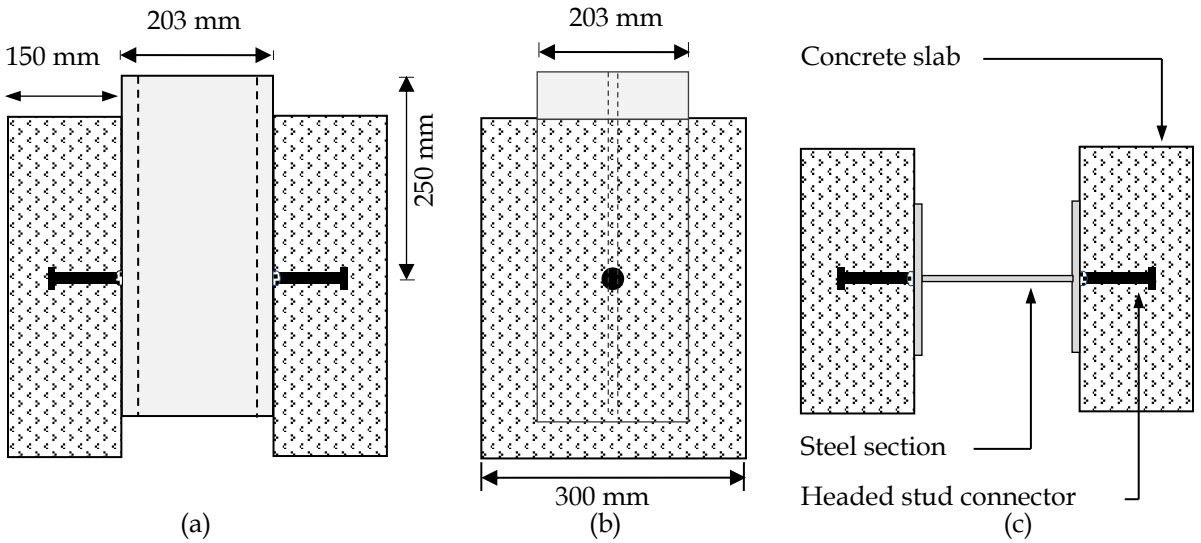

Fig. 5-2: Unreinforced steel-concrete composite specimen; (a) front view, (b) side view and (c) top view

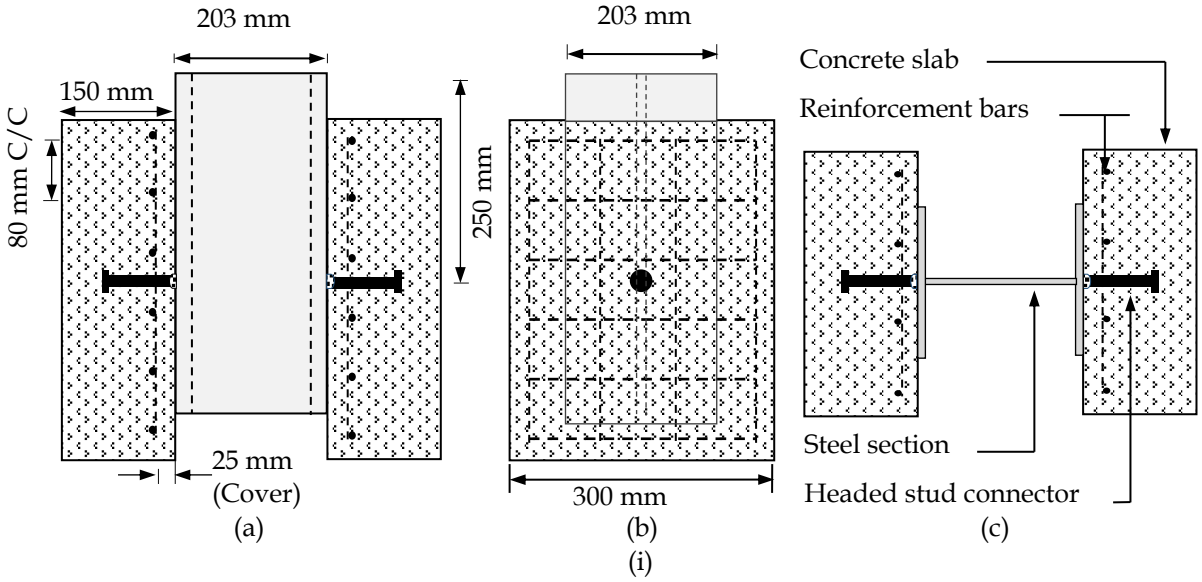
203 mm
150 mm
80 mm C/C
250 mm
25 mm
(Cover)
(a)
203 mm
300 mm
(b)
(i)
Concrete slab
Reinforcement bars
Steel section
Headed stud connector
(c)

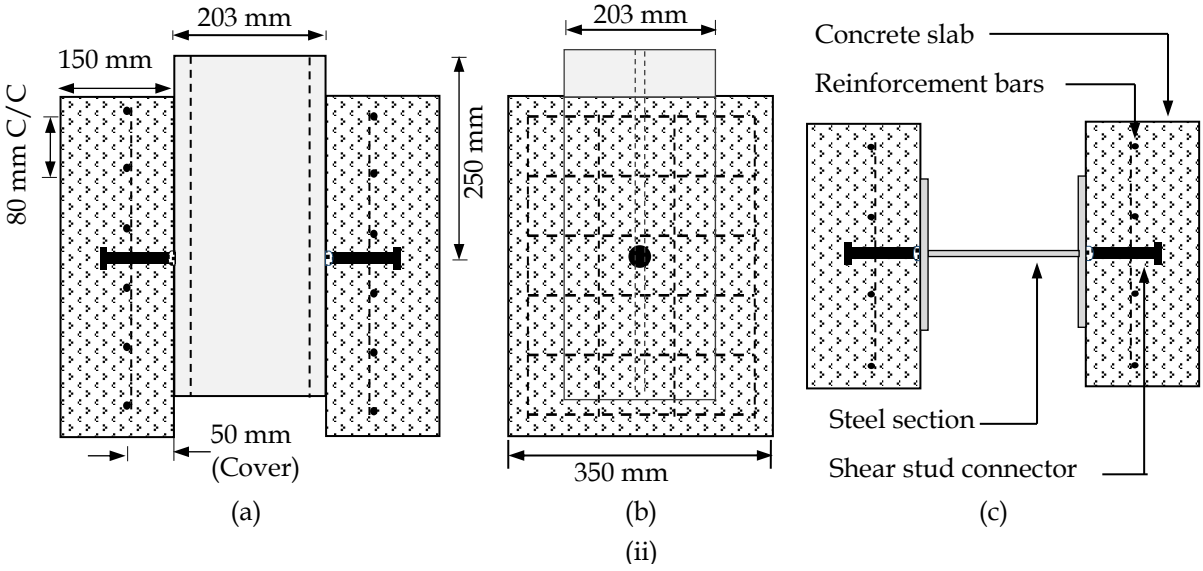
203 mm
150 mm
80 mm C/C
250 mm
50 mm
(Cover)
(a)
203 mm
350 mm
(b)
(ii)
Concrete slab
Reinforcement bars
Steel section
Shear stud connector
(c)

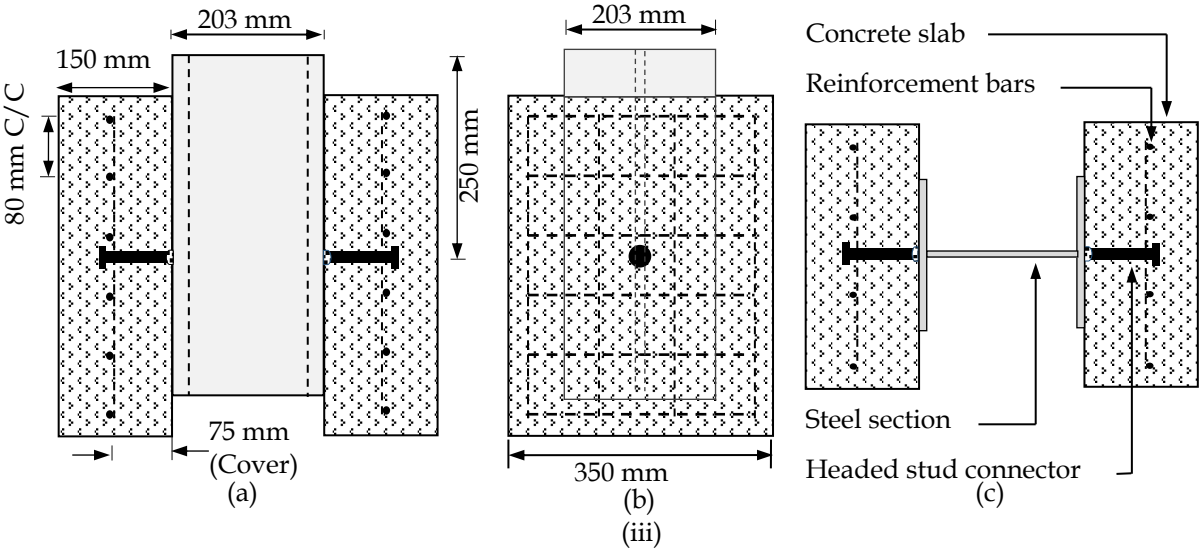
203 mm
150 mm
80 mm C/C
250 mm
75 mm
(Cover)
(a)
203 mm
350 mm
(b)
(iii)
Concrete slab
Reinforcement bars
Steel section
Headed stud connector
(c)

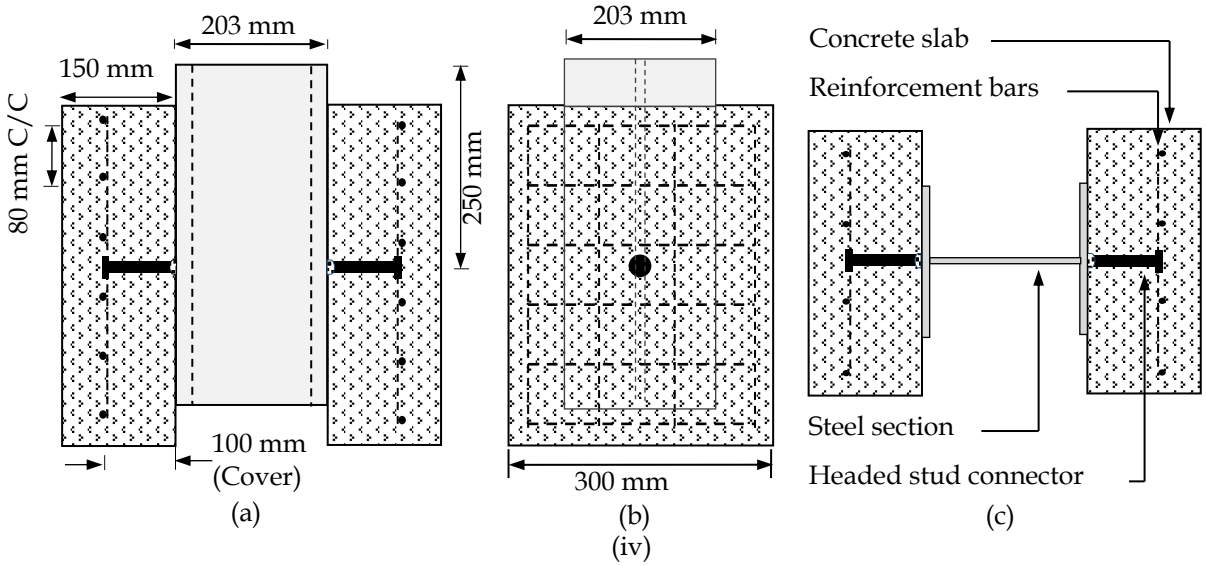

Fig. 5-3: Steel-concrete composite specimen with single reinforcement layer; (i) at 25 mm, (ii) 50 mm, (iii) 75 mm and (iv) 100 mm, from root of stud; (a) front view, (b) side view and (c) top view

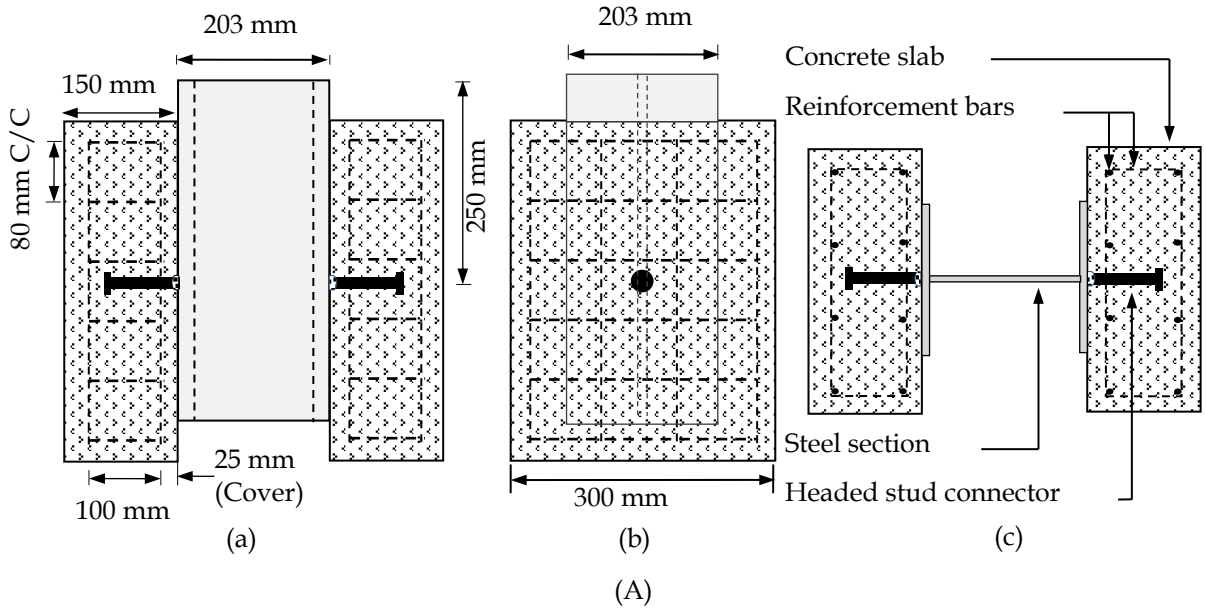

Fig. 5-4(A): Steel-concrete composite specimen with 100 mm double reinforcement layer cage at 25 mm from root of stud; (a) front view, (b) side view and (c) top view

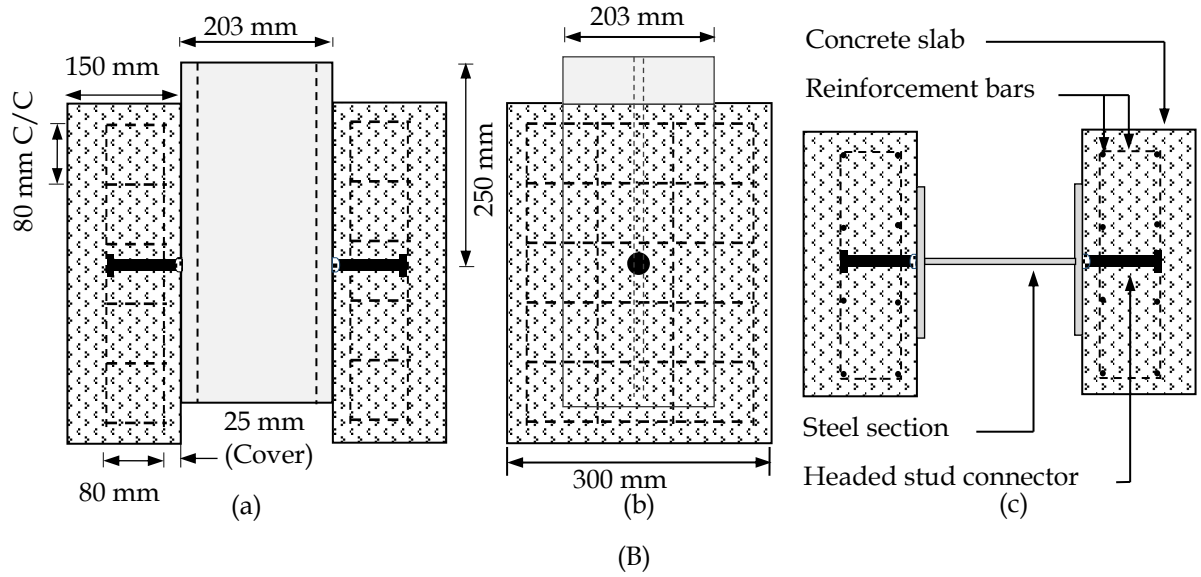

Fig. 5-4(B): Steel-concrete composite specimen with 80 mm double reinforcement layer cage at 25 mm from root of stud; (a) front view, (b) side view and (c) top view

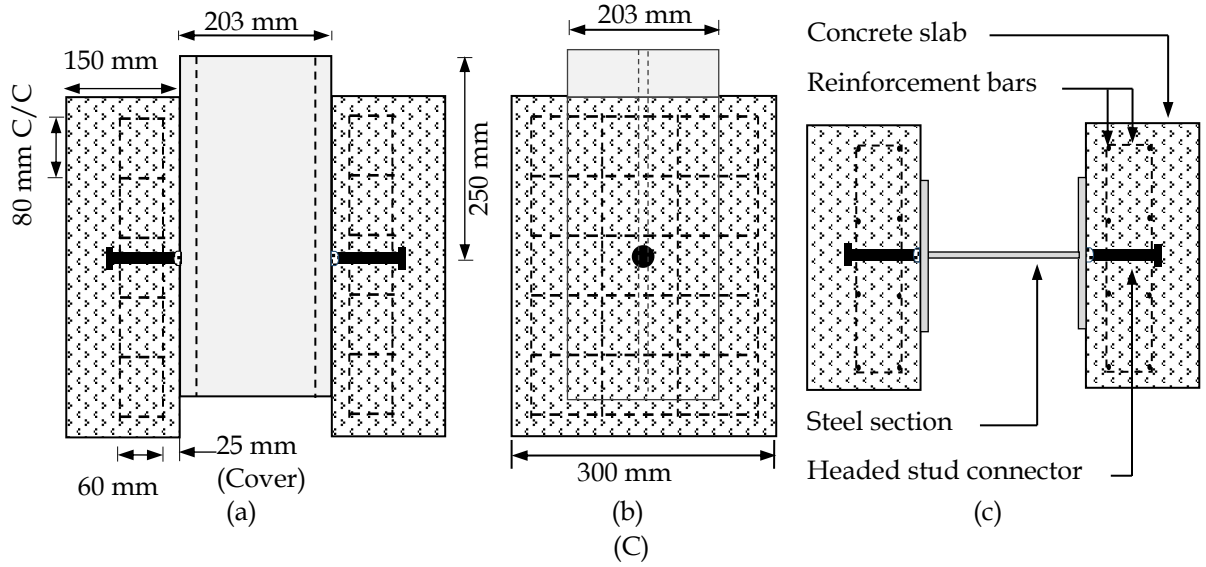

Fig. 5-4(C): Steel-concrete composite specimen with 60 mm double reinforcement layer cage at 25 mm from root of stud; (a) front view, (b) side view and (c) top view

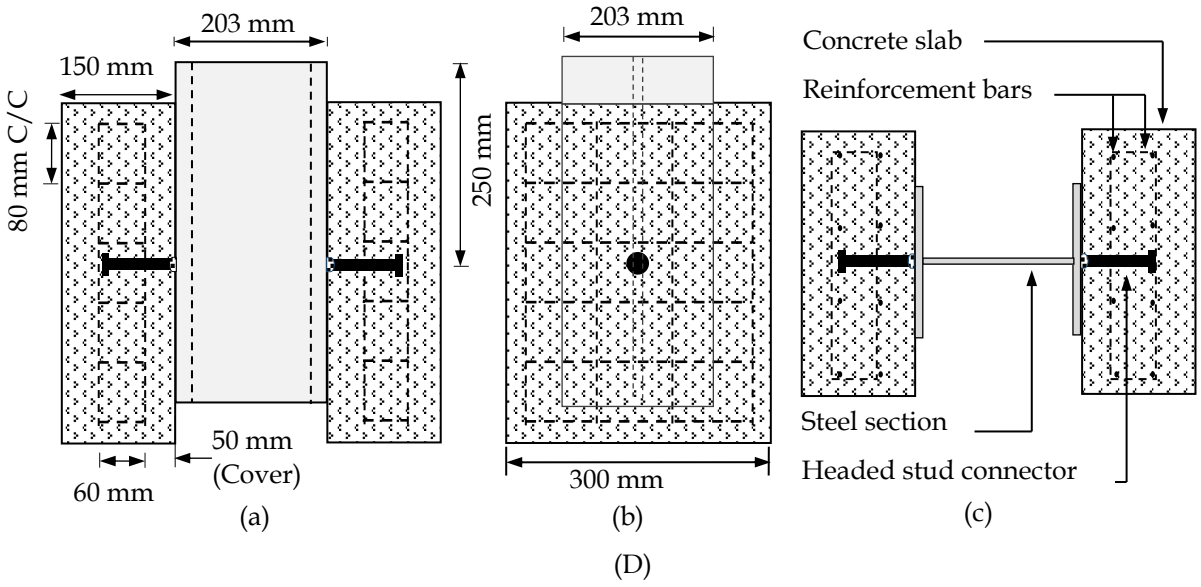

Fig. 5-4(D): Steel-concrete composite specimen with 60 mm double reinforcement layer cage at 50 mm from root of stud; (a) front view, (b) side view and (c) top view

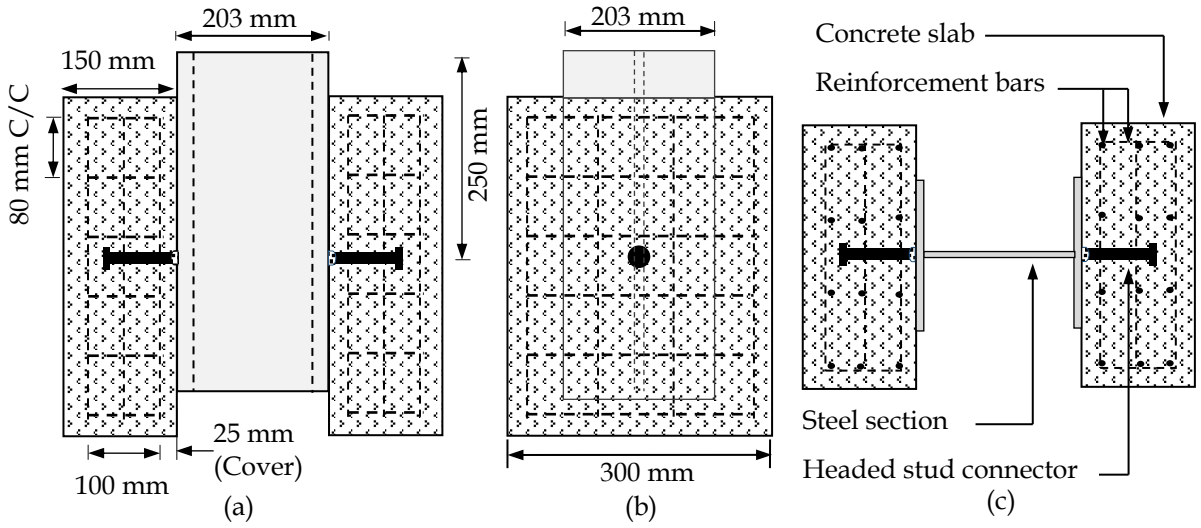

Fig. 5-5: Steel-concrete composite specimen with triple reinforcement layer at 25 mm from root of stud; (a) front view, (b) side view and (c) top view

5.4 Effect of Variation in Concrete Strength

5.4.1 Load-Slip Behaviour

The behaviour of headed stud connected push out test specimens with varying concrete strength (C_1, C_2, C_3, C_4 and C_5) has been experimentally investigated. Tests have been conducted by applying monotonic loading over composite specimens and the engendered relative slip at corresponding load levels have been recorded. *Table 5-3* presents the maximum load capacity of single headed stud connector along with the ultimate relative slip for each specimen. The ultimate strength of connections with headed studs increases with increase in concrete strength, and a linear relationship has been observed. With increase in strength of concrete element from C_1 (32.50 MPa) to C_5 (73.46 MPa), an increase of 52.53 MPa in the connection strength has been observed. However, with the increase in strength of concrete elements, a reduction in ultimate slip of the connections has been observed. A significant reduction of 44.47% (almost half) has been observed in the ultimate slip of connections, when the strength of concrete elements has been increased from C_1 to C_5. The averaged applied load vs. relative slip curves, for all specimens, have been plotted and shown in *Fig. 5-6*. The curves show a significant increase in strength and reduction in deformability of connections, with an increase in strength of concrete elements.

Table 5-3: Applied load and ultimate relative slip values for composite specimens

Specimen details	Concrete strength (MPa)	Applied load (kN)	Ultimate slip (mm)
C_1(a, b and c)2RL100S25	32.50	138.58	9.67
C_2(a, b and c)2RL100S25	38.55	146.15	7.17
C_3(a, b and c)2RL100S25	46.50	157.83	7.33
C_4(a, b and c)2RL100S25	57.71	170.75	6.71
C_5(a, b and c)2RL100S25	73.46	191.10	5.37

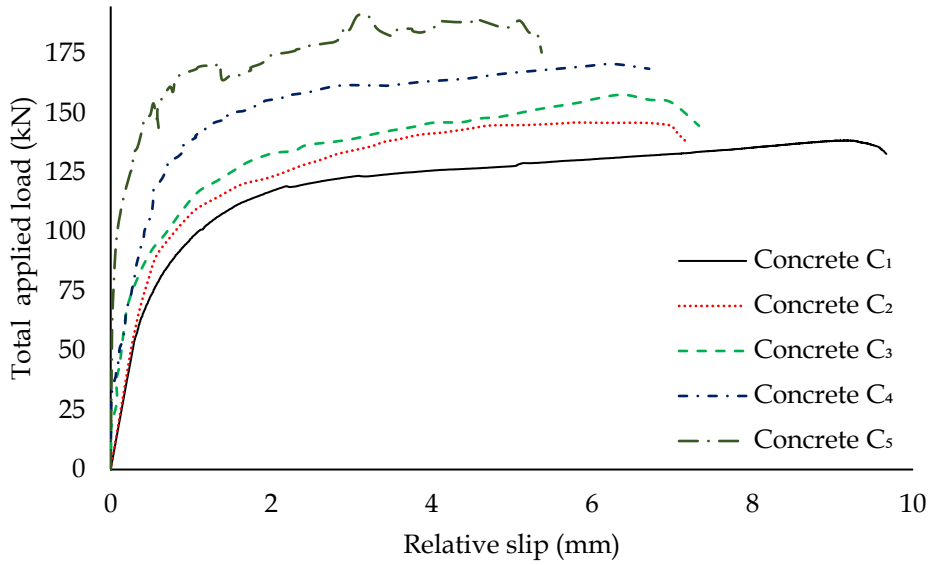

Fig. 5-6: Applied load –relative slip curves for steel-concrete composite specimens with varying concrete strength (from C_1, C_2, C_3, C_4 and C_5)

5.4.2 Failure Pattern

This section presents an in-depth discussion about the effects of variation in the strength of concrete elements on the failure pattern of composite specimens. In principle, with an increase in the strength of concrete elements, the connection strength and rigidity increases. This in-turn reduces the extent of damage in the concrete elements of the push-out specimens. This further leads to a change in failure pattern from failure of headed studs away from the root of stud owing to significant rotation due to yielding of concrete (in case of lower strengths of concrete), to failure of headed stud at the root of stud owing to concentration of shear stresses in the weld region (in case of higher strengths of concrete). This is also evident through the observed failure patterns of the tested specimens, shown in *Figs. 5-7* to *5-10*, for concrete slabs with strengths varying from C_1 concrete to C_5 concrete. The figures also depict that with an increase in strength of concrete elements, the deformability of the connectors decreases while the connection strength increases.

In cases where the strength of concrete elements is relative lower (C_1 and C_2), failure occurs due to concrete crushing leading to large deformation in headed studs (*Fig. 5-7*). For specimens having relatively moderate strength of concrete

elements (C_3 and C_4), the observed failure is due to combined deformation in headed stud with small amount of concrete crushing (*Figs. 5-8* and *5-9*). In case of specimens having relatively higher strength of concrete elements (C_5), the resistance offered by the concrete element is very high and the failure of weld at the root of the studs has been observed (*Fig. 5-10*).

(a) (b)

Fig. 5-7: Failure of steel-concrete composite connection having C_1 and C_2 concrete; (a) shank failure at steel surface and (b) concrete crushing on the bearing side

(a) (b)

Fig. 5-8: Failure of steel-concrete composite connection having C_3 concrete; (a) concrete crushing at the bearing portion and (b) shank failure of headed stud at steel surface

(a) (b)

Fig. 5-9: Failure of steel-concrete composite connection having C_4 concrete; (a) concrete crushing at the bearing portion and (b) shank failure of headed stud at steel surface

(a) (b)

Fig. 5-10: Failure of steel-concrete composite connection having C_5 concrete; weld failure with fracture in headed stud connected portion

5.4.3 Shear Stiffness

The behaviour of a steel-concrete composite member depends primarily on the shear stiffness of the connections between the elements. The applied load vs engendered slip curves of the push out test specimens have been idealized to obtain the initial stiffness (k_i) and post-yield stiffnesses (k_{py}) of the connections, using the energy balance approach. The bilinear idealization of the non-linear load-slip curves represents the pre- and post-yield shear stiffnesses of the composite connections. The initial shear stiffness is represented by the slope of first line of the idealized curve, while the slope of second part of the idealized curve represents the post-yield stiffness. The initial stiffness of the connection has been taken as the secant modulus of the actual load-slip curve. This secant line is further extended to a point between P_y and P_u, such that its intersection with the second line defines the yield point. *Fig. 5-11* shows a typical representation of the actual and idealized load-slip curves of a composite connection. Assuming that the hatched area (area under actual and over idealized curve) in the figure represents positive energy and the area marked with vertical lines (area under idealized curve and over actual curve) represents negative energy, the coordinates defining the idealized curve have been obtained such that, the algebraic sum of the positive and negative areas is zero, while minimizing the summation of both the areas. The step by step procedure to carry out the bilinear idealization of the load-slip curve has been given as:

Origin and $\left(s_{p_u}, P_u\right)$ is known, and the energy under the actual load-slip curve $\left(e_a\right)$ can be given as

$$e_a = \int_s p(s)\,ds \qquad (5-2)$$

A bilinear idealization of the actual load-slip curve obtained through experiment has been obtained as,

$$p'(s) = \begin{cases} k_i s & \forall \ (s \le s_1) \\ k_{py} s + D_0 & \forall \ (s \ge s_1) \end{cases} \qquad (5-3)$$

where, $k_i = P_1/s_1$, $k_{py} = \left(\frac{P_u - P_1}{s_u - s_1}\right)$ and D_0 is the constant representing the intercept at abscissa.

The energy under the bilinear curve has been estimated as a variable depending upon the yield and ultimate points.

$$e_b = \int_0^{s_u} p'(s)\,ds \qquad (5-4)$$

The variable energy under the bilinear curve is equated to the energy under the actual curve $(e_b = e_a)$, which provides the locus of the point (s_1, P_1) for the bilinear curve.

The area between the bilinear and the actual load-slip curve (e_{a-b}), is then minimized to provide the unique point (s_1, P_1).

$$e_{a-b} = \int |p(s) - p'(s)|\,ds \qquad (5-5)$$

The origin is then joined to (s_1, P_1), to obtain the first line of bilinear curve, representing the initial stiffness. Also, (s_1, P_1) is joined to (s_{p_y}, P_u) to obtain the second line of bilinear curve representing the post-yield stiffness of the connection.

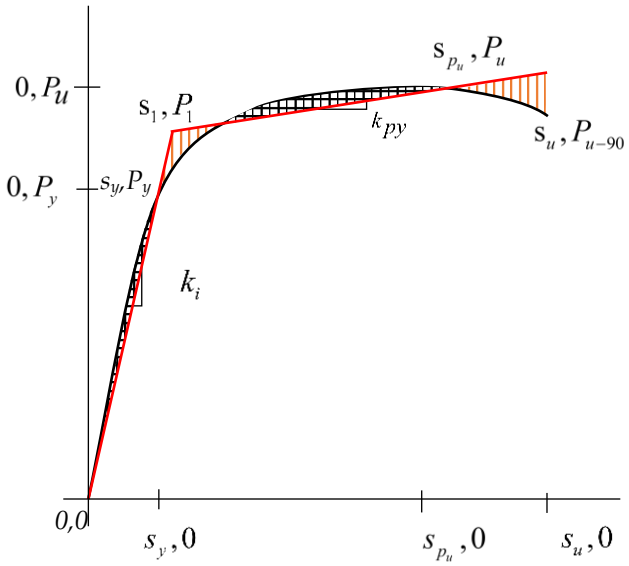

Fig. 5-11: Actual and bilinear idealized load-slip curves for typical composite connection

As the area under the two curves is same, the obtained bilinear approximation has been assumed to provide simplified an yet and accurate yet estimation of the actual load-slip curve of the connection.

The actual (experimental) as well as idealized load-slip behaviours of the specimens having concrete elements of different strengths (from C_1 to C_5) have been shown in *Figs. 5-12* to *5-16* respectively. The estimated values of the initial and post yield stiffnesses of the connections have been shown in *Table 5-3*. Both, the initial and post-yield stiffnesses have been observed to increase with an increase in the strength of concrete. The observed maximum increase in initial stiffness is 202.37 kN/mm (133.20%), while an increase of 4.47 kN/mm (142.10%) has been noted in case of post-yield stiffness, with an increase of 40.96 MPa (126.03%) in the strength of concrete elements from C_1 to C_5 (32.50 MPa to 73.46 MPa).

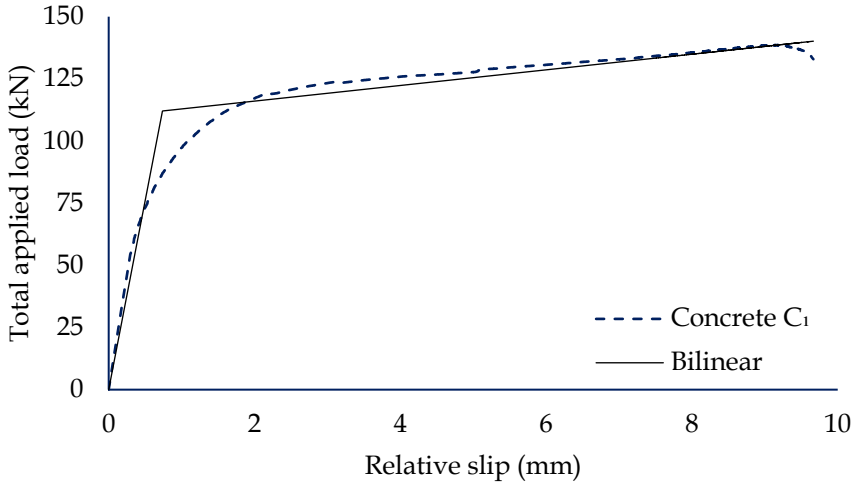

Fig. 5-12: Initial and post yield stiffness of steel-concrete composite specimens with C_1 concrete.

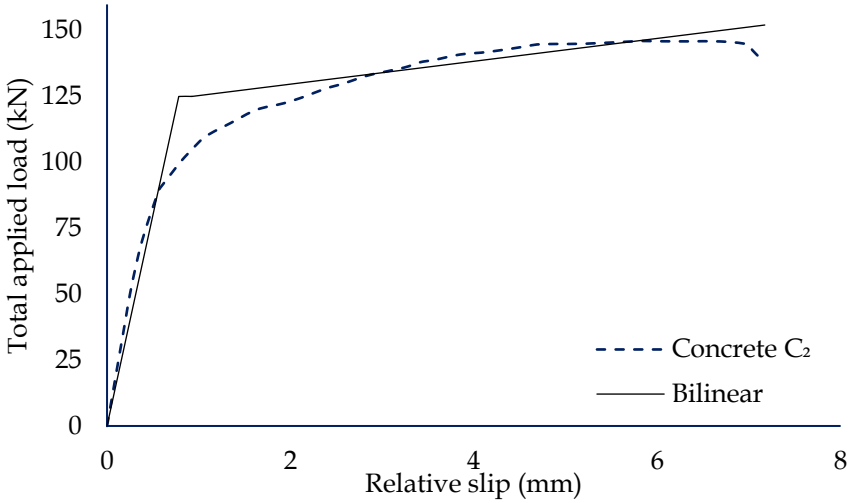

Fig. 5-13: Initial and post yield stiffness of steel-concrete composite specimens with C_2 concrete.

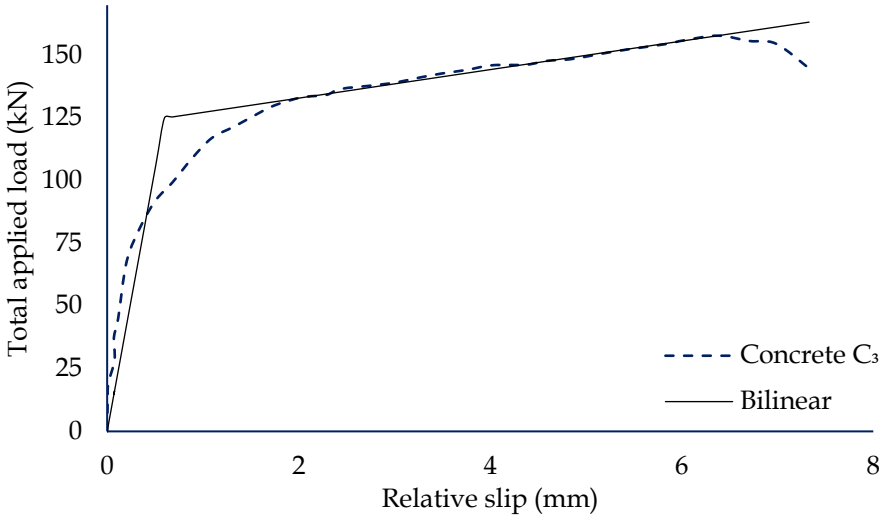

Fig. 5-14: Initial and post yield stiffness of steel-concrete composite specimens with C_3 concrete.

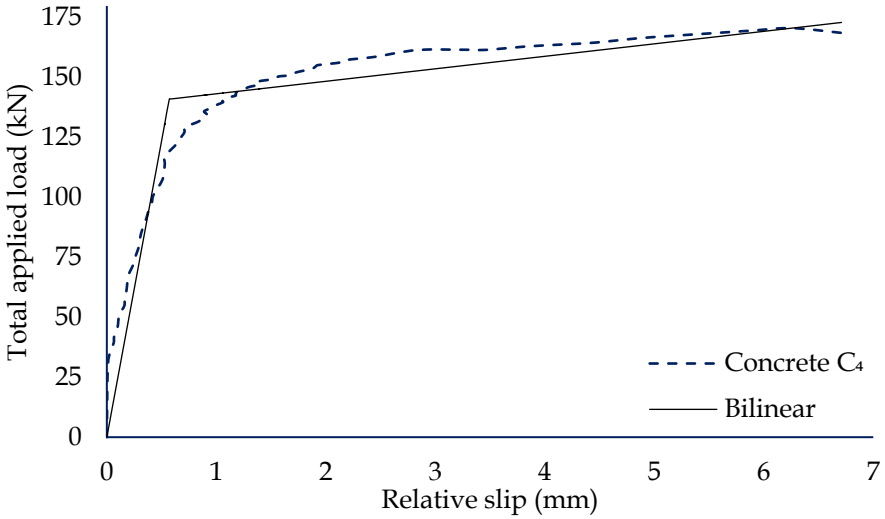

Fig. 5-15: Initial and post yield stiffness of steel-concrete composite specimens with C_4 concrete.

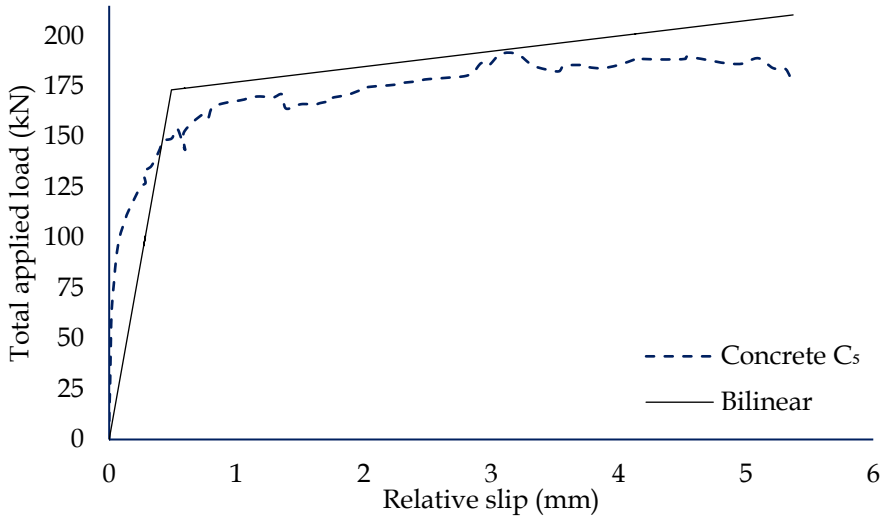

Fig. 5-16: Initial and post yield stiffness of steel-concrete composite specimens with C_5 concrete.

Table 5-4: Initial shear stiffness and post –yield stiffness values for various composite specimens.

Specimen details	Initial shear stiffness (k_i)	Post yield stiffness (k_{py})
	(kN/mm)	(kN/mm)
C_1(*a, b* and *c*)*2RL100S25*	151.94	3.14
C_2(*a, b* and *c*)*2RL100S25*	159.90	4.34
C_3(*a, b* and *c*)*2RL100S25*	209.11	5.79
C_4(*a, b* and *c*)*2RL100S25*	247.32	5.21
C_5(*a, b* and *c*)*2RL100S25*	354.31	7.61

5.5 Influence of Confining Reinforcement on Connection Behaviour

This section presents a discussion on the connection behaviour of steel-concrete composite specimens connected using headed shear studs, in the light of the influence of confining reinforcement. The results obtained, by conducting push out tests on specimens with unreinforced concrete elements, and concrete elements having single, double and triple layers of reinforcement, have been discussed individually. The effects of quantity and arrangement of confinement reinforcement, on the connection behaviour have also been presented.

5.5.1 Unreinforced Specimens

The specimens having concrete elements with no reinforcement (*Fig. 5-2*), when subjected to incremental push-out loading, exhibit an elastoplastic with strain hardening load-slip behaviour. The load-slip behaviour of these connections bears striking similarity to the force-deformation behaviour of a single headed stud connector (please see *section 3.2.4.1*). This implies that the contribution of unreinforced concrete element in the connection rigidity is marginal. The results of push out tests, on unreinforced steel-concrete composite (*G-1*) specimens, under monotonic loading have been presented in *Table 5-5*. The average values of shear capacity and ultimate engendered slip, obtained for the three identical specimens with each concrete strength (C_1 and C_2), have been reported. Although, the average value of ultimate engendered slip for the tested specimens is of the order of approximately 6 mm, one of the specimens with unreinforced concrete element having C_2 concrete exhibited an ultimate engendered slip of only 1.88 mm, representing premature failure. The probable reasons for the observed premature

failure of the third specimen with C_2 concrete may be the formation of excessive hair-line cracks on the concrete surface, owing to large settlement and plastic shrinkage. The averaged applied load vs engendered relative slip curves for specimens with concrete elements having no reinforcement have been shown in *Fig. 5-17*. The results of the study suggest that the ultimate strength of connections, for both (C_1 and C_2) concrete strengths is almost equal, with a marginal variation of only 8.98 kN (7.63%). Also, the ultimate engendered slip decreases with increase in concrete strength (from C_1 to C_2) marginally by 0.38 mm (5.95%). The photographs of specimens having unreinforced concrete elements, after the testing, have been shown in *Figs. 5-18(a)* and *(b)*. *Fig. 5.18(a*) shows a significant crushing of concrete near the interface along with overturning of steel section from its original position, with respect to headed stud connector. *Fig. 5-18(b)* shows crushing of concrete elements along with a propagation of cracks in the transverse direction owing to absence of confining reinforcement around the shear stud.

Table 5-5: Dowel strength capacity and induced relative slip at steel-concrete interface for unreinforced composite specimens.

Specimens details	Reinforcement amount	Capacity/ stud	Ultimate slip
	(%)	(kN)	(mm)
C_1(a, b and c)0RL0S0	0.00	117.69	6.39
C_2(a, b and c)0RL0S0	0.00	126.67	6.01 (avg. of two specimen) 1.88 (premature failure)

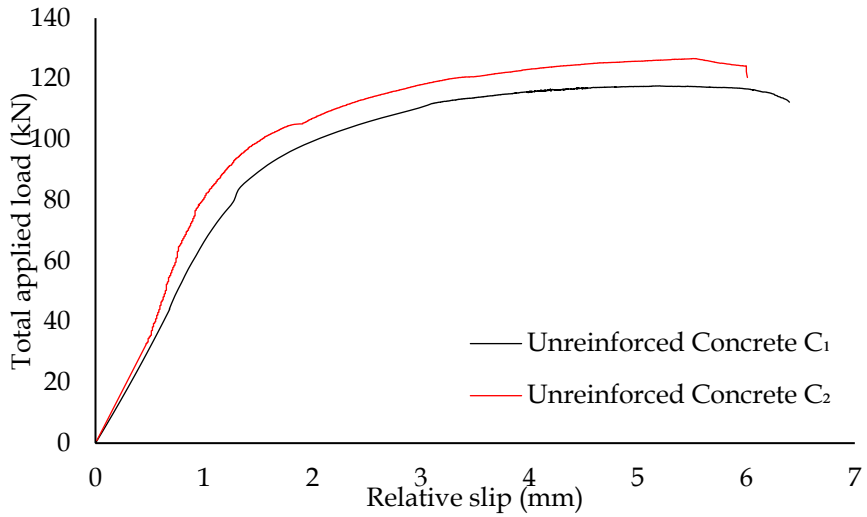

Fig. 5-17: Applied load-relative slip curves for unreinforced steel-concrete composite specimens having C_1 and C_2 concrete.

(a) (b)

Fig. 5-18: Failure of specimens having unreinforced concrete elements with; (a) overturning of steel-section from original position with respect to concrete element and (b) ripping of concrete from position of stud

5.5.2 Single Layer Reinforced Specimens

5.5.2.1 Single Layer Reinforced Specimen with C_1 Concrete

This section presents the study on the behaviour of steel-concrete composite pushout specimens having single layer of reinforcement in C_1 concrete element. The specimens have been prepared with reinforcement layers at four different distances from the root of headed stud (25 mm, 50 mm, 75 mm and 100 mm). Overall, four groups of specimens have been tested, each consisting of three specimens with identical concrete elements (having same distance between reinforcement layer and root of stud). The headed studs, in each specimen, have been positioned at 250 mm from the loading end of steel section. The amount of reinforcement in each concrete element has been maintained at 0.6% of the total cross-sectional area of concrete element.

The results of the push out tests on steel-concrete composite specimens having single layer of reinforcement in C_1 concrete, in terms of the individual shear capacity of studs along with the ultimate relative slip have been listed in Table 5-6. The maximum shear capacity of headed stud has been found to be 137.34 kN, when reinforcement cage has been placed at 25 mm from root of stud. While, the minimum shear capacity of headed stud has been observed to be 119.10 kN when

the reinforcement cage has been placed at 100 mm from root of stud. The variation in location of reinforcement layer, from 25 mm to 100 mm from the root of stud, exhibits a significant change, of about 15.31% (18.24 kN), on the shear capacity of the connection. The results of the push out tests suggest that, the shear capacity of headed stud connections with concrete elements having single reinforcement layer decreases with increase in the distance of reinforcement layer from root of stud. With an increase in distance between reinforcement layer and root of stud, from 25 mm to 50 mm, 75 mm and 100 mm, the shear capacity of the connection has been observed to reduce by 4.1%, 9.13% and 13.28%, respectively. The shear strength of composite specimen having single layer reinforcement at 100 mm from root of stud has been observed to be almost equal to that of the unreinforced specimen (difference in strength being 1.20%). The post yield dowel strength of singly reinforced specimens also undergoes a significant degradation with increase in the distance between reinforcement layer and root of stud.

The effect of variation in location of reinforcement layers, on the maximum engendered slip of the connections is significant. The results of the experimental investigation suggest that the ultimate slip, observed at connection interface, indicates increasing ductile behaviour with increase in distance between root of stud and reinforcement layer, from 25 mm to 75 mm (*Fig. 5-19*). However, in case of specimens with 100 mm distance between root of stud and reinforcement layer, the connection exhibits a brittle behaviour. This can be attributed to the negligible confining effect of the reinforcement layer placed at 100 mm from root of stud. The observed relative slip (*Table 5-6*) of the connections increases by 19.82% (1.6 mm) and 51.82% (4.18 mm), in cases when the distance between root of stud and reinforcement layer are increased to 50 mm and 75 mm, respectively, from 25 mm. Such a behaviour is typical to the low reinforcement sections of typical reinforced concrete members. However, a reduction of 23.04% (1.86 mm) has been observed in relative slip when the distance between root of stud and reinforcement layer is increased to 100 mm from 25 mm. The ultimate failure of specimen having reinforcement cage at 100 from root of stud is sudden and is strikingly like unreinforced specimen (the difference being only 2.82% or 0.18 mm).

Table: 5-6: Dowel strength and induced relative slip at composite interface for single layer reinforcement steel-concrete composite push-out specimen.

Specimens details	Reinforcement amount	Capacity/stud	Ultimate slip
	(%)	(kN)	(mm)
C_1a(a, b and c)1RL0C25	0.60	137.34	8.07
C_1(a, b and c)1RL0C50	0.60	131.60	9.67
C_1(a, b and c)1RL0C75	0.60	124.8	12.25
C_1(a, b and c)1RL0C100	0.60	119.10	6.21

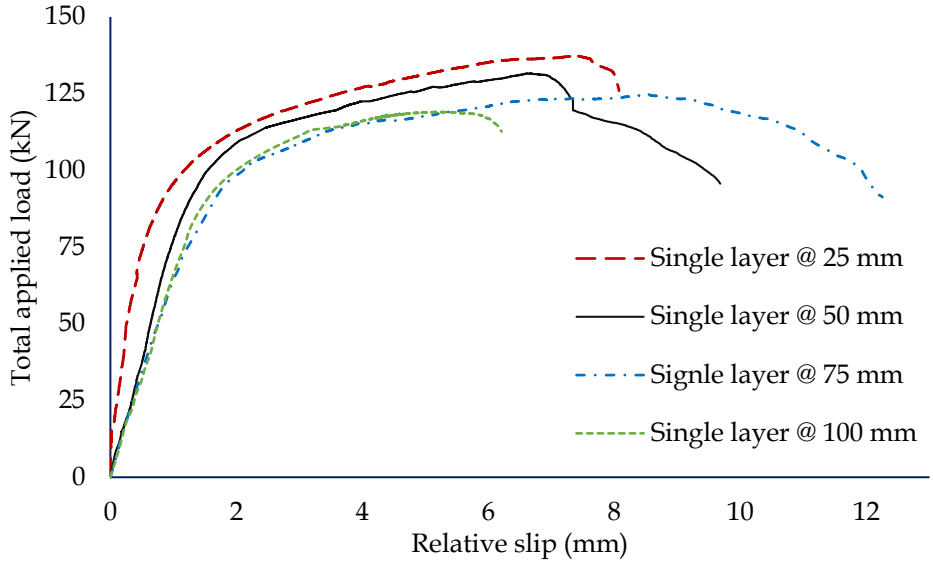

Fig. 5-19: Applied load- relative slip curves steel-concrete composite specimens with C_1 concrete and single layer reinforcement at 25 mm, 50 mm, 75 mm and 100 mm distance from root of headed stud

5.5.2.2 Single Layer Reinforced Specimen with C_2 Concrete

In this section, the effects of change in strength of concrete element having single layer of reinforcement have been discussed. The results of the push out tests, in terms of the shear capacity and ultimate slip of single stud connector, have been listed in *Table 5-7*. The specimens prepared for this study are exactly like those prepared with C_1 concrete except the concrete mix. In case of specimens with concrete element having strength C_2 and reinforcement layer is placed 25 mm from the root of stud, the shear capacity of the stud has been observed to be 138.2 MPa, which is almost similar to that of the corresponding specimens with C_1 concrete elements. However, with an increase in the strength of concrete elements (from C_1 to C_2), a very slight reduction in the ultimate slip of the specimens has been

observed, for all the cases of the reinforcement layer location. The behaviour of specimens with C_2 concrete exhibits slightly higher ultimate strength and lower deformability (ultimate slip), owing to the higher strength and thus enhanced contribution from the brittle concrete element. It is to be noted that in case of the specimen with C_2 concrete having 100 mm distance between reinforcement layer and root of stud, although the shear strength of the connection is comparable to other specimens, there is a significant reduction in the ultimate slip (35.11%), and the resulting ultimate slip (5.21 mm) which is even below the minimum limit specified for ductile connections (6 mm) in EC4 (2005).

Based on the results obtained, an empirical relation for the dowel strength of headed stud connector (Q_u) has been proposed in terms of strength of concrete, as,

$$Q_u \propto \left(\Delta f_c\right)^{0.5} \qquad (5-2)$$

where, f_c is the compressive strength of concrete in MPa. The applied load- relative slip curves for steel-concrete composite specimens with C_2 concrete and single layer reinforcement at 25 mm, 50 mm, 75 mm and 100 mm distance from root of headed have been shown in *Fig. 5-20*. The behaviour of all composite specimens with C_2 concrete has been obsrved to be similar to as C_1 concrete composite specimens.

Table 5-7: Dowel strength and induced relative slip at composite interface for single layer reinforcement steel-concrete composite push-out specimen with C_2 concrete.

Specimens details	Reinforcement amount	Capacity/stud	Ultimate slip
	(%)	(kN)	(mm)
C_2(a, b and c)1RL0C25	0.60	138.12	8.03
C_2(a, b and c)1RL0C50	0.60	132.21	9.70
C_2(a, b and c)1RL0C75	0.60	127.25	10.51
C_2(a, b and c)1RL0C100	0.60	122.23	5.21

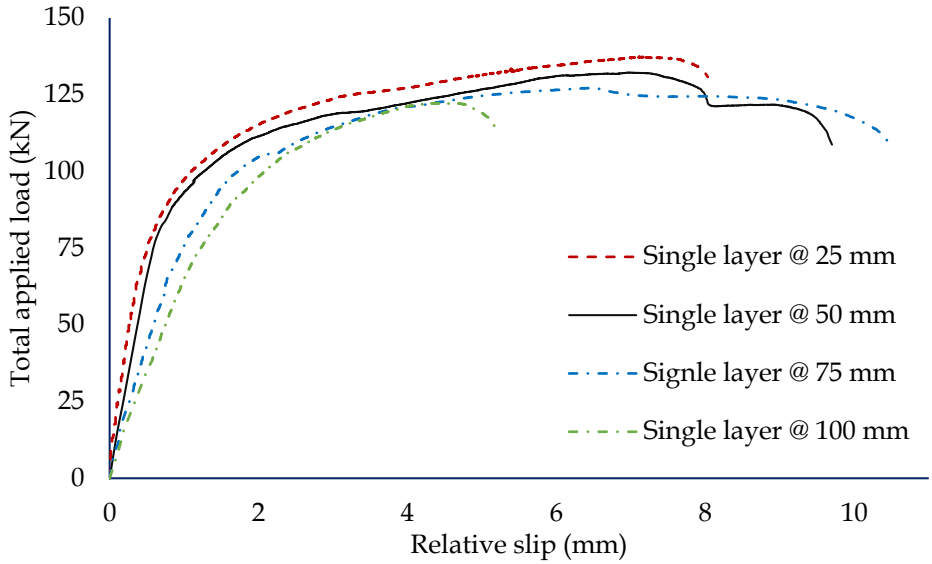

Fig. 5-20: Applied load- relative slip curves steel-concrete composite specimens with single layer reinforcement at 25 mm, 50 mm, 75 mm and 100 mm distance from root of headed stud having concrete C_2

The typical failures of steel-concrete composite specimens with reinforcement layer at 25 mm, 50 mm, 75 mm and 100 mm from root of stud have been shown in *Figs. 5-21(a), (b), (c) and (d).* The failure of composite specimens with reinforcement layer at 25 mm from root of studs has been shown in *Fig. 5-21(a).* The failure occurs in concrete slabs at the position of reinforcement layer. The behaviour has been observed in case of composite specimens having reinforcement layer at 50 mm and 75 mm from root of studs as evident in *Figs. 5-21(b)* and *(c)*. The concrete crushing failure has not been evident in composite specimens having reinforcement layer at 100 mm from root of stud is evident from *Fig. 5-21(d)*.

(a)

(b)

(c)

(d)

Fig. 5-21: Typical failure of steel-concrete composite specimens; (a) at 25 mm, (b) at 50 mm, (c) at 75 mm and (d) at 100 mm from root of stud

5.5.3 Double Layer Reinforced Specimen

5.5.3.1 Double Layer Reinforced Specimen with C_1 Concrete

In this section, the behaviour of steel-concrete composite specimens having two layers of reinforcement in C_1 concrete has been discussed in detail. The effects of various positions of reinforcement layers along with the effects of distance of reinforcement cage from root of stud, on the behaviour of connections has been investigated. The confining width of the reinforcement cage has been altered by increasing the distance between the two reinforcement layers. The monotonic loading has been applied on composite specimens and the applied loading vs relative slip curves for connection strength per headed stud connector have been plotted. The observed ultimate values for dowel strength and relative slip have been listed in *Table 5-8*. The results suggest that, in case of specimens with concrete elements having 25 mm distance between root of stud and first layer of reinforcement, with an increase in confining width of reinforcement cage, the ultimate shear strength of the composite specimens reduces, while the ultimate slip of the connections increases. The probable reason for this observed behaviour (reduction in strength with increase in ultimate slip) with increase in confining width may be the reduction in concrete confinement around the stud root and/or shank. The applied load vs. relative slip behaviour of connections have been plotted and shown in *Fig. 5-22*. It is evident from the graphs that the at higher confinement levels of concrete, the slope of the load-slip curves increases significantly, indicating higher stiffness of the connections. It has also been observed that with an increase in the distance of reinforcement cage from root of stud, the shear strength of the connections decreases significantly, along with an evident reduction in the ultimate slip of the connections. *Fig. 5-7* depicts the failure patterns of connections with C_1 concrete and two layers of reinforcement.

Table 5-8: Dowel strength and induced relative slip at composite interface for double layer reinforced specimens with C_1 concrete strength.

Specimen details	Reinforcement amount	Capacity/stud	Ultimate slip
	(%)	(kN)	(mm)
C_1(a, b and c)2RL100C25	1.20	138.58	9.67
C_1(a, b and c)2RL80C25	1.20	141.80	8.23
C_1(a, b and c)2RL60C25	1.20	146.35	6.36
C_1(a, b and c)2RL60C50	1.20	136.52	7.63

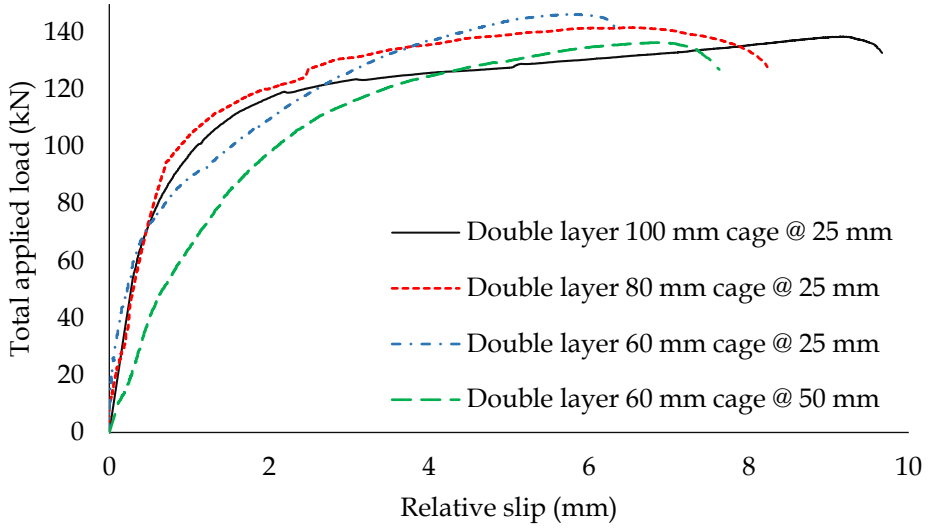

Fig. 5-22: Applied load- relative slip curves steel-concrete composite specimens with double layer reinforcement cages of 100 mm, 80 mm and 60 mm at 25 mm, and 60 mm at 50 mm from root of studs having strength C_1 of concrete elements

5.5.3.2 Double Layer Reinforced Specimen with C_2 Concrete

The specimens with C_2 concrete elements having two layers of reinforcement, with different distances between reinforcement layers (confining width of 60 mm, 80 mm and 100 mm), as well as between root of stud and first reinforcement layer (25 mm and 50 mm), have been discussed in this section. Table 5.9 enlists the experimentally obtained maximum values, of shear strength (per headed stud) and relative slip, for the tested specimens. Similar specimens have been prepared, with the C_2 concrete elements and having two layers of reinforcement (1.2%) placed at 25 mm and 50 mm from root of stud. The results obtained follow an almost similar pattern, as those described in the previous section (with C_1 strength concrete

elements), exhibiting an increase in shear strength and a reduction in ultimate slip. *Fig. 5-23* shows the applied load vs relative slip curves of the tested specimens. The load-slip curves suggest that the ultimate slip for all the tested specimens have almost same values. An important observation, from the load-slip behaviour of the specimen with the reinforcement cage placed at 25 mm from root of stud and having confining width of 100 mm, and the specimen with the reinforcement cage placed at 50 mm from root of stud and having confining width of 60 mm, is that both the specimens exhibit almost same shear strength, while their load-slip curves follow entirely different paths. It has been noted that the relative increment in connection strengths, with the increase in concrete elements strength from C_1 to C_2, exhibits almost linear variation. With an increase in strength of concrete element (from C_1 to C_2) by 6.05 MPa (18.61%), an increase in shear strength of connections by 7.57 kN (5.46%), has been observed.

Table 5-9: Dowel strength and induced relative slip at composite interface for double layer reinforced specimens with C_2 concrete.

Specimen	Reinforcement amount	Capacity/stud	Ultimate slip
	(%)	(kN)	(mm)
C_2(a, b and c)2RL100C25	1.20	146.15	9.90
C_2(a, b and c)2RL80C25	1.2	152.10	9.24
C_2(a, b and c)2RL60C25	1.20%	159.85	7.77
C_2(a, b and c)2RL60C50	1.20	144.28	7.88

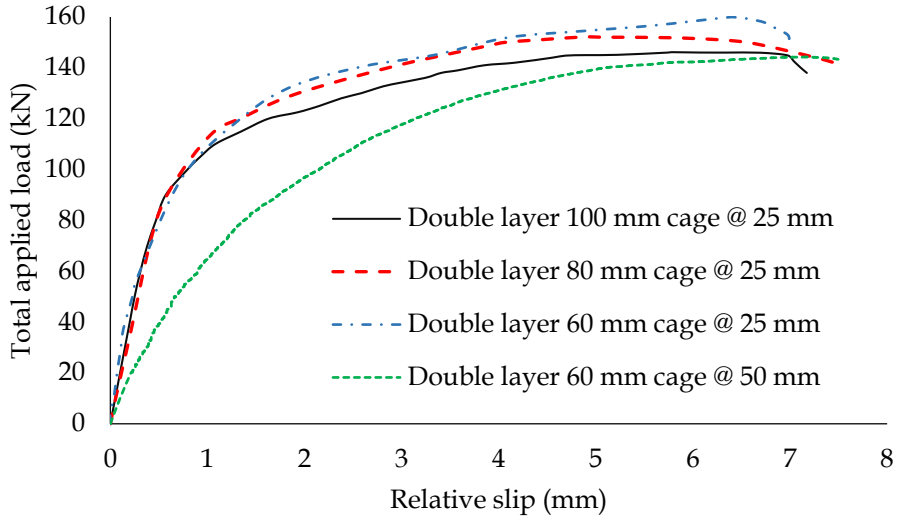

Fig. 5-23: Applied load- relative slip curves steel-concrete composite specimens with double layer reinforcement cages of 100 mm, 80 mm and 60 mm at 25 mm, and 60 mm at 50 mm from root of studs having strength C_2 of concrete elements

5.5.4 Triple Layered Reinforced Specimen

The performance of steel-concrete composite connections having three layers of reinforcement in concrete elements with C_1 and C_2 strengths, have been discussed in the present section. The effects of change in strength of concrete elements, on the behaviour of highly reinforced (1.8% reinforcement, as compared to 0.15% nominal reinforcement) composite connections have been investigated. The experimentally obtained values of ultimate strength and relative slip have been listed in *Table 5-10*. The shear capacity of connections for C_1 and C_2 strength concrete have been found to be 149.72 kN and 163.87 kN, respectively, while the ultimate slips for the two specimens have been obtained as 8.67 mm and 6.29 mm, respectively. The maximum shear strength of the connection increases by 14.15 kN (9.45%), while the ultimate slip of the connections reduces by 2.38 mm (29.24%), with an increase in the strength of concrete element by 6.5 MPa (18.61%).

The applied load vs relative slip curves of the composite push out test specimens with three layer of reinforcement have been shown in *Fig. 5-24*. The two characteristic features of the specimens having three layers of reinforcement are the high initial stiffness and significant ductility of the connections, as observed from the load-slip behaviour. The load-slip behaviour of the specimens suggest that the high initial stiffness of the specimens is owing to the contribution of concrete. However, after the yielding of concrete, the stiffness of the specimens reduces significantly, and the reinforcement bars and confined concrete together with the headed stud govern the post yield load-slip behaviour. The failure pattern of tested specimens has been shown in *Fig. 5-25*. It has been observed that the concrete elements sustain no visible cracking even at lower concrete strengths (C_1 and C_2), owing to high degree of confinement. However, crushing of concrete at the bearing zone of the headed stud has been observed. Considering that all the other governing parameters are constant, the relation between the shear strength of connector (Q_u) and concrete strength is,

$$Q_u \propto (\Delta f_{ck})^{1.0} (A_{r\%})^3 \qquad (5-3)$$

where, $A_{r\%}$ is the percentage reinforcement and Δf_{ck} is change in strength of concrete element in MPa.

Table 5-10: Ultimate dowel strength and induced slip at triple layer reinforced steel-concrete composite specimen interfaces.

Specimen details	Reinforcement amount (%)	capacity/stud (kN)	Ultimate slip (mm)
C_1(a, b and c)3RL50C25	1.80	153.34	8.67
C_2(a, b and c)3RL50C25	1.80	162.32	6.29

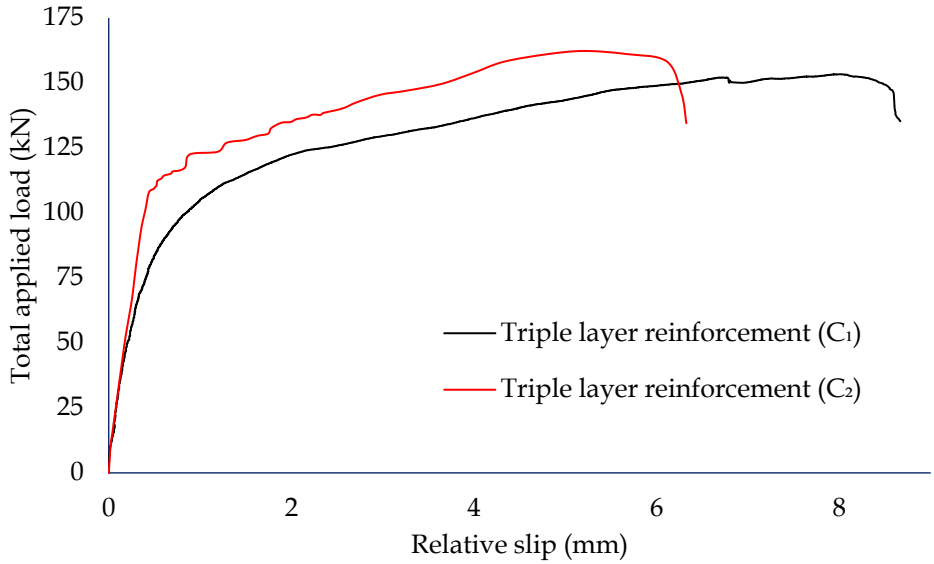

Fig. 5-24: Applied load relative slip for steel-concrete composite specimens having three layers of reinforcement with C_1 and C_2 concrete

Fig. 5-25: Typical failure of triple layered specimen from both faces (one side stud and other side weld) at the same time

5.6 Stiffness Comparison

This section aims at investigating the initial and post yield shear stiffnesses of composite specimens, using the concept of energy balance for the various composite specimens tested during the present study.

5.6.1 Unreinforced Specimens

The stiffnesses of unreinforced steel-concrete composite specimens have been evaluated using the equivalent energy approach. The area under the actual load-slip (representing energy) has been used to estimate the bilinear load-slip behaviour of the specimens, representing its initial and post yield stiffnesses. The values obtained for initial and post-yield stiffness have been reported in *Table 5-11*. In case of unreinforced composite specimens, the initial stiffnesses and post yield stiffnesses of the connections are 59.01 kN/mm and 3.36 kN/mm, respectively for specimen with C_1 strength concrete slab. While the corresponding values for unreinforced concrete slab having strength C_2 are 71.21 kN/mm and 4.16 kN/mm, respectively. The change in strength of concrete element from C_1 to C_2 (6.05 MPa or 18.62%), leads to an increase in initial stiffness and post yield stiffness by 12.20 kN/mm (or 20.67%) and 0.80 kN/mm (or 23.89%), respectively. The stiffnesses along with the actual and idealized load-slip curves for unreinforced specimens have been plotted and shown in *Figs. 5-26* and *5-27*.

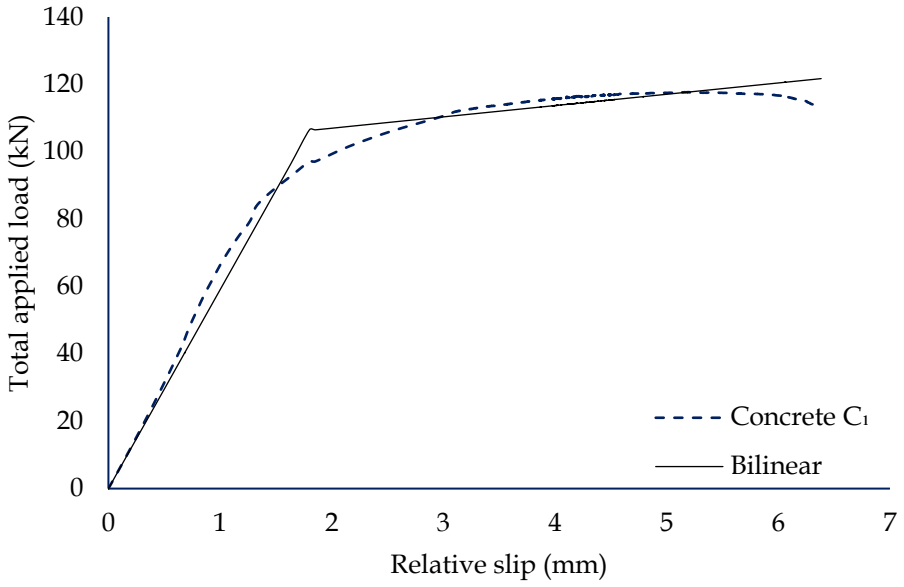

Fig. 5-26: Stiffness idealization for unreinforced composite specimen having concrete strength of C_1

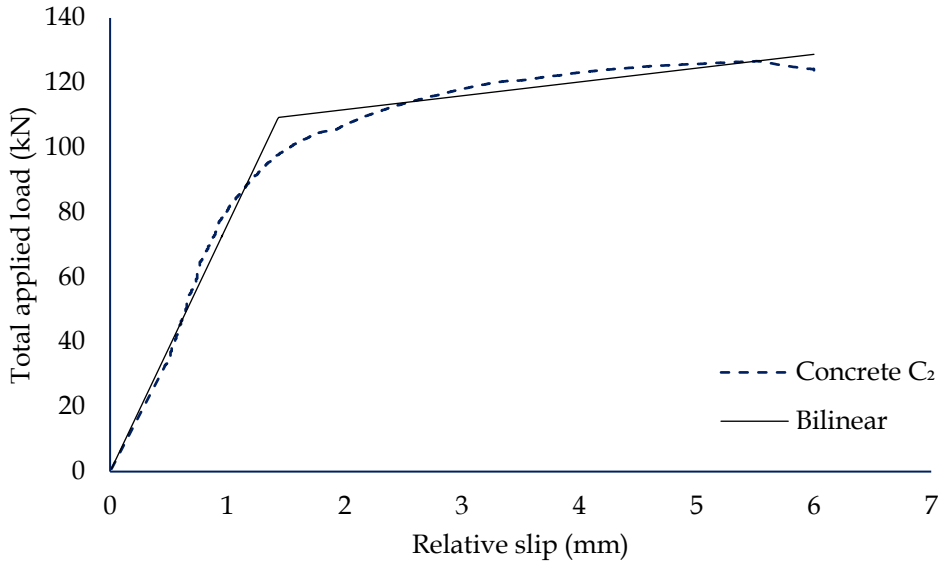

Fig. 5-27: Stiffness idealization for unreinforced composite specimen having concrete strength of C_2

Table 5-11: Initial and post-yield stiffnesses of unreinforced steel-concrete composite specimens

Specimen details	Initial stiffness (k_i) (kN/mm)	Change	Post-yield stiffness (k_{py}) (kN/mm)	Change
C_1 (a, b and c) 0RL0S0	59.01	12.20	3.36	0.80
C_2 (a, b and c) 0RL0S0	71.21	(20.67%)	4.16	(23.89%)

5.6.2 Single Layer Reinforced Specimen

This section presents a discussion on the shear stiffnesses (initial and post yield) of steel-concrete composite specimens with concrete elements having single layer of reinforcement. The specification and behaviour of the specimens have already been discussed in *sections 5.3.2* and *5.5.2*, respectively. The bilinear idealization of the load-slip behaviour of the specimens has been carried out as per the method discussed in *section 5.4.3.* The actual as well as idealized load-slip curves of the specimens have been plotted and shown in *Figs. 5-28* to *5-35*. The initial and post-yield stiffnesses of various specimens having single layer of reinforcement in concrete slab have been listed in *Table 5-12*. As compared to the specimens with unreinforced concrete slab, the initial stiffness of specimens with concrete elements having single layer of reinforcement exhibits an increase of 67.43 kN/mm (114.27%) and 80.89 kN/mm (113.59%) in shear stiffness for concrete element

strength C_1 and C_2, respectively. However, the post yield stiffness exhibits negligible change. It can thus be concluded that the introduction of single reinforcement layer in concrete element leads to a significant increase in initial stiffness only. Further, it has been observed that, with increase in distance between the reinforcement layer and the root of headed stud the initial stiffness of the connection reduces, and is almost equal to the values of initial and post yield stiffness of specimens with unreinforced concrete elements (as is evident from *Table 5-12*).

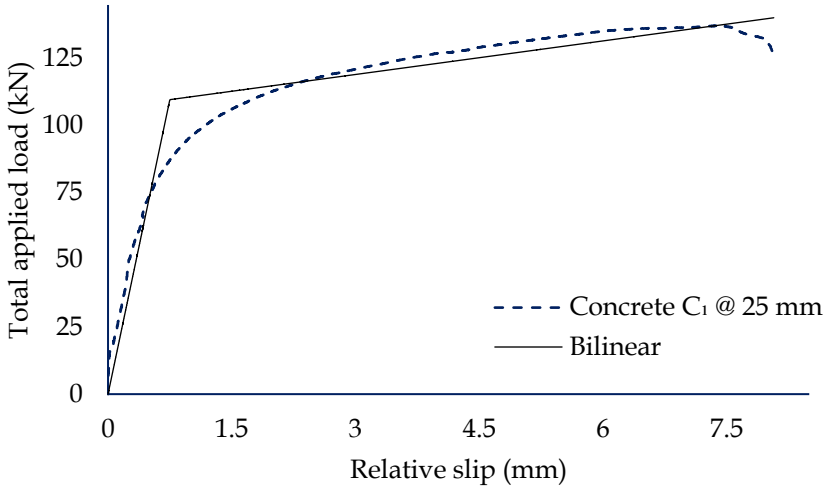

Fig. 5-28: Stiffness idealization for composite specimen with single layer reinforcement at 25 mm from root of stud having C_1 concrete

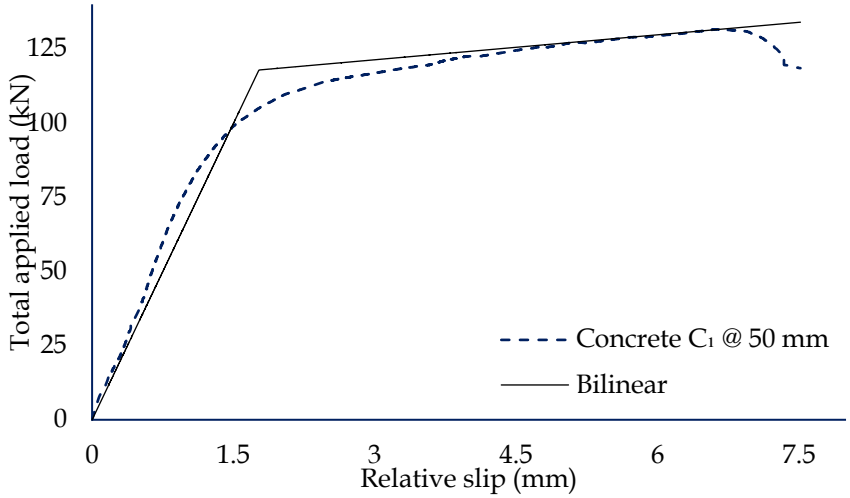

Fig. 5-29: Stiffness idealization for composite specimen with single layer reinforcement at 50 mm from root of stud having concrete strength of C_1

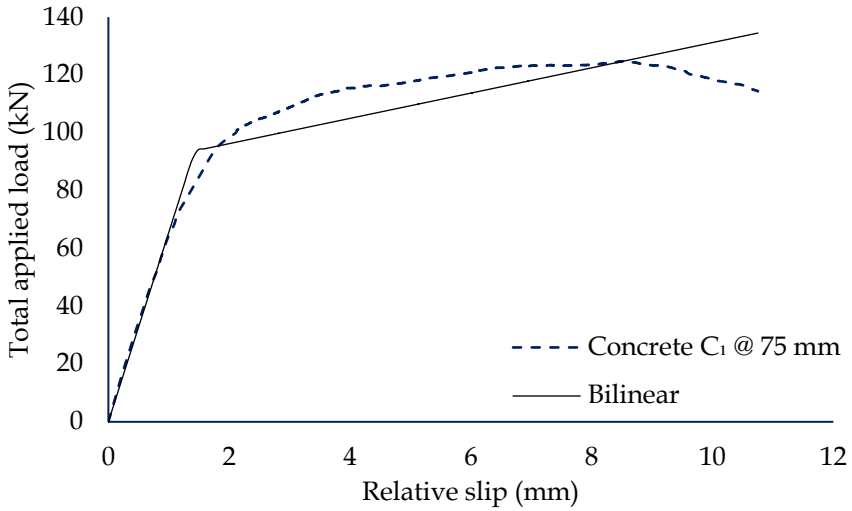

Fig. 5-30: Stiffness idealization for composite specimen with single layer reinforcement at 75 mm from root of stud having concrete strength of C_1

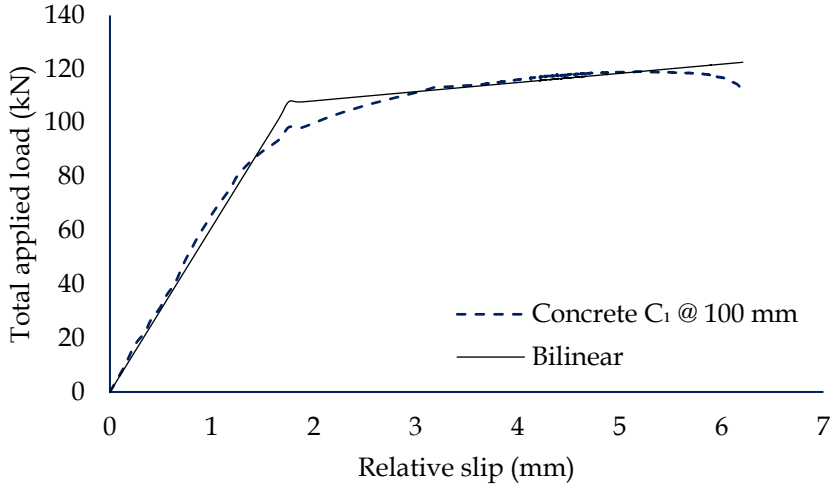

Fig. 5-31: Stiffness idealization for composite specimen with single layer reinforcement at 100 mm from root of stud having concrete strength of C_1

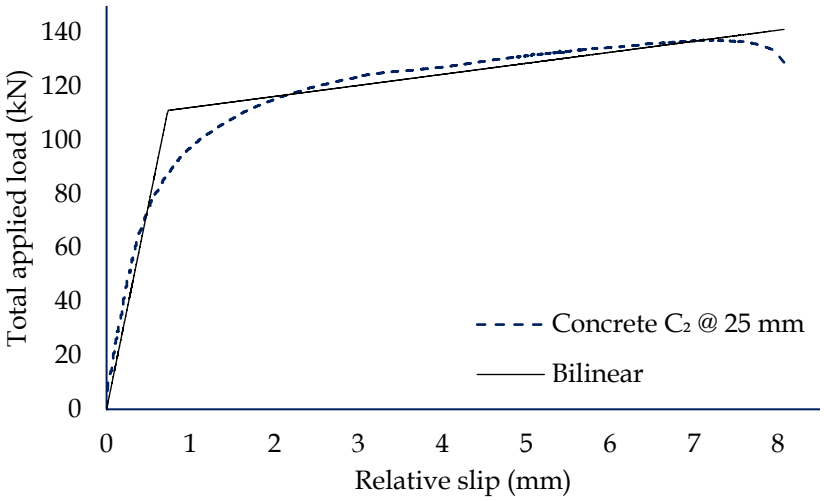

Fig. 5-32: Stiffness idealization for composite specimen with single layer reinforcement at 25 mm from root of stud having concrete strength of C_2

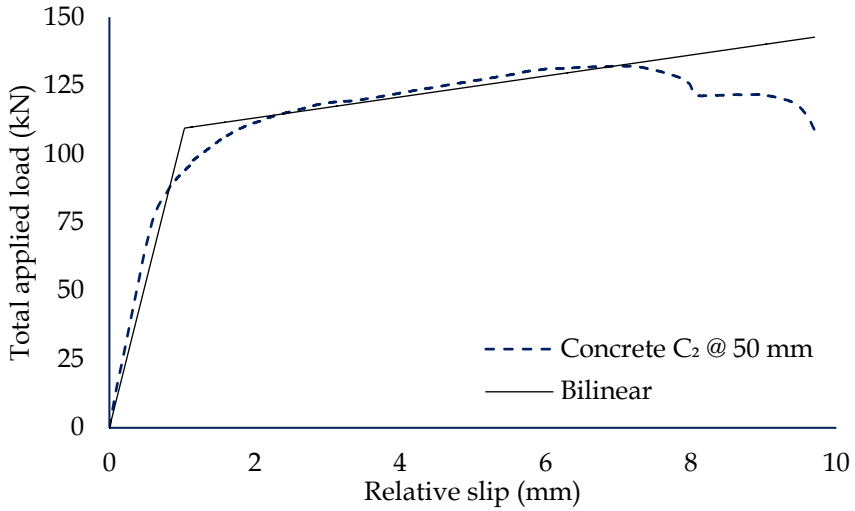

Fig. 5-33: Stiffness idealization for composite specimen with single layer reinforcement at 50 mm from root of stud having concrete strength of C_2

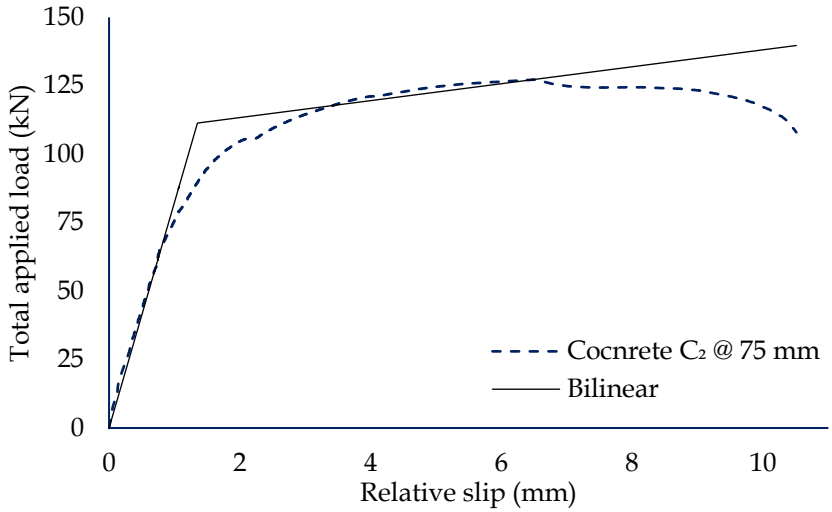

Fig. 5-34: Stiffness idealization for composite specimen with single layer reinforcement at 75 mm from root of stud having concrete strength of C_2

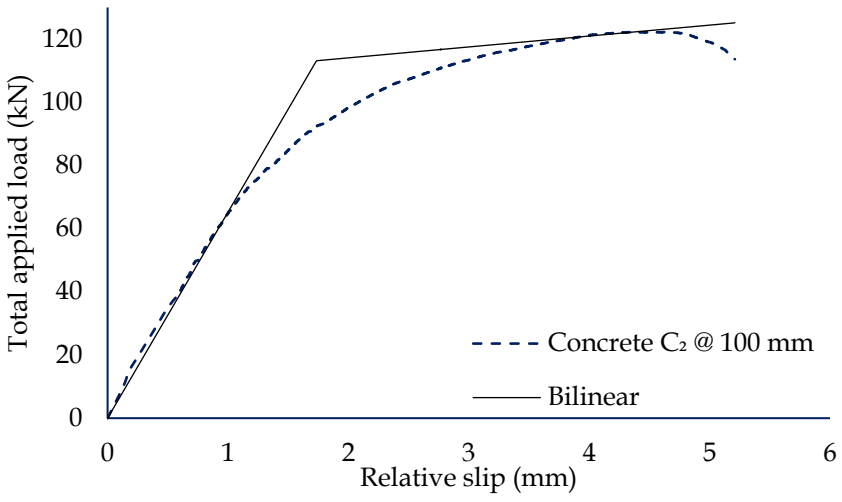

Fig. 5-35: Stiffness idealization for composite specimen with single layer reinforcement at 100 mm from root of stud having concrete strength of C_2

Table 5-12: Initial and post-yield stiffnesses of single layer reinforced steel-concrete composite specimens

Specimen	Initial stiffness (k_i)	Post-yield stiffness (K_{py})
	(kN/mm)	(kN/mm)
C_1(a, b and c)1RL0S25	146.45	4.17
C_2(a, b and c)1RL0S25	152.10	4.11
C_1(a, b and c)1RL0S50	66.58	2.80
C_2(a, b and c)1RL0S50	106.00	3.83
C_1(a, b and c)1RL0S75	65.57	4.37
C_2(a, b and c)1RL0S75	82.40	3.09
C_1(a, b and c)1RL0S100	61.29	3.41
C_2(a, b and c)1RL0S100	65.21	3.45

5.6.3 Double Layer Reinforced Specimens

In this section, the initial and post yield stiffnesses of steel-concrete composite specimens with concrete elements having two layers of reinforcement at different spatial locations have been presented. The actual as well as the bilinear load-slip curves (representing the initial and post yield stiffnesses) of the tested specimens have been shown in *Figs. 5-36* to *5-41*. The estimated values of the initial and post yield stiffnesses of all the tested specimens have been shown in *Table 5-13*. The composite specimens with concrete elements having single layer of reinforcement at 25 mm from root of stud and double layer of reinforcement with 100 mm cage at 25 mm from root of stud exhibits almost similar stiffness values. However, with increase in confinement of concrete in the specimens, the initial and post yield stiffnesses have been observed to increase. The effects of increase in confining width from 100 mm to 60 mm are increase in initial stiffness (by 34.18 kN/mm or 22.50%) and post yield stiffness (by 2.48 kN/mm or 78.97%) for concrete strength C_1. Similarly, for the specimens with concrete element having C_2 strength and spacing between reinforcement layers reduced from 100 mm to 60 mm, increase in initial stiffness (by 64.15 kN/mm 40.12%) and post yield stiffness (by 2.16 kN/mm or 49.88%) has been observed. The change is very high (almost 50%) in initial as well as post yield stiffnesses for both the concrete strengths. The results clearly indicate that the stiffnesses of connections are significantly affected by the geometry and location of reinforcement cage. It can also be concluded that with increase in the distance between first reinforcement layer and root of stud, the

connection strength and stiffness reduces. The stiffness idealization curves for composite specimens with 100 mm reinforcement cage at 25 mm from root of stud having C_1 and C_2 concrete have been shown in *Figs. 5-12* and *5-13*.

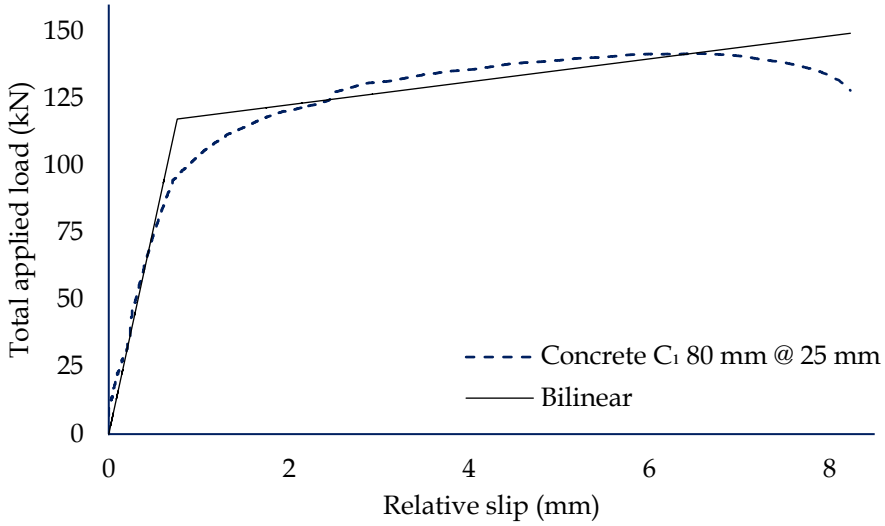

Fig. 5-36: Stiffness idealization for composite specimen with double layer reinforcement with 80 mm cage at 25 mm from root of stud having concrete strength of C_1

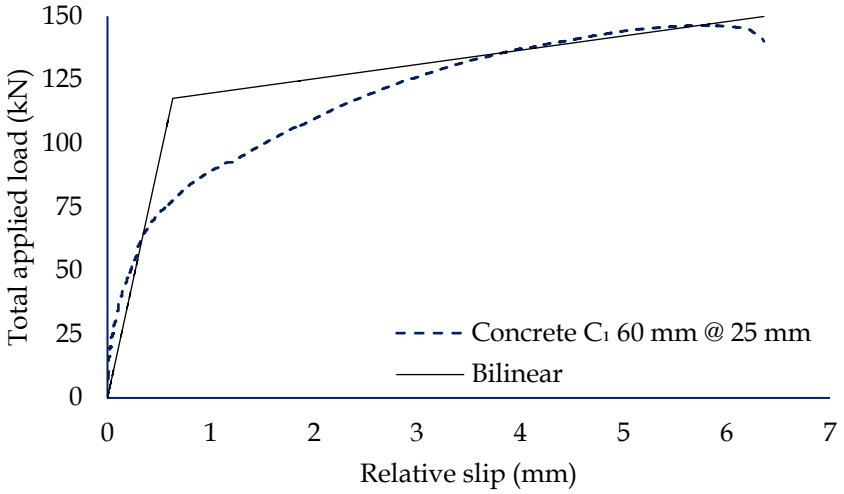

Fig. 5-37: Stiffness idealization for composite specimen with double layer reinforcement with 60 mm cage at 25 mm from root of stud having concrete strength of C_1

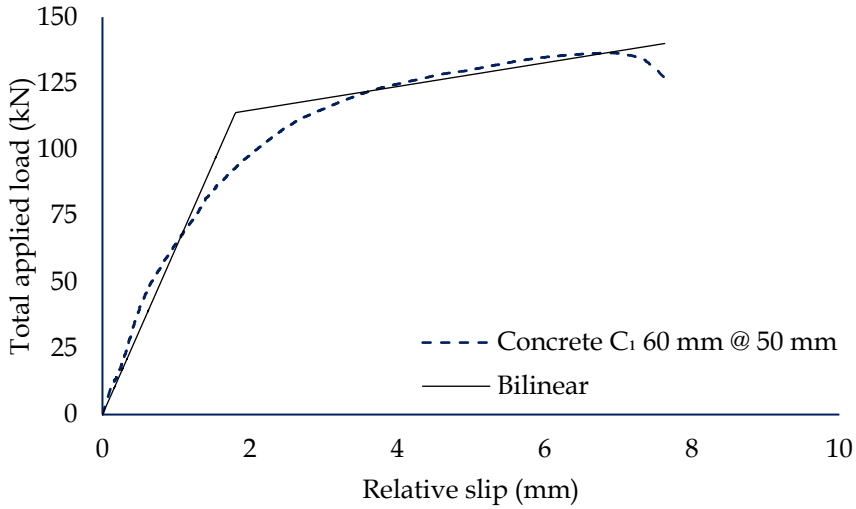

Fig. 5-38: Stiffness idealization for composite specimen with double layer reinforcement with 60 mm cage at 50 mm from root of stud having concrete strength of C_1

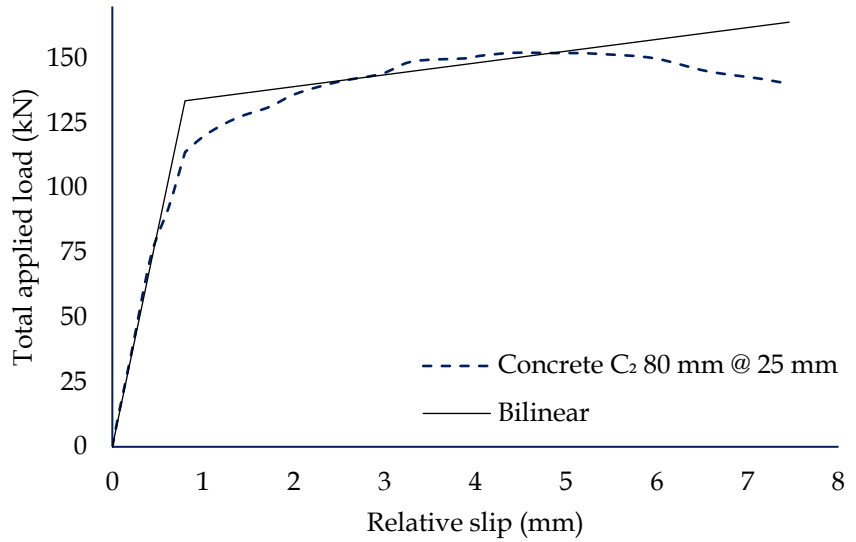

Fig. 5-39: Stiffness idealization for composite specimen with double layer reinforcement with 80 mm cage at 25 mm from root of stud having concrete strength of C_2

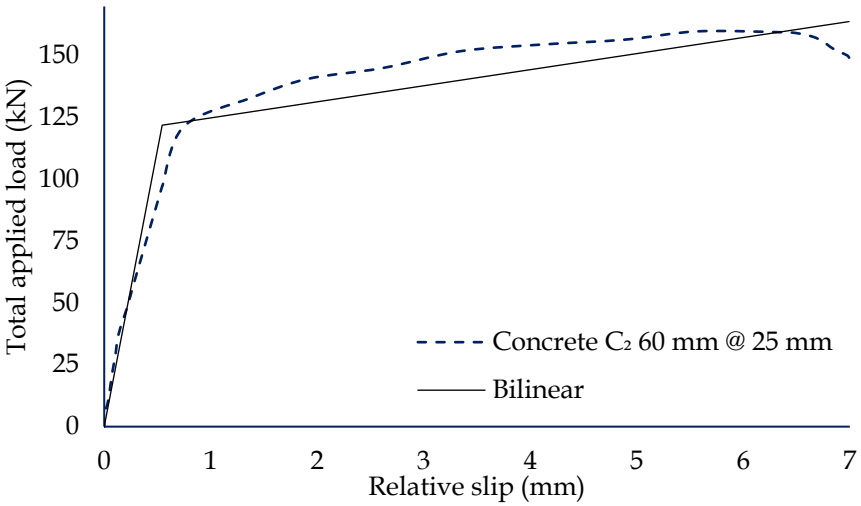

Fig. 5-40: Stiffness idealization for composite specimen with double layer reinforcement with 60 mm cage at 25 mm from root of stud having concrete strength of C_2

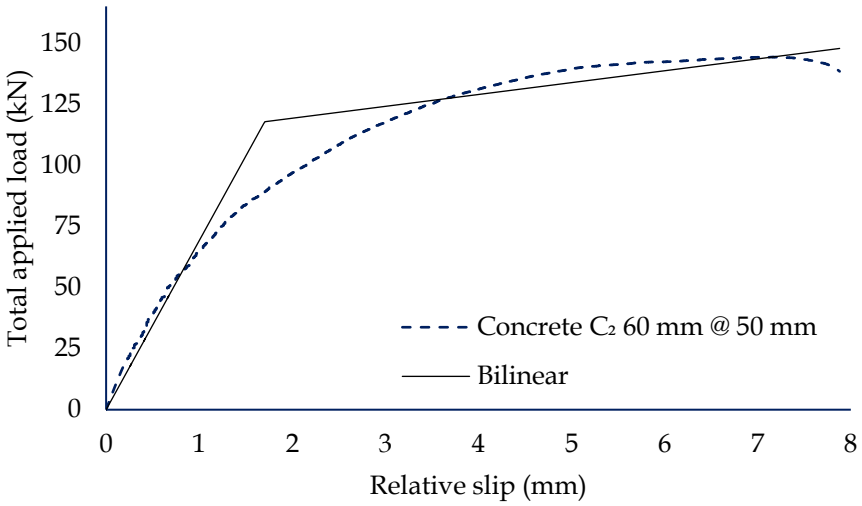

Fig. 5-41: Stiffness idealization for composite specimen with double layer reinforcement with 60 mm cage at 50 mm from root of stud having concrete strength of C_2

Table 5-13: Initial and post-yield stiffnesses of double layer reinforced steel-concrete composite specimens.

Specimen details	Initial shear stiffness (k_i) (kN/mm)	Post-yield stiffness (k_{py}) (kN/mm)
C_1(a, b and c)2RL100S25	151.93	3.14
C_2(a, b and c)2RL100S25	159.90	4.34
C_1(a, b and c)2RL80S25	154.48	4.28
C_2(a, b and c)2RL80S25	166.78	4.66
C_1(a, b and c)2RL60S25	186.11	5.62
C_2(a, b and c)2RL60S25	224.06	6.51
C_1(a, b and c)2RL60S50	63.13	4.48
C_2(a, b and c)2RL60S50	69.14	4.86

5.6.4 Triple Layer Reinforced Specimens

The initial and post yield stiffnesses of composite specimens with concrete elements having three layers of reinforcement have been detailed in this section. The bilinear idealized load-slip curves along with the actual load-slip behaviour of specimens with triply reinforced concrete elements having strengths of C_1 and C_2 have been shown in *Figs. 5-42* and *5-43*, respectively. The initial and post yield stiffnesses of the tested specimens have been listed in *Table 5-14*. A significant variation in the stiffness values has been observed in comparison to the corresponding values for specimens with concrete elements having 100 mm confining width and 25 mm distance between root of stud and first reinforcement

layer. For composite specimens with C_1 concrete elements, the observed increment in initial stiffnesses is 49.32 kN/mm (32.46%) while that for post yield stiffness is 3.02 kN/mm (96.21%). Similarly, for composite specimen with C_2 concrete, the increase in initial and post yield stiffness have been observed to be 98.46 kN/mm (61.57%) and 3.08 kN/mm (71.03%), respectively. As compared to the specimens having unreinforced concrete elements, the specimens with three layers of reinforcement exhibit an increase in initial and post yield stiffnesses by almost 3.5 times and 1.8 times, respectively.

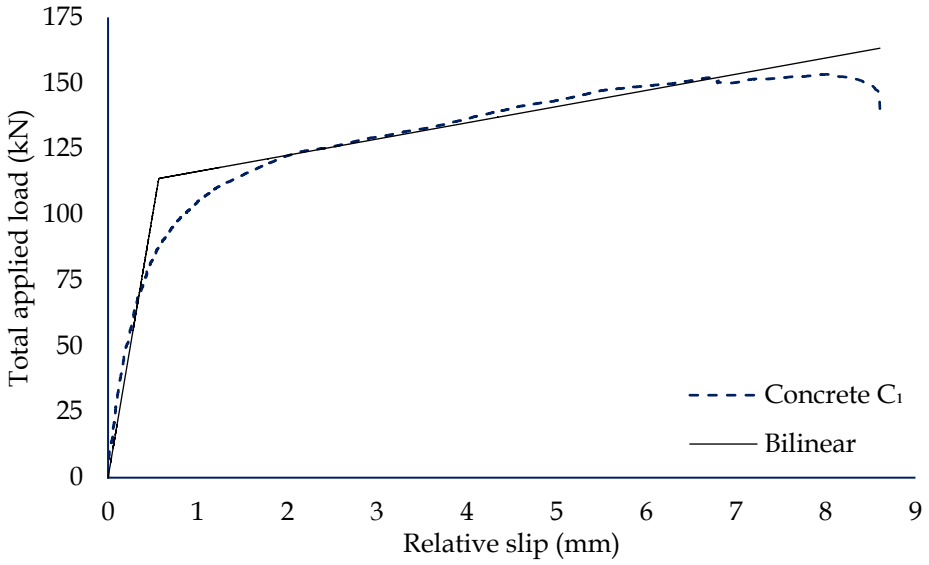

Fig. 5-42: Stiffness idealization for composite specimen with triple layer reinforcement having concrete strength of C_1

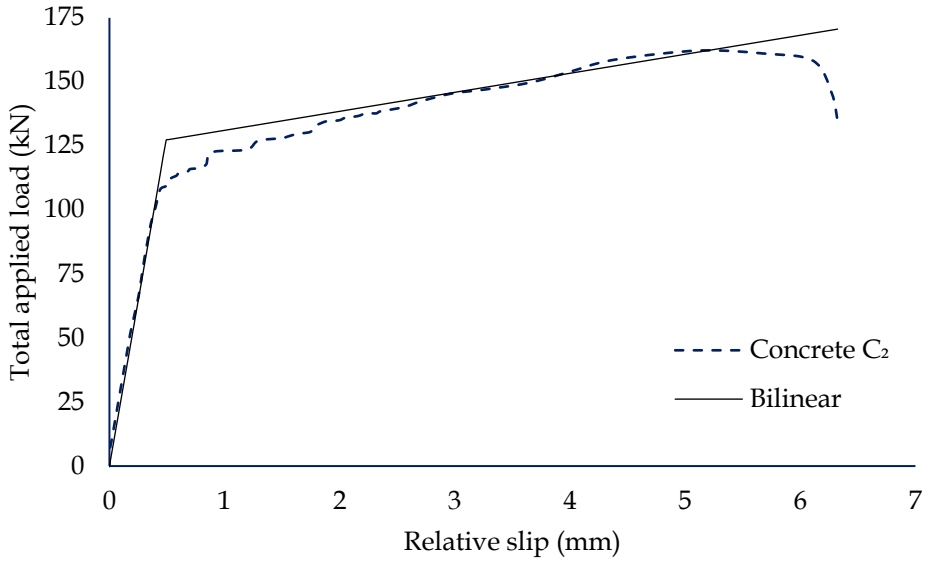

Fig. 5-43: Stiffness idealization for composite specimen with triple layer reinforcement having concrete strength of C_2

Table 5-14: Initial and post-yield stiffnesses of triple layer reinforced steel-concrete composite specimens.

Specimen details	Initial stiffness (k_i)	Post-yield stiffness (k_{yp})
	(kN/mm)	(kN/mm)
C_1(a, b and c)3RL50S25	201.25	6.16
C_2(a, b and c)3RL50S25	258.37	7.42

5.7 Conclusions

The behaviour of mechanical headed stud connected composite specimens under monotonic loading has been investigated in the present chapter. The parameters considered to investigate the behaviour of composite connections are, the strength of concrete elements (from C_1 to C_5) and the quantity and location of the reinforcement. The following are the precise conclusions, drawn from the study:

- The compressive strength of concrete elements significantly affects the dowel strength of headed stud connector(s). A linear relation exists between the dowel strength of shear connector and compressive strength of concrete elements considered in present study.
- There exists an inverse relationship between the strength of concrete element and the ultimate relative slip of the connection. The observed ultimate slip for a composite specimen having C_5 strength concrete is as low as 5.37 mm, which is lower than the minimum relative slip of 6 mm specified by Eurocode 4 for ductile connections.
- Another notable effect of increase in the strength of concrete element is the reduction in deformability along with a downward shift of fracture height of the studs (towards the root of stud). It has been observed that, for the specimen having concrete element of strength C_5, the failure of stud occurs due to fracture of weld, along with minimal crushing of concrete at the bearing zone.
- The increase in strength of concrete element leads to significant increase in the initial and post yield stiffnesses of the connections increases significantly. An increase of upto 133.20% in the initial stiffness and 142.10% in the post yield stiffness has been observed with the change in strength of concrete elements from C_1 to C_5 (126.03%).

- The effect of increase in quantity of reinforcement (from 0 to 1.8%) is that the ultimate strength of the connection increases with density of reinforcement. However, for the steel-concrete composite specimens having very high strength of concrete elements, the failure of headed stud governs the performance.
- The shear strength of steel-concrete composite connection reduces with an increase in the distance between first layer of reinforcement and the root of stud. When this distance is increased from 25 mm to 100 mm, the connection strength reduces, by 15.31% (137.34 kN to 119.10 kN) in case of C_1 concrete, and by 11.50% (138.12 kN to 122.23 kN) in case of C_2 concrete.
- The ductility of connection has been observed to increase with the increase in distance between root of stud and reinforcement cage. However, this effect is observed only when the reinforcement cage lies in the zone of influence of the headed studs.
- Premature failure has been observed in single layer reinforced steel-concrete composite specimens, primarily owing to cracking of concrete at the level of reinforcement layer.
- The stiffness, strength and ductility of composite connections increases with an increase in the percentage of reinforcement in the concrete layer due to enhanced confinement effect.
- The load-slip behaviour of specimen with unreinforced concrete element is almost similar to that of the specimen with concrete element having single layer of reinforcement at 100 mm from root of shear stud. It can thus be concluded that the effect of reinforcement, outside the influence zone of the headed stud, is negligible.
- The composite specimen with concrete element having 100 mm reinforcement cage at 25 mm from root of stud and specimen with concrete element having 60 mm reinforcement cage at 50 mm from root of stud exhibits almost same ultimate strength. However, the load-slip curves of the two specimens follow entirely different paths. The initial stiffness of

specimen with concrete element having 60 mm reinforcement cage at 50 mm from root of stud has been found to be governed by concrete only.

- Double layer reinforced specimens having 100 mm cage with 25 mm spacing from root of stud and 60 mm cage with 50 mm spacing from root of stud follow almost identical path in load-slip curve under monotonic loading.
- Although, the effect of reinforcement layers on the post yield stiffness of connections is marginal, the initial stiffnesses of connections having no reinforcement and single layer of reinforcement increases by 67.43 kN/mm (114.27%) for C_1 strength concrete and by 80.89 kN/mm (113.59%) for C_2 strength concrete.
- The reduction in the confining width of reinforcement from 100 mm to 60 mm leads to increase in the initial and post yield stiffnesses of steel-concrete composite specimens. In case of specimens with C_1 concrete, the initial stiffness increases by 34.18 kN/mm (22.50%) and post yield stiffness increases by 2.479 kN/mm (78.97%). Also, for specimens with concrete element having C_2 strength the increase in initial stiffness is about 64.15 kN/mm (40.12%) and increase in post yield stiffness is about 2.16 kN/mm (49.88%). These observations underscore the importance of confinement of concrete element in terms of strength and stiffness of the connections.
- The strength and stiffness of the connections is inversely related to the distance between the root of stud and the first layer of reinforcement, i.e., the strength and stiffness of the connection reduces with increase in the distance between the root of stud and first reinforcement layer.
- The specimens with concrete element having three layers of reinforcement exhibits significantly higher initial stiffness (3.5 times) and post yield stiffness (1.8 times) than the corresponding specimens having unreinforced concrete elements.

Chapter: 6

Effect of Adhesive Layer Thickness on Behaviour of Bonded Connections

6.1 Overview

The performance of steel-concrete composite members depends on the connection at the steel-concrete interface. Of the two connection methodologies considered in this study, the thickness of adhesive layer at composite interface is the most critical parameter, in case of bonded connections, that determines the connection performance. In this chapter, the effect of the change in thickness of adhesive layer, on the capacity of connection, the ultimate slip at the interface and the initial shear stiffness of connection have been analysed. Steel-concrete composite specimens, bonded with adhesive layers of different thicknesses, have been prepared as push-out test specimens. The cast and prepared specimens have been tested under compressive shear, to determine the behaviour of composite connections.

The applied load - relative slip curves for all bonded specimens have been plotted. The ultimate strength and engendered slip, for all adhesive layer thicknesses of steel-concrete specimens, have been obtained through load-slip curves. The failure patterns of bonded connections has been critically observed and discussed in detail. The initial shear stiffness of bonded connections have also been estimated through the load-slip curves. The behaviour obtained from experimental studies has been substantiated through finite element (FE) verification.

6.2 Materials Used

6.2.1 Concrete

The concrete slabs used for the bonded steel-concrete composite push-out test specimens, in the present study, have been prepared using the high strength concrete (C_5) (*Table 3-2*). The 28 days compressive strength of cured concrete cube is 73.46 MPa. The mix proportioning details and other relevant properties of the concrete has already been discussed in Chapter three (*section 3.2.1)*.

6.2.2 Structural Steel

The steel sections used to prepare the steel-concrete composite specimens, are standard universal column sections. The properties of selected steel section have been shown in *Table 6-1*. The bonded specimens employ Universal Steel Column UC 112@23 kg/m sections, cut to the length of 350 mm. *Fig. 6-1* shows a typical schematic view of structural steel section.

Table 6-1: Geometric details of structural steel section used in bonded composite specimen

Description	Sectional weight	Total depth	Flange width	Thickness of web	Thickness of flange	Area
	(kg/m)	(mm)	(mm)	(mm)	(mm)	(mm^2)
UC 112 × 112 × 23	23.1	112.0	103.0	7.4	10	1899

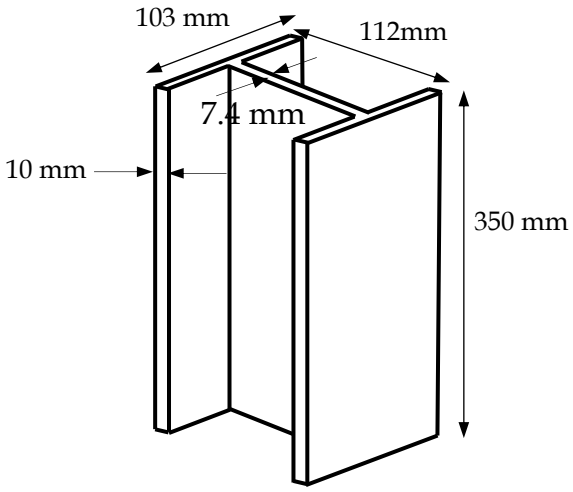

Fig. 6-1: Schematic representation of steel column (UC 112@23kg/m) used in bonded composite specimen

6.2.3 Structural Adhesive

The epoxy based structural adhesive, selected on the basis of a preliminary study, as discussed in *section 3.2.5.1*, has been used for the present study. The properties of selected adhesive have been discussed in detail in the Chapter three (*section 3.2.5.2*). The prepared concrete and steel sections have been shown in *Fig. 6-2*. To prevent the flow of adhesive outside the desired area, and to maintain a uniform thickness of adhesive layer, double sided polyurethane tape has been used to mark the bonded area. The adhesive tape has been applied along three edges of the bonded area in concrete slab (as shown in *Fig. 6-2*), while one edge of bonded area

in concrete slab has been left without tape to squeeze out surplus adhesive from the bonded area. The area surrounding the adhesive tape has been greased, to prevent alteration in the bonded area.

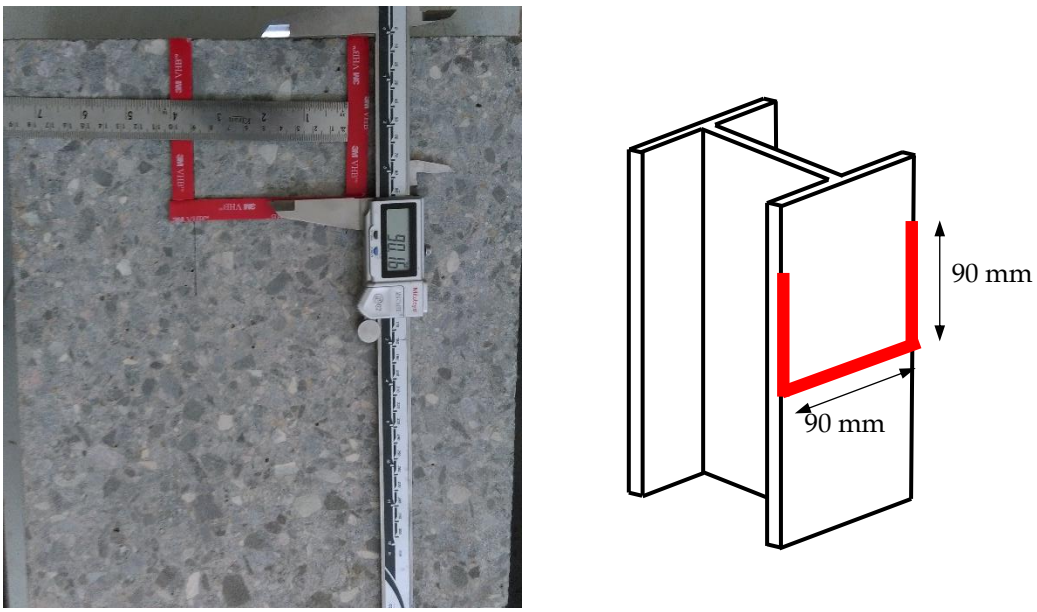

Fig. 6-2: Prepared specimen; (a) concrete section prepared for adhesive bonding and (b) steel section prepared for bonding

6.3 Push-Out Test: General Arrangement

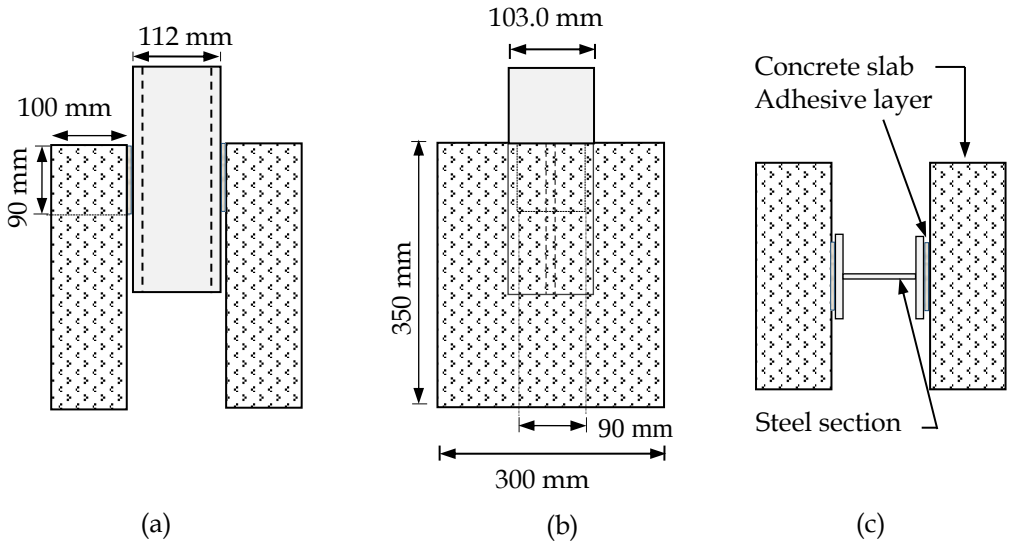

Fig. 6-3: Geometric detail of push-out test specimen with arrangement; (a) front view, (b) side view and (c) top view

The geometrical arrangement of push out test specimen has been adopted from the Eurocode 4 (EC4 2004) specifications (procedure discussed in *section 3.3.1*), while the dimensional details have been adopted from Si-Larbi et al. (2007).

The bonded area on each of the two faces of a specimen is 90 mm × 90 mm, maintaining an aspect ratio of one. A schematic representation of the detailed geometry of push out test specimen and connection at steel-concrete interface has been shown in *Fig. 6-3*. The experimental push-out test setup with instrumentation details has been shown in *Fig. 6-4*.

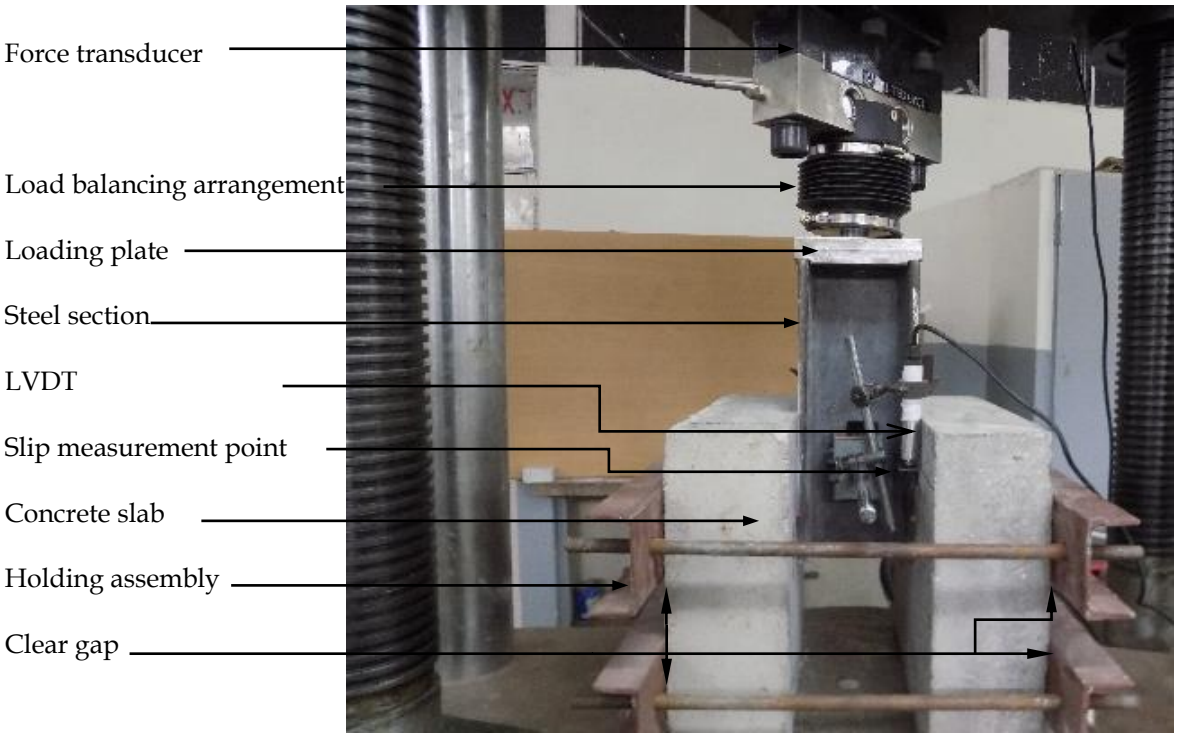

Fig. 6-4: Push out test: Detailed arrangements of testing equipment and composite specimen on loading frame

6.4 Methodology

The experimental programme has been designed to evaluate the optimum bond thickness of connections, using twenty-five push out test specimens. The effect of bond layer thickness on the performance of connections has been analysed through a parametric experimental study, with specimens having five different bond layer thicknesses of 1 mm, 2 mm, 3 mm, 4 mm and 5 mm. Five push out test specimens for each bond layer thickness have been prepared, and analysed. The primary purpose of preparing five specimens for each adhesive layer thickness, is to obtain a better estimate of strength and slip capacity of the connections. Five different values of thicknesses provide an insight on the failure modes of connection interfaces in the specimens.

6.5 Analytical Verification

Analytical verification of experimental results has been carried out through finite element (FE) analysis software package ABAQUS 6.13 (Simulia HSK 2013). All elements (concrete slab, steel section and adhesive layer) have been modelled as three dimensional elements for increased computational accuracy. A uniform mesh has been developed using three dimensional eight noded brick elements with reduced integration (C3D8R). Owing to the symmetry of the push-out specimens in terms of loading, boundary conditions and geometry, a quarter model has been analysed to simulate the experimental conditions. The details of the modelled specimens along with boundary conditions are shown in *Fig. 6-5*. Different mesh sizes have been tried to achieve the convergence of FE analysis results. The selected mesh size has an aspect ratio of three. A typical meshed quater finite element model, having 3413 elements, has been shown in *Fig. 6-6*. The number of elements and element size varies with variation in adhesive layer thicknesses.

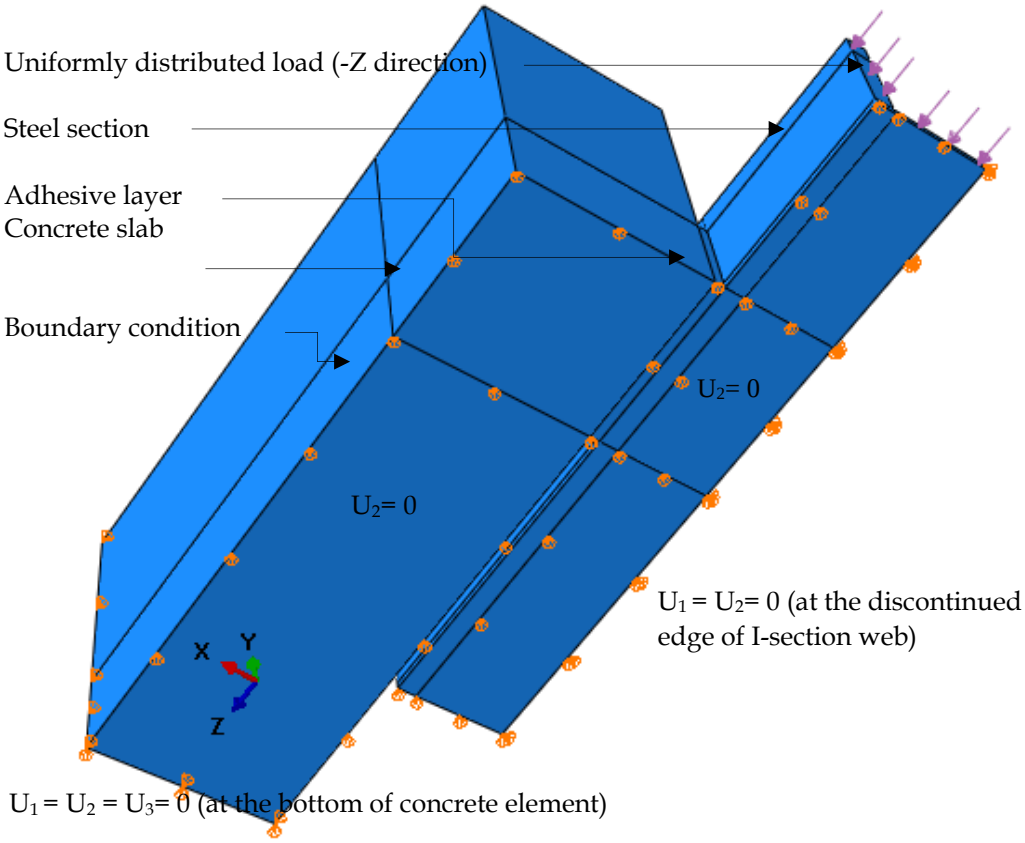

Fig. 6-5: Geometric details of FE quarter model of steel-concrete composite push out specimen

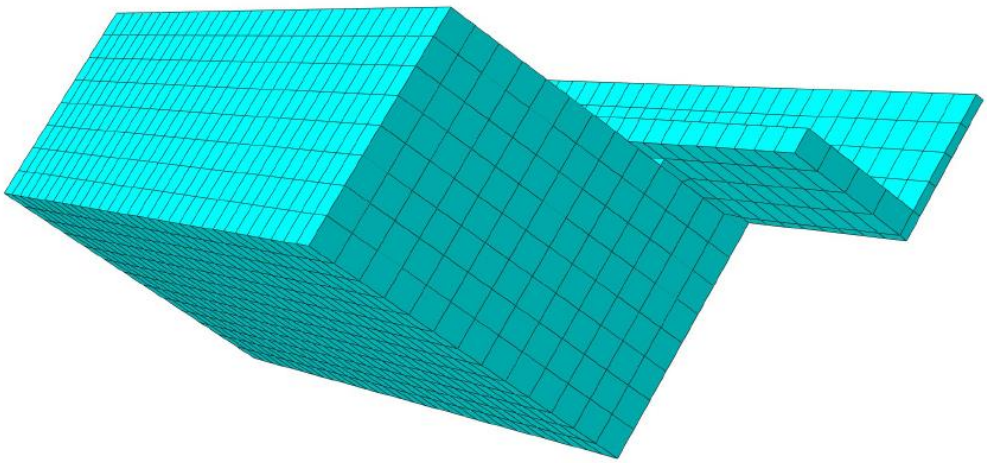

Fig. 6-6: FE quarter model (having 3413 elements) for bonded composite specimen with three mm thick adhesive layer

6.6 Effect of Adhesive Layer Thickness

The behaviour of epoxy bonded steel-concrete composite push out test specimens, having different thicknesses of bond layer, subjected to direct compressive shear loading has been discussed in this section. The results of finite element analyses have also been discussed to support the experimental findings.

6.6.1 Bond Layer Thickness of One mm

The push-out tests on specimens with one mm thickness of adhesive layer has been performed. During the tests, the observed relative slip in the specimens has been plotted against the applied load. The variations in total applied load with respect to the interfacial slip for both experimental and FE analyses have been shown in *Fig. 6-7*. The figure depicts a close interaction between the ultimate capacity and relative slip at interface for all specimens. The total applied load and the engendered relative slip follow a linear path up to the failure, which represents a constant rigidity in composite connection. The average values of load capacity and the ultimate relative slip obtained from experiments are 165.88 kN and 20.5 microns (μm) respectively. The FE values for ultimate load and relative slip are 153.45 kN and 21.94 μm respectively. The percentage variation between experimental and FE analysis results, for ultimate load and relative slip are 7.49% and 7.02%, respectively. *Fig. 6-8* shows the observed failure pattern of concrete-

epoxy-steel connection. Adhesion failure has been observed in all specimen i.e., the complete adhesive layer has been ripped off either from epoxy-steel interface or from concrete-epoxy interface. The primary reason for this ripping-off of the surfaces is high stress concentration at connected interfaces, which is evident in *Figs. 6-9(a)* and *(b)*. The high stress concentration at bearing portion (loading end) leads to cracking of the concrete surrounding the bonded area as observed in *Fig. 6-9(a)*. It has been found that the crack propagates from the bearing end into the concrete, as observed in *Fig. 6-9(b)*.

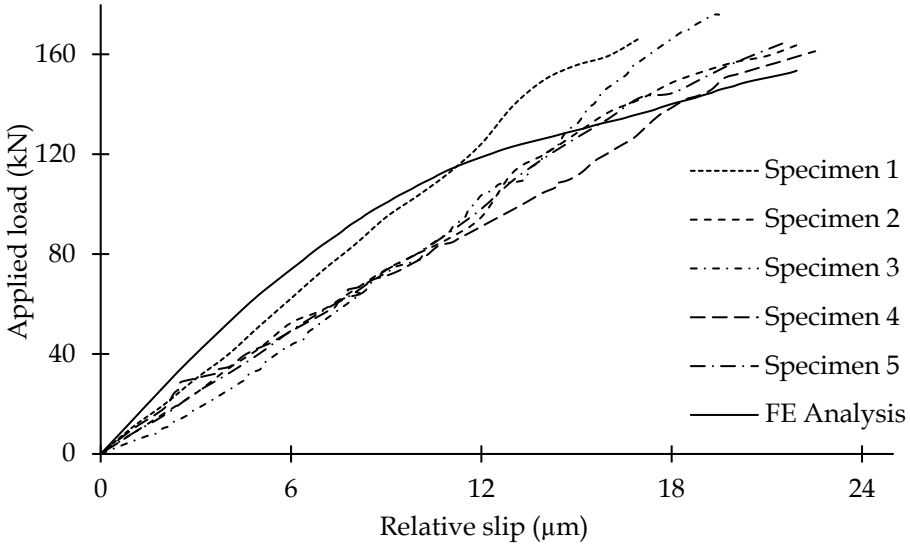

Fig. 6-7: Variation of relative slip with total applied load for composite specimens bonded with one mm thick adhesive layer

Fig. 6-8: Adhesion failure of one mm thick adhesive layer from epoxy-steel interface

(a) (b)

Fig. 6-9: Bearing zone failure in concrete specimen at interface for one mm thick adhesive layer; (a) crack lines at bearing end of interface after failure and (b) diagonally propagated shear crack in concrete specimen

6.6.2 Bond Layer Thickness of Two mm

Fig. 6-10 shows the variation of total applied load against the measured interfacial slip, for experimental and FE analysis of specimens having two mm thickness of adhesive layer. It has been observed that at higher load levels, the connection stiffness decreases slightly in comparison to specimen having one mm thickness of adhesive layer. However, no significant increase in connection ductility has been observed with increase in thickness of adhesive layer. The average value of load capacity and ultimate slip obtained from experiments are 173.9 kN and 26.0 μm, respectively. The FE values for ultimate load and relative slip are 164.11 kN and 26.47 μm, respectively. The percentage variation in values of ultimate load and relative slip between experimental and FE analysis are 5.63% and 1.18%, respectively. The failure pattern of concrete-epoxy and epoxy-steel interfaces have been shown in *Fig. 6-11*. Adhesive failure mode is clearly evident in the figure, as there are no observable slipping contours in the adhesive layer. The failure pattern is similar to the one observed in case of one mm thick adhesive layer. However, the stress concentration at bearing portion reduced significantly, leading to prevention of premature failure and increased strength of composite connection.

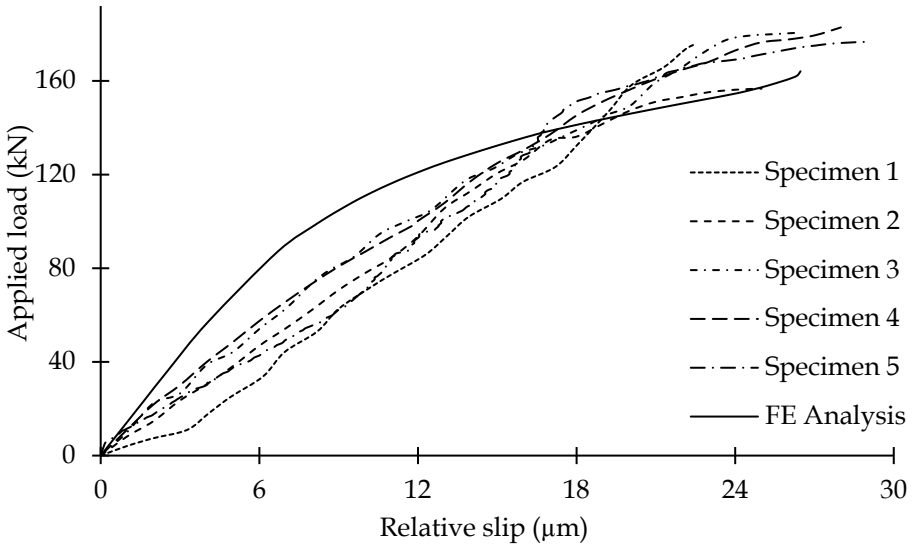

Fig. 6-10: Variation of relative slip with total applied load for composite specimens bonded with two mm thick adhesive layer

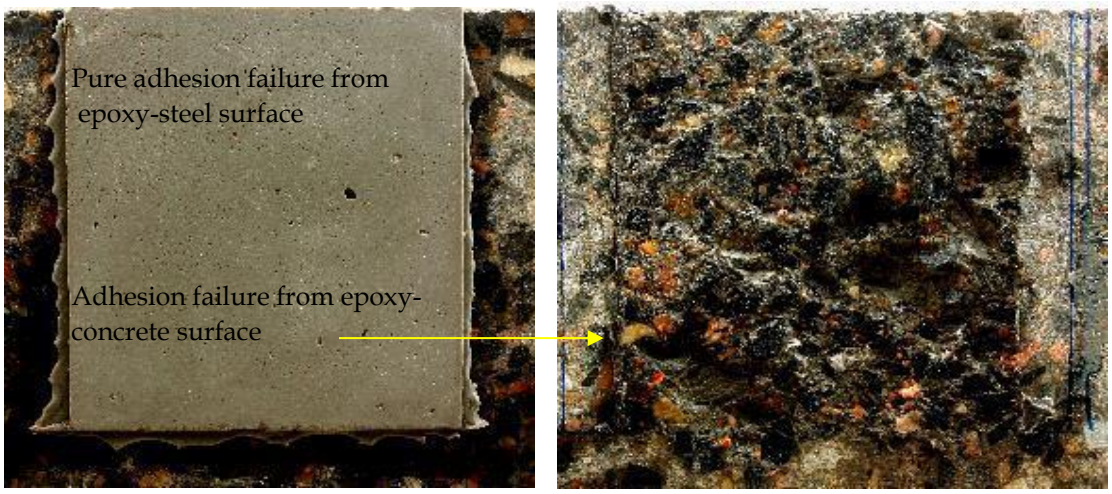

Fig. 6-11: Adhesive failure of interface in composite specimen for two mm thick adhesive layer

6.6.3 Bond Layer Thickness of Three mm

The relationship between total applied load and interfacial slip for experimental and FE analysis having three mm thickness of adhesive layer has been shown in *Fig. 6-12*. The average values of load capacity and ultimate slip, obtained in this experimental study are 194.3 kN and 33.0 μm, respectively; these properties are observed to be directly proportional to the thickness of the adhesive layer. The FE values for ultimate load and relative slip are 182.07 kN and 32.90 μm, respectively. The percentage variation in ultimate load and relative slip between experimental

and FE analysis are 6.29% and 0.30%, respectively. *Fig. 6-13* shows the observed failure modes in connection having 3 mm thickness of the adhesive layer. *Fig. 6-13(a)* clearly shows a mixed mode of failure in the concrete-epoxy-steel interface, while *Fig. 6-13(b)* shows an adhesive bond failure. It can be observed that in the case of the mixed mode of failure, the failure plane is inclined at an angle of 45° from the direction of loading.

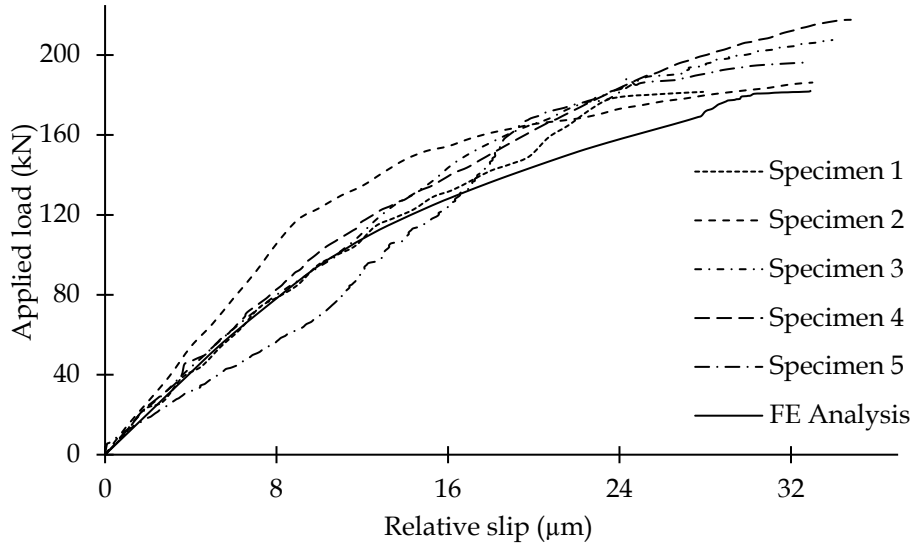

Fig. 6-12: Variation of relative slip with total applied load for composite specimens bonded with three mm thick adhesive layer

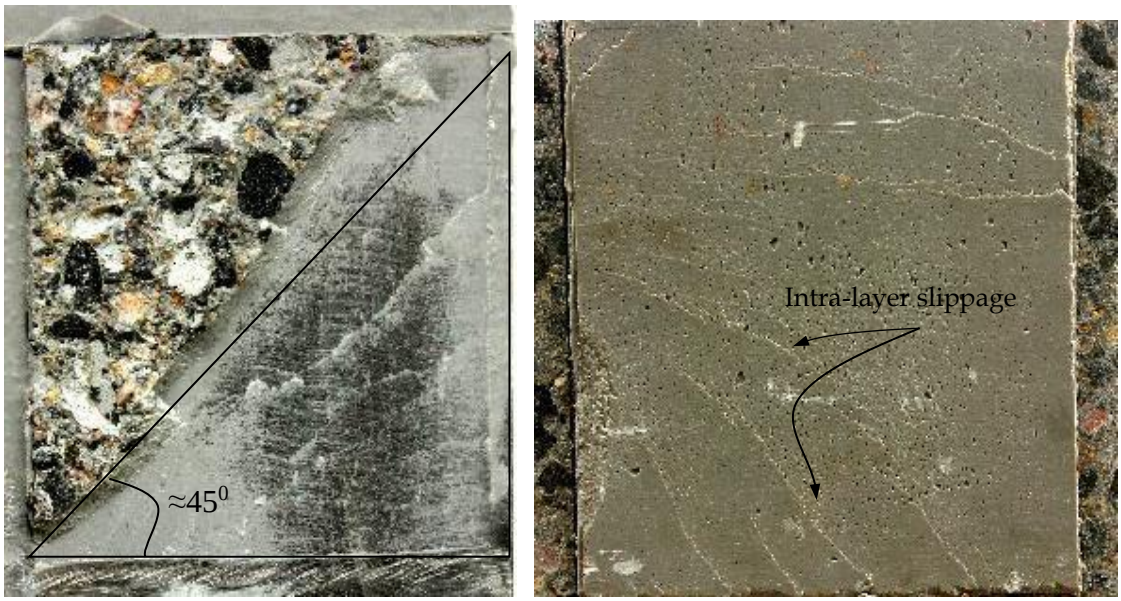

Fig. 6-13: Mode of failure for three mm thick adhesive layer: (a) Mixed mode failure of concrete-epoxy-steel interface and (b) Adhesive bond failure

6.6.4 Bond Layer Thickness of Four mm

The load-slip curves for experimental and FE analysis of the specimens with four mm thick adhesive layer have been shown in *Fig. 6-14*. A significant reduction in the stiffness of the connection is observed, as compared to the connections with lesser thickness of adhesive layers. However, improved connection ductility has been observed in the case of connections with 4 mm thickness of adhesive layer. The average values of load capacity and ultimate slip obtained from experiments are 165.54 kN and 37.5 µm, respectively, while, the FE values for ultimate load and relative slip are 166.18 kN and 41.24 µm, respectively. The percentage variation in the value of ultimate load and relative slip between experimental and FE analysis are 0.39% and 9.97%, respectively. A decrease in connection strength capacity has also been observed with an increase in thickness in both cases (FE analysis and experimental study). *Fig. 6-15* shows the connection failure pattern, which is purely governed by cohesion. Failed surface in *Fig. 6-15* has clear signs of diagonal shear cracking around the adhesive layer. Intra-layer slipping of cross-linked layers has also been observed in failed adhesive layer. The observed shear cracks have been inclined in the range of 30° to 60° from the loading plane.

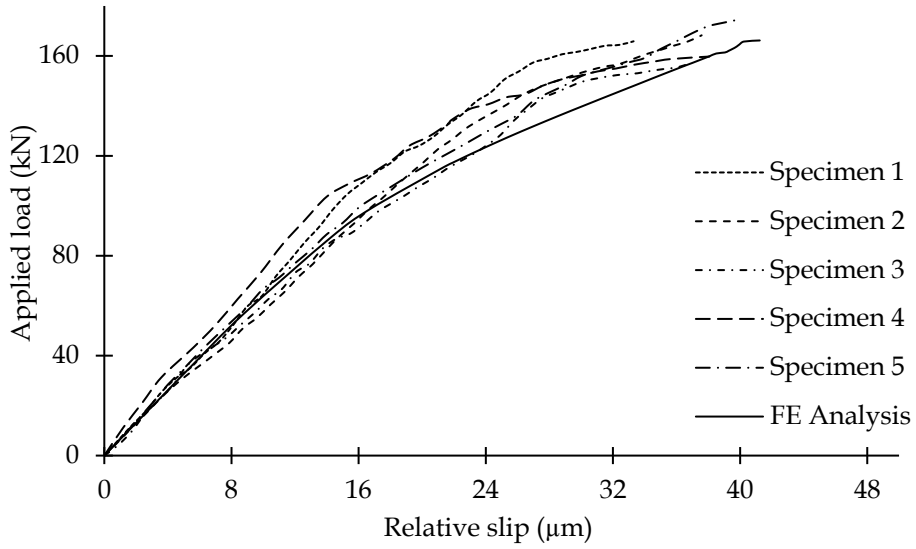

Fig. 6-14: Variation of relative slip with total applied load for composite specimens with four mm thick adhesive layer

Fig. 6-15: Cohesive failure mode of composite specimen for four mm thick adhesive layer

6.6.5 Bond Layer Thickness of Five mm

Fig. 6-16 shows the variation of total applied load with respect to the interfacial slip for experimental and FE analysis for specimens with five mm thick adhesive layer. The experimental load capacity and ultimate slip of the connections have an average value of 150.58 kN and 44.5 μm, respectively. The FE values for ultimate load and relative slip are 147.06 kN and 44.99 μm, respectively. The percentage variation between experimental and FE analysis results are 2.34% in ultimate load

and 1.10% in relative slip. An increase in the ultimate slip at the connection interface has also been observed with an increase in the bond thickness. *Fig. 6-17* shows the photograph of a specimen after failure of composite bond; it is evident that weak bond (crosslink of adhesive chains) breaks owing to the crack resulting from intra-layer slippage. These intra-layer cracks propagate towards the concrete-epoxy and epoxy-steel interface and lead to permanent bond failure. It can also be observed from *Fig. 6-17* that the failure of the interface, even though random, is cohesive in nature having no distinctly observable failure shapes. This may be attributed to the scattering of weak cross links of adhesive. Nonetheless, the absence of tensile failure or adhesive mode failure in concrete is also evident.

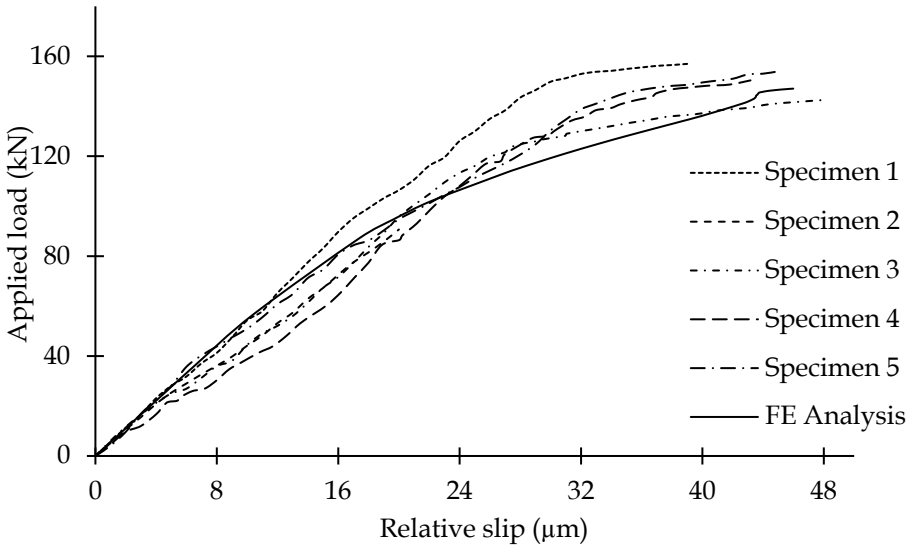

Fig. 6-16: Variation of relative slip with applied load for composite specimens with five mm thick adhesive layer

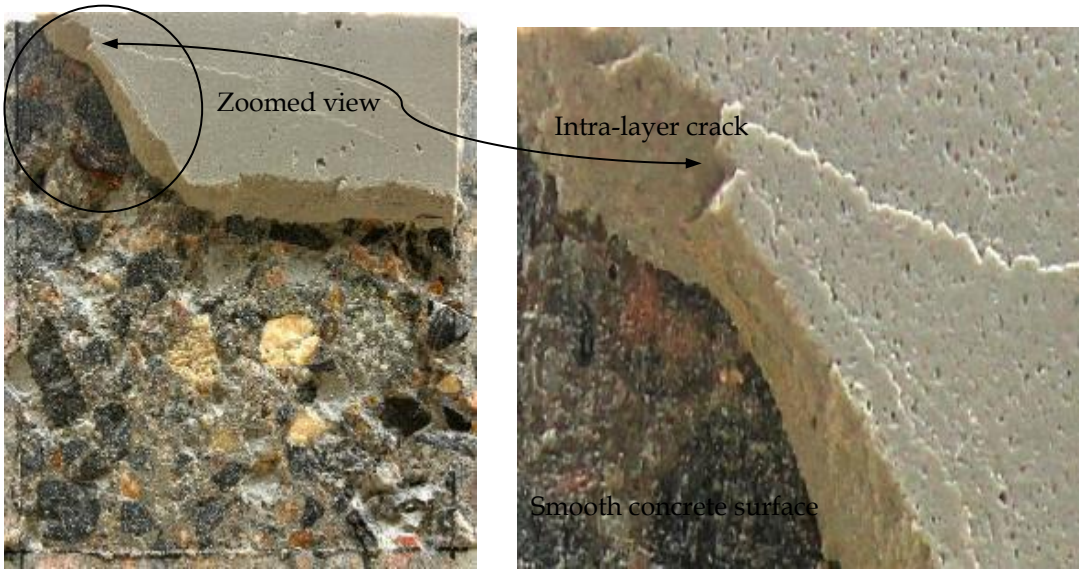

Fig. 6-17: Failure of composite concrete-epoxy-steel interface in cohesion mode for five mm thick adhesive layer

6.7 Comparative Performance of Distinct Bond Layer Thicknesses

6.7.1 Connection Behaviour and Failure Patterns

The relation between the total applied load and engendered relative slip for connections with all five adhesive layer thicknesses have been plotted and shown in Fig. 6-18. The curve represents the average experimental load-slip behaviours of all the five specimens of each thickness of the adhesive layer. It can be observed from the figure, that the stiffness as well as the strength of the connection increases initially, and then decreases with an increase in thickness of the adhesive layer. It is also evident that the change in strength and stiffness remain marginal upto a certain, optimum thickness of bonded layer, beyond which, even a slight increase in the thickness of bonded layer reduces the strength as well as stiffness, significantly. However, the trend in connection ductility has been observed to be directly proportional to the thickness of the bonded layer. The maximum load resistance and resultant ultimate slip for experimental and FE analysis have been reported in *Table 6-2*. The difference in FE analysis and experimental load values for all five adhesive layer thicknesses is limited to 7.5%, while a maximum difference of 10.00% has been observed in case of engendered relative slip. The FE analysis values show a close correspondance with experimental results.

The failure pattern of bonded connections changes from adhesive to mixed (adhesive and cohesive) and from mixed to cohesive modes on increasing the bond layer thickness. For adhesive layers with thickness lesser than 3 mm, the adhesive mode of failure has been observed, between concrete-epoxy and epoxy-steel interface with higher overall connection rigidity. However, when thickness of adhesive is greater than 3 mm, cohesive mode of failure of interface has been generally observed.

Table 6-2: Results of static push out test specimen for varying thicknesses

Adhesive thickness (t_a)	Applied load(Exp.) (P_u) (kN)	Applied load (FE) (P_u) (kN)	Diff. (%)	Ultimate slip (Exp.) (s_u) (μm)	Ultimate slip (FE) (s_u) (μm)	Diff. (%)
1.00	165.88	153.45	7.49	20.5	21.94	7.02
2.00	173.99	164.11	5.63	26.0	26.47	1.81
3.00	194.33	182.07	6.29	33.0	32.90	0.30
4.00	165.54	166.18	0.39	37.5	41.24	9.97
5.00	150.58	147.06	2.34	44.5	44.99	1.10

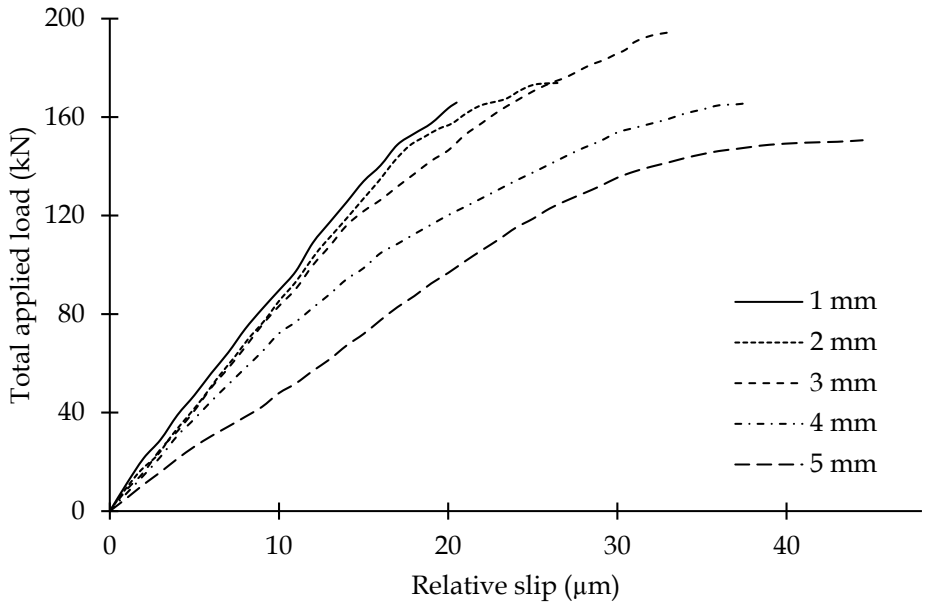

Fig. 6-18: Change in relative slip with total applied load for varying thickness adhesive layer

6.7.2 Shear Stiffness of Adhesive Bonded Connection

The initial shear stiffnesses of bonded connections have been obtained using the method described in Chapter four (*section 4.3.1*). The shear stiffnesses of connections with different thicknesses have been listed in *Table 6-3*. The variation in shear stiffness with respect to the thickness of adhesive bonded layer (*Fig. 6-19*) bears a non-linear inverse relationship. Reduction in shear stiffness between one mm and five mm thick adhesive layers is almost 42.16%. It is also evident that the reduction in shear stiffness, upto an adhesive layer thickness of 3 mm, is lower (15.48%) as compared to the rapid reduction observed for adhesive layers thicker than 3 mm.

Table 6-3: Shear stiffness calculations of composite connections

Adhesive thickness	Total applied load (P_u)	0.7 P_u	(0.7 P_u)/2	Slip at 0.7 P_u	Initial shear stiffness (k_i)
(mm)	(kN)	(kN)	(kN)	(μm)	(kN/mm)
1.00	165.88	116.12	58.06	12.9	4515.09
2.00	173.99	121.70	60.85	14.3	4242.83
3.00	194.33	136.03	68.02	17.8	3815.94
4.00	165.54	115.88	57.94	18.9	3068.29
5.00	150.58	104.13	52.06	21.6	2611.36

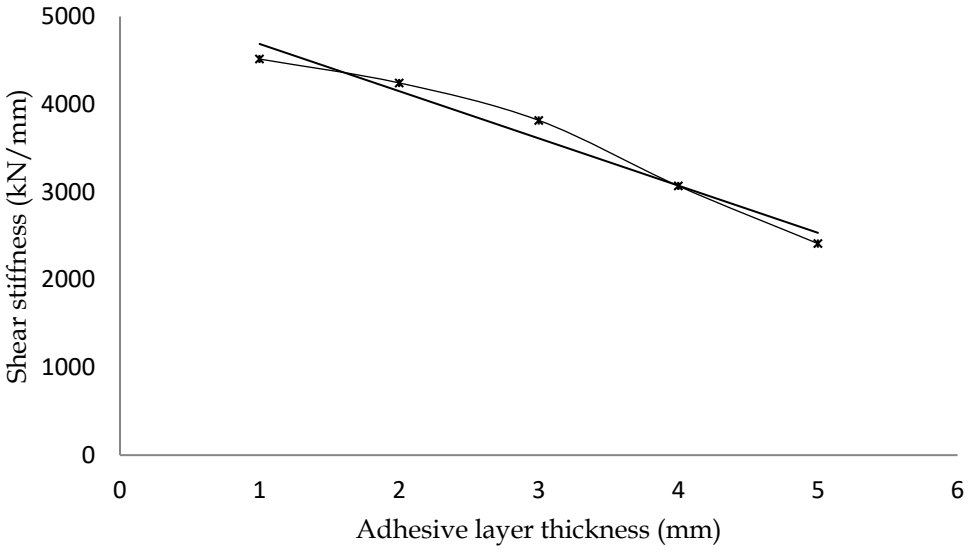

Fig. 6-19: Variation of shear stiffness with adhesive layer thickness

6.8 Stress Variation in the Bonded Area

The variation of stresses, along the length and width of the bonded area, determines the behaviour of connections. An finite element study has been carried out to investigate the distribution of stresses in the bonded area, in order to gain insight on the behaviour of connections under compressive shear loading. For this purpose, the specimen with optimum thickness of adhesive layer (three mm), has been analysed using ABAQUS software package. The typical shear stress *(S_{xz})* variation across the width of three mm thick adhesive layer has been shown in *Fig. 6-20*. The figure shows the variation of shear stress in adhesive layer, across the width of the bonded area, at the top, mid and bottom lengths (*Fig. 6-21*).

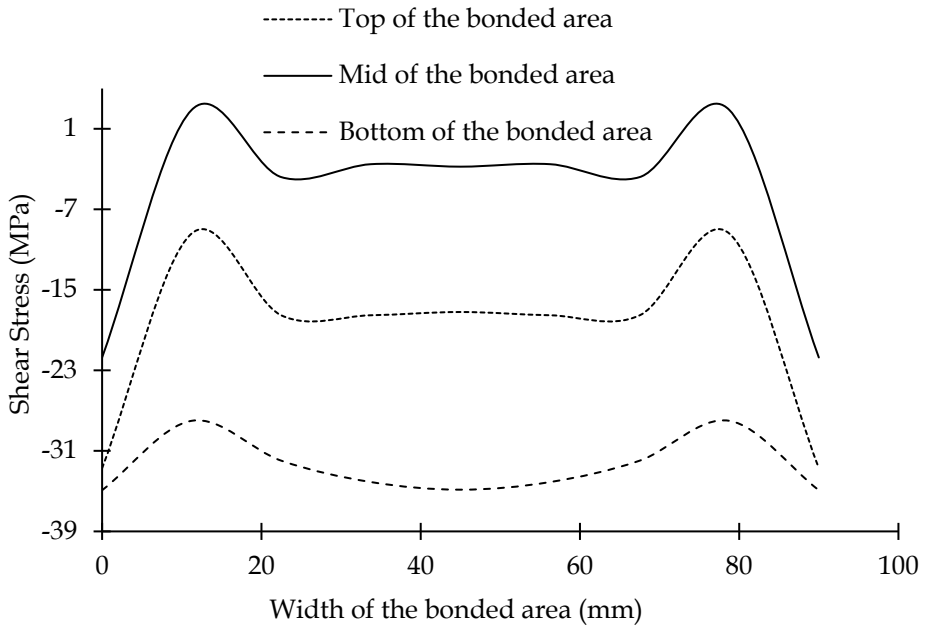

Fig. 6-20: Shear stress variation in adhesive layer along the width of the bonded area

The intensity of stress has been observed to be higher at top and bottom lengths of the bonded area as compared to the mid length. The maximum intensity of stress is found at the corners of the top and bottom of the bonded area. This may lead to failure in the adhesive layer, starting from the corners. The shear stress variation in adhesive layer along the length of bonded area at middle of the width of bonded area is shown in *Fig. 6-22*. The variation in stress clearly shows that the

stress intensity is maximum at top and bottom of bonded area. The nonuniform variation in shear stress at the start and end points may be exhibited due to difference in young's modulus of steel, concrete and epoxy (*Fig. 6-21*).

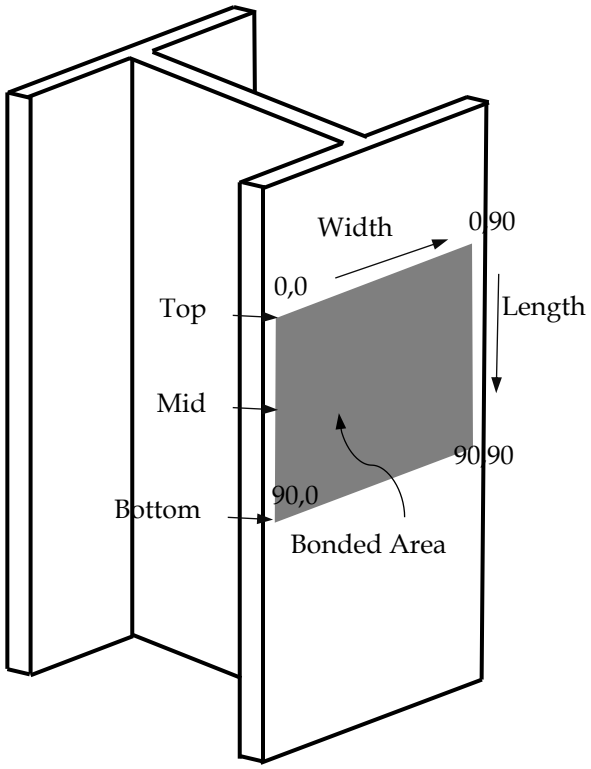

Fig. 6-21: Representation of bonded area on steel section surface along with the Co-ordinational representation of width and length of bonded area

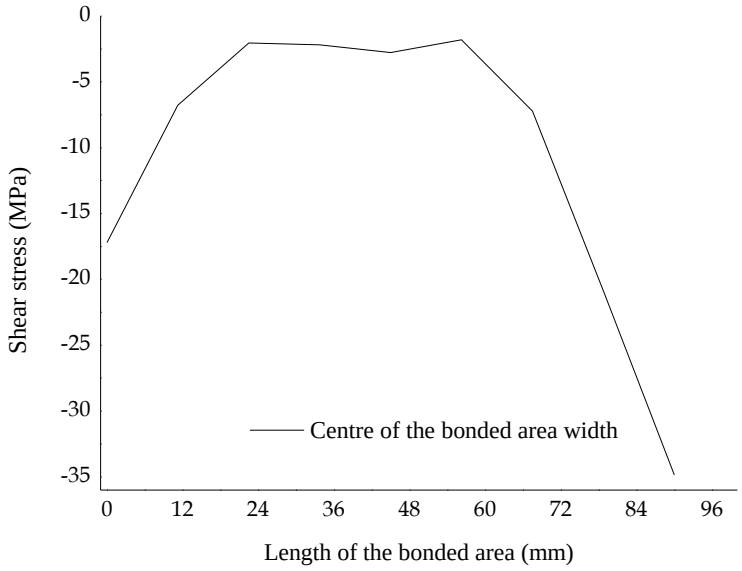

Fig. 6-22: Shear stress variation in adhesive layer along the length of bonded area

6.9 Conclusions

This chapter presented the behaviour of steel concrete composite connections, bonded using epoxy based adhesive. The comparative performances and behaviour of push-out test specimens having different bond layer thicknesses were examined. The optimum thickness of the bonded layer along with the failure modes and relative strength and stiffnesses of connections have also been investigated, experimentally, as well as analytically. Following are the broad conclusions derived from this study:

- The failure pattern of bonded connections changes from adhesive to mixed (adhesive and cohesive), and from mixed to cohesive mode on increasing the bond layer thickness. For adhesive layers having thickness less than 3 mm, the adhesive mode of failure has been observed between concrete-epoxy and epoxy-steel interfaces with desirable overall connection rigidity. However, when the thickness of adhesive is greater than 3 mm, cohesive mode of failure of interface has been observed, while at the optimum thickness (3 mm), the composite interfaces experience mixed mode of failure.
- Increase in the thickness of adhesive layer increases the shear capacity of bonded connection up to an optimum (3 mm) thickness. Beyond this, an increase in thickness decreases the strength of connections.
- The relative slip at the interface of composite connection increases with an increase in the adhesive layer thickness.
- The shear stiffness of connection decreases with increase in the bond thickness. Also, the rate of decrement in shear stiffness increases with increase in the thickness of connection. The stiffness of connection reduces to almost half of its original value with change in bond layer thickness from 1 mm to 5 mm.
- The results obtained from FE analysis are in close agreement with experimental results. The difference in FE analysis and experimental values for all five adhesive layer thicknesses is limited to 7.5% and 10.00% for total applied load and engendered relative slip, respectively.

- The maximum intensity of shear stress has been found at boundary line of the bonded area. However, highest shear stress has been obtained at end bearing line of the bonded area.

Chapter: 7

Flexural Behaviour of Composite Beams

7.1 Overview

This chapter investigates the flexural behaviour of full scale steel-concrete composite beam specimens. The specimens have been prepared, using the two connection schemes, namely, mechanical headed stud connected and adhesive bonded, and have been subjected to two-point bending. The observed flexural behaviour has been discussed in detail along with a comparative analysis of the suitability of both the connection schemes. The full scale beam tests have been conducted to gain better insight on the overall flexural behaviour of the composite members.

The full scale simply supported composite beam specimens, two specimen connected using mechanical headed studs and one specimen connected using adhesive layer, have been subjected to two-point bending. The two specimens connected using mechanical headed stud connectors have different arrangement of headed studs along the span. One specimen has the headed studs arranged inline, while the other specimen has a staggered arrangement of the headed studs. The difference in the behaviour of specimens with the two schemes of arrangement of the headed studs has been discussed in detail. The investigation has been carried out under incremental monotonic loads. The applied load vs relative slip curves along with the load-deflection profile and the deflected shape of composite beams have also been observed and discussed in detail.

7.2 Material Used

7.2.1 Concrete

The concrete slab for the composite beam specimen has been cast using the C_1 concrete, the details of which have already been discussed in Chapter three (*Table 3-1*). The prepared concrete element has an overall length of 5100 mm with a cross-sectional geometry as shown in *Fig. 7-1* below. The concrete slab has been reinforced with 8 mm diameter HYSD bars spaced uniformly at 150 mm in

transverse direction along with 5 bars of the same diameter in longitudinal direction, as shown in *Fig. 7-1*.

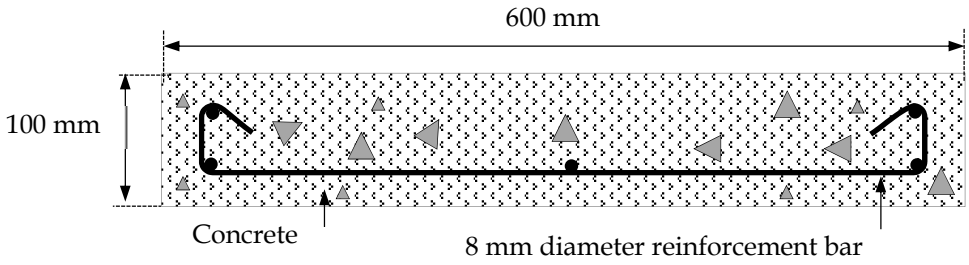

Fig. 7-1: Geometric details of reinforced concrete slab

7.2.2 Structural Steel

The steel element of the composite beams has comprises of standard hot rolled Universal Beam sections. The rolled steel sections have been cut to the length of *5100* mm to obtain the steel elements. The geometric details of beam section have been listed in *Table 7-1*.

Table 7-1: Geometric details of hot rolled steel beam section

Description	Total depth	Flange width	Web thickness	Flange thickness	Root radius	Area
	(mm)	(mm)	(mm)	(mm)	(mm)	(mm^2)
UB 305 × 165 × 46	306.6	165.7	6.7	11.8	8.9	5875.0

7.2.3 Headed Stud

Standard headed studs having a diameter of 16 mm and height 78 mm have been used to form the connection at steel-concrete composite interface. The tensile property of the material of headed studs has already been discussed in Chapter three (*section 3.2.5*). The typical geometry of headed stud connector has been shown in Fig. 7-2.

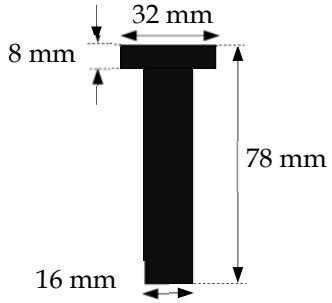

Fig. 7-2: Geometric detail of headed stud connector

7.3 Experimental Program

The objective of the present study is to investigate the flexural behaviour of full scale steel concrete composite beams connected using different connection schemes. The simply supported composite beam specimens have been subjected to two point loading. Two-connection strategies, one providing mechanical connection using headed studs and other ensuring the connection using structural adhesive, have been investigated. Two different schemes of arrangement of headed stud connectors have been studied, one having inline arrangement of headed studs and other having a staggered (zigzag) arrangement of headed studs. However, the composite beams prepared using different connection strategies and arrangements thereof, have almost identical geometrical properties.

A schematic representation of the beam along with its geometrical properties and loading and support conditions has been shown in *Fig. 7-3(a)*. The load has been applied at *375* mm from the mid span, on both the halves of the beam. The load is applied such that it acts symmetrically at the cross-sectional vertical centroidal axis. The cross-sectional schematic view of the beam, connected using headed shear studs with inline arrangement, with its geometrical properties has been shown in shown in *Fig. 7-3(b)*. The location of strain gauges, to capture the strain measurement at various locations, has been indicated in the *Fig 7-4*, in a half span schematic representation.

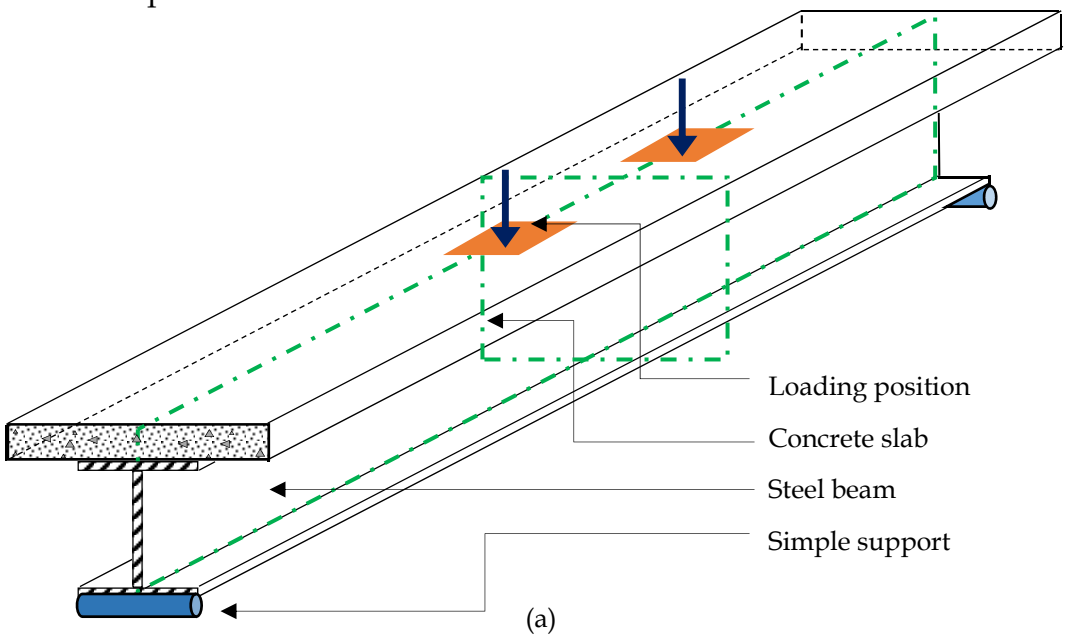

(a)

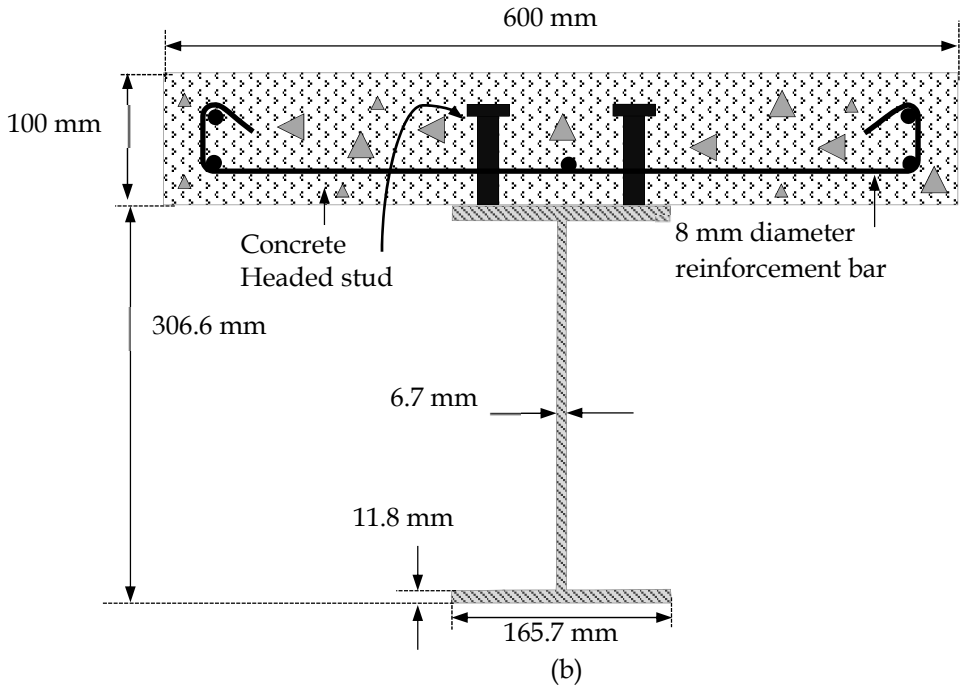

Fig. 7-3: Geometry of composite beam; (a) isometric view and (b) cross-section view

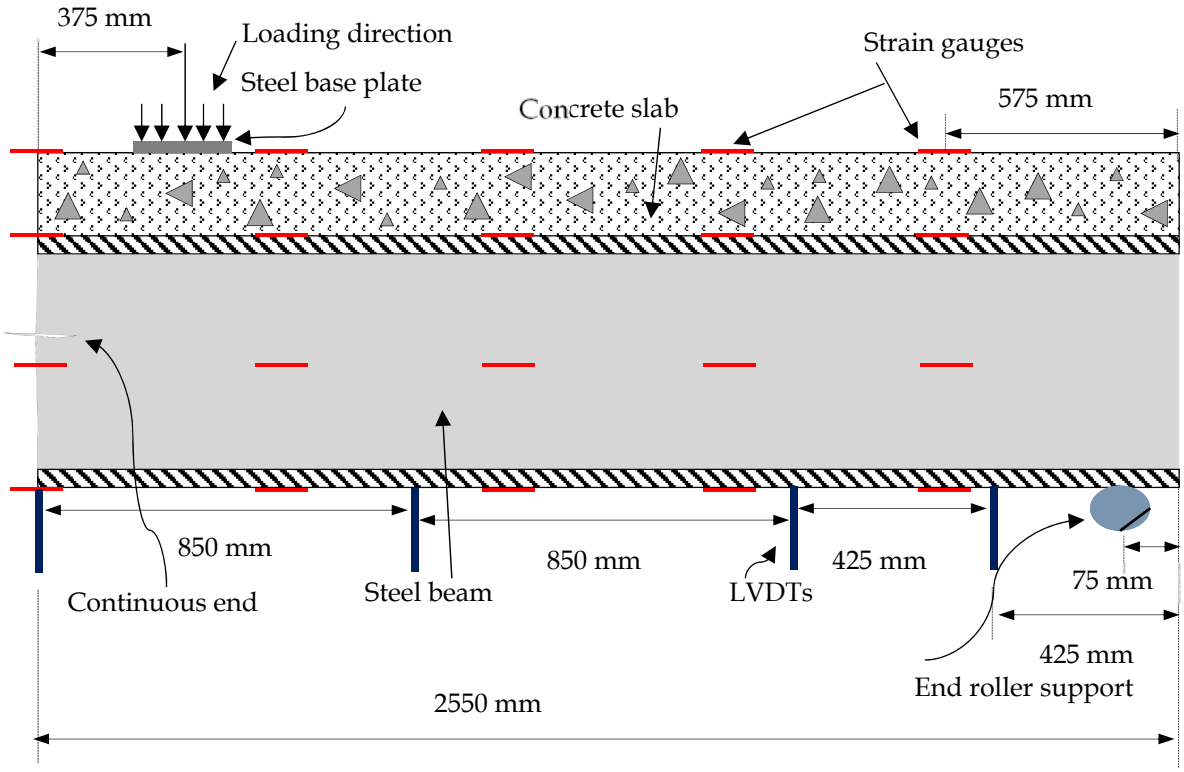

Fig. 7-4: Side view of steel-concrete composite beam (half span)

7.4 Steel-Concrete Composite Beam having Headed Studs in Inline Pattern

This section presents a discussion on the behaviour of the steel-concrete composite beam, having mechanical connection using headed studs arranged inline pattern, and subjected to an incremental monotonic flexural loading. The performance of the connection has been evaluated in terms of the applied load vs engendered slip curves at the support and the load deflection curves at various positions of spans in the beam. *Fig. 7-5(a), (b) and (c)* shows the various details of the tested specimen during its preparation, while *Fig. 7-6* shows the beam specimen, ready to be tested with all necessary instrumentations.

(a)

(b)

(c)

Fig. 7-5: Preparation of steel-concrete composite beam; (a) steel beam with headed stud connectors in inline pattern, (b) steel beam with form work and (c) freshly cast concrete slab over steel beam

Fig. 7-6: steel-concrete composite beam with the instrumentation arrangement

7.4.1 Load-Slip Behaviour

The load slip behaviour, at the connected interface of a steel concrete composite beam provides significant insight on the overall degree of interaction of the connection between elements. The significance of degree of interaction has already been discussed, in detail, in Chapter one (*section 1.3.2.3*). This section presents discussion on the connection properties of the investigated beam specimen, primarily in terms of the connection stiffness. *Fig. 7-7* shows the experimentally obtained load slip curve of the beam specimen having inline arrangement of headed studs. The slip, as plotted in the abscissa of the graph, has been measured at the connection interface level near the beam ends, as the maximum slip is anticipated in this region only. The initial noise in the load-slip curve represents the rearrangement of load distribution in the composite beam specimen. The drops at certain points in the load slip curve (at the load values of 244.77 kN, 289.81 kN, 320.06 kN and 351.90 kN) represent the probable distortion and failure in some of the headed stud connectors along with localised cracking and crushing of concrete surrounding those connectors. During the experiment, a distinct loud snapping sound, characterising the failure of headed stud, has been noticed at various instances. The results of the testing suggest that, for a steel concrete composite beam connected using headed studs arranged inline, the ultimate load capacity and relative slip are 363.18 kN and 1.089 mm, respectively.

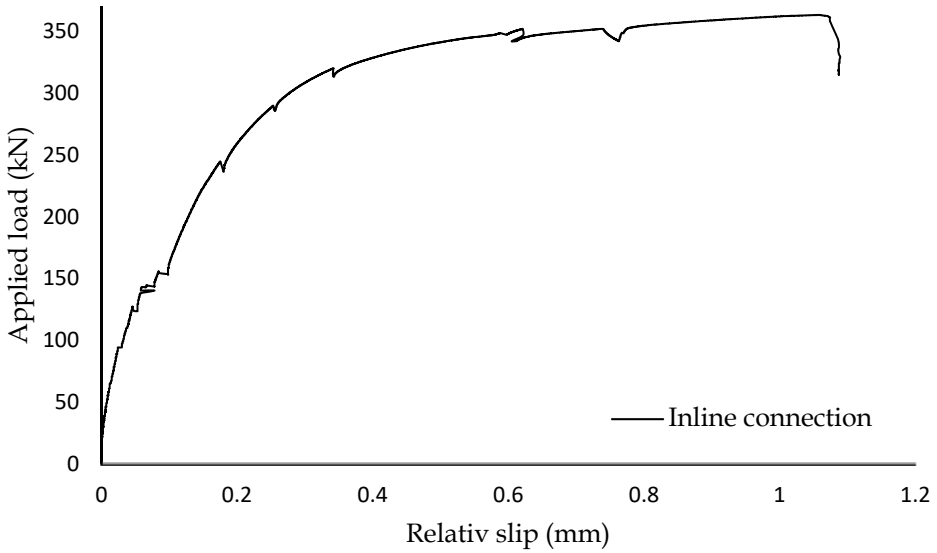

Fig. 7-7: Applied load vs relative slip curve of the steel-concrete composite beam connected with inline headed stud connectors

7.4.2 Load-Deflection Behaviour

The vertical deflection of the steel concrete composite beam having inline studs has been recorded at four locations in the half span of the beam specimen, at distances of 425 mm, 850 mm, 1700 mm and 2550 mm, from the simply supported end. The observed vertical deflections at the selected points, i.e. at 425 mm, 850 mm, 1700 mm and 2550 mm from the supported end, have been shown in *Fig. 7-8*. Sudden undulations in the load deflection curves at same load levels (of 244.77 kN, 289.81 kN, 320.06 kN and 351.90 kN), in all the four considered locations are clearly evident in the figure. This sudden drop is expected to be the indication of failure of certain headed studs and/or cracking (or crushing) of the concrete surrounding the studs, and the subsequent redistribution of the forces. The first drop has been observed at 244.77 kN (67.40% of ultimate load), while at a load level of around 320.06 kN (around 90% of ultimate load) minor cracking in concrete element of the beam has been observed in middle one third span and at the ends of the composite beam. This cracking leads to excessive deformation and yielding of headed studs and crushing of the surrounding concrete.

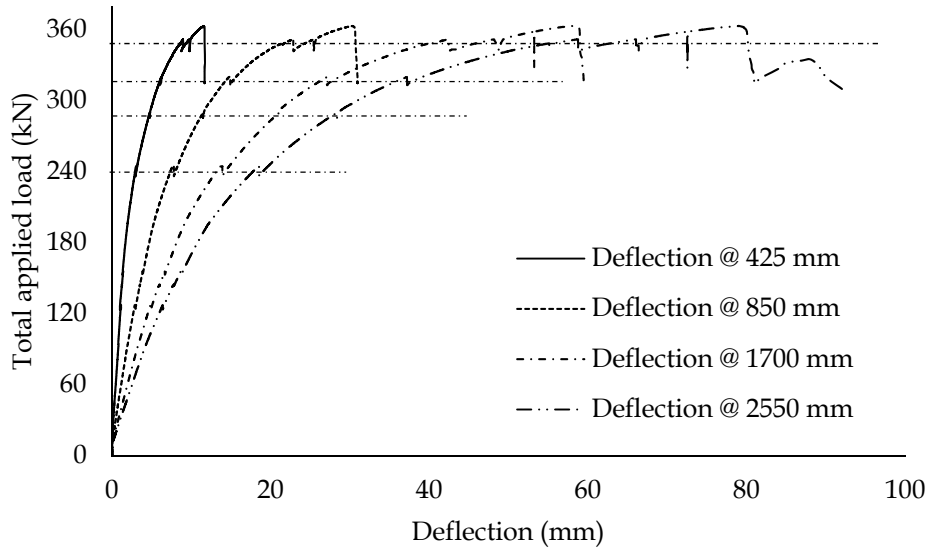

Fig. 7-8: Combined load deflection curves for inline composite beam at distance 425 mm, 850 mm and 1700 mm, 2550 mm from end of beam

7.4.3 Deflected Profile

The deflected profile of the composite beam (with headed stud connectors arranged inline pattern) along the span has been shown in *Fig. 7-9*. The figure shows the deflection profiles at eleven different load levels, spaced at intervals of l0% of ultimate load. The deflection profiles have been observed to follow a parabolic path, with an almost linear increase in the degree of skewness of the curve with increase in applied load. However, a sharp increase in the degree of skewness of the curves can be observed beyond a load level of 288 kN (79.30% of ultimate load), representing initiation of nonlinearity in the behaviour. It can thus be assumed that the nonlinearity in the behaviour of steel concrete composite beam initiates at a load level corresponding to about 80% of the ultimate strength.

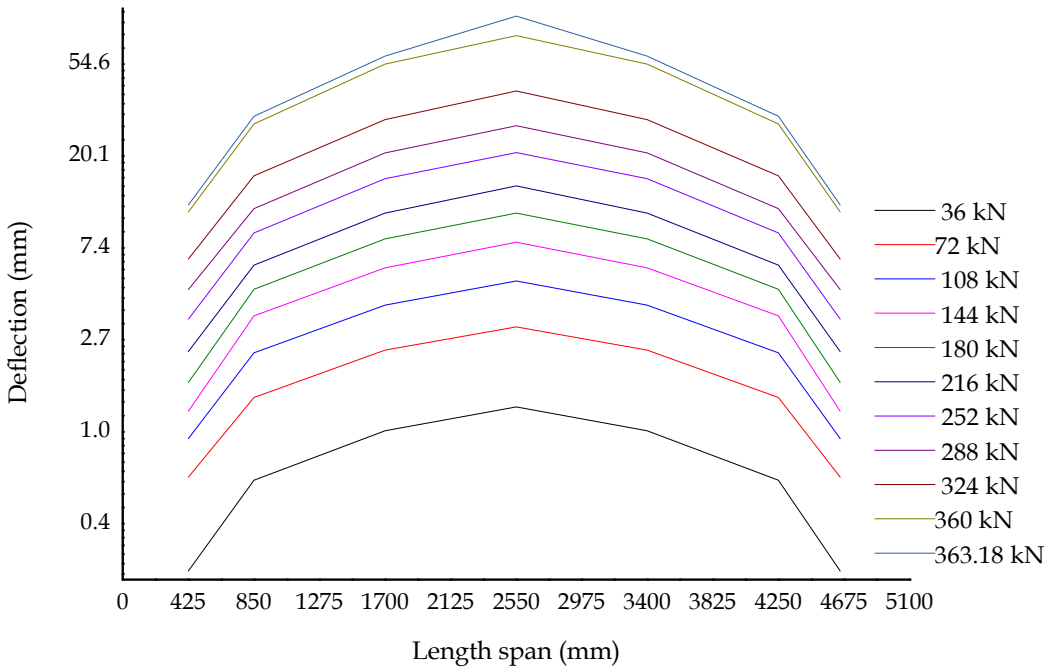

Fig. 7-9: Deflected profile of the composite beam connected with composite beam in inline pattern along the length of the span.

7.4.4 Failure Pattern

The behaviour of the steel concrete composite beam specimen has been closely monitored and even the prima facie changes in the physical properties of the beam have been recorded during the flexural testing. *Fig. 7-10* shows the critical states of the beam specimen, as observed during the testing, and represents the initial cracking, preliminary yielding and ultimate (failure) state. In *Fig. 7-10(a)*, the initiation of cracking in concrete element, between the two loading points along the longitudinal direction directly above the location of headed studs, has been shown. A clearer representation of this initial cracking along the longitudinal direction, between the points of load application and above the location of headed studs has been presented in *Fig. 7-10(b)*. Thick steel plates have been employed for the application of load over the concrete element of the composite beam, around which, significant cracking of the concrete has been observed, and has been shown in *Fig. 7-10(c)*.

(a) (b)

(c) (d)

(e) (f)

Fig. 7-10: Failure of steel-concrete composite beam; (a) cracking in concrete slab in the line of headed stud connector (one side), (b) cracking in concrete slab in the line of headed stud connector (both side), (c) cracking in concrete around the loaded area, (d) excessive crushing of concrete (concrete top), (e) cracking in concrete throughout the cross-section and yield in steel and (f) cracked portion of composite slab with yielded profile

Fig. 7-10(d) shows the excessive cracking of concrete element, between the two points of loading, at higher load levels, representing the failure of the beam in the middle one-third span of the beam. The disintegration of the concrete element (cracking in concrete throughout the cross-section) along with the yielding of steel element at higher load levels has been shown in *Fig. 7-10(e)*. The post-failure deflected profile of composite beam has been captured and shown in *Fig. 7-10(f)*.

7.5 Steel-Concrete Composite Beam having Headed Studs in Staggered Pattern

(a) (b) (c)

Fig. 7-11: Steel-concrete composite beam; (a) mechanical headed studs welded over steel beam in staggered pattern, (b) Prepared steel beam for concrete pouring along with reinforcement arrangement and (c) in place cast concrete slab

The behaviour of steel-concrete composite beam connected with mechanical headed stud connectors arranged in staggered pattern has been discussed in the present section. The overall flexural behaviour has been investigated in terms of the load-slip curves at beam ends, load-deflection profiles at certain locations and strain induced at certain points along the span. The systematic process of welding the headed stud connectors in staggered pattern, the arrangement of reinforcement bars over the steel element and the fresh cast concrete element over the prepared steel element have been shown in *Figs. 7-11(a)*, *(b)* and *(c)*, respectively. The instrumentation arrangements and a closer view of load balancing arrangement have been shown in *Figs. 7-12(a)* and *(b)*, respectively.

(a)

(b)

Fig. 7-12: Mechanical headed stud connected steel-concrete composite beam; (a) instrumentation arrangements and (b) close view of load balancing and application arrangement

7.5.1 Load-Slip Behaviour

The relative slip, induced at steel-concrete composite beam has been measured at the beam ends. The beam has geometric properties and loading symmetry along the mid span. Therefore, the load-slip curve drawn in *Fig. 7-13* is veraged curve for both ends. The load-slip curve shows some redistribution of stresses at a load-level of 150 kN (39.88% of ultimate load). The maximum values obtained for applied load and ultimate slip are 376.11 kN and 0.83 mm, respectively. The slip follows a smooth curve with the change in loading. The excessive yielding in connectors or concrete cracking is evident at two points (309.19 kN and 327.13 kN) in entire loading process. After the level of 363.89 kN, the excessive concrete cracking in composite beam occurs, which leads to some redistribution in load and noise in corresponding relative slip.

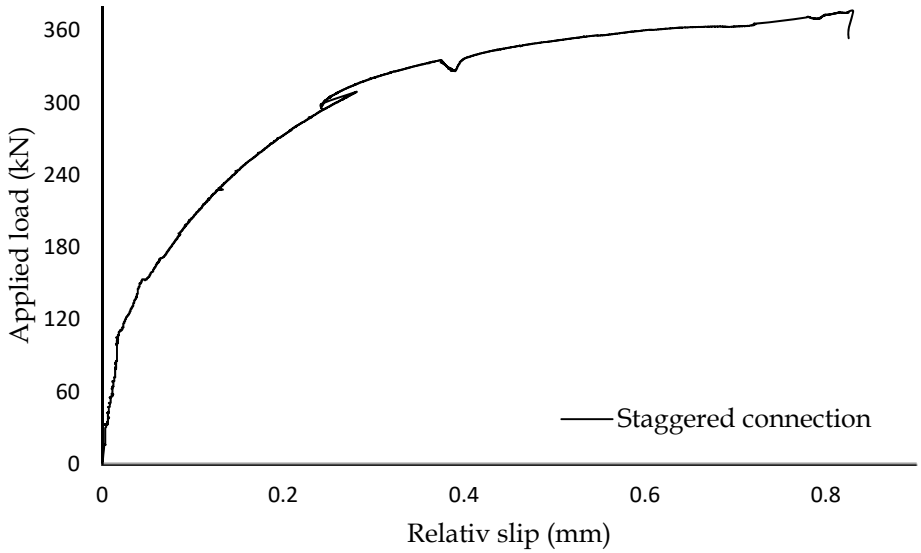

Fig. 7-13: Applied load-relative slip curve for composite beam having mechanical headed studs in staggered pattern

7.5.2 Load-Deflection Behaviour

The vertical deflection of the steel-concrete composite beam is a first-hand indication of the degree of interaction of the connection between the elements of the beam. In this case also, the vertical deflections at four distinct distances (of 425 mm, 850 mm, 1700 mm and 2550 mm) from one end of the beam have been recorded and discussed in this section. The applied load vs observed vertical

deflection curves for the beam have been shown in *Fig 7-14*. During the entire loading process, the load-deflection curves have depicted sharp jumps at two load levels, of 309.19 kN and 327.13 kN, at all the four considered points of measurement. These undulations represent the failure of headed studs and/or cracking (or crushing) of concrete surrounding the headed studs and the subsequent redistribution of forces. Although the undulations characterize the damage, the extent of the damage in case of staggered arrangement of headed studs has been observed to be significantly less than that in case of headed studs arranged inline.

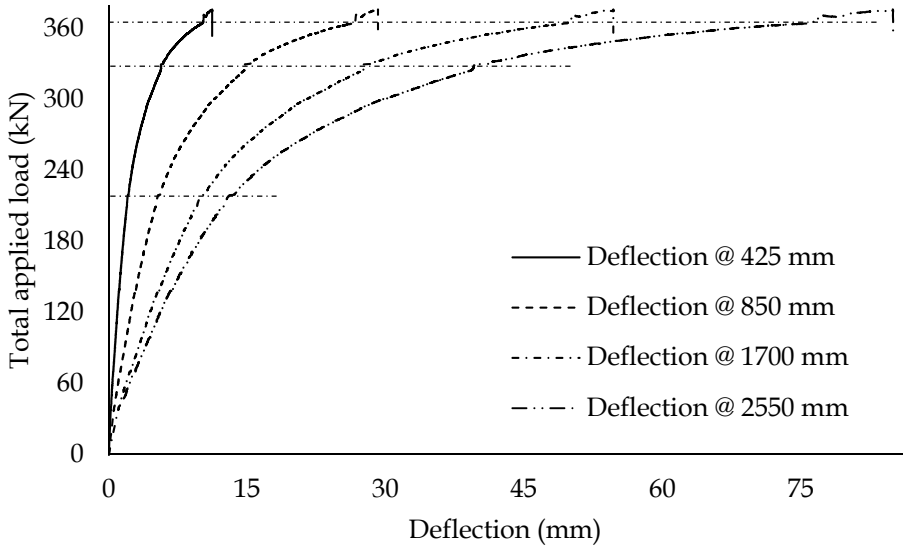

Fig. 7-14: Load-deflection curves for staggered composite beam at distance 425 mm, 850 mm, 1700 mm and 2550 mm from beam ends

7.5.3 Deflected Profile

The deflected profile of a beam provides a significant insight on its overall performance. This section presents a discussion on the deflected profile of the simply supported composite beam, connected using headed studs arranged in staggered fashion along its span. The deflection profiles of the beam, at eleven different load levels spaced at intervals of l0% of ultimate load, have been shown in *Fig. 7-15*. The deflection profiles of composite beam have been observed to follow a parabolic curve, with an almost linear increase in the degree of skewness with respect to the applied load. However, the degree of skewness in deflection

profiles of composite beam connected using staggered headed studs (*Fig. 7-15*) is relatively lower than that observed for beam with headed studs arranged inline (*Fig. 7-9*). The curves suggest that the skewness becomes prominent beyond a load level of 288 kN (79.30% of ultimate load), which represents the initiation of nonlinearity in the beam. It can thus be safely stated that the nonlinearity, in the behaviour of steel concrete composite beam, initiates at a load level corresponding to about 80% of the ultimate strength. Another observation, based on the comparative analysis of the deflected profiles, is that the nonlinear behaviour of composite beam with staggered headed studs is better (more uniform) than that of the beam with headed studs arranged inline.

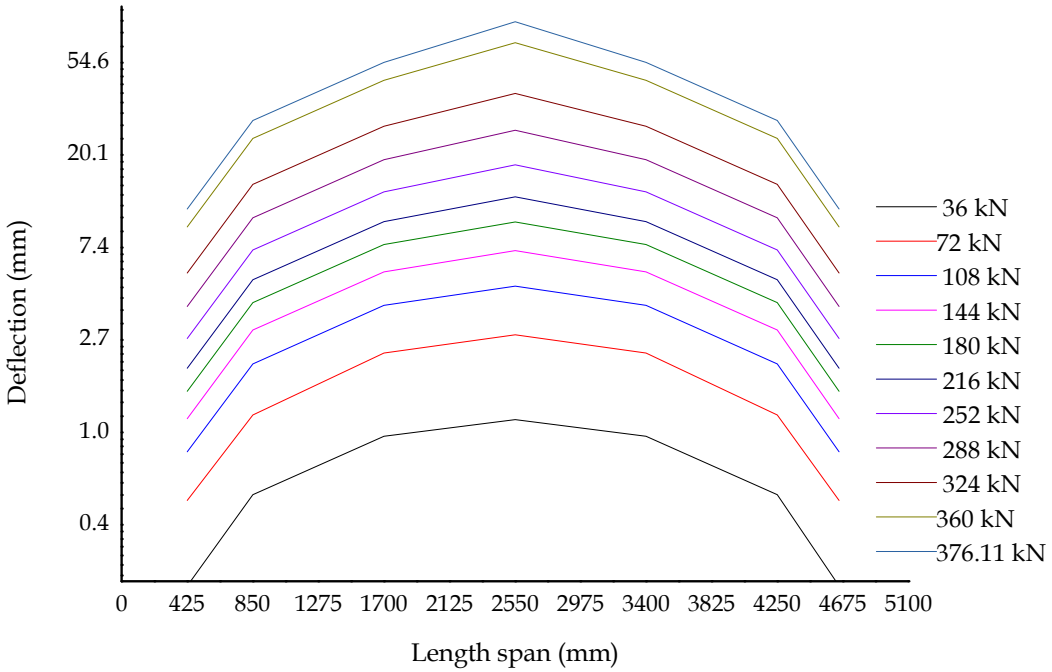

Fig. 7-15: Deflected profile of composite beam connected with headed studs in staggered pattern along the length of span

7.5.4 Failure Pattern

The flexural behaviour of a steel concrete composite beam specimen, connected using headed studs arranged in staggered fashion, has been evaluated through experimental investigation, and the performance of the beam specimen has been

discussed in this section. The various states of the beam specimen at different stages of the testing have been shown through *Figs. 7.16(a) – (e)*. The deflected profile of the specimen, after the two-point bending test, has been shown in *Fig. 7-16(a)*. Significant deflection in composite member near the mid span can be clearly observed in the figure. The *Fig. 7-16(b)* shows the transverse cracking in concrete slab near the mid span of the beam specimen. The flexural failure in concrete slab (side view) near the mid span of the beam is evident in *Fig 7-16(c)*. The most probable reason for the observed prominent transverse cracking of the concrete slab is excessive deformation of the headed studs, leading to the splitting of concrete slab into two parts about the mid span of composite beam. The cracking and splitting of the concrete element along the entire cross-section has been shown in *Fig. 7-15(d)*. The *Fig. 7-15(e)* shows the significant cracking of the concrete element along the longitudinal span, below and around the point of application of load.

(a)

(b)

(c)

(d)

(e)

Fig. 7-16: Failure in steel-concrete composite beam having headed stud connector in staggered pattern; (a) deflected profile of composite beam, (b) cracking in concrete at top surface, (c) Separation of concrete in two parts at mid span under bending, (d) crack propagation in entire cross–section and (e) massive crushing below the load and cracking along the span.

7.6 Structural Adhesive Bonded Steel-Concrete Composite Beam

This section presents a discussion on the flexural behaviour of a simply supported steel-concrete composite beam specimen, connected using structural adhesive, and subjected to two-point loading. The process of application of the adhesive along with the methodology to achieve adhesive bonded connection between steel and concrete interfaces have also been presented in this section. The parameters used for characterisation of the behaviour of composite beam are the applied load vs engenderred slip at the support, and the applied load vs vertical deflection curves of the specimen observed at four points along the half-span of the beam.

The step by step procedure for the preparation of adhesive bonded composite beam has been shown in *Fig. 7-17*. The strucutral section, used for the preparation of adhesive bonded specimen has been shown in *Fig. 7-17(a)*. The formation of the formwork to cast the RCC slab over the steel element has been shown in *Fig. 7-17(b)*. Also, *Fig. 7-17(c)* shows the prepared formwork with the arrangement of reinforcement, ready for concrete pouring. The cast RCC element, lifted though jacks (thereby creating a gap between steel and concrete elements), for application of adhesive over the surface of steel element has been shown in *Fig. 7-17(d)*. *Fig. 7-*

17(e) shows the test ready adhesive bonded steel concrete composite beam along with the arrangement of LVDTs and strain gauges.

(a)

(b)

(c)

(d)

(e)

Fig. 7-17: Structural adhesive bonded steel-concrete composite beam, (a) plane structural steel I-section of desired length, (b) formwork preparation for RCC slab casting, (c) prepared shuttering with reinforcement for RCC slab, (d) clear gap between steel beam and precast concrete surface for adhesive application and (e) prepared steel-beam with LVDTs and strain gauges arrangements

7.6.1 Load-Slip Behaviour

The load-slip behaviour, at the simply supported ends of the adhesive bonded steel concrete composite beam at the level of connected interface, has been discussed in the present section. The applied load as well as the engendered slip values, recorded at both the ends, have been averaged, owing to the symmetry of the specimen, in terms of loading geometry and support conditions, along the mid span. The averaged load-slip curve as shown in *Fig. 7-18*, exhibits an elastoplastic behaviour along with a prominent undulation at the (tentative) yield point. The curve represents an undulation at the level of 329.97 kN (i.e. 90.63% of ultimate strength). The probable reason for the observed undulation may be a localized cracking in concrete element or failure of certain bonded portion in a span. However, no clear evidence of bond failure or significant concrete crushing has been observed at this load level. Further, it has been observed that with further

increase in load, the engendered slip increases significantly, in a highly nonlinear fashion. The failure of the specimen has been observed at a load of 364.08 kN exhibiting an engendered slip of 0.12 mm.

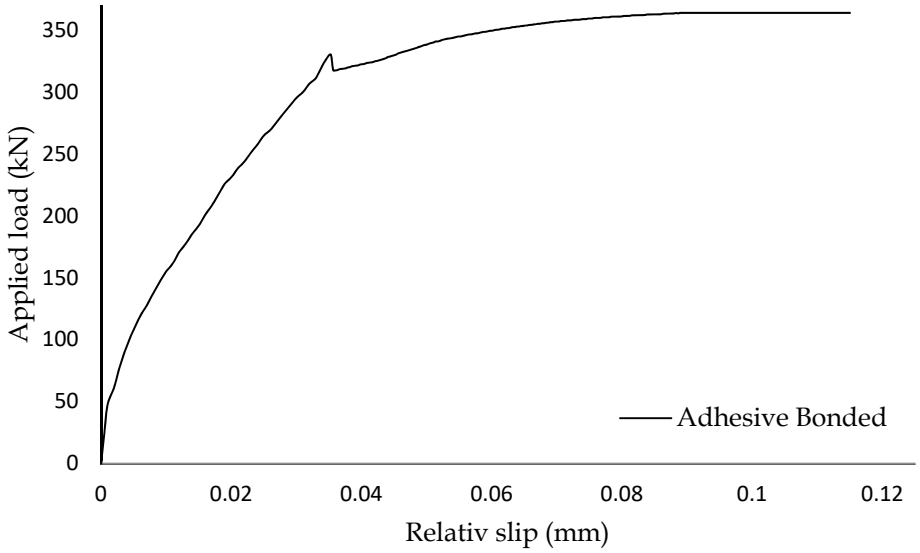

Fig. 7-18: Applied load-relative slip curve for adhesive bonded steel-concrete composite beam

7.6.2 Load-Deflection Behaviour

The vertical deflection of the simply supported adhesive bonded steel-concrete composite beam has been obtained through experimental study. The load deflection curves of the composite beam at four distinct points (at 425 mm, 850 mm, 1700 mm and 2550 mm from end of beam) have been shown in *Fig. 7-19*. It can be clearly observed from the graph that load-deflection curves at all the four locations sustain a pronounced undulation at the same load level of 329.97 kN. The cracking of concrete in RCC slab or the failure of bond at span may be the probable reasons for the observed undulation. The load-deflection curve has been observed to follow a smooth path exhibiting a perfect bond until failure.

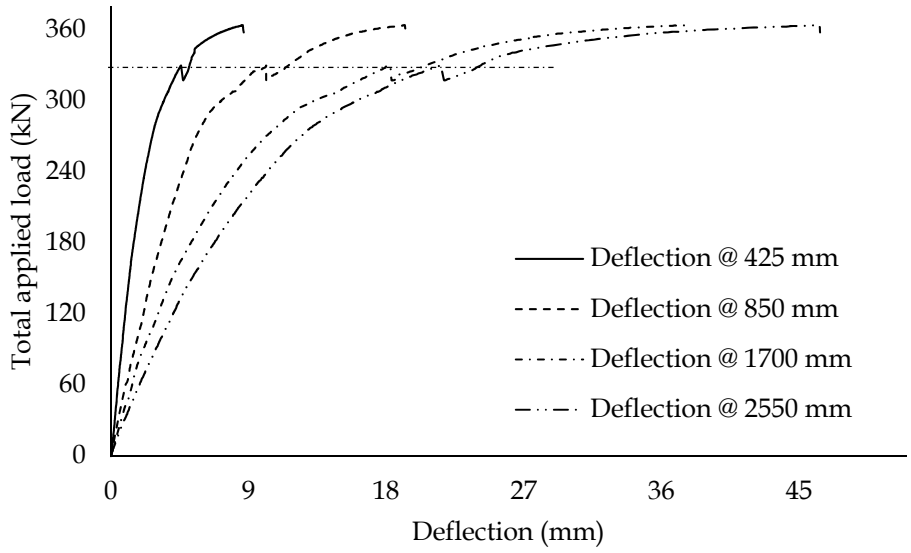

Fig. 7-19: Combined load deflection curves for adhesive bonded composite beam at distance 425 mm, 850 mm, 1700 mm, 2550 mm from end of beam

7.6.3 Deflected Profile

The deflected profile of simply supported composite beam connected using structural adhesive has been discussed in this section. *Fig. 7-20* shows the deflected profile of bonded composite beam at eleven different load points, with equal static increments of 10% of the ultimate load along the length of span, on a semi-log scale. The deflection profiles of adhesive bonded beam show an increase in deflection from the simply supported end to the centre of the beam, beyond which an inverse trend (after mid span) has been observed. This trend become more pronounced beyond a load of 216 kN (60% of ultimate load). The obtained force-deflection behaviour of the composite beam suggests that in case of adhesive bonded connections, the strain remains localized at or near the mid span of the beam, irrespective of the loading conditions. The localization of strain at the mid-span (below the loaded areas) of the beam reduces the flexural performance of the beams with adhesive bonded connections, in terms of distribution of stresses. The localised distribution of stresses, ultimately lead towards failure in bonded beam. However, change in deflected profile and increase in degree of skewness have not been observed upto the failure.

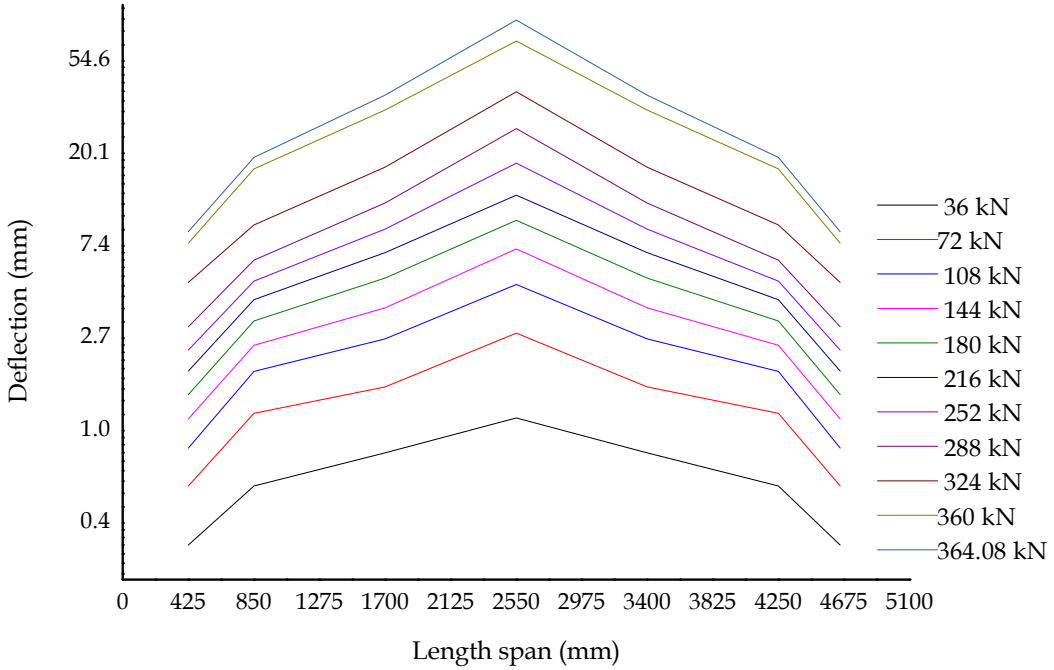

Fig. 7-20: Deflected profile of bonded composite beam along the length of span

7.6.4 Failure Pattern

The overall flexural behaviour of the adhesive bonded composite beam specimen has been discussed in detail in this section. The simply supported beam specimen has been subjected to two-point flexural loading at the one third spans of the beam, and the load has been applied using a simple loading assembly. The observed behaviour of the beam specimen at various stages of the testing has been shown in *Fig. 7-21*. The *Fig. 7-21(a)* shows cracking of the concrete slab directly below the loading assembly, while *Fig. 7-21(b)* and *(c)* shows the further widening of flexural cracks at higher load levels. It has been observed that the cracking in the concrete element initiates at the bottom of the concrete element (tension cracking), almost directly below the point of application of the load, and propagates upwards. This can be explained by the brittle nature of interfacial connection and deflection below the point of load application. The through transverse cracking of the concrete element can be clearly observed in *Fig. 7-21(d)*. Ultimately, the failure of bonded portion at the connected interface is evident in *Fig. 7-21(e)*.

(a)

(b)

(c)

(d)

(e)

Fig. 7-21: Adhesive bonded steel-concrete composite beam failure; (a) minor cracking in concrete slab below the loaded area (one point), (b) tensile crack opening in concrete slab below the loaded area, (c) increment in crack opening width, (d) through transvers cracking at bottom and (e) bond failure at steel-concrete composite interface

7.7 Comparative Behaviour

This section presents a comparison of the behaviour of different connection schemes tested during this study. The flexural behaviour of composite beams connected using mechanical headed studs (inline and staggered orientations) and adhesive bond has been critically analysed to determine the adeptness of a connection methodology. The parameters selected for the comparison are the load-slip behaviour, the load-deflection behaviour and the initial and post yield stiffnesses of the beam specimens.

7.7.1 Load-Slip Behaviour

The influence of connection strategy on the performance of steel-concrete composite connections is generally represented by the load-slip behaviour of the connections. It provides significant insight on the behaviour of connection in terms of its rigidity, stiffness and rotation. A comparative plot of the experimentally evaluated load-slip curves of the beams with both the connection methodologies has been shown in *Fig. 7-22*. The figure clearly shows that in case of headed stud connectors, the change in arrangement of connectors, from inline to staggered, increases the ultimate engendered slip, although the ultimate strength remains the same. However, with the change in connection strategy from headed stud connected to adhesive bonded, the load-slip behaviour at steel-concrete interface undergoes a drastic change. The ultimate values for applied load and relative slip for all the tested specimens have been enlisted in *Table 7-2*. The maximum value of applied load has been obtained in case of composite beam connected using headed studs arranged in staggered pattern, and is 376.11 kN. The ultimate strength in case of beam with staggered arrangement of headed studs is 3.56% higher than that of the beam with headed studs arranged inline, and 3.32% higher than the adhesive bonded composite beam.

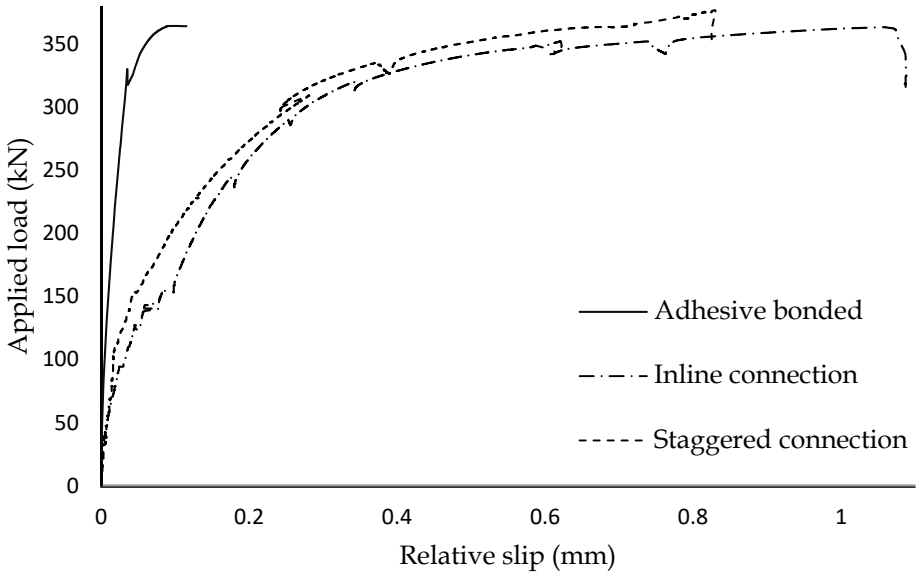

Fig. 7-22: Comparative applied load-relative slip behaviour of steel-concrete composite beams

Table 7-2: Maximum load and ultimate slip for inline and staggered mechanical headed stud connected composite beams

Connection strategy	Maximum load(P_u)	Ultimate slip(s_u)
	(kN)	*(mm)*
Adhesive bonded	364.08	0.115
Inline connection	363.18	1.089
Staggered connection	376.11	0.83

7.7.2 Load-Deflection Behaviour

The comparative load-deflection profiles of all the three steel concrete composite beams, at a distance on 425 mm, 850 mm, 1700 mm and 2550 mm from the simply supported end, have been shown in *Figs. 7-23* to *7-26*, respectively. The load-deflection curves of the three tested beam specimens, at 425 mm from the simply supported end of the beams has been shown in *Fig. 7-23*. It can be observed from the figure that the load-deflection profiles of all the beams follow almost the same path upto a load level of 150.44 kN (40% of ultimate), beyond which, the connection stiffness dominates the load deflection behaviour. This effect has been observed to be more pronounced in the load-deflection curves at higher distances from the simply supported end, as evident through *Figs. 7-24* to *7-26*. *Table 7-3* enlists the observed ultimate values of vertical deflection of the beams. It has been

observed that the ultimate vertical deflection is minimum near the supports and maximum at the mid span of the beams. It has also been observed, that the maximum ductility has been achieved in case of composite beams connected with headed studs arranged in inline fashion, while the minimum ductility is offered by adhesive bonded composite beams.

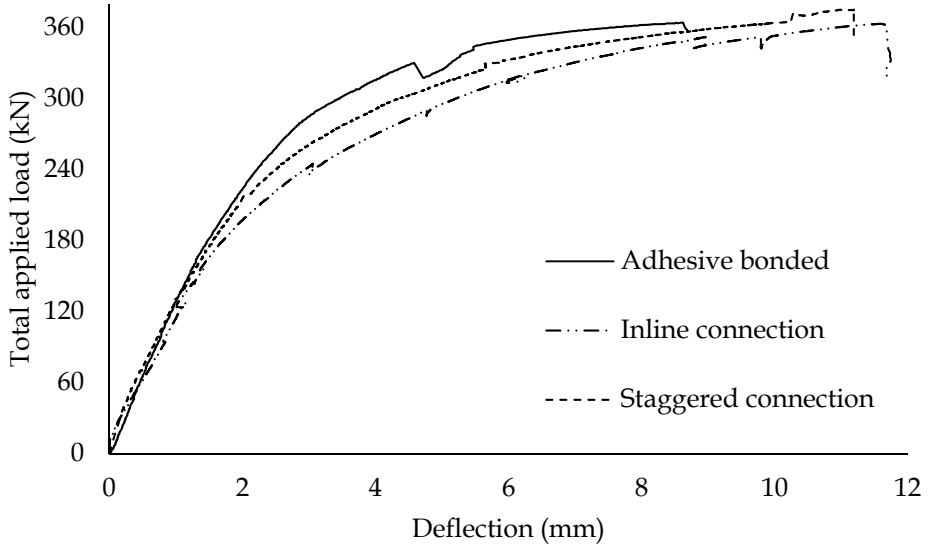

Fig. 7-23: Comparative load-deflection behaviour of steel-concrete composite beams at 425 mm from beam end

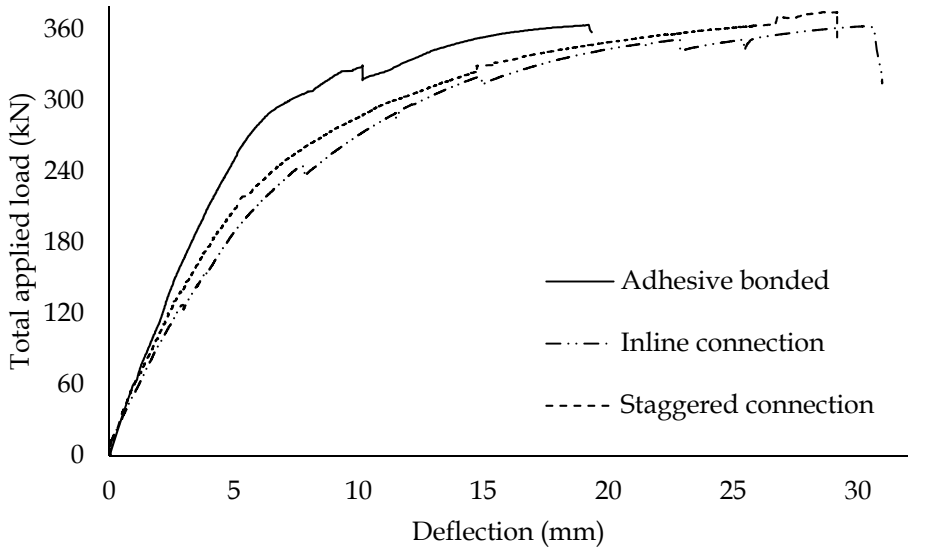

Fig. 7-24: Comparative load-deflection behaviour of steel-concrete composite beams at 850 mm from beam end

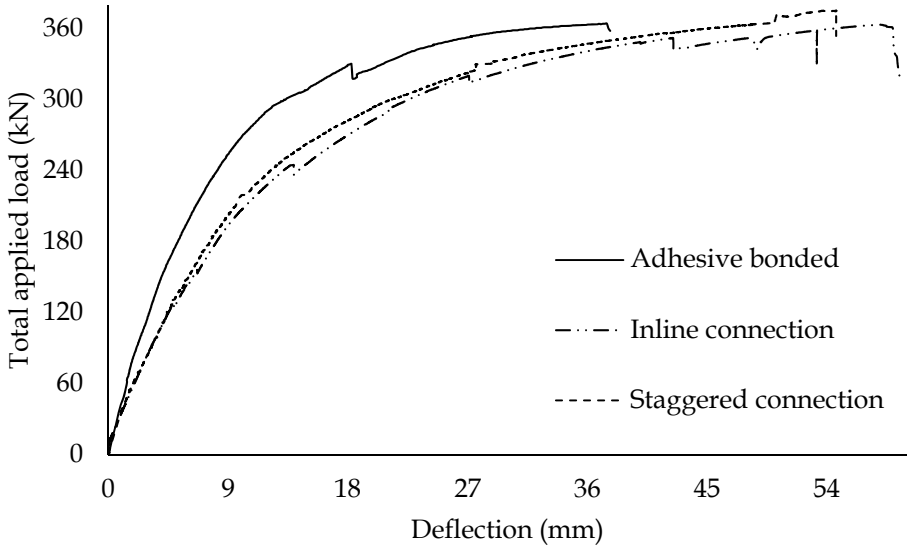

Fig. 7-25: Comparative load-deflection behaviour of steel-concrete composite beams at 1700 mm from beam end

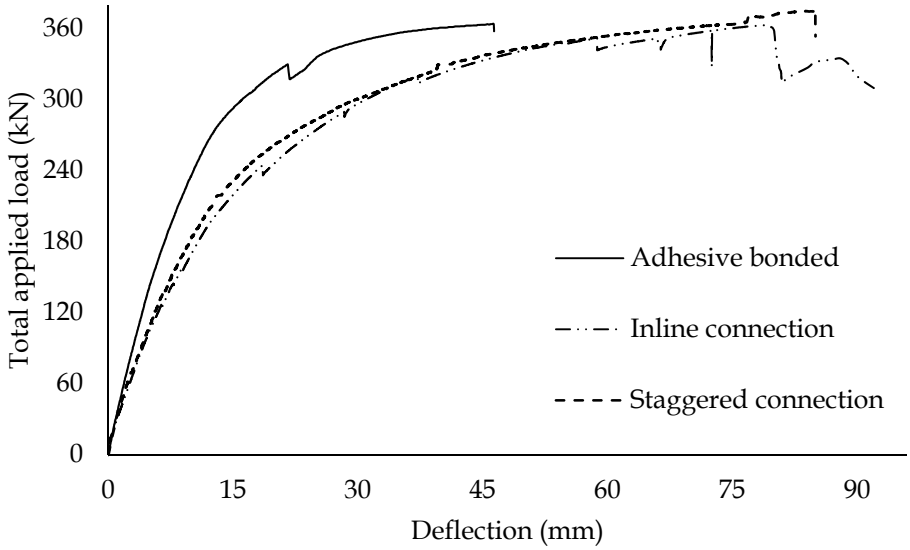

Fig. 7-26: Comparative load-deflection behaviour of steel-concrete composite beams at 2550 mm from beam end

Table 7-3: Ultimate load and deflection values for headed studs and adhesive bonded steel-concrete composite beams

Connection strategy	Maximum load(P_u)	Ultimate deflection (δ_{max})			
		425	850	1700	2550
	(kN)	Mm	mm	mm	mm
Adhesive bonded	364.08	8.68	19.33	37.70	46.36
Inline connection	363.18	11.74	30.96	59.48	92.00
Staggered connection	376.11	11.19	29.17	54.69	84.99

7.7.3 Shear Stiffness

The initial as well as post-yield shear stiffness of the tested composite beams have been estimated using the energy balanced approach, as described in Chapter five (*section 5.3*). The estimated values of the initial and the post-yield shear stiffness of the beams have been presented in *Table 7-4*. The bilinear idealized load-slip curves, representing the shear stiffness of the three beams, have been shown in *Fig. 7-27*. The results suggest that the initial shear stiffness of the adhesive bonded composite beam is greater than that of the composite beams connected using mechanical headed studs, connected in inline and staggered patterns, by 7.89 and 4.39 times, respectively. The significant difference in the values of initial stiffness of the three beam specimens underlines the effect of adopted connection strategy on the behaviour of connection. It has also been observed that in case of composite beams connected using mechanical headed studs, the change in arrangement of connectors from inline to staggered, decreases the interfacial slip at the same load level, leading to a significant increase in the connection shear stiffness.

Table 7-4: Initial and post yield stiffness of headed studs and adhesive bonded steel-concrete composite beams

Connection strategy	Initial stiffness *(k_i)*	Post-yield stiffness *(k_{py})*
	(kN/mm)	(kN/mm)
Adhesive bonded	11870.90	733.88
Inline connection	1504.22	32.95
Staggered connection	2701.42	129.82

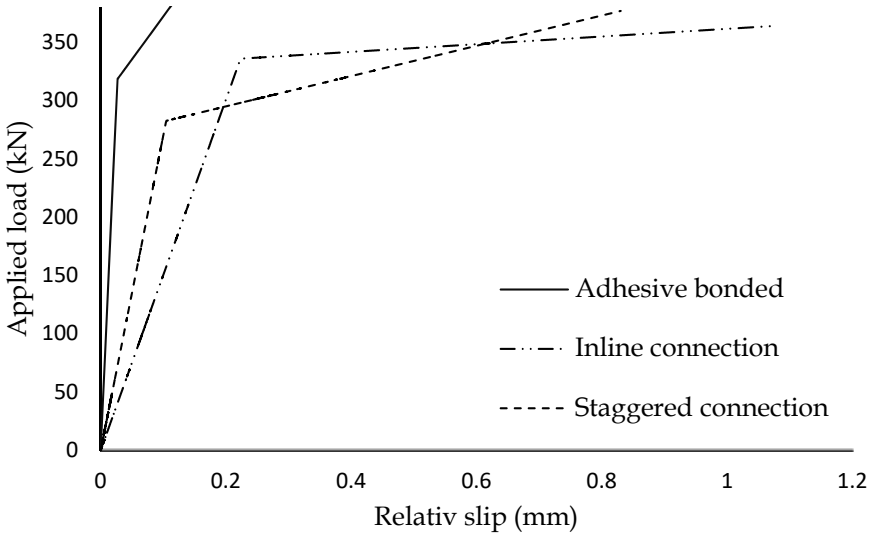

Fig. 7-27: Bilinear idealization of load-slip behaviour of steel-concrete composite beams

7.8 Conclusions

This chapter presented an investigation on the flexural behaviour of single span simply supported steel-concrete composite beams under two-point loading. Three composite beams have been prepared, using two material based connection methodologies, first using mechanical headed stud connectors (flexible) and the second using structural adhesive (rigid). The composite beam specimens with mechanical headed stud connectors have been prepared to investigate the effect of arrangement of headed studs along the span of the beam. The effects of inline and staggered arrangement of headed stud connectors, on the flexural behaviour of composite beams have been studied. The load- slip and load-deflection curves of the beams have been used as the parameters for estimation of the behaviour of the beams. The initial and post-yield stiffnesses for composite beams have also been evaluated on the basis of the energy balance approach. Based on the results of the experimental study, following precise conclusions have been drawn:

- Almost equal load capacities (3.56% variation) have been obtained for all the three beams. The composite beam with staggered arrangement of headed studs offers the maximum strength of 376.11 kN, while composite beams, with headed studs arranged inline and adhesive bonded, offers an almost equal strength of 364 kN.
- The relative slips engendered at connected interface for composite beams, connected with adhesive, mechanically headed stud connecters in staggered pattern and in inline pattern are 0.115 mm, 0.83 mm and 1.089, respectively. This change in beam connection strategy leads to an increase in relative slip, which in-turn decreases the degree of interaction.
- The values obtained for ultimate deflection at mid-span of the composite beams are 46.39 mm, 84.99 mm and 92.00 mm, for adhesive bonded, mechanically headed stud connected in staggered pattern and in inline pattern, respectively. With the change in connection strategy from adhesive bonded to mechanical headed stud connected, the increase in ultimate deflection values are almost 1.80 (staggered pattern) to 2.00 (inline pattern) times.

- The changes in the deflected profiles of the composite beam specimens in all the three cases exhibits an almost similar behaviour, i.e., the skewness of the curves defining the deflected profile increases with an increase in load beyond 80% of the ultimate strength. Such a trend characterises the initiation of nonlinear behaviour beyond the load level of 80% of ultimate.
- The redistribution of loads and stresses, distortion and failure of headed stud connector or a group of connectors, localised cracking and crushing in RCC slab have been observed to be the possible reasons for drops in load-slip and load-deflection curves for all beams. The formation of all drops at same lead levels reinforces this conclusion.
- Large number of drops in load-slip and load-deflection curves in composite beam connected with headed stud connectors arranged in inline pattern, as compared to those arranged in staggered pattern, signifies a better and more uniform transfer of stresses between the connected elements in the latter. This observation leads to a conclusion that the composite beams with mechanical headed studs arranged in staggered pattern exhibits a better behaviour than those with headed suds arranged in inline pattern.
- In case of composite beams connected with mechanical headed stud connectors arranged inline the predominant failure is due to cracking in concrete along both the lines of connectors. However, the in case of composite beam with staggered arrangement of headed studs, the failure occurs by cracking in concrete along the longitudinal span at mid-portion and diagonally from centre. Furthermore, for adhesive bonded composite beams, the flexural failure of concrete has been observed with the cracking of concrete element from bottom to top, almost at the mid-span of the beam.
- The initial stiffness of adhesive boned composite beam (11870.90 kN) is 7.89 times higher than that of the beam connected with mechanical headed stud connecters arranged inline (1504.22 kN), and 4.39 times higher than the beam connected with staggered headed studs (2701.42 kN).
- The post-yield stiffness of adhesive boned composite beam (733.88 kN) is 24.50 times higher than that of the beam connected with mechanical headed

stud connecters arranged inline (29.95 kN), and 5.65 times higher than the beam connected with staggered headed studs (129.82 kN).

Chapter: 8

Summary and Conclusions

8.1 Overview

This thesis explores the integrity of steel-concrete composite members, on the basis of the interfacial connections between the two constituent elements. The behaviour of the composite members has been observed to be significantly affected by the properties of the connection. The connection methodologies, selected based on member function, degree of connection, degree of interaction and material based approaches have been analysed and discussed. A comparative statement on the performance of composite members, connected using two fundamentally different connection methodologies has been presented. The comparative behaviour of both connection methodologies has been analysed under monotonic as well as extreme loading through vertical push-out and drop weight impact tests. The factors influencing the connection performance have also been critically observed and analysed. The flexural behaviour of full scale simply supported steel-concrete composite beams, connected using both the connection methodologies, has also been investigated under two-point loading. In this chapter, the salient findings of the experimental and analytical studies, conducted during the course of this thesis, have been presented.

8.2 Summary and Conclusions

This section discusses the chapter-wise findings of the various investigations carried out in this thesis. The effectiveness and performance of interfacial connections decide the behaviour of composite members. To understand the state of art about the interfacial connections, and to gain insight on the connection behaviour, a detailed literature review has been carried out. The literature review has been categorized on the basis of connection strategies adopted to connect the two elements of composite members. The literature suggest that the comparative behaviour of ideologically and characteristically different connection methodologies has not been explicitly compared yet. Composite connection characteristics have been defined on the basis of the materials used to connect the

two interfaces and can be classified broadly as flexible and rigid shear connections. The connections made using mechanical headed stud are the most common flexible shear connections while those with structural adhesive exhibits a predominantly rigid behaviour. The physical, mechanical, chemical and microstructural properties of materials used in in the present study have also been studies in detail. Experimental investigations have been conducted to gain insight into the behaviour of constitutive materials (material ingredients) and derive input parameters to carry out Finite Element simulations, for concrete, structural steel, reinforcement bar, headed studs and adhesive. The following conclusions have been drawn from the experimental investigations on the constituent material:

- The quality of welding, employed to connect steel element and headed studs has been subjected to the Bend test. The results suggest that the Metal inert gas type welding is the most appropriate welding technique.
- The epoxy resin based structural adhesive has been selected on the basis of the results of a preliminary study. The tensile behaviour of the adhesive has been observed to be brittle. The presence of bond at concrete and adhesive interface has been validated with the results of chemical and microstructural analysis.
- The chemical bond behaviour studied through FT-IR suggests that the composite interface possess a bond band which is stronger than concrete but slightly weaker than epoxy. The interfacial strength influencing bond band has been observed at 990.06 cm^{-1} for concrete, 1081.33 cm^{-1} for epoxy, 1008.95 cm^{-1} for the composite interface.
- The microstructural investigation (BSE imaging) reveals a near perfect bonding behaviour between concrete and adhesive layer.
- Dynamic mechanical analysis of selected epoxy adhesive suggests the applicability in structural operating range for temperatures in steel-concrete composite construction.

The behaviour of steel-concrete composite vertical push-out test specimens prepared using both connecting strategies (headed stud connector and structural adhesive) have been investigated. The area of influence for mechanically

connected and adhesive bonded specimens has been kept identical in the present study, for accurate prediction of strength. The behaviour of both the connections under static and impact loading have been experimentally evaluated, and presented. The following conclusions can be drawn on the basis of this experimental study:

- The static strength capacity for both connection strategies differ by 10.88% with respect to mechanically headed stud connected specimen. Although, the variation in effective area is only 2.51%.
- The initial shear stiffness of specimen having bonded connection is twenty two times higher than the stiffness of mechanical headed stud connector connected specimen.
- The overall ductility of adhesive bonded connection is almost negligible, while mechanically headed stud connected connections are ductile in nature. The ultimate failure of adhesively bonded composite specimen is brittle in nature and failure of concrete is observed under the action of impact load.
- The number of blows required for crack initiation in adhesive bonded composite specimens are 1.4 times higher than that required for crack initiation in mechanical stud connected specimens. The number of blows required for the final failure of adhesively bonded composite specimens are 0.72 times (significantly less) than that required for causing a serviceability failure (slip of 3 mm) in mechanically connected specimens.

The factors influencing the connection strength of mechanical headed stud connected composite specimen have also been investigated under monotonic loading. The parameters considered to investigate the behaviour of composite connections are, the strength of concrete elements (from C_1 to C_5) and the quantity and location of the reinforcement. The following salient conclusions have been drawn from the study:

- The compressive strength of concrete elements significantly affects the dowel strength of headed stud connector(s). A linear relation exists between the dowel strength of shear connector and compressive strength of concrete

elements considered in present study. However, an inverse relationship exists between the strength of concrete elements and the ultimate relative slip of the connection.

- With increase in the strength of concrete elements, a reduction in deformability along with a downward shift of fracture height of the studs (towards the root of stud) has been observed. It has also been observed that, for the specimen having concrete element of strength C_5, the failure of stud occurs due to fracture of weld, along with minimal crushing of concrete at the bearing zone.
- The increase in strength of concrete element leads to significant increase in the initial and post yield stiffness of the connections. An increase of upto 133.20% in the initial stiffness and 142.10% in the post yield stiffness has been observed with the change in strength of concrete elements from C_1 to C_5 (126.03%).
- The effect of increase in quantity of reinforcement (from 0 to 1.8%) is that the ultimate strength of the connection increases with density of reinforcement. However, for the steel-concrete composite specimens having very high strength of concrete elements, the failure of headed stud governs the performance.
- The shear strength of steel-concrete composite connection reduces with an increase in the distance between first layer of reinforcement and the root of stud. When this distance is increased from 25 mm to 100 mm, the connection strength reduces, by 15.31% (137.34 kN to 119.10 kN) in case of C_1 concrete, and by 11.50% (138.12 kN to 122.23 kN) in case of C_2 concrete.
- The ductility of connection has been observed to increase with the increase in distance between root of stud and reinforcement cage. However, this effect is observed only when the reinforcement cage lies in the zone of influence of the headed studs.
- Premature failure has been observed in single layer reinforced steel-concrete composite specimens, primarily owing to cracking of concrete at the level of reinforcement layer.

- The stiffness, strength and ductility of composite connections increases with an increase in the percentage of reinforcement in the concrete layer due to enhanced confinement effect.
- The load-slip behaviour of specimen with unreinforced concrete element is almost similar to that of the specimen with concrete element having single layer of reinforcement at 100 mm from root of shear stud. It can thus be concluded that the effect of reinforcement, outside the influence zone of the headed stud, is negligible.
- The composite specimen with concrete element having 100 mm reinforcement cage at 25 mm from root of stud and specimen with concrete element having 60 mm reinforcement cage at 50 mm from root of stud exhibits almost same ultimate strength. However, the load-slip curves of the two specimens follow entirely different paths. The initial stiffness of specimen with concrete element having 60 mm reinforcement cage at 50 mm from root of stud has been found to be governed by concrete only.
- Double layer reinforced specimens having 100 mm cage with 25 mm spacing from root of stud and 60 mm cage with 50 mm spacing from root of stud follow almost identical path in load-slip curve under monotonic loading.
- Although, the effect of reinforcement layers on the post yield stiffness of connections is marginal, the initial stiffness of connections having no reinforcement and single layer of reinforcement increases by 67.43 kN/mm (114.27%) for C_1 strength concrete and by 80.89 kN/mm (113.59%) for C_2 strength concrete.
- The reduction in the confining width of reinforcement from 100 mm to 60 mm leads to increase in the initial and post yield stiffness of steel-concrete composite specimens. In case of specimens with C_1 concrete, the initial stiffness increases by 34.18 kN/mm (22.50%) and post yield stiffness increases by 2.479 kN/mm (78.97%). Also, for specimens with concrete element having C_2 strength the increase in initial stiffness is about 64.15 kN/mm (40.12%) and increase in post yield stiffness is about 2.16 kN/mm

(49.88%). These observations underscore the importance of confinement of concrete element in terms of strength and stiffness of the connections.

- The strength and stiffness of the connections is inversely related to the distance between the root of stud and the first layer of reinforcement, i.e., the strength and stiffness of the connection reduces with increase in the distance between the root of stud and first reinforcement layer.
- The specimens with concrete element having three layers of reinforcement exhibits significantly higher initial stiffness (3.5 times) and post yield stiffness (1.8 times) than the corresponding specimens having unreinforced concrete elements.

The comparative performances of bonded push-out test specimens having different bond layer thickness have been examined. The optimum thickness of the bonded layer along with the failure modes and relative strength and stiffness of connections have also been investigated, experimentally, as well as analytically. For achieving the above objective, the compressive strength (C_5) of concrete element and structural adhesive have been selected to be almost identical for correct estimation of optimum thickness and failure pattern. Following conclusions can be drawn from this study:

- The failure pattern of bonded connections changes from adhesive to mixed (adhesive and cohesive), and from mixed to cohesive mode on increasing the bond layer thickness. For adhesive layers having thickness less than 3 mm, the adhesive mode of failure has been observed between concrete-epoxy and epoxy-steel interfaces with desirable overall connection rigidity. However, when the thickness of adhesive is greater than 3 mm, cohesive mode of failure of interface has been observed, while at the optimum thickness (3 mm), the composite interfaces experience mixed mode of failure.
- Increase in the thickness of adhesive layer increases the shear capacity of bonded connection up to an optimum (3 mm) thickness. Beyond this, an increase in thickness decreases the strength of connections.

- The relative slip at the interface of composite connection increases with an increase in the adhesive layer thickness.
- The shear stiffness of connection decreases with increase in the bond thickness. Also, the rate of decrement in shear stiffness increases with increase in the thickness of connection. The stiffness of connection reduces to almost half of its original value with change in bond layer thickness from 1 mm to 5 mm.
- The results obtained from FE analysis are in close agreement with experimental results. The difference in FE analysis and experimental values for all five adhesive layer thickness is limited to 7.50% and 10.00% for total applied load and engendered relative slip, respectively.
- The maximum intensity of shear stress has been found at boundary line of the bonded area. However, highest shear stress has been obtained at end bearing line of the bonded area.

The single span simply supported steel-concrete composite beams under two-point loading have been experimentally investigated to analyse the flexural behaviour under monotonic loading. Three composite beams have been prepared, using two material based connection methodologies, first using mechanical headed stud connectors (flexible) and the second using structural adhesive (rigid). The composite beam specimens with mechanical headed stud connectors have been prepared to investigate the effect of arrangement of headed studs. The effects of inline and staggered arrangement of headed stud connectors have been studied. The load- slip and load-deflection curves of the beams have been used as the parameters for estimation of the behaviour of the beams. The initial and post-yield stiffnesses for composite beams have also been evaluated on the basis of the energy balance approach. On the basis of the experimental results, following conclusions have been drawn:

- Almost equal load capacities (3.56% variation) have been obtained for all the three beams. The ultimate values for engendered relative slips at connected interface for all three composite beams namely, adhesive bonded, headed stud connected in staggered pattern and in inline pattern

are 0.115 mm, 0.83 mm and 1.09 mm, respectively. This significant change in relative slip, in-turn decreases the degree of interaction.

- With the change in connection strategy from adhesive bonded to mechanical headed stud connected, the increase in ultimate deflection values are almost 1.80 (staggered pattern) to 2.00 (inline pattern) times. The change in skewness of the deflected profile of composite has been observed beyond a load level of 80% of the ultimate strength.
- The redistribution of loads and stresses, distortion and failure of headed stud connector or a group of connectors, localised cracking and crushing in RCC slab have been observed to be the possible reasons for drops in load-slip and load-deflection curves for all beams. The formation of all drops at same load levels reinforces this conclusion.
- Large number of drops in load-slip and load-deflection curves in composite beam connected with headed stud connectors arranged in inline pattern, as compared to those arranged in staggered pattern, signifies a better and more uniform transfer of stresses between the connected elements in the latter. This observation leads to a conclusion that the composite beams with mechanical headed studs arranged in staggered pattern exhibits a better behaviour than those with headed studs arranged in inline pattern.
- The initial stiffness of adhesive bonded composite beam (11870.90 kN) is 7.89 times higher than that of the beam connected with mechanical headed stud connectors arranged inline (1504.22 kN), and 4.39 times higher than the beam connected with staggered headed studs (2701.42kN). However, the post-yield stiffness of adhesive bonded composite beam (733.88 kN) is 24.50 times higher than that of the beam connected with mechanical headed stud connectors arranged inline (29.95 kN), and 5.65 times higher than the beam connected with staggered headed studs (129.82 kN). The increase in stiffness of composite beams increases the degree of connection.

8.3 Scope of Future Work

Although, the outcomes from this research work signifies the adeptness of individual connection methodology on the basis of the degree of interaction and degree of connection, the following points can be addressed in the future as an extension of current research work:

- The instantaneous design aspects (strength, slip, deflection and stiffness) of two ideologically different connection methodology (flexible and rigid) based on connecting material have been considered in present study. However, for an enhanced clarity and in-depth understanding, studies on some other relevant aspects such as bonded area geometry and aggregate size may be taken up.
- The performance comparison of both connection methodologies in dynamic and creep loading may also be considered to propose proper design guidelines.
- The durability of steel-concrete composite connection bonded with structural adhesive may be considered as an aspect.

References

AASHTO-LRFD (2007). " Bridge Design specifications.", American Association of State Highway Transportation Officials., Washington, DC.

ABAQUS (HKS, 2013). "ABAQUS 6.13 User's manual." *Simulia, Dassault Systems, Providence, RI*.

Aboobucker, M., Wang, T., and Liew, J. R. (2009). "An experimental investigation on shear bond strength between steel and fresh cast concrete using epoxy." *The IES Journal Part A: Civil & Structural Engineering*, 2(2), 107-115.

ACI 211 (2008). "Guide for selecting proportions for high-strength concrete using portland cement and other cementitious materials." *ACI 211.4R-08*, American Concrete Institute, Farmington Hills, MI.

ACI 318 (1977). "Building Code Requirements for Reinforced Concrete." *ACI 318-77,* American Concrete Institute, Farmington Hills, MI.

ACI 349 (2001). "Code Requirements for Nuclear Safety Related Concrete Structures " *ACI 349R-01*, American Concrete Institute, Farmington Hills, MI.

ACI 544 (2009). "Measurement of Properties of Fiber Reinforced Concrete, *ACI 544.2 R-89,* 1989 (Reapproved 2009)." American Concrete Institute, Farmington Hills, MI.

ACI AASHO (1957). "Standard Specification for Highway Bridges.", American Association of Highway Officials., Washington, DC.

Adekola, A. (1968). "Partial interaction between elastically connected elements of a composite beam." *International Journal of Solids and Structures*, 4(11), 1125-1135.

Adekola, A. (1974). "The dependence of shear lag on partial interaction in composite beams." *International Journal of Solids and Structures*, 10(4), 389-400.

Adhikary, B. B., and Mutsuyoshi, H. (2002). "Numerical simulation of steel-plate strengthened concrete beam by a non-linear finite element method model." *Construction and Building Materials*, 16(5), 291-301.

Adhikary, B. B., and Mutsuyoshi, H. (2006). "Shear strengthening of RC beams with web-bonded continuous steel plates." *Construction and Building Materials*, 20(5), 296-307.

Adhikary, B. B., Mutsuyoshi, H., and Sano, M. (2000). "Shear strengthening of reinforced concrete beams using steel plates bonded on beam web: experiments and analysis." *Construction and Building materials*, 14(5), 237-244.

Ahn, J.-H., Lee, C.-G., Won, J.-H., and Kim, S.-H. (2010). "Shear resistance of the perfobond-rib shear connector depending on concrete strength and rib arrangement." *Journal of Constructional Steel Research*, 66(10), 1295-1307.

AISC-ANSI 360 (1978). " Specifications for the design, fabrication and erection of structural steel for buildings." American Institute of Steel Construction., New York.

AISC-ANSI 360 (2010). "360-10,“Specification for Structural Steel”.", American Institute of Steel Construction, Chicago (IL).

Alenezi, K., Tahir, M., Alhajri, T., Badr, M., and Mirza, J. (2015). "Behavior of shear connectors in composite column of cold-formed steel with lipped C-channel assembled with ferro-cement jacket." *Construction and building materials*, 84, 39-45.

Ali, M. M., Oehlers, D. J., and Bradford, M. A. (2005). "Debonding of steel plates adhesively bonded to the compression faces of RC beams." *Construction and building materials*, 19(6), 413-422.

Ali, M. M., Oehlers, D., and Bradford, M. (2000). "Shear peeling of steel plates adhesively bonded to the sides of reinforced concrete beams." *Proceedings of the Institution of Civil Engineers-Structures and Buildings*, 140(3), 249-259.

Alqedra, M., and Ashour, A. (2005). "Prediction of shear capacity of single anchors located near a concrete edge using neural networks." *Computers & structures*, 83(28), 2495-2502.

An, L., and Cederwall, K. (1996). "Push-out tests on studs in high strength and normal strength concrete." *Journal of Constructional Steel Research*, 36(1), 15-29.

Ashour, A., and Alqedra, M. (2005). "Concrete breakout strength of single anchors in tension using neural networks." *Advances in Engineering Software*, 36(2), 87-97.

ASTM C469/C469M (2014). "Standard Test Method for Static Modulus of Elasticity and Poisson’s Ratio of Concrete in Compression." *C469/C469M*, ASTM International, West Conshohocken, PA, 2014.

ASTM C881 (2010). "Standard Specification for Epoxy-Resin-Base Bonding Systems for Concrete." *C881,* ASTM International, West Conshohocken, PA.

ASTM D638 (2010). "Standard test method fort tensile properties of plastics." *D 638*, ASTM International, West Conshohocken, PA.

ASTM D695 (2015). "Standard test method for compressive properties of rigid plastics " *D 695,* ASTM International, West Conshohocken, PA.

Ataei, A., Bradford, M. A., and Liu, X. (2016). "Experimental study of composite beams having a precast geopolymer concrete slab and deconstructable bolted shear connectors." *Engineering Structures*, 114, 1-13.

Ataei, A., Bradford, M., and Liu, X. "Sustainable composite beams and joints with deconstructable bolted shear connectors." *Proc., 23th Australian conference on the Mechanics of structures and materials, Byron Bay, Australia*.

Badie, S. S., Tadros, M. K., Kakish, H. F., Splittgerber, D. L., and Baishya, M. C. (2002). "Large shear studs for composite action in steel bridge girders." *Journal of Bridge Engineering*, 7(3), 195-203.

Badoux, J. C. (1965). "Horizontal shear connection in composite concrete beams under repeated loading." Lehigh University.

Ban, H., Uy, B., Pathirana, S. W., Henderson, I., Mirza, O., and Zhu, X. (2015). "Time-dependent behaviour of composite beams with blind bolts under sustained loads." *Journal of constructional steel research*, 112, 196-207.

Baran, E., and Topkaya, C. (2012). "An experimental study on channel type shear connectors." *Journal of Constructional Steel Research*, 74, 108-117.

Baran, E., and Topkaya, C. (2014). "Behavior of steel–concrete partially composite beams with channel type shear connectors." *Journal of Constructional Steel Research*, 97, 69-78.

Barnaf, J., Bajer, M., and Vyhnankova, M. (2012). "Bond strength of chemical anchor in high-strength concrete." *Procedia Engineering*, 40, 38-43.

Barnard, P. R., and Johnson, R. (1965). "ULTIMATE STRENGTH OF COMPOSITE BEAMS." *Proceedings of the Institution of Civil Engineers*, 32(2), 161-179.

Barnes, R. A., and Mays, G. C. (2006). "Strengthening of reinforced concrete beams in shear by the use of externally bonded steel plates: Part 1–Experimental programme." *Construction and Building Materials*, 20(6), 396-402.

Benzarti, K., Chataigner, S., Quiertant, M., Marty, C., and Aubagnac, C. (2011). "Accelerated ageing behaviour of the adhesive bond between concrete specimens and CFRP overlays." *Construction and building materials*, 25(2), 523-538.

Berthet, J., Yurtdas, I., Delmas, Y., and Li, A. (2011). "Evaluation of the adhesion resistance between steel and concrete by push out test." *International Journal of Adhesion and Adhesives*, 31(2), 75-83.

BIS 10262 (2009). "Concrete Mix proportioning-Guidelines." Bureau of Indian Standards, New Delhi, India.

BIS 11384 (1985 2003,). "Code of practice for composite construction in structural steel and concrete." *IS:11384*New Delhi, India.

BIS 1608 (2005). "Metallic materials-Tensile testing at ambient temperature " *IS: 1608*, BIS New Delhi, India.

BIS 1786 (2008). "High Strength Deformed Steel Bars and Wires for Concrete Reinforcement—Specification." *Bureau of Indian Standards, New Delhi*.

BIS 383 (2016). "Coarse and fine aggregate for concrete-Specifications." *IS: 383*, BIS, New Delhi, India.

Bizindavyi, L., and Neale, K. (1999). "Transfer lengths and bond strengths for composites bonded to concrete." *Journal of composites for construction*, 3(4), 153-160.

Bouazaoui, L., and Li, A. (2008). "Analysis of steel/concrete interfacial shear stress by means of pull out test." *International Journal of Adhesion and Adhesives*, 28(3), 101-108.

Bouazaoui, L., Jurkiewiez, B., Delmas, Y., and Li, A. (2008). "Static behaviour of a full-scale steel–concrete beam with epoxy-bonding connection." *Engineering Structures*, 30(7), 1981-1990.

Bouazaoui, L., Perrenot, G., Delmas, Y., and Li, A. (2007). "Experimental study of bonded steel concrete composite structures." *Journal of Constructional Steel Research*, 63(9), 1268-1278.

Branco, F. J., Tadeu, A. J., and Nogueira, J. A. (2003). "Bond geometry and shear strength of steel plates bonded to concrete on heating." *Journal of materials in civil engineering*, 15(6), 586-593.

British Standard, B. (1997). "8110-97. Structural use of concrete, Part 1, Code of practice for design and construction." *British Standards Institution, London*.

Brozzetti, J. (2000). "Design development of steel-concrete composite bridges in France." *Journal of Constructional Steel Research*, 55(1), 229-243.

BS (1989). "Bonding agents for use with gypsum plasters and cement. Specification for polyvinyl acetate (PVAC) emulsion bonding agents for indoor use with gypsum building plasters." *BS 5270*, British Standards Institution London.

BS 5400-5 (1978). "Steel, concrete and composite bridges—Part 5: Code of practice for the design of composite bridges." *British Standards Institution, BS, London, UK.*, 5400-5405.

BS 5400-5 (2005). "Steel, concrete and composite bridges—Part 5: Code of practice for the design of composite bridges." *British Standards Institution, BS*, 5400-5405.

BS EN ISO 14555 (2014). "BS EN ISO 14555,." *Welding. Arc Stud Welding of Metallic Materials*, British Standards Institution, London, United Kingdom.

Buyukozturk, O., and Hearing, B. (1998). "Failure behavior of precracked concrete beams retrofitted with FRP." *Journal of composites for construction*, 2(3), 138-144.

Cândido-Martins, J., Costa-Neves, L., and Vellasco, P. d. S. (2010). "Experimental evaluation of the structural response of Perfobond shear connectors." *Engineering Structures*, 32(8), 1976-1985.

Carlberger, T., and Stigh, U. (2010). "Influence of layer thickness on cohesive properties of an epoxy-based adhesive—an experimental study." *The Journal of adhesion*, 86(8), 816-835.

Carreira, D. J., and Chu, K.-H. "Stress-strain relationship for plain concrete in compression." *Proc., Journal Proceedings*, 797-804.

Carreira, D. J., and Chu, K.-H. "Stress-strain relationship for reinforced concrete in tension." *Proc., Journal Proceedings*, 21-28.

Chand, S. (1979). "Cracks in building and their remedial measures." *Indian Concrete Journal* 268-272.

Chapman, J., and Balakrishnan, S. (1964). "Experiments on composite beams." *The Structural Engineer*, 42(11), 369-383.

Chen, J., and Teng, J. (2003). "Shear capacity of FRP-strengthened RC beams: FRP debonding." *Construction and Building Materials*, 17(1), 27-41.

Chen, S. (2003). "Load carrying capacity of composite slabs with various end constraints." *Journal of Constructional Steel Research*, 59(3), 385-403.

Chiang, M. Y., and Herzl, C. (1994). "Plastic deformation analysis of cracked adhesive bonds loaded in shear." *International Journal of Solids and Structures*, 31(18), 2477-2490.

Chinn, J. (1961). *The Use of Nelson Studs with Idealite Lightweight-aggregate Concrete in Composite Construction: Part I: Tests of 3/4 and 7/8" Studs, 4" High with 6" Slabs, 6 Sack Mix*, University of Colorado Engineering Experiment Station.

Chung, H. "Epoxy repair of bond in reinforced concrete members." *Proc., Journal Proceedings*, 79-82.

Clouston, P., Bathon, L. A., and Schreyer, A. (2005). "Shear and bending performance of a novel wood–concrete composite system." *Journal of Structural Engineering*, 131(9), 1404-1412.

Cognard, J. Y., Davies, P., Gineste, B., and Sohier, L. (2005). "Development of an improved adhesive test method for composite assembly design." *Compos Sci Technol*, 65(3), 359-368.

Colajanni, P., La Mendola, L., and Monaco, A. (2014). "Stress transfer mechanism investigation in hybrid steel trussed–concrete beams by push-out tests." *Journal of Constructional Steel Research*, 95, 56-70.

Colak, A. (2001). "Parametric study of factors affecting the pull-out strength of steel rods bonded into precast concrete panels." *Int J Adhes Adhes*, 21(6), 487-493.

Çolak, A., Çoşgun, T., and Bakırcı, A. E. (2009). "Effects of environmental factors on the adhesion and durability characteristics of epoxy-bonded concrete prisms." *Construction and Building materials*, 23(2), 758-767.

Cooper, V., Ivankovic, A., Karac, A., McAuliffe, D., and Murphy, N. (2012). "Effects of bond gap thickness on the fracture of nano-toughened epoxy adhesive joints." *Polymer*, 53(24), 5540-5553.

Coronado, C. A., and Lopez, M. M. (2008). "Experimental characterization of concrete-epoxy interfaces." *Journal of Materials in Civil Engineering*, 20(4), 303-312.

Crasto, A., Kim, R., and Mistretta, J. (2001). "The application of composites for the rehabilitation of concrete bridge infrastructure." *Advanced Composite Materials*, 10(2-3), 147-157.

Culver, C., and Coston, R. (1961). "Tests of composite beams with stud shear connectors, Proc. ASCE, 87,(ST2),(February 1961), Reprint No. 174 (61-3)."

Custódio, J., Broughton, J., and Cruz, H. (2009). "A review of factors influencing the durability of structural bonded timber joints." *International journal of adhesion and adhesives*, 29(2), 173-185.

D1002-98, A. (2010). "Standard Test Method for Apparent Shear Strength of Single-Lap-Joint Adhesively Bonded Metal Specimens by Tension Loading (Metal-to-Metal)." *D1002*, American Society for Testing Materials, West Conshohocken, PA,US.

Da Silva, L. F. M., das Neves, P. C., Adams, R. D., Wang, A., and Spelt, J. K. (2009b). "Analytical models of adhesively bonded joints-Part II: Comparative study." *Int J Adhes Adhes*, 29(3), 331-341.

Da Silva, L. F. M., das Neves, P. J. C., Adams, R. D., and Spelt, J. K. (2009a). "Analytical models of adhesively bonded joints-Part I: Literature survey." *Int J Adhes Adhes*, 29(3), 319-330.

Dai, X., Lam, D., and Saveri, E. (2015). "Effect of concrete strength and stud collar size to shear capacity of demountable shear connectors." *Journal of Structural Engineering*, 141(11), 04015025.

Dallam, L. N. (1968). *Pushout tests with high strength bolt shear connectors*, Missouri State Highway Department.

Dallam, L. N., and Harpster, J. L. (1968). *Composite beam tests with high-strength bolt shear connectors*, Missouri State Highway Department.

Daniels, B., Brekelmans, J., and Stark, J. (1993). "State-of-the-art report for composite bridge research." *Journal of Constructional Steel Research*, 27(1-3), 123-141.

Daniels, J. H., and Fisher, J. W. (1967). "Static behavior of composite beams with variable load position." Fritz Engineering Laboratory, Department of Civil Engineering, Lehigh University.

Daniels, J. H., and Fisher, J. W. (1968). *Fatigue behavior of continuous composite beams*, Lehigh University.

Davison, J., and Longworth, J. (1969). "Composite beams in negative bending."

De Andrade, S., Vellasco, P. d. S., Ferreira, L., and de Lima, L. (2007). "Semi-rigid composite frames with perfobond and T-rib connectors Part 2: Design models assessment." *Journal of Constructional Steel Research*, 63(2), 280-292.

de Lima Araújo, D., Sales, M. W. R., de Paulo, S. M., and de Cresce El, A. L. H. (2016). "Headed steel stud connectors for composite steel beams with precast hollow-core slabs with structural topping." *Engineering Structures*, 107, 135-150.

Dedic, D. J., and Klaiber, F. W. (1984). "High-strength bolts as shear connectors in rehabilitation work." *Concrete international*, 6(7), 41-46.

Derewonko, A., Godzimirski, J., Kosiuczenko, K., Niezgoda, T., and Kiczko, A. (2008). "Strength assessment of adhesive-bonded joints." *Comp Mater Sci*, 43(1), 157-164.

Deric, J. O., and Bradford, M. A. (1995). "Composite Steel and Concrete Structural Members." *Fundamental Behaviour, Australia*.

Dorton, R. A., Holowka, M., and King, J. (1977). "The Conestogo River Bridge—Design and Testing." *Canadian Journal of Civil Engineering*, 4(1), 18-39.

Driscoll Jr, G., and Slutter, R. (1961). "Research on composite design at Lehigh University, Proc. AISC, National Engineering Conference,(1961), Reprint No. 180 (61-8)."

Easterling, W. S., Gibbings, D. R., and Murray, T. M. (1993). "Strength of shear studs in steel deck on composite beams and joists." *Engineering Journal*, 30(2), 44-55.

EC4 (2004). "Eurocode 4: Design of composite steel and concrete structures. Part 1-1: General rules and rules for buildings." *EN 1994-1-1*Brussels, Belgium.

Ekenel, M., and Myers, J. J. (2007). "Durability performance of RC beams strengthened with epoxy injection and CFRP fabrics." *Construction and Building Materials*, 21(6), 1182-1190.

Ekenel, M., Rizzo, A., Myers, J. J., and Nanni, A. (2006). "Flexural fatigue behavior of reinforced concrete beams strengthened with FRP fabric and precured laminate systems." *Journal of Composites for Construction*, 10(5), 433-442.

El-Ghazzi, M. N. (1972). "Longitudinal shear capacity of the slabs of composite beams."

El-Hawary, M. M. (1999). "Evaluation of bond strength of epoxy-coated bars in concrete exposed to marine environment." *Construction and Building Materials*, 13(7), 357-362.

Ellobody, E. (2014). *Finite element analysis and design of steel and steel–concrete composite bridges*, Butterworth-Heinemann.

El-Tawil, S., and Deierlein, G. G. (1999). "Strength and ductility of concrete encased composite columns." *Journal of Structural engineering*, 125(9), 1009-1019.

Epackachi, S., Esmaili, O., Mirghaderi, S. R., and Behbahani, A. A. T. (2015). "Behavior of adhesive bonded anchors under tension and shear loads." *Journal of Constructional Steel Research*, 114, 269-280.

Ernst, S., Bridge, R. Q., and Wheeler, A. (2010). "Correlation of beam tests with pushout tests in steel-concrete composite beams." *Journal of structural engineering*, 136(2), 183-192.

Farhey, D. N., Adin, M. A., and Yankelevsky, D. Z. (1995). "Repaired RC flat-slab-column subassemblages under lateral loading." *Journal of Structural Engineering*, 121(11), 1710-1720.

Fernando, D., Yu, T., and Teng, J.-G. (2013). "Behavior of CFRP laminates bonded to a steel substrate using a ductile adhesive." *Journal of Composites for Construction*, 18(2), 04013040.

Fisher, J. W., Daniels, J. H., and Slutter, R. (1972). "Continuous composite beams for steel-concrete bridges, Final Report, April 1972."

Frigione, M., Aiello, M., and Naddeo, C. (2006). "Water effects on the bond strength of concrete/concrete adhesive joints." *Construction and building materials*, 20(10), 957-970.

Galambos, T. V. (2000). "Recent research and design developments in steel and composite steel–concrete structures in USA." *Journal of Constructional Steel Research*, 55(1), 289-303.

Gara, F., Ranzi, G., and Leoni, G. (2010). "Short-and long-term analytical solutions for composite beams with partial interaction and shear-lag effects." *International Journal of Steel Structures*, 10(4), 359-372.

Garcia, I., and Daniels, J. (1972). "Variables affecting the negative moment behavior of composite beams, April 1972."

Gattesco, N., Giuriani, E., and Gubana, A. (1997). "Low-cycle fatigue test on stud shear connectors." *Journal of Structural Engineering*, 123(2), 145-150.

Hamada, S., and Longworth, J. (1973). "Ultimate strength of continuous composite beams."

Han, L.-H., Li, W., and Bjorhovde, R. (2014). "Developments and advanced applications of concrete-filled steel tubular (CFST) structures: members." *Journal of Constructional Steel Research*, 100, 211-228.

Hanswille, G., Porsch, M., and Ustundag, C. (2007a). "Resistance of headed studs subjected to fatigue loading Part II: Analytical study." *Journal of constructional steel research*, 63(4), 485-493.

Hanswille, G., Porsch, M., and Ustundag, C. (2007b). "Resistance of headed studs subjected to fatigue loading: Part I: Experimental study." *Journal of constructional steel research*, 63(4), 475-484.

He, J., Liu, Y., and Pei, B. (2013). "Experimental study of the steel-concrete connection in hybrid cable-stayed bridges." *Journal of Performance of Constructed Facilities*, 28(3), 559-570.

Henderson, I., Zhu, X., Uy, B., and Mirza, O. (2015). "Dynamic behaviour of steel–concrete composite beams with different types of shear connectors. Part I: Experimental study." *Engineering Structures*, 103, 298-307.

Hindo, K. R. (1990). "In-place bond testing and surface preparation of concrete." *Concrete International*, 12(4), 46-48.

Hollaway, L. (2003). "The evolution of and the way forward for advanced polymer composites in the civil infrastructure." *Construction and Building Materials*, 17(6), 365-378.

Höök, M., and Stehn, L. (2008). "Applicability of lean principles and practices in industrialized housing production." *Construction Management and Economics*, 26(10), 1091-1100.

Horgnies, M., Willieme, P., and Gabet, O. (2011). "Influence of the surface properties of concrete on the adhesion of coating: characterization of the interface by peel test and FT-IR spectroscopy." *Progress in Organic Coatings*, 72(3), 360-379.

Hosain, M., and Pashan, A. (2006). "Channel Shear Connectors in Composite Beams: Push-Out Tests." *Composite Construction in Steel and Concrete V*, 501-510.

Hui, E. C. (2001). "Measuring affordability in public housing from economic principles: Case study of Hong Kong." *Journal of Urban Planning and development*, 127(1), 34-49.

IRC 22 (1986). "Standard Specifications and Code of practice for Road Bridges." *Composite Construction (Working State Design)*, The Indian Roads Congress, New Delhi, India.

Johnson, R. P. (2008). *Composite structures of steel and concrete: beams, slabs, columns, and frames for buildings*, John Wiley & Sons.

Johnson, R., and May, I. (1975). "Partial-interaction design of composite beams." *Structural Engineer*, 8(53).

Johnson, S. M. (1965). "Deterioration, maintenance, and repair of structures."

Julio, E. N., Branco, F. A., and Silva, V. t. D. (2004). "Concrete-to-concrete bond strength. Influence of the roughness of the substrate surface." *Construction and Building Materials*, 18(9), 675-681.

Julio, E. N., Branco, F. A., Silva, V. D., and Lourenco, J. F. (2006). "Influence of added concrete compressive strength on adhesion to an existing concrete substrate." *Building and environment*, 41(12), 1934-1939.

Jurkiewiez, B., Meaud, C., and Ferrier, E. (2014). "Non-linear models for steel–concrete epoxy-bonded beams." *Journal of Constructional Steel Research*, 100, 108-121.

Jurkiewiez, B., Meaud, C., and Michel, L. (2011). "Non linear behaviour of steel–concrete epoxy bonded composite beams." *Journal of Constructional Steel Research*, 67(3), 389-397.

Kahraman, R., Sunar, M., and Yilbas, B. (2008). "Influence of adhesive thickness and filler content on the mechanical performance of aluminum single-lap joints bonded with aluminum powder filled epoxy adhesive." *J Mater Process Tech*, 205(1), 183-189.

Kalyanasundaram, P., Rajeev, S., and Udayakumar, H. (1990). "REPCON: expert system for building repairs." *Journal of computing in civil engineering*, 4(2), 84-101.

Kang, T. H.-K., Howell, J., Kim, S., and Lee, D. J. (2012). "A state-of-the-art review on debonding failures of FRP laminates externally adhered to concrete." *International Journal of Concrete Structures and Materials*, 6(2), 123-134.

Karayannis, C., Chalioris, C., and Sideris, K. (1998). "Effectiveness of RC beam-column connection repair using epoxy resin injections." *Journal of Earthquake Engineering*, 2(02), 217-240.

Karbhari, V. M., and Zhao, L. (2000). "Use of composites for 21st century civil infrastructure." *Computer methods in applied mechanics and engineering*, 185(2), 433-454.

Kim, H.-Y., and Jeong, Y.-J. (2006). "Experimental investigation on behaviour of steel–concrete composite bridge decks with perfobond ribs." *Journal of Constructional Steel Research*, 62(5), 463-471.

King, D., Slutter, R., and Driscoll Jr, G. (1965). "Fatigue strength of 1/2 inch diameter stud shear connectors, Highway Research Record No. 103, Publication No. 294."

Klaiber, F., and Wipf, T. "An alternate shear connector for composite action." *Proc., Mid-Continent Transportation Symposium Proceedings*, 115-120.

Kwon, G., Engelhardt, M. D., and Klingner, R. E. (2010a). "Behavior of post-installed shear connectors under static and fatigue loading." *Journal of Constructional Steel Research*, 66(4), 532-541.

Kwon, G., Engelhardt, M. D., and Klingner, R. E. (2010b). "Experimental behavior of bridge beams retrofitted with postinstalled shear connectors." *Journal of Bridge Engineering*, 16(4), 536-545.

Lam, D. (2007). "Capacities of headed stud shear connectors in composite steel beams with precast hollowcore slabs." *Journal of Constructional Steel Research*, 63(9), 1160-1174.

Lam, D., and El-Lobody, E. (2005). "Behavior of headed stud shear connectors in composite beam." *J Struct Eng*, 131(1), 96-107.

Larbi, A. S., Ferrier, E., Jurkiewiez, B., and Hamelin, P. (2007). "Static behaviour of steel concrete beam connected by bonding." *Engineering structures*, 29(6), 1034-1042.

Lee, P.-G., Shim, C.-S., and Chang, S.-P. (2005). "Static and fatigue behavior of large stud shear connectors for steel–concrete composite bridges." *Journal of Constructional Steel Research*, 61(9), 1270-1285.

Leffler, K., Alfredsson, K., and Stigh, U. (2007). "Shear behaviour of adhesive layers." *Int J Solids Struct*, 44(2), 530-545.

Liang, Q. Q., Uy, B., Bradford, M. A., and Ronagh, H. R. (2004). "Ultimate strength of continuous composite beams in combined bending and shear." *Journal of Constructional Steel Research*, 60(8), 1109-1128.

Lloyd, R., and Wright, H. (1990). "Shear connection between composite slabs and steel beams." *Journal of Constructional Steel Research*, 15(4), 255-285.

Loh, H., Uy, B., and Bradford, M. (2004). "The effects of partial shear connection in the hogging moment regions of composite beams: Part I—Experimental study." *Journal of Constructional Steel Research*, 60(6), 897-919.

López-González, J. C., Fernández-Gómez, J., and González-Valle, E. (2012). "Effect of adhesive thickness and concrete strength on FRP-concrete bonds." *Journal of Composites for Construction*, 16(6), 705-711.

Louw, J., van Dyk, A., and Roux, A. (1970). "Stud Shear Connectors In Composite Steel And Concrete Construction Under Impact." *WIT Transactions on The Built Environment*, 8.

Lukaszewska, E., Johnsson, H., and Fragiacomo, M. (2008). "Performance of connections for prefabricated timber–concrete composite floors." *Materials and Structures*, 41(9), 1533-1550.

Luo, Y., Li, A., and Kang, Z. (2012). "Parametric study of bonded steel–concrete composite beams by using finite element analysis." *Engineering Structures*, 34, 40-51.

MacDonald, M., and Calder, A. (1982). "Bonded steel plating for strengthening concrete structures." *International Journal of Adhesion and Adhesives*, 2(2), 119-127.

Mahrenholtz, P., and Eligehausen, R. (2015). "Post-installed concrete anchors in nuclear power plants: Performance and qualification." *Nuclear Engineering and Design*, 287, 48-56.

Maleki, S., and Bagheri, S. (2008a). "Behavior of channel shear connectors, Part I: Experimental study." *Journal of Constructional Steel Research*, 64(12), 1333-1340.

Maleki, S., and Bagheri, S. (2008b). "Behavior of channel shear connectors, Part II: Analytical study." *Journal of Constructional Steel Research*, 64(12), 1341-1348.

Maleki, S., and Mahoutian, M. (2009). "Experimental and analytical study on channel shear connectors in fiber-reinforced concrete." *Journal of Constructional Steel Research*, 65(8), 1787-1793.

Manfredi, G., Fabbrocino, G., and Cosenza, E. (1999). "Modeling of steel-concrete composite beams under negative bending." *Journal of engineering mechanics*, 125(6), 654-662.

Marshall, W., Nelson, H., and Banerjee, H. (1971). "AN EXPERIMENT STUDY OF THE USE OF HIGH-STRENGTH FRICTION GRIP BOLTS AS SHEAR CONNECTORS IN COMPOSITE BEAMS." *Structural Engineer*.

Martiny, P., Lani, F., Kinloch, A., and Pardoen, T. (2012). "A multiscale parametric study of mode I fracture in metal-to-metal low-toughness adhesive joints." *Int J Fracture*, 173(2), 105-133.

Mattock, A. H. (1977). "NATIONAL SCIENCE FOUNDATION GRANT NO. ENG74-21131 FINAL REPORT PART 3."

Mays, G. C., and Hutchinson, A. R. (2005). *Adhesives in civil engineering*, Cambridge University Press.

Mays, G., and Vardy, A. (1982). "Adhesive-bonded steel/concrete composite construction." *International Journal of Adhesion and Adhesives*, 2(2), 103-107.

Meaud, C., Jurkiewiez, B., and Ferrier, E. (2014). "Steel–concrete bonding connection: An experimental study and non-linear finite element analysis." *International Journal of Adhesion and Adhesives*, 54, 131-142.

Mette, C., Stammen, E., and Dilger, K. (2016). "Challenges in joining conductive adhesives in structural application–Effects of tolerances and temperature." *International Journal of Adhesion and Adhesives*, 67, 49-53.

Miller, T. C., Chajes, M. J., Mertz, D. R., and Hastings, J. N. (2001). "Strengthening of a steel bridge girder using CFRP plates." *Journal of Bridge Engineering*, 6(6), 514-522.

Mirza, O., and Uy, B. (2010). "Effects of the combination of axial and shear loading on the behaviour of headed stud steel anchors." *Engineering Structures*, 32(1), 93-105.

Mottram, J., and Zheng, Y. (1996). "State-of-the-art review on the design of beam-to-column connections for pultruded frames." *Composite structures*, 35(4), 387-401.

Moynihan, M. C., and Allwood, J. M. (2014). "Viability and performance of demountable composite connectors." *Journal of Constructional Steel Research*, 99, 47-56.

Naithani, K., Gupta, V., and Gadh, A. (1988). "Behaviour of shear connectors under dynamic loads." *Materials and Structures*, 21(5), 359-363.

Nakamura, S.-i., Momiyama, Y., Hosaka, T., and Homma, K. (2002). "New technologies of steel/concrete composite bridges." *Journal of Constructional Steel Research*, 58(1), 99-130.

Nethercot, D. (2003). *Composite construction*, CRC Press.

Newmark, N. M., Siess, C. P., and Viest, I. (1951). "Tests and analysis of composite beams with incomplete interaction." *Proc. Soc. Exp. Stress Anal*, 9(1), 75-92.

Nguyen, H. T., and Kim, S. E. (2009). "Finite element modeling of push-out tests for large stud shear connectors." *Journal of Constructional Steel Research*, 65(10), 1909-1920.

Nie, J.-G., Li, Y.-X., Tao, M.-X., and Nie, X. (2014). "Uplift-Restricted and Slip-Permitted T-Shape Connectors." *Journal of Bridge Engineering*, 20(4), 04014073.

Noel, M., Wahab, N., and Soudki, K. (2016). "Experimental investigation of connection details for precast deck panels on concrete girders in composite deck construction." *Engineering Structures*, 106, 15-24.

Nozaka, K., Shield, C. K., and Hajjar, J. F. (2005). "Effective bond length of carbon-fiber-reinforced polymer strips bonded to fatigued steel bridge I-girders." *Journal of Bridge Engineering*, 10(2), 195-205.

Oehlers, D., and Coughlan, C. (1986). "The shear stiffness of stud shear connections in composite beams." *Journal of Constructional Steel Research*, 6(4), 273-284.

Oehlers, D. J. (1989). "Splitting induced by shear connectors in composite beams." *Journal of Structural Engineering*, 115(2), 341-362.

Oehlers, D. J. (1989). "Splitting induced by shear connectors in composite beams." *Journal of Structural Engineering*, 115(2), 341-362.

Oehlers, D. J. (2001). "Development of design rules for retrofitting by adhesive bonding or bolting either FRP or steel plates to RC beams or slabs in bridges and buildings." *Composites Part A: applied science and manufacturing*, 32(9), 1345-1355.

Oehlers, D. J., and Bradford, M. A. (1999). *Elementary behaviour of composite steel and concrete structural members*, Elsevier.

Oehlers, D. J., and Bradford, M. A. (2013). *Composite Steel and Concrete Structures: Fundamental Behaviour: Fundamental Behaviour*, Elsevier.

Oehlers, D., and Coughlan, C. (1986). "The shear stiffness of stud shear connections in composite beams." *Journal of Constructional Steel Research*, 6(4), 273-284.

Oehlers, D., and Coughlan, C. (1986). "The shear stiffness of stud shear connections in composite beams." *Journal of Constructional Steel Research*, 6(4), 273-284.

Oehlers, D., Park, S., and Ali, M. M. (2003). "A structural engineering approach to adhesive bonding longitudinal plates to RC beams and slabs." *Composites Part A: Applied Science and Manufacturing*, 34(9), 887-897.

Oguejiofor, E., and Hosain, M. (1992). "Behaviour of perfobond rib shear connectors in composite beams: full-size tests." *Canadian Journal of Civil Engineering*, 19(2), 224-235.

Oguejiofor, E., and Hosain, M. (1994). "A parametric study of perfobond rib shear connectors." *Canadian Journal of Civil Engineering*, 21(4), 614-625.

Oguejiofor, E., and Hosain, M. (1997). "Numerical analysis of push-out specimens with perfobond rib connectors." *Computers & Structures*, 62(4), 617-624.

Ollgaard, J. G., Slutter, R. G., and Fisher, J. W. (1971). "Shear strength of stud connectors in lightweight and normal weight concrete." *AISC Engineering Journal*, 8(2), 55-64.

Omar, H. A., Yusoff, N. I. M., Ceylan, H., Sajuri, Z., Jakarni, F. M., and Ismail, A. (2016). "Investigation of the relationship between fluidity and adhesion strength of unmodified and modified bitumens using the pull-off test method." *Construction and Building Materials*, 122, 140-148.

O'Neill, J. W. (2009). "The fire performance of timber-concrete composite floors."

Pan, A. D., and Moehle, J. P. (1992). "An experimental study of slab-column connections." *Structural Journal*, 89(6), 626-638.

Pang, A. (1979). "Composite steel: Concrete design. A comparison of the monograph on tall buildings, AISC-ACI, BS 5400 and the German code of practice for the design of steel composite beams." *NASA STI/Recon Technical Report N*, 80, 21619.

Papastergiou, D., and Lebet, J.-P. (2014). "Experimental investigation and modelling of the structural behaviour of confined grouted interfaces for a new steel–concrete connection." *Engineering Structures*, 74, 180-192.

Pashan, A., and Hosain, M. (2009). "New design equations for channel shear connectors in composite beams." *Canadian Journal of Civil Engineering*, 36(9), 1435-1443.

Pathirana, S. W., Uy, B., Mirza, O., and Zhu, X. (2015). "Strengthening of existing composite steel-concrete beams utilising bolted shear connectors and welded studs." *Journal of Constructional Steel Research*, 114, 417-430.

Pathirana, S. W., Uy, B., Mirza, O., and Zhu, X. (2016a). "Flexural behaviour of composite steel–concrete beams utilising blind bolt shear connectors." *Engineering Structures*, 114, 181-194.

Pathirana, S. W., Uy, B., Mirza, O., and Zhu, X. (2016b). "Bolted and welded connectors for the rehabilitation of composite beams." *Journal of Constructional Steel Research*, 125, 61-73.

Phillips, D., and Binsheng, Z. (1993). "Direct tension tests on notched and un-notched plain concrete specimens." *Magazine of Concrete Research*, 45(162), 25-35.

Queiroz, F., Vellasco, P., and Nethercot, D. (2007). "Finite element modelling of composite beams with full and partial shear connection." *Journal of Constructional Steel Research*, 63(4), 505-521.

Qureshi, J., Lam, D., and Ye, J. (2011). "Effect of shear connector spacing and layout on the shear connector capacity in composite beams." *Journal of constructional steel research*, 67(4), 706-719.

Rehman, N., Lam, D., Dai, X., and Ashour, A. F. (2016). "Experimental study on demountable shear connectors in composite slabs with profiled decking." *Journal of Constructional Steel Research*, 122, 178-189.

Robertson, I. N., and Johnson, G. (2004). "Repair of slab-column connections using epoxy and carbon fiber reinforced polymer." *Journal of Composites for Construction*, 8(5), 376-383.

Rodrigues, J. P. C., and Laím, L. (2011). "Behaviour of Perfobond shear connectors at high temperatures." *Engineering Structures*, 33(10), 2744-2753.

Rodrigues, J. P. C., and Laím, L. (2014). "Experimental investigation on the structural response of T, T-block and T-perfobond shear connectors at elevated temperatures." *Engineering structures*, 75, 299-314.

Roediger, L. (1951). "Composite construction and its applications." *Civil Engineering= Siviele Ingenieurswese*, 1(8), 237-254.

Sadek, F., El-Tawil, S., and Lew, H. (2008). "Robustness of composite floor systems with shear connections: Modeling, simulation, and evaluation." *Journal of Structural Engineering*, 134(11), 1717-1725.

Sakla, S. S., and Ashour, A. F. (2005). "Prediction of tensile capacity of single adhesive anchors using neural networks." *Computers & structures*, 83(21), 1792-1803.

Santos, D. S., Santos, P. M., and Dias-da-Costa, D. (2012). "Effect of surface preparation and bonding agent on the concrete-to-concrete interface strength." *Construction and Building Materials*, 37, 102-110.

Santos, P. M., and Julio, E. N. (2007). "Correlation between concrete-to-concrete bond strength and the roughness of the substrate surface." *Construction and Building Materials*, 21(8), 1688-1695.

Sarnes Jr, F. W. (1975). "Prestressing continuous composite steel-concrete bridges, MS thesis September 1975."

Schnerch, D., Dawood, M., Rizkalla, S., and Sumner, E. (2007). "Proposed design guidelines for strengthening of steel bridges with FRP materials." *Construction and building materials*, 21(5), 1001-1010.

Selden, K. L., Fischer, E. C., and Varma, A. H. (2015). "Experimental investigation of composite beams with shear connections subjected to fire loading." *Journal of Structural Engineering*, 142(2), 04015118.

Shanmugam, N., and Lakshmi, B. (2001). "State of the art report on steel–concrete composite columns." *Journal of constructional steel research*, 57(10), 1041-1080.

Shariati, A., RamliSulong, N., and Shariati, M. (2012). "Various types of shear connectors in composite structures: A review." *International Journal of Physical Sciences*, 7(22), 2876-2890.

Shariati, M., Sulong, N. R., Shariati, A., and Kueh, A. (2016). "Comparative performance of channel and angle shear connectors in high strength concrete composites: An experimental study." *Construction and Building Materials*, 120, 382-392.

Shash, A. (2005). "Repair of concrete beams–a case study." *Construction and Building Materials*, 19(1), 75-79.

Shaw, J. (1990). "Adhesives in the construction industry: Materials and case histories." *Construction and Building Materials*, 4(2), 92-97.

Siess, C. P., and Viest, I. M. (1952). "Studies of slab and beam highway bridges, Part V: Tests of continuous right I-beam bridges. A report of an investigation/Engineering Experiment Station structural research series; no. S-12." *University of Illinois. Engineering Experiment Station. Studies of slab and beam highway bridges, pt. 5*.

Siess, C. P., Viest, I. M., and Newmark, N. M. (1952). "Studies of slab and beam highway bridges: part III: small-scale tests of shear connectors and composite t-beams." University of Illinois at Urbana Champaign, College of Engineering. Engineering Experiment Station.

Siewczyńska, M. (2012). "Method for determining the parameters of surface roughness by usage of a 3D scanner." *archives of civil and mechanical engineering*, 12(1), 83-89.

Slutter, R. G., and Driscoll Jr, G. C. "RESEARCH ON COMPOSITE DESIGN AT LEHIGH UNIVERSITY." *Proc., Proc. AISC National Engineering Conference*.

Slutter, R. G., and Driscoll Jr, G. C. (1963). "Flexural strength of steel and concrete composite beams."

Slutter, R. G., and Fisher, J. W. (1966). "Fatigue strength of shear connectors." *Highway research record*, 147, 65-88.

Slutter, R., and Fisher, J. (1965). "Tentative design procedure for shear connectors in composite beams, August 1965."

Soty, R., and Shima, H. (2011). "Formulation for maximum shear force on L-shape shear connector subjected to strut compressive force at splitting crack occurrence in steel-concrete composite structures." *Procedia Engineering*, 14, 2420-2428.

Soty, R., and Shima, H. (2013). "Formulation for shear force–relative displacement relationship of L-shape shear connector in steel–concrete composite structures." *Engineering Structures*, 46, 581-592.

Souici, A., Berthet, J. F., Li, A., and Rahal, N. (2013). "Behaviour of both mechanically connected and bonded steel-concrete composite beams." *Engineering Structures*, 49, 11-23.

Souici, A., Berthet, J., Li, A., and Rahal, N. (2013). "Behaviour of both mechanically connected and bonded steel–concrete composite beams." *Engineering Structures*, 49, 11-23.

Stallmeyer, J., Munse, W., and Selby, K. (1965). "Fatigue Tests of Plates and Beams with Stud Shear Connectors." *Highway Research Record*(76).

Stigh, U., Biel, A., and Walander, T. (2014). "Shear strength of adhesive layers–models and experiments." *Eng Fract Mech*, 129, 67-76.

Stras, J. C. (1964). "An experimental and analytical study of prestressed composite beams." Rice University.

Subedi, N., and Coyle, N. (2002). "Improving the strength of fully composite steel-concrete-steel beam elements by increased surface roughness—an experimental study." *Engineering structures*, 24(10), 1349-1355.

Tadeu, A. J., and Branco, F. J. (2000). "Shear tests of steel plates epoxy-bonded to concrete under temperature." *Journal of Materials in civil Engineering*, 12(1), 74-80.

Täljsten, B. (2006). "The importance of bonding—A historic overview and future possibilities." *Advances in Structural Engineering*, 9(6), 721-736.

Taplin, G., and Grundy, P. "Incremental slip of stud shear connectors under repeated loading." *Proc., Composite construction-conventional and innovative. International conference*, 145-150.

Taranath, B. S. (2016). *Structural analysis and design of tall buildings: steel and composite construction*, CRC press.

Tavakkolizadeh, M., and Saadatmanesh, H. (2003). "Strengthening of steel-concrete composite girders using carbon fiber reinforced polymers sheets." *Journal of Structural Engineering*, 129(1), 30-40.

Taylor, T. P., and Matlock, H. (1968). *A finite-element method of analysis for composite beams*, Center for Highway Research, the University of Texas.

Teo, D., Mannan, M. A., Kurian, V., and Ganapathy, C. (2007). "Lightweight concrete made from oil palm shell (OPS): structural bond and durability properties." *Building and Environment*, 42(7), 2614-2621.

Thanoon, W. A., Jaafar, M. S., Kadir, M. R. A., and Noorzaei, J. (2005). "Repair and structural performance of initially cracked reinforced concrete slabs." *Construction and Building Materials*, 19(8), 595-603.

Thurlimann, B. "Fatigue and static strength of stud shear connectors." *Proc., Journal Proceedings*, 1287-1302.

Thurlimann, B. (1958). "Composite beams with stud shear connectors." *Highway Research Board Bulletin*(174).

Tilly, G. (1985). "Fatigue of land-based structures." *International Journal of Fatigue*, 7(2), 67-78.

Toprac, A. (1965). "Strength of three new types of composite beams."

Tremper, B. "Repair of damaged concrete with epoxy resins." *Proc., Journal Proceedings*, 173-182.

Upadhyaya, P., and Kumar, S. (2015). "Pull-out capacity of adhesive anchors: an analytical solution." *International Journal of Adhesion and Adhesives*, 60, 54-62.

Valente, I., and Cruz, P. J. (2004). "Experimental analysis of Perfobond shear connection between steel and lightweight concrete." *Journal of Constructional Steel Research*, 60(3), 465-479.

Van Gemert, D. (1980). "Force transfer in epoxy bonded steel/concrete joints." *International Journal of Adhesion and Adhesives*, 1(2), 67-72.

Van Gemert, D., and Maesschalck, R. (1983). "Structural repair of a reinforced concrete plate by epoxy bonded external reinforcement." *International Journal of Cement Composites and Lightweight Concrete*, 5(4), 247-255.

Veldanda, M., and Hosain, M. (1992). "Behaviour of perfobond rib shear connectors: push-out tests." *Canadian Journal of Civil Engineering*, 19(1), 1-10.

Vianna, J. d. C., Costa-Neves, L., Vellasco, P. d. S., and de Andrade, S. (2008). "Structural behaviour of T-Perfobond shear connectors in composite girders: An experimental approach." *Engineering Structures*, 30(9), 2381-2391.

Vianna, J. d. C., Costa-Neves, L., Vellasco, P. d. S., and De Andrade, S. (2009). "Experimental assessment of Perfobond and T-Perfobond shear connectors' structural response." *Journal of Constructional Steel Research*, 65(2), 408-421.

Viest, I. "Investigation of stud shear connectors for composite concrete and steel T-beams." *Proc., Journal Proceedings*, 875-892.

Viest, I. M. (1951). "Full-scale tests of channel shear connectors and composite t-beams." University of Illinois at Urbana Champaign, College of Engineering. Engineering Experiment Station.

Viest, I. M. (1960). "Review of research on composite steel-concrete beams." *Transactions of the American Society of Civil Engineers*, 126(2), 1101-1120.

Viest, I. M., Siess, C. P., Appleton, J., and Newmark, N. M. (1952). "Studies of Slab and Beam Highway Bridges: Part IV. Full Scale Tests of Channel Shear Connectors and Composite T-Beams." *University of Illinois Engineering Excerpt, Station Bulletin*, 405.

Viest, I., Fountain, R. S., and Siess, C. (1958). "Development of the New AASHO Specifications for Composite Steel and Concrete Bridges." *Highway Research Board Bulletin*(174).

Volnyy, V. A., and Pantelides, C. P. (1999). "Bond length of CFRP composites attached to precast concrete walls." *Journal of Composites for Construction*, 3(4), 168-176.

Wake, W. (1978). "Theories of adhesion and uses of adhesives: a review." *Polymer*, 19(3), 291-308.

Wang, D., Wu, D., He, S., Zhou, J., and Ouyang, C. (2015). "Behavior of post-installed large-diameter anchors in concrete foundations." *Construction and Building Materials*, 95, 124-132.

Wang, D., Wu, D., Ouyang, C., and Zhai, M. (2016). "Performance and design of post-installed large diameter anchors in concrete." *Construction and Building Materials*, 114, 142-150.

Wang, F., Li, M., and Hu, S. (2014). "Bond behavior of roughing FRP sheet bonded to concrete substrate." *Construction and Building Materials*, 73, 145-152.

Wang, Q., Zhao, D., and Guan, P. (2004). "Experimental study on the strength and ductility of steel tubular columns filled with steel-reinforced concrete." *Engineering Structures*, 26(7), 907-915.

Wang, Y. C. (1998). "Deflection of steel-concrete composite beams with partial shear interaction." *J Struct Eng*, 124(10), 1159-1165. ABAQUS (HKS, 2013). "ABAQUS 6.13 User's manual." *Simulia, Dassault Systems, Providence, RI*.

Wright, H., Evans, H., and Harding, P. (1987). "The use of profiled steel sheeting in floor construction." *Journal of Constructional Steel Research*, 7(4), 279-295.

Yam, L., and Chapman, J. (1968). "The inelastic behaviour of simply supported composite beams of steel and concrete." *Proceedings of The Institution of Civil Engineers*, 41(4), 651-683.

Yao, J., Teng, J., and Chen, J. (2005). "Experimental study on FRP-to-concrete bonded joints." *Composites Part B: Engineering*, 36(2), 99-113.

Yilmaz, S., Özen, M. A., and Yardim, Y. (2013). "Tensile behavior of post-installed chemical anchors embedded to low strength concrete." *Construction and Building Materials*, 47, 861-866.

Yoshitaka, U., Tetsuya, H., and Kaoru, M. "An experimental study on shear characteristics of perfobond strip and its rational strength equations." *Proc., International symposium on connections between steel and concrete*, RILEM Publications SARL, 1066-1075.

Yu-Hang, W., Jian-Guo, N., and Jian-Jun, L. (2014). "Study on fatigue property of steel–concrete composite beams and studs." *Journal of Constructional Steel Research*, 94, 1-10.

Zellner, W. "Recent designs of composite bridges and a new type of shear connectors." *Proc., Composite Construction in Steel and Concrete:*, ASCE, 240-252.

Zhao, G., and Li, A. (2008). "Numerical study of a bonded steel and concrete composite beam." *Computers & Structures*, 86(19), 1830-1838.

Zhao, X.-L., and Zhang, L. (2007). "State-of-the-art review on FRP strengthened steel structures." *Engineering Structures*, 29(8), 1808-1823. Bouazaoui, L., Perrenot, G., Delmas, Y., and Li, A. (2007). "Experimental study of bonded steel concrete composite structures." *Journal of Constructional Steel Research*, 63(9), 1268-1278.

List of Publications from Present Work:

International Journal:

Kumar, P., Patnaik, A., and Chaudhary, S. (2017). "A review on application of structural adhesives in concrete and steel–concrete composite and factors influencing the performance of composite connections." *International Journal of Adhesion and Adhesives*, 77, 1-14.

Kumar, P., Chaudhary, S., and Gupta, R. (2017). "Behaviour of Adhesive Bonded and Mechanically Connected Steel-concrete Composite under Impact Loading." *Procedia Engineering*, 173, 447-454.

Kumar, P., Patnaik A., and Chaudhary, S. (2017). "Effect of Bond Layer Thickness on Behaviour of Steel-Concrete Composite Connections." *Engineering Structures*, (Under Re-review)

Kumar, P., and Chaudhary, S. (2017). "Effect of Reinforcement Detailing on Performance of Composite Connections with Headed Studs." *Engineering Structures*, (Under Re-review)

International Conference:

Kumar, P., and Chaudhary, S. (2013) "Experimental Investigations for Shear Bond Strength of Steel and Concrete Bonded by Epoxy" *Proc., YRGS Int. Symp. on Current Challenges in Structural Engineering*, Chaudhary S. and Tripathi B., eds., Excel India Publications, New Delhi, Jaipur 165-171.

Kumar, P., Kasar, A. A., Naqvi S. A. A., and Chaudhary, S. (2017) "FE Analysis of Interfacial Failure Mechanism in Steel-concrete composite Bond." *International Conference on Composite Materials and Structures,* Hyderabad, India.